CORONAVIRUSES IN POULTRY: AN ONGOING PANDEMIC?

Coronavirus-induced diseases further clarified
with studies on comparative pathology and dual infection

Erik A.W. S. Weerts

Coronaviruses in poultry: an ongoing pandemic?

Coronavirus-induced diseases further clarified with studies
on comparative pathology and dual infection

Erik A.W.S. Weerts

Lay out: Erik A.W.S. Weerts
Print: Ipskamp Printing

ISBN: 978-94-6473-140-8

Coronaviruses in poultry: an ongoing pandemic?

Coronavirus-induced diseases further clarified with studies on comparative pathology and dual infection

Coronavirussen in pluimvee: een aanhoudende pandemie?

Coronavirus-geïnduceerde ziekten nader verklaard middels studies naar vergelijkende pathologie en duale infecties

(met een samenvatting in het Nederlands)

Proefschrift

ter verkrijging van de graad van doctor aan de Universiteit Utrecht
op gezag van de rector magnificus, prof. dr. H.R.B.M. Kummeling,
ingevolge het besluit van het college voor promoties
in het openbaar te verdedigen op

donderdag 8 juni 2023 des middags te 12.15 uur

door

Erik Anthonius Wilhelmus Siebertus Weerts

geboren op 30 juni 1983
te Oeffelt

Promotor:

Prof. dr. A. Gröne

Copromotoren:

Dr. M.G.R. Matthijs
Dr. M.H. Verheije

Beoordelingscommissie:

Prof. dr. F. Broere
Dr. R. Dijkman
Prof. dr. R. Ducatelle
Prof. dr. S. Rottenberg
Prof. dr. J.A. Stegeman

Content

1 Introduction

The COVID-19 pandemic, caused by the severe acute respiratory syndrome coronavirus 2 (SARS-CoV2), over the last years made the world's human population thoroughly aware of the existence of coronaviruses (CoVs) and the severe diseases they can cause.[18,43,53,59,60,64] Veterinarians, veterinary researchers and livestock farmers, however, have been battling coronavirus-induced diseases already for decades. The first ever reported disease that retrospectively appeared to be caused by a member of this virus family was 'infectious bronchitis' (IB) in chickens. In 1931, researchers Schalk and Hawn published about an 'apparently new respiratory disease' in chickens in North Dakota.[51] Bushnell and Brandly in 1933 discovered that this disease could be reproduced by injecting chicks with airway discharges of diseased birds, even after these discharges were passed over so-called Berkefield filters, which would prevent passage of bacteria and protozoal parasites.[14] Further confirmation of involvement of an alternative, yet unknown infectious agent came after Hudson and Beaudette in 1937 managed to culture the agent in embryonated chicken eggs. This technique had made people aware earlier on of existence of other non-bacterial infectious agents in chickens, for example the causative agent of fowl pox, which were back then considered to be a 'virus' more *per exclusionem* than based on true visualization of the agent.[8] In 1967 Almeida and Tyrrell were finally able to visualize the cause of IB via electron microscopy. They discovered structures of similar morphology within body fluids of chickens, mice and humans that suffered from diseases suspected to be caused by viruses. The observed spherical structures were named 'coronavirus' after their characteristic halo that resembled the solar 'corona' (Fig. 1). This observation marked the discovery of the infectious bronchitis virus (IBV) as first avian coronavirus (AvCoV) and retrospectively as cause of the first ever recognized coronaviral disease.[3] Currently, IBV has spread globally and causes significant problems with chicken welfare and productions losses almost all over the world.[24,33]

Infectious bronchitis is primarily a respiratory disease. Since the description of the IBV variant that is regarded as the IBV prototype in Massachusetts in 1941 (IBV M41), many different genotypes of IBV have been found and characterized. Several of these can cause disease outside the respiratory tract, but all variants found so far usually seem to be able to induce rhinitis and tracheitis (Fig. 2).[25,56]

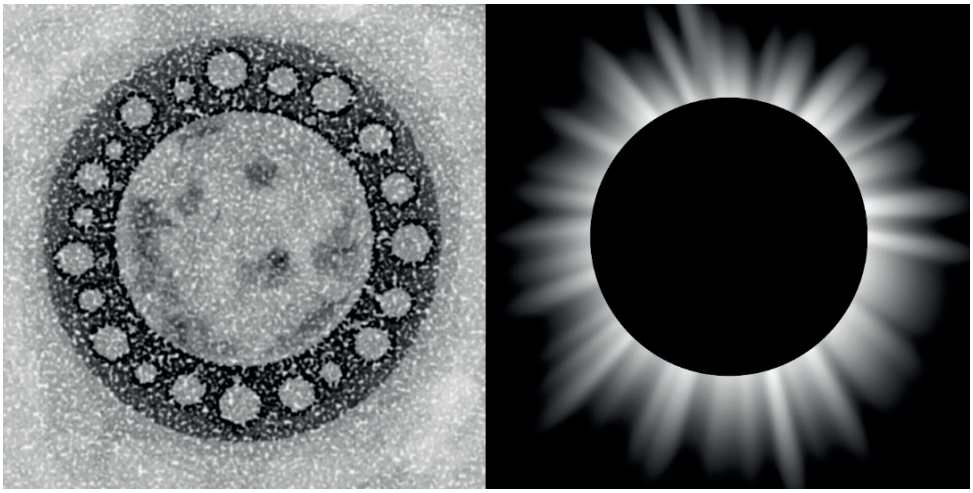

Figure 1: Artistic impression of the morphology of a coronavirus particle as visualized by electron microscopy (left panel), compared an artistic impression of the solar corona (right panel).

Severity of these upper respiratory diseases can vary per viral variant and depending on the type, age and immune status of the infected chicken. With exception of few IBV variants that are known for their relatively high pathogenicity, such as the Australian T strain and Delaware 072, mortality due to IBV infection by especially non-nephropathogenic virus variants is generally very low. Mortality tends to be the highest in younger-aged chicks with up to 25% of mortality among flocks during the first 6 weeks of age.[50] During infection, the respiratory epithelium goes through a phase of degeneration and subsequently a phase of hyperplasia before it changes back to its original morphology during a recovery phase.[25] Inflammatory cell infiltration progresses from heterophilic in the degenerative phase to mainly lymphohistiocytic in the hyperplastic phase. Mainly during the degenerative phase, an intraluminal exudate of heterophils mixed with desquamated infected epithelial cells can be observed within the upper airways.[62] IBV-induced pneumonia and airsacculitis do occur, but these generally become more clinically relevant after subsequent infection with a bacterium, for example the avian pathogenic *Escherichia coli* (APEC).[27,30,45,46] IBV can be excreted via nasal and tracheal discharges and can be often found in tracheal swabs.

IBV can infect other epithelia than the respiratory epithelium and the clinical

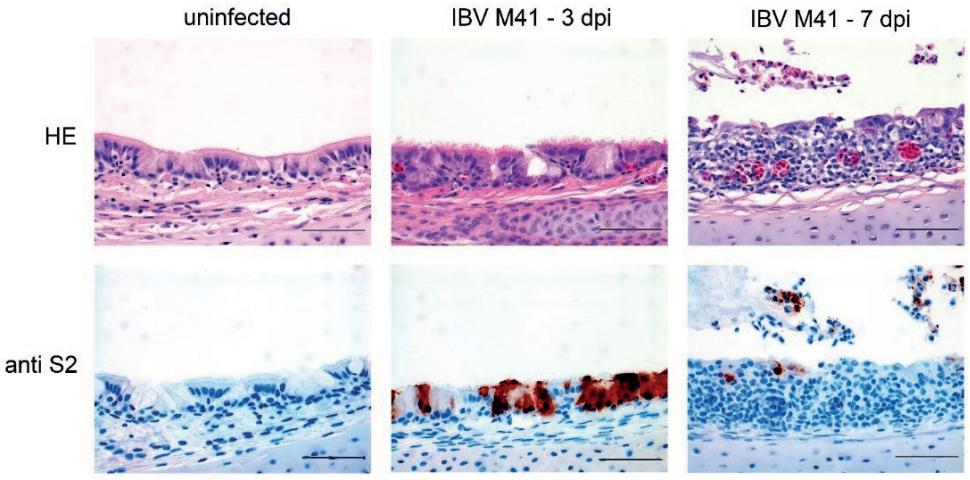

Figure 2: Chicken tracheal mucosa; uninfected (left panels); infected with IBV M41, 3 days post infection (dpi) - tissue architecture barely changed but with abundant viral protein expression (middle panels); infected with IBV M41, 7 dpi - loss of cilia and goblet cells, lymphohistiocytic infiltration of the epithelium, heterophils and mucus in the lumen, viral protein expression in the remaining epithelium and desquamated cells. Scale bar = 50 µm. *Adapted from: Ambepitiya Wickramasinghe, I.N., et al. The avian coronavirus spike protein. Virus Research 2014; 194; 37-48.*

impact of an IBV infection tends to increase when the virus is able to spread from the airways to other tissues.[48] Several IBV variants disseminate to the kidneys, for example the classic nephropathogenic type B1648 and the IBV QX variants. These cause tubular necrosis and tubulointersititial nephritis (Fig. 3), which might be lethal especially in young chicks.[4,19-21,25,35] In addition, some IBV variants can spread to the female reproductive tract and cause salpingitis, via which they reduce egg production and decrease of eggshell quality.[23,25,36,37] A severe result of oviduct infection can sometimes be observed in young chicks, mainly after infection with IBV QX variants. Such infections can induce cystic malformations of the oviduct that permanently impede egg production, a situation that is referred to as the so-called 'false layer syndrome'.[9] Male genital infection does occur, but the clinical impact of such infections is unclear.[61] Proventriculitis after IBV infection has been reported, but this seems more an exceptional than a regular sequel.[4] IBV is known to infect the intestinal tract, but generally not considered a virus associated with intestinal disease.[4,15,25] The cecal tonsil has been suggested as potential location of latent infection, but it is not clear whether such infection truly involves the lymphoid cell component

instead of merely the local cecal epithelium.[25] The virus can often be found in the cloaca and on cloacal swabs, but the relative contributions to the cloacal viral load from viral replication in the urogenital tract, the intestines and the airways (via swallowing) are unclear and will likely vary per IBV variant.[25,50] Of additional interest are the Harderian glands, in which IBV can replicate and cause adenitis. Via infection of these glands, the virus can get spread within tear drops.[52] IBV has so far not been associated with infections of the liver, pancreas or the nervous system.

Other poultry species, most notably turkeys but also Guinea fowl, quail and pheasants, can also suffer from coronavirus-induced disease.[16] While the associated tissue injury in pheasants and sometimes quail seems to resemble that of IBV infection in chickens with involvement of the respiratory and urinary tract,[5,17,31,44,54,55] coronaviruses of turkeys, Guinea fowl and regularly quail are known to cause enteric symptoms.[2,5,26,29,42] Intestinal disease is best studied in turkeys infected with the turkey coronavirus (TCoV) and to lesser extent in Guinea fowl infected with the Guinea fowl coronavirus (GfCoV). TCoV, which has distinct US and French (Fr) variants, and GfCoV are genetically closely related and seem to have IBV ancestors.[13] Turkeys infected with TCoV develop diarrhea and anorexia and show decreased growth.[2,29,50] Disease caused by TCoV was first described as 'mud fever' by Peterson and Hymas in 1951 and later became referred to as 'bluecomb disease'.[47] In 1973, the causative viral agent of this

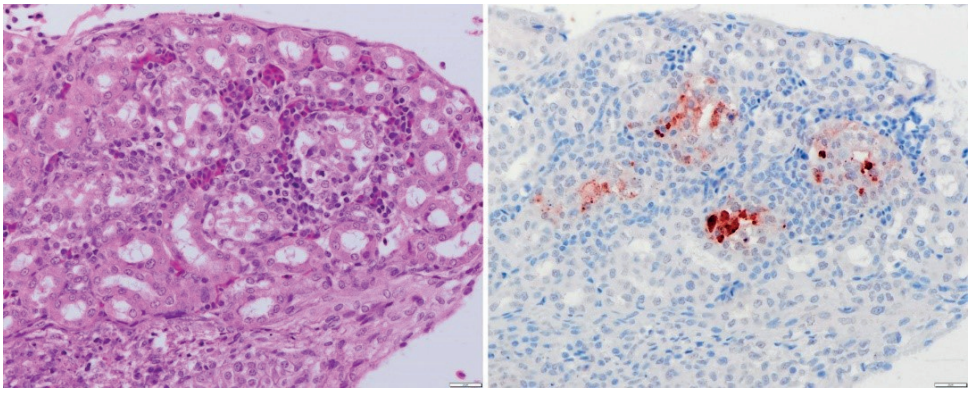

Figure 3: Chicken kidney infected with IBV QX; tubular necrosis and lymphoplasmacytic interstitial nephritis (left panel, HE) with intralesional viral protein expression (right panel, anti S2). Scale bar = 20 µm.

disease was discovered via electron microscopy and identified as a coronavirus.[50] GfCoV-induced enteric disease in industrially-kept Guinea fowl is known in France since the 1970s. Due to the often severe clinical presentation with high mortality, but the lack of knowledge on the exact cause, this was referred to as 'fulminating disease'.[22,26,42] GfCoV was demonstrated to be the cause of this severe enteric disease in 2014. Especially for GfCoV, little details about the disease, its pathogenesis and the full viral tropism are known and researchers only very recently in 2021 managed to isolate the virus from diseased birds.[22]

Immune responses against avian coronaviruses are most extensively studied for IBV. The chicken immune system protects against IBV infection via both innate and adaptive pathways. First defense is provided by epithelial barriers, which in the airways are equipped with the so-called mucocillairy apparatus. Apart from its physical barrier function against IBV, the epithelium likely also plays a role during initiation of inflammatory and immune responses once infection occurs.[49] Heterophils are an additional line of first defense and also macrophages and natural killer cells are known to play a role in the early anti-IBV response.[6,25,34] Adaptive immunity against IBV infection comprises humoral and cellular responses with generation of memory cells. B cell-dependent production of the immunoglobulins IgM and IgG has been repeatedly demonstrated during vaccine trials and also local mucosal immunity with IgA production is known to occur.[25,41] T cell-mediated cellular responses have been shown in the airways and do comprise presence of both T helper and cytotoxic T cell subsets.[7,39,41,45] Several of these responses are known to be mediated by specific cytokines. Of these responses, at least interferon (IFN) release but also release of other interleukins have been specifically evaluated.[40] Studies have shown that IBV is able to modulate several of these responses and it has been suggested that this modulation might influence the occurrence of secondary bacterial infections.[6]

Protection against IBV infections in the poultry industry is mostly based on stimulation of immune responses via vaccination. Vaccination strategies are commonly based on the use of live-attenuated vaccines, which are mostly produced by viral culture in embryonated chicken eggs and administered via

spray or aerosol techniques.[15,24,32] The many different IBV variants are known to belong to several serotypes and therefore it has been shown impossible to protect against infection by any IBV field variant via vaccination with one strain only. Therefore, combining various viral variants within a vaccination scheme is necessary and has been demonstrated to lead to better protection. More recently, steps have been undertaken to produce recombinant vaccines with the aim to combine the immunogenic parts of several IBV variants within one pluripotent vaccine.[28,38,57,58]

IBV, TCoV and GfCoV belong to the gammacoronaviruses, the genus of coronaviridae in which to date most of the avian coronaviruses (AvCoVs) are classified. Many recently discovered avian coronaviruses in wild birds belong to the newest of the four known genera, the deltacoronaviruses.[16,54] Among these, no equivalents of IBV, TCoV and GfCoV as causative agents of clinical disease or threats to lifestock have yet been pinpointed. Most of the other coronaviruses proven to be clinically relevant among animal species and humans belong to the genera of alpha- and betacoronaviruses, of which SARS-CoV2 is currently one of the most impactful examples of the latter genus.[18,43] All coronaviruses are positive single-stranded RNA viruses with a variable size of 80 to 120 nm. Structurally they consist of a lipid bilayer that contains three of the four structural proteins. Of these proteins, the envelope (E) and membrane (M) proteins function mostly to define the shape of the viral particle, whereas the spike (S) protein is needed to bind to the cells of the host. A fourth structural protein, the nucleocapsid (N) protein, is found inside the viral particle where it packages the viral RNA.[62]

The S protein consists of two subunits, of which the more variable S1 part contains the receptor binding domain (RBD) and interacts with the host receptor determinants, while the more conserved S2 part has a major role in fusion of the viral particle with the host cell membrane.[62] The S protein mostly defines the host and tissue tropism of the specific coronavirus and is also the dominant protein that modulates the host's immune response.[62] Several IBV variants use the S protein to bind to α2,3-linked sialic acids, which is so far the best known receptor determinant for IBV.[1,63] Recently it was discovered that IBV QX variants seem to bind to another, yet undetermined group of sialic acids.[12] TCoV and

GfCoV have been shown to bind to other surface molecules, such as nonsialylated poly-LacNAc-containing glycans.[5,11] To date, additional protein receptors are suspected to exist, but no studies have been able to discover these so far.[10] With discovery of the different glycan receptor molecules, some studies have been performed to gain knowledge about similarities and differences of tissue tropisms for different IBV variants and TCoV and GfCoV,[5,11] but several questions remain and especially for Guinea fowl comparative studies on *in vivo* tissue tropism and pathogenesis are lacking so far, though very much needed for understanding disease.

With the continuous discovery of new IBV variants and other coronaviruses that might become a threat to livestock or even the human population in the future, more knowledge is needed about the diseases coronaviruses cause. For IBV in chickens, many questions remain about the role of the virus in dual respiratory infections with bacteria like APEC, but also with other viruses like the avian influenza virus (AIV). Only few *in vivo* evaluations of dual viral infections in chicken flocks that include IBV have been reported and mechanistically viral interference in poultry is still poorly understood. Only limited knowledge exists on the relevance of IBV-induced intestinal infection and how enteric involvement in IB differs from TCoV infection in turkeys and GfCoV infection in Guinea fowl. For GfCoV, on the other hand, only little information exists on potential tissue tropism outside the intestines. Furthermore it is unclear why GfCoV infection is usually associated with severe 'fulminating disease', while turkeys and chickens infected with respectively TCoV and IBV tend to encounter less severe intestinal problems with less lethal outcome. To address these topics, this thesis presents the following studies:

In **Chapter 2**, the effects of attenuation of an IBV QX vaccine variant on lesion severity and coinciding viral replication dynamics are compared with its wild-type ancestor virus. Studies on attenuated IBV vaccine variants tend to focus on gaining proof of successful attenuation mostly by scoring ciliostasis in the trachea and development of kidney lesions and not so much on further characteristics of lesion development and viral excretion that more comprehensively explain the attenuated phenotype. The hypothesis in this study is that respiratory and renal lesions will develop also after attenuation,

but that these will be significantly less severe and these will coincide with only limited shedding of virus via nasal and cloacal discharges.

In **chapter 3**, interference of IBV and avian influenza viruses (AIVs) is studied in a trachea organ culture (TOC) model. Studies on viral interference in birds are rare and with continuing outbreaks of AIV and the ongoing discovery of new IBV variants, such interferences are very relevant for the poultry field. They might influence disease severity and preventive measures, especially since these viruses share common receptor determinants to bind to the host's cells. It might be likely that infection of the trachea by one virus will hamper replication by another virus due to loss of susceptible cells, but the study in this chapter aims to elucidate whether this is mostly the result of pure cell loss or that additional factors, for example changes in receptor expression, could play a role.

The study in **chapter 4** is set up to gain more knowledge about dual infections with respiratory viruses and APEC. It aims to find correlations between airway pathology and immune responses after infection with APEC when this is preceded by an infection with IBV or two additional important chicken respiratory viruses, the Newcastle disease virus (NDV) and the avian metapneumovirus (aMPV). Virus-enhanced colibacillosis is a big threat to the poultry industry and the airways have been proven to play a major role in the development of this disease. This phenomenon has been mainly studied with IBV as preceding virus, but the present study aims to compare the effect on lesion development and immune responses when NDV or aMPV are used as initial infectious agent. Based on knowledge from studies in for example mice as model for human influenza virus-enhanced streptococcal pneumonia, the hypothesis for this work is that the viruses will lead to more extensive airway lesions and certain associated inflammatory stimuli that will hamper anti-bacterial responses.

Chapter 5 elaborates further on the individual contributions of IBV and APEC to airsacculitis as part of IBV-enhanced colibacillosis, probably the most famous example of a dual infection in chickens with a virus and bacterium. Previous studies of this kind highlighted the importance of the air sac in development of disease, because these particularly seem to develop significantly more severe

lesions than other respiratory tissues after dual infection than with APEC alone. Since control groups infected with IBV alone mostly lacked in these previous studies, this study aims to gain new insights into IBV-APEC-induced air sacculitis by more comprehensive comparison with birds that only received virus. The hypothesis for this study was that IBV might define lesion morphology more extensively than previously thought and that APEC probably mostly enhances the virus-induced damage, rather than that the bacterium induces most of the damage, assisted by hampered antibacterial immune responses due to interference of the virus.

Another avian coronavirus is introduced in **chapter 6**. In this chapter, transmission and excretion kinetics of the Fr TCoV are studied in association with the localization of the virus within the different segments of the intestines. Compared to the US variant of TCoV, which is known for decades now, the Fr variant is less well characterized and additional studies on the aforementioned aspects will help to better understand development of TCoV-induced intestinal disease over time when the virus gets introduced in a commercial flock of turkeys. The infection hypothetically will likely lead to mucosal damage through the intestinal tract with viral protein expression in balance with viral shedding. The study also aims to define the region of the intestinal tract most prominently targeted by Fr TCoV.

The study in **chapter 7** evaluates and compares in detail morphologic changes within the intestinal tract of chickens, turkeys and Guinea fowl infected with respectively IBV, TCoV and GfCoV. The intestinal tract seems to be the only organ system that is targeted by all three AvCoVs, but the usual clinical presentation of these infections is markedly different in these poultry species. The study in this chapter aims to find an explanation for these clinical differences by performing a retrospective histological analysis of paraffin-embedded intestinal samples with the hypothesis that the Guinea fowl will have more severe enteritis and more abundant intralesional viral protein. This chapter in addition reports about lesions and viral tropism in other organ systems, because these were not very well studied for GfCoV before.

To conclude, results from these six studies are combined and discussed in **chapter 8** and remaining knowledge gaps and future perspectives on research and field relevance are addressed.

In the end, this thesis presents new knowledge on pathogeneses, immune responses and viral excretion and transmission of AvCoVs, that will help to design and improve preventive and therapeutic strategies for the known but also potentially emerging coronavirus-induced diseases in poultry and probably other species.

References

1. Abd El Rahman S, El-Kenawy AA, Neumann U, et al. Comparative analysis of the sialic acid binding activity and the tropism for the respiratory epithelium of four different strains of avian infectious bronchitis virus. *Avian Pathol*. 2009;38:41-45.

2. Adams NR, Ball RA, Hofstad MS. Intestinal lesions in transmissible enteritis of turkeys. *Avian Dis*. 1970;14:392-399.

3. Almeida JD, Tyrrell DA. The morphology of three previously uncharacterized human respiratory viruses that grow in organ culture. *J Gen Virol*. 1967;1:175-178.

4. Ambali AG, Jones RC. Early pathogenesis in chicks of infection with an enterotropic strain of infectious bronchitis virus. *Avian Dis*. 1990;34:809-817.

5. Ambepitiya Wickramasinghe IN, de Vries RP, Weerts EAWS, et al. Novel receptor specificity of avian gammacoronaviruses that cause enteritis. *J Virol*. 2015;89:8783-8792.

6. Ariaans MP, Matthijs MGR, van Haarlem D, et al. The role of phagocytic cells in enhanced susceptibility of broilers to colibacillosis after infectious bronchitis virus infection. *Vet Immunol Immunopathol*. 2008;123:240-250.

7. Arstila TP, Vainio O, Lassila O. Central role of CD4+ T cells in avian immune response. *Poult Sci*. 1994;73:1019-1026.

8. Beaudette FR, Hudson CB. Cultivation of the virus of infectious bronchitis. *J Am Vet Med Ass*. 1937;90:51-60.

9. Benyeda Z, Szeredi L, Mató T, et al. Comparative histopathology and immunohistochemistry of QX-like, Massachusetts and 793/B serotypes of infectious bronchitis virus infection in chickens. *J Comp Pathol*. 2010;143:276-283.

10. Bickerton E, Maier HJ, Stevenson-Leggett P, et al. The S2 subunit of infectious bronchitis virus Beaudette is a determinant of cellular tropism. *J Virol*. 2018;92:e01044-18,1-18.

11. Bouwman KM, Delpont M, Broszeit F, et al. Guinea fowl coronavirus diversity has phenotypic consequences for glycan and tissue binding. *J Virol*. 2019;93:e00067-19,1-11.

12. Bouwman KM, Parsons LM, Berends AJ, et al. Three amino acid changes in avian coronavirus spike protein allow binding to kidney tissue. *J Virol*. 2020;94:e01363-19,1-14.

13. Brown PA, Touzain F, Briand FX, et al. First complete genome sequence of European turkey coronavirus suggests complex recombination history related with US turkey and Guinea fowl coronaviruses. *J Gen Virol*. 2016;97:110-120.

14. Bushnell LD, Brandly CA. Laryngotracheitis in chicks. *Poult Sci*. 1933;12:55-60.

15. Cavanagh D. Coronavirus avian infectious bronchitis virus. *Vet Res*. 2007;38:281-297.

16. Cavanagh D. Coronaviruses in poultry and other birds. *Avian Pathol*. 2005;34:439-448.

17. Cavanagh D, Mawditt K, Welchman D de B, et al. Coronaviruses from pheasants (*Phasianus colchicus*) are genetically closely related to coronaviruses of domestic fowl (infectious bronchitis virus) and turkeys. *Avian Pathol*. 2002;31:81-93.

18. Chauhan S. Comprehensive review of coronavirus disease 2019 (COVID-19). *Biomed J*. 2020;43:334-340.

19. Chen BY, Hosi S, Nunoya T, et al. Histopathology and immunohistochemistry of renal lesions due to infectious bronchitis virus in chicks. *Avian Pathol*. 1996;25:269-283.

20. Chen BY, Itakura C. Histopathology and immunohistochemistry of renal lesions due to avian infectious bronchitis virus in chicks uninoculated and previously inoculated with highly virulent infectious bursal disease virus. *Avian Pathol*. 1997;26:607-624.

21. Chong KT, Apostolov K. The pathogenesis of nephritis in chickens induced by infectious bronchitis virus. *J Comp Pathol*. 1982;92:199-211.

22. Courtillon C, Briand F-X, Allée C, et al. Description of the first isolates of Guinea fowl corona and picornaviruses obtained from a case of Guinea fowl fulminating enteritis. *Avian Pathol*. 2021;50:507-521.

23. Crinion RA, Ball RA, Hofstad MS. Pathogenesis of oviduct lesions in immature chickens following exposure to infectious bronchitis virus at one day old. *Avian Dis*. 1971;15:32-41.

24. De Wit JJ, Cook JK, van der Heijden HM. Infectious bronchitis virus variants: a review of the history, current situation and control measures. *Avian Pathol.* 2011;40:223-235.

25. Dhinakar Raj G, Jones RC. Infectious bronchitis virus: immunopathogenesis of infection in the chicken. *Avian Pathol.* 1997;26:677-706.

26. Ducatez MF, Liais E, Croville G, Guerin JL. Full genome sequence of Guinea fowl coronavirus associated with fulminating disease. *Virus Genes*. 2015;50:514-517.

27. Dwars RM, Matthijs MGR, Daemen AJ, et al. Progression of lesions in the respiratory tract of broilers after single infection with *Escherichia coli* compared to superinfection with *E. coli* after infection with infectious bronchitis virus. *Vet Immunol Immunopathol*. 2009;127:65-76.

28. Ellis S, Keep S, Britton P, de Wit S, et al. Recombinant infectious bronchitis viruses expressing chimeric spike glycoproteins induce partial protective immunity against homologous challenge despite limited replication *in vivo. J Virol*. 2018;92:e01473-18,1-18.

29. Gomes DE, Hirata KY, Saheki K, et al. Pathology and tissue distribution of turkey coronavirus in experimentally infected chicks and turkey poults. *J Comp Pathol*. 2010;143:8-13.

30. Goren E. Observations on experimental infection of chicks with *Escherichia coli*. *Avian Pathol*. 1978;7:213-224.

31. Gough RE, Cox WJ, Winkler CE, et al. Isolation and identification of infectious bronchitis virus from pheasants. *Vet Rec*. 1996;138:208-209.

32. Ignjatovic J, Sapats S. Avian infectious bronchitis virus. *Rev Sci Tech*. 2000;19:493-508.

33. Jackwood MW. Review of infectious bronchitis virus around the world. *Avian Dis*. 2012;56:634-641.

34. Jansen CA, de Geus ED, van Haarlem DA, et al. Differential lung NK cell responses in avian influenza virus infected chickens correlate with pathogenicity. *Sci Rep*. 2013;3: 2478,1-10.

35. Jones RC. Nephrosis in laying chickens caused by Massachusetts-type infectious bronchitis virus. *Vet Rec*. 1974;95**:**319.

36. Jones RC, Jordan FT. Persistence of virus in the tissues and development of the oviduct in the fowl following infection at day old with infectious bronchitis virus. *Res Vet Sci*. 1972;13:52-60.

37. Jones RC, Jordan FT. The site of replication of infectious bronchitis virus in the oviduct of experimentally infected hens. *Vet Rec*. 1971;89:317-318.

38. Keep S, Sives S, Stevenson-Leggett P, et al. Limited cross-protection against infectious bronchitis provided by recombinant infectious bronchitis viruses expressing heterologous spike glycoproteins. *Vaccines (Basel)*. 2020;8:330,1-19.

39. Kim TS, Shin EC. The activation of bystander CD8+ T cells and their roles in viral infection. *Exp Mol Med*. 2019;51:154,1-9.

40. Kint J, Fernandez-Gutierrez M, Maier HJ, et al. Activation of the chicken type I interferon response by infectious bronchitis coronavirus. *J Virol*. 2015;89:1156-1167.

41. Kjærup RM, Dalgaard TS, Norup LR, et al. Characterization of cellular and humoral immune responses after IBV infection in chicken lines differing in MBL serum concentration. *Viral Immunol*. 2014;27:529-542.

42. Liais E, Croville G, Mariette J, et al. Novel avian coronavirus and fulminating disease in Guinea fowl, France. *Emerg Infect Dis*. 2014;20:105-108.

43. Lin CN, Chan KR, Ooi EE, et al. Animal coronavirus diseases: parallels with COVID-19 in humans. *Viruses*. 2021;13:1507,1-15.

44. Lister SA, Beer JV, Gough RE, et al. Outbreaks of nephritis in pheasants (*Phasianus colchicus*) with a possible coronavirus aetiology. *Vet Rec*. 1985;117:612-613.

45. Matthijs MGR, Ariaans MP, Dwars RM, et al. Course of infection and immune responses in the respiratory tract of IBV infected broilers after superinfection with *E. coli*. *Vet Immunol Immunopathol*. 2009;127:77-84.

46. Matthijs MGR, van Eck JHH, Landman WJM, et al. Ability of Massachusetts-type infectious bronchitis virus to increase colibacillosis susceptibility in commercial broilers: a comparison between vaccine and virulent field virus. *Avian Pathol*. 2003;32:473-481.

47. Peterson EH, Hymas TA. Antibiotics in the treatment of an unfamiliar turkey disease. *Poult Sci*. 1951;30:466-468.

48. Reddy VRAP, Trus I, Desmarets LMB, et al. Productive replication of nephropathogenic infectious bronchitis virus in peripheral blood monocytic cells, a strategy for viral dissemination and kidney infection in chickens. *Vet Res*. 2016;47:70,1-19.

49. Robinson KM, Kolls JK, Alcorn JF. The immunology of influenza virus-associated bacterial pneumonia. *Curr Opin Immunol*. 2015;34:59-67.

50. Saif YM, Fadly AM, Glisson JR, et al. *Diseases of Poultry*. 12th ed. Iowa State University Press; 2008.

51. Schalk AF, Hawn MC. An apparently new respiratory disease of baby chicks. *J Am Vet Med Ass*. 1931;78:413-422.

52. Toro H, Godoy V, Larenas J, et al. Avian infectious bronchitis: viral persistence in the harderian gland and histological changes after eyedrop vaccination. *Avian Dis*. 1996;40:114-120.

53. Torres Acosta MA, Singer BD. Pathogenesis of COVID-19-induced ARDS: implications for an ageing population. *Eur Respir J*. 2020;56:2002049,1-12.

54. Torres CA, Listorti V, Lupini C, et al. Gamma and deltacoronaviruses in quail and pheasants from Northern Italy. *Poult Sci*. 2017;96:717-722.

55. Torres CA, Villarreal LY, Ayres GR, et al. An avian coronavirus in quail with respiratory and reproductive signs. *Avian Dis*. 2013;57:295-299.

56. Valastro V, Holmes EC, Britton P, et al. S1 gene-based phylogeny of infectious bronchitis virus: an attempt to harmonize virus classification. *Infect Genet Evol.* 2016;39:349-364.

57. Van Beurden SJ, Berends AJ, Krämer-Kühl A, et al. A reverse genetics system for avian coronavirus infectious bronchitis virus based on targeted RNA recombination. *Virol J*. 2017;14:109,1-13.

58. Van Beurden SJ, Berends AJ, Krämer-Kühl A, et al. Recombinant live attenuated avian coronavirus vaccines with deletions in the accessory genes 3ab and/or 5ab protect against infectious bronchitis in chickens. *Vaccine*. 2018;36:1085-1092.

59. Van den Brand JM, Haagmans BL, Leijten L, et al. Pathology of experimental SARS coronavirus infection in cats and ferrets. *Vet Pathol*. 2008;45:551-562.

60. Van den Brand JM, Smits SL, Haagmans BL. Pathogenesis of Middle East respiratory syndrome coronavirus. *J Pathol*. 2015;235:175-184.

61. Villarreal LY, Brandao PE, Chacon JL, et al. Orchitis in roosters with reduced fertility associated with avian infectious bronchitis virus and avian metapneumovirus infections. *Avian Dis*. 2007;51:900-904.

62. Wickramasinghe IN, van Beurden SJ, Weerts EAWS, Verheije MH. The avian coronavirus spike protein. *Virus Res*. 2014;194:37-48.

63. Winter C, Schwegmann-Wessels C, Cavanagh D, et al. Sialic acid is a receptor determinant for infection of cells by avian infectious bronchitis virus. *J Gen Virol*. 2006;87:1209-1216.

64. Yao XH, He ZC, Li TY, et al. Pathological evidence for residual SARS-CoV-2 in pulmonary tissues of a ready-for-discharge patient. *Cell Res*. 2020;30:541-543.

2

Attenuated live infectious bronchitis virus QX vaccine disseminates slowly to target organs distant from the site of inoculation

A. Laconi [a,b,#], E.A.W.S. Weerts [a,#], J.C.G. Bloodgood [a], J.P. Deniz Marrero [a], A.J. Berends [a], G. Cocciolo [c], J.J. de Wit [a,d], M.H. Verheije [a]

[a] Division of Pathology, Department Biomolecular Health Sciences, Faculty of Veterinary Medicine, Utrecht University, Utrecht, the Netherlands

[b] Department of Comparative Biomedicine and Food Science, University of Padua, Legnaro (PD), Italy

[c] Department of Veterinay Medicine, University of Bari, Valenzano, Italy

[d] Royal GD Animal Health, Deventer, the Netherlands

[#] *contributed equally*

published: Vaccine, 2020; 38: 1486-1493.

Abstract

Infectious bronchitis (IB) is a highly contagious respiratory disease of poultry, caused by the avian coronavirus infectious bronchitis virus (IBV). Currently, one of the most relevant genotypes circulating worldwide is IBV-QX (GI-19), for which vaccines have been developed by passaging virulent QX strains in embryonated chicken eggs. Here we explored the attenuated phenotype of a commercially available QX live vaccine, IB Primo QX, in specific pathogens free broilers. At hatch, birds were inoculated with QX vaccine or its virulent progenitor IBV-D388, and postmortem swabs and tissues were collected each day up to eight days post infection to assess viral replication and morphological changes. In the trachea, viral RNA replication and protein expression were comparable in both groups. Both viruses induced morphologically comparable lesions in the trachea, albeit with a short delay in the vaccinated birds. In contrast, in the kidney, QX vaccine viral RNA was nearly absent, which coincided with the lack of any morphological changes in this organ. This was in contrast to high viral RNA titers and abundant lesions in the kidney after IBV D388 infection. Furthermore, QX vaccine showed reduced ability to reach and replicate in conjunctivae and intestines including cloaca, resulting in significantly lower titers and delayed protein expression, respectively. Nephropathogenic IBVs might reach the kidney also via an ascending route from the cloaca, based on our observation that viral RNA was detected in the cloaca one day before detection in the kidney. In the kidney distal tubular segments, collecting ducts and ureter were positive for viral antigen. Taken together, the attenuated phenotype of QX vaccine seems to rely on slower dissemination and lower replication in target tissues other than the site of inoculation.

Keywords

infectious bronchitis virus – nephropathogenicity – broilers – attenuation – vaccine – virulence

Introduction

Infectious bronchitis (IB) is an acute, highly contagious respiratory disease of chickens (Gallus gallus) caused by infectious bronchitis virus (IBV).[1] The virus belongs to the genus Gammacoronavirus within the family Coronaviridae, order Nidovirales.[2] IBV poses a major economic threat worldwide, especially due to reduced egg quality and quantity in layer chickens and predisposition to bacterial infections in broilers. IBV initially targets the epithelium of the respiratory tract, but depending on the viral strain it can also infect other organs, mostly the reproductive tract and the kidneys. New IBV variants, resulting in different genotypes, serotypes and pathotypes, are continuously reported.[3]

Based on its clinical symptoms in the field and on its global dissemination, one of the most threatening IBV genotypes is QX (GI-19). The first QX strain circulating was reported from China in 1998,[4] and QX-like IBV strains are now circulating in many other countries. These viruses are associated with respiratory problems, renal failure, drops in egg production and 'false layers' syndrome.[5-9] In Europe, it is the second most prevalent IBV genotype.[10]

The control of IB occurs by vaccination, typically using live attenuated vaccines derived from virulent strains serially passaged in embryonated chicken eggs. As a result the virus adapts to the embryo, with a concomitant attenuation for hatched, juvenile and adult chickens.[11-13] Similarly, QX field virulent strains have been attenuated via passage in embryonated chicken eggs.[14] The basis of the attenuation of live IBV vaccines and its effects on the resulting phenotype are, however, poorly understood.

Here we set out to elucidate the attenuated phenotype of the QX vaccine, NOBILIS IB Primo, by comparing its viral replication, protein expression and induction of lesions in various target tissues to that of its progenitor, IBV-D388.[9] Viral distribution was investigated at the site of inoculation, the trachea, and in the kidneys, conjunctivae and the gastrointestinal tract, specifically including the cloaca, over the first eight days after experimental infection of day-old broilers. Our data show that the attenuation of QX vaccine phenotypically

results in reduced ability to spread and to replicate in tissues beyond the site of infection.

Materials and methods

Viruses and chickens

IBV-D388 was isolated by GD Animal Health (Deventer, The Netherlands) in March 2004 from 19-day-old broiler breeders with respiratory signs and increased mortality due to renal failure.[9] NOBILIS IB Primo QX (MSD/Animal Health, The Netherlands; batch A006A1J01; $10^{4.0}$–$10^{5.5}$ EID_{50} per vial) is a live attenuated avian infectious bronchitis QX virus derived from strain D388. Full genome sequences of the vaccine and its progenitor virulent strain are not currently available.

Experimental design

Fifty-six specific pathogens free (SPF) broiler-type chickens (GD Animal Health, Deventer, The Netherlands) of mixed gender were used in accordance with GD Animal Health institutional guidelines (Ethical animal experimentation approval 2017-071). At day of hatch, the animals were divided into three groups, containing eight (negative controls), 24 (QX vaccine), and 24 (IBV-D388) chickens respectively, and each group was kept in separate isolators under controlled housing conditions, including filtered supply and exhaust air. At day 0, the control group was inoculated with PBS, and the experimental groups were inoculated intratracheally with one dose of 10^3 EID_{50} IBV-D388 or QX vaccine in 0.1 ml sterile water. Back titration showed that birds were inoculated with a dose of $10^{3.1}$ EID_{50} of IBV-D388 and a dose of $10^{5.0}$ EID_{50} QX vaccine, respectively.

All animals were checked daily for clinical symptoms, but it is of note that clinical symptoms including mild dyspnea, mildly increased respiratory sounds, and mild serous ocular and nasal discharge are difficult to record when animals are housed in isolators. Here, both the onset, the frequency and the number of birds showing clinical respiratory symptoms listed above were comparable between the groups (data not shown). Every day, one bird of the control group, three IBV-D388 and three QX vaccine inoculated animals were euthanized. From each

animal, swabs were taken from the trachea, the conjunctivae and the cloaca, and stored at 4 °C after drying for two hours in a laminar flow cabinet. Tissue samples were collected from trachea and kidneys daily. Samples from the gastrointestinal (GI) tract, including the cloaca, were taken at days 1, 4, 7, and 8. Tissues were fixed in neutral-buffered 10% formalin in PBS for 24 h, stored in 70% ethanol and finally paraffin-embedded. Additional kidney tissue samples were placed in liquid nitrogen immediately during necropsy and subsequently stored in -80 °C for viral RNA isolation.

Viral RNA analysis

RNA was extracted from individual dry swabs and kidneys. Briefly, the swabs were eluted in 500 ml of PBS and the viral RNA was extracted using a QIAamp viral RNA minikit (QIAGEN, Hilden, Germany) following the manufacturer's protocol, whereas 30 mg of each kidney was homogenized using MagNA Lyser Instrument (Roche, Germany) and the RNA was isolated using the RNeasy minikit (QIAGEN, Hilden, Germany), following the manufacturer's recommendations. In each round of RNA isolation, a QX isolate with known titer (10^6 EID_{50}/ml) was included as positive control, while PBS was used as negative control. qRT-PCRs were performed using the iTaq universal SYBR Green one-step kit (Bio-Rad Laboratories, Hercules, California, USA). A genotype QX specific SYBR Green qRT-PCR developed and validated in our laboratory[15] based on the S1 gene sequence was used to detect and quantify viral RNA. The limit of detection of the assay was equal to $10^{1.31}$ EID_{50}/100 ml. The qRT-PCR reactions were carried out in a Bio-Rad CFX Connect real-time PCR system. In each qRT-PCR round, three ten-fold dilutions of the positive control were used to create a standard curve to quantify the viral RNA in the samples.

Histopathology and anti-IBV immunohistochemistry

Tissue slides were cut from the formalin-fixed, dehydrated, and paraffin-embedded tracheas, kidneys, cloacas and other segments of the gastrointestinal tract. For histopathological examination, tissue slides of trachea and kidney were stained with haematoxylin and eosin (HE) according to standard laboratory procedures. Histopathologic changes were critically evaluated via light

microscopy by two veterinary pathologists, who after individual evaluation came to a consensus. Immunohistochemical staining was performed on tissue slides as previously described by van Beurden et al. (2017),[16] using a monoclonal antibody directed against the IBV S2 protein (Prionics - Thermo Fisher Scientific, Waltham, MA, USA). Percentages of cells showing viral protein expression were scored for each organ by light microscopic evaluation, similarly as described by Van den Brand et al. (2011).[17] For the trachea, this was done with the total piece of tissue divided into ten parts; in each tenth, the percentage of cells showing viral protein expression was defined in 10% increments. An average viral protein expression percentage for the total trachea was then calculated by dividing the total sum of the ten separate percentages by ten. For the kidney and cloaca, similar procedures were followed, but, due to the more variable tissue sample shape, each tissue piece was divided into five instead of ten parts for technical convenience. The GI tract was evaluated for presence of viral protein expression without percentage-wise scoring and with division of the total GI tract into four parts: (1) stomachs (proventriculus and gizzard), (2) small intestines (duodenum, jejunum, ileum), (3) large intestines (caeca, large intestinal segment connecting ileocaecal junction with cloaca) and (4) cloaca.

Statistical analysis

A two-way analysis of variance (ANOVA) was used to assess whether the viral RNA and the viral replication in each tissue were significantly different between the vaccine and its virulent progenitor.

Results

Tracheal viral RNA and viral protein expression are comparable between IBV-D388 and QX vaccine inoculated chickens

At each time point, postmortem swabs were taken from the animals before further collection of tissues. From the swabs taken from the most caudal part of the trachea, viral RNA isolation and qRT-PCR were performed to determine the amount of viral RNA present in the trachea per animal per time point (Fig. 1A). Viral RNA could be detected in the trachea from the first day onward and viral

RNA titers remained constant over time until day 8 in both the IBV-D388 and QX vaccine inoculated groups (Fig. 1A). There were no significant differences in viral RNA titers between time points or between the field and vaccine strain ($p > 0.05$).

To investigate whether RNA titers were derived from local viral replication or only from the inoculum itself, RNA presence was compared with viral protein expression, visualized via immunohistochemical staining. The percentages of cells showing viral protein expression per trachea per time point are shown in Fig. 1B. For IBV-D388, viral protein expression could be detected from day 2 onward, while the first viral protein detection after QX vaccine infection was first observed on day 4. Viral protein expression was detected in all three trachea samples from day 4 onward after IBV-D388 inoculation, while protein expression was only present for all three samples on day 5 after QX vaccine inoculation. However, there were no statistically significant differences between the groups at any time point. For both the IBV-D388 and QX vaccine-inoculated birds, a representative example of trachea stained with an antibody against IBV is shown in Fig. 1C.

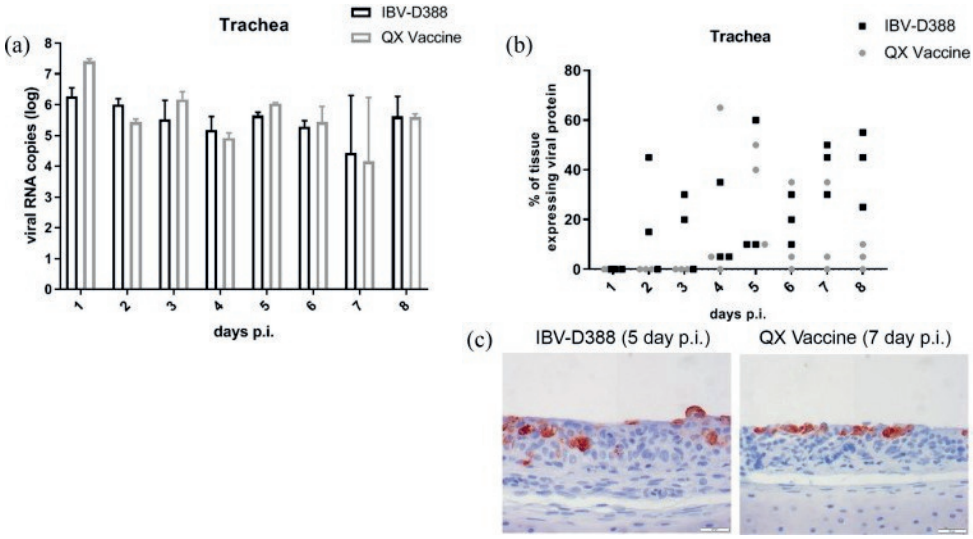

Fig. 1. IBV QX viruses in trachea of experimentally infected broilers. (A) Viral RNA was isolated from swabs from the most caudal part of the trachea of each bird upon necropsy. qRT-PCR using primers directed against the S1 gene was performed in duplicate. Viral titers were calculated based on a standard curve, and the mean and standard deviation of three birds are shown; (B/C) Trachea sections were stained by immunohistochemistry using an anti-IBV S2 antibody. The percentage of cells within the trachea section that expressed viral proteins is depicted in (B) and (C) representative images. No statistically significant differences between the groups were observed.

Tracheal lesions resulting from infection by IBV-D388 and QX vaccine are similar, but are induced earlier, more abruptly and initially more severely by the progenitor virus

To study the pathogenicity of both viruses, the tracheal histopathologic lesions were compared over time (Fig. 2). From day 2 to day 4 post infection, tracheal sections of the QX-D388 infected birds showed scattered epithelial cells with signs of cell death, marked desquamation of epithelial cells, and infiltration and exocytosis of heterophils, resulting in accumulations of both cell types in the tracheal lumen. At the same time points, the QX vaccine inoculated tracheas only showed a mild reduction of goblet cells and cilia, with few dying cells scattered through the mucosal lining. In the latter, a transition to more abundant epithelial desquamation and heterophilic infiltration was only seen from day 6 onward. From day 7 onward, tracheal changes were comparable for both groups, and included the classic IBV-induced lesions such as complete loss of goblet cells and cilia, epithelial metaplasia, and chronic mononuclear inflammatory cell infiltration throughout the mucosa and submucosa. Tracheal sections of mock-infected birds did not show any morphological changes at any time point (histologic pictures over time comparable to the infected tracheas 1 day post infection (d.p.i.) (data not shown).

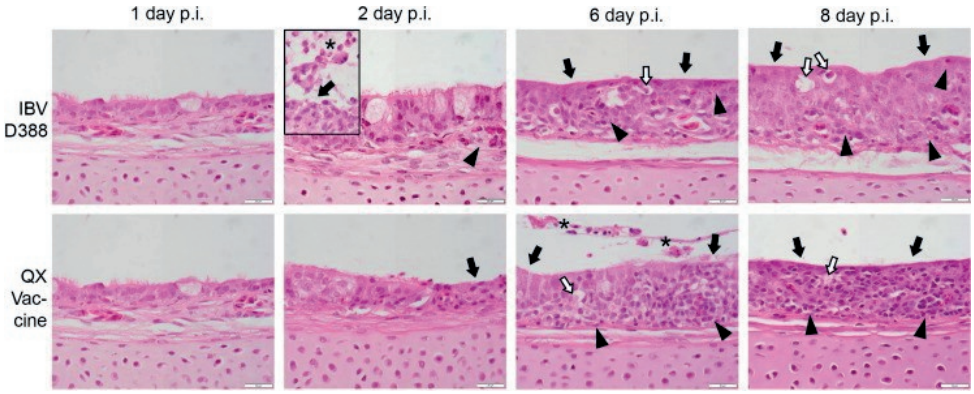

Fig. 2. Histopathological changes in trachea of experimentally infected broilers. Trachea sections were stained by H&E and evaluated for lesions by light microscopy. Lesions comprised loss of cilia and goblet cells (black arrows), vacuoles containing single dead cells (white arrows) which often show high level of viral protein expression in immunohistochemical staining (not shown), inflammatory cell infiltration (arrow heads) and epithelial desquamation and heterophil presence after exocytosis (asterisk). Inset picture IBV D388, 2 day p.i.: trachea of other than primarily-depicted animal with most prominent epithelial desquamation and heterophil presence (main picture presents average trachea on this time point regarding inflammatory cell infiltration into the tissue better).

IBV-D388 is more efficient in reaching and replicating in the kidney compared to QX vaccine

We next analysed whether there were differences between IBV-D388 and its derivative vaccine in replication in the kidney. Viral RNA from kidney tissues was quantified by qRT-PCR (Fig. 3A), showing that IBV-D388 viral RNA was present from day 3 onward and further increased on day 4 (Fig. 3A). In contrast, viral RNA titers of QX vaccine were much lower, and the titers of the two viruses were significantly different from day 4 onward. Immunohistochemical staining and quantification of viral antigen-expressing cells confirmed that the vaccine virus did not replicate significantly over time in this tissue, while clear expression of S2 protein was observed from day 4 onward in D388-inoculated animals (Fig. 3B). Viral antigen expression was only seen in renal tubular structures, often with an emphasis on the more distal tubular segments, collecting ducts and (when present in the sample) the ureter (Fig. 3C).

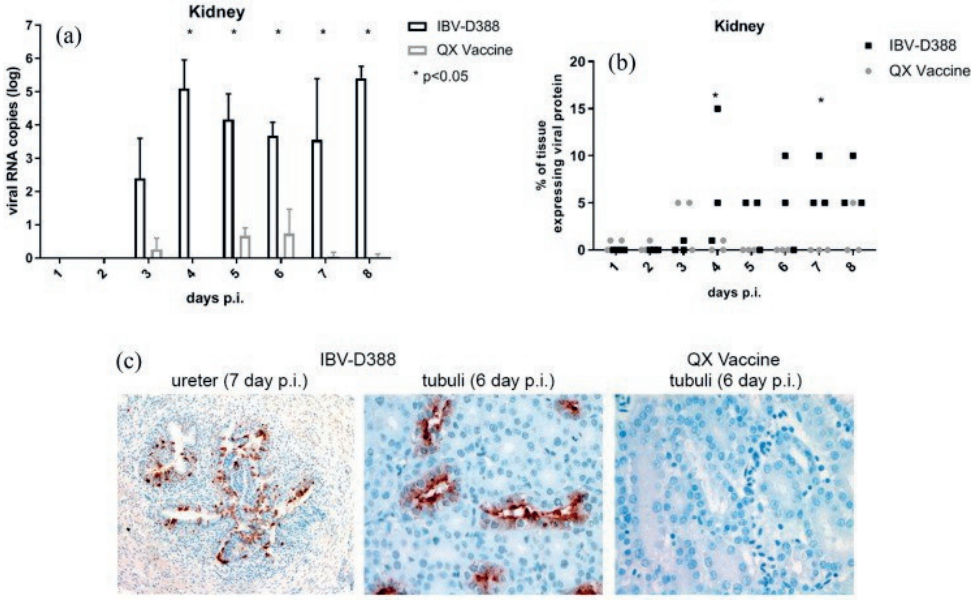

Fig. 3. IBV QX viruses in kidney of experimentally infected broilers. (A) Viral RNA was isolated from kidney tissue, and qRT-PCR was performed in duplicate. Viral titers were calculated based on a standard curve, and the mean and standard deviation of three birds are shown; (B/C) Kidney tissues were stained by immunohistochemistry using an anti-IBV antibody (C). The percentage of cells within the kidney that expressed viral proteins is depicted for each animal (B) and representative images are given (C). * $p < 0.05$.

Renal lesions are only induced upon infection with IBV-D388

Representative histological pictures of kidney for both IBV-D388 and QX vaccine inoculated birds taken at 4 and 6 d.p.i. are depicted in Fig. 4. Morphological changes could be observed in the kidneys of birds infected with IBV-D388 from 3 d.p.i. onward, with death and desquamation into the lumen of single tubular epithelial cells. Over time, visible from day 6 onwards, these cell death-defined lesions changed towards marked, mononuclear, peritubular interstitial inflammation with few remaining scattered cells showing signs of cell death throughout the tissue. Kidney sections of vaccinated birds, as well as mock-infected birds (not shown), did not show any relevant changes throughout the experiment.

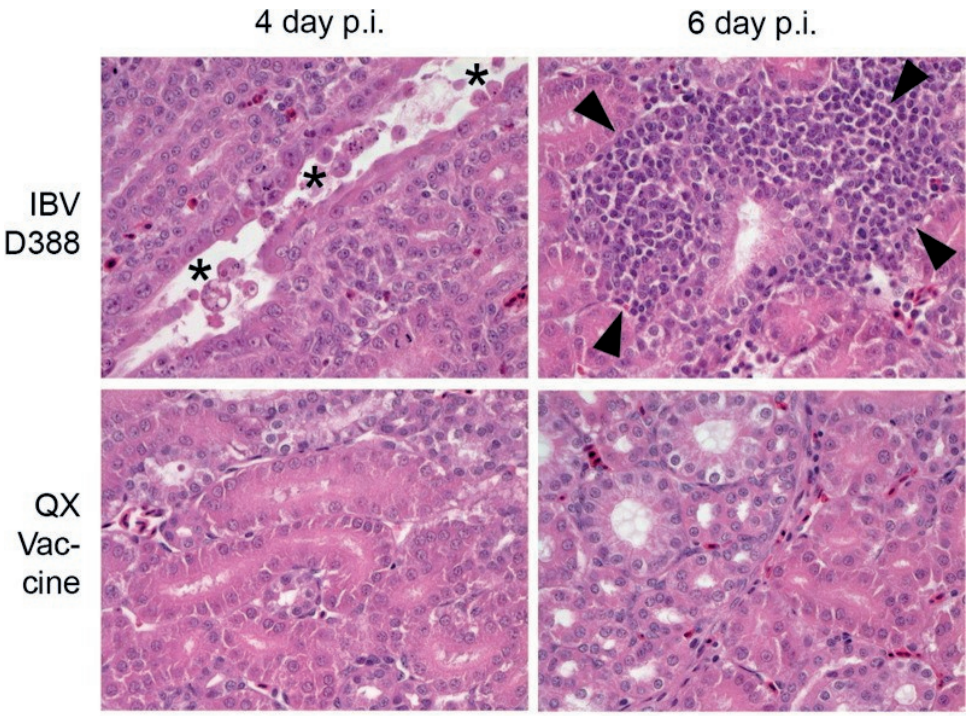

Fig. 4. Histopathological changes in the kidney of experimentally infected broilers. Kidney sections were stained by H&E and evaluated for lesions by light microscopy. Lesions included death and desquamation of single tubular epithelial cells (asterisk) and interstitial, peritubular inflammatory cell infiltration (arrow heads).

IBV-D388 reaches the conjunctivae and cloaca earlier and with higher titers than QX vaccine

To further investigate the ability of the two viruses to reach secondary target organs, we assessed the presence of viral RNA in swabs collected from the conjunctivae and the cloaca. IBV-D388 viral RNA could be detected in the conjunctivae with significantly higher titers than QX vaccine on days 1, 4, 6, 7, and 8 (Fig. 5A). In the cloaca of birds infected with IBV-D388, RNA was detected from day 2 onward with higher RNA titers observed than after QX vaccine inoculation. In the vaccine-inoculated group, viral RNA could not be detected earlier than 4 d.p.i. (Fig. 5B). Statistically significant differences in the two groups were observed at days 2 and 3.

QX can replicate in the gastrointestinal tract

To further gain insight into the dissemination of the two viruses throughout the body, we analysed GI tissues collected at days 1, 4, 7, and 8 post infection for the expression of IBV viral proteins. The number of animals expressing viral proteins in stomachs (proventriculus, gizzard), small intestines (duodenum, jejunum, ileum), large intestines (caecum, large intestinal segment connecting ileocaecal junction with cloaca) and cloaca per time point is depicted in Table 1. With exception of the proventriculus and at most time points also of the cranial small intestine (duodenum and jejunum), all tissues analysed (from caeca to cloaca mostly) support replication of IBV-D388 and its derivative vaccine.

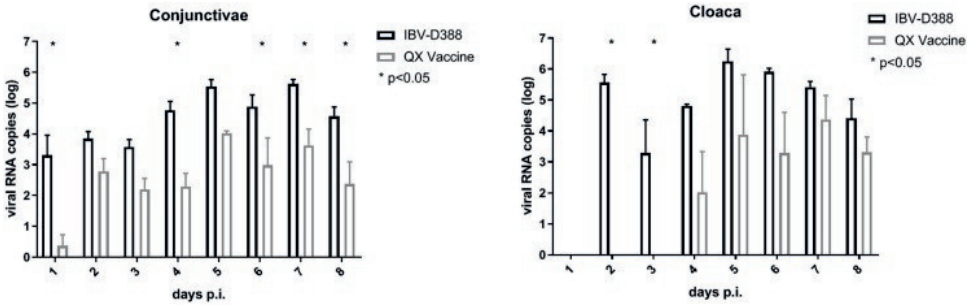

Fig. 5. IBV QX viruses in ocular and cloacal swabs. Viral RNA was isolated from swabs of conjunctivae (A) and cloaca (B) and qRT-PCR was performed in duplicate. Viral titers were calculated based on a standard curve, and the mean and standard deviation of three birds are shown. * $p < 0.05$.

However, viral protein expression was clearly more abundant and present earlier after IBV-D388 infection (4 d.p.i., compared to protein expression in comparable numbers of cells after QX vaccine only at 8 d.p.i.). In the birds' stomachs, a limited number of positive cells were observed in the gizzard, but not in the proventriculus. More detailed analysis of the cloaca indicated no statistical differences between IBV-D388 and QX vaccine regarding percentage of tissue expressing viral proteins (Fig. 6A), and comparable preferences for epithelial cells, which showed viral protein expression predominantly (Fig. 6B).

Table 1
Immunohistochemistry of gastrointestinal tract tissues of IBV-D388 and QX vaccine. The number of IBV protein positive tissues (total out of three) at 1, 4, 7 and 8 days post infection (d.p.i.). [$] Only protein expression seen in the gizzard, never in the proventriculus; [#] Very limited protein expression (approximately 10 cells or less in one or two small clusters).

Virus	days p.i.	Stomach[$]	Small intestine	Large intestine	Cloaca
IBV-D388	1	0	0	0	0
	4	0	3	3	2
	7	3	3	3	3
	8	2	2	3	3
IB Primo QX	1	0	0	0	0
	4	0	1[#]	0	1
	7	1[#]	0	0	2[#]
	8	1	2	2	2

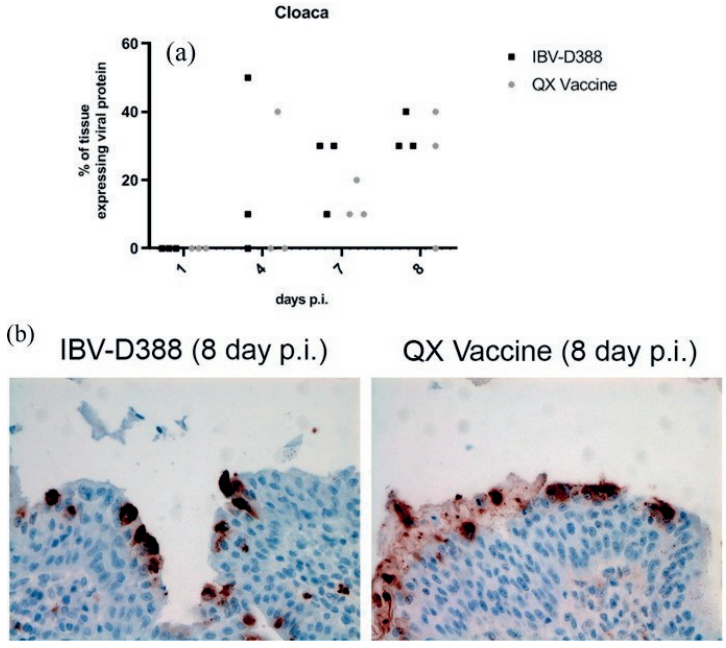

Fig. 6. IBV QX viruses in gastrointestinal tract of experimentally infected broilers. Cloaca tissues were stained by immunohistochemistry using the anti-IBV antibody. (A) The percentage of cells that expressed viral proteins is depicted for each animal, and (B) representative images are shown.

Discussion

In this manuscript, we investigated the attenuated phenotype of a commercially available IBV vaccine strain at early time points after inoculation of SPF broiler chickens. While replication of the QX vaccine was comparable to that of its virulent progenitor at the site of inoculation, the vaccine virus showed a remarkable delay of viral protein expression and lower viral RNA production in other target organs.

The ability of a virus to infect and replicate in tissues beyond the site of infection depends on the route of transport and the susceptibility of a respective organ. Since the 1960s, viremia has been proposed as one of the routes of IBV dissemination,[18] with only recent evidence for involvement of mononuclear cells in transportation of the virus throughout the body.[19,20] In our study, mononuclear cells expressing viral proteins were only rarely detected (data not shown), so it is yet unclear whether they truly contribute to IBV dissemination. In addition, virions excreted by coughing, sneezing and rales, or taken up by ingestion, can contribute to the dissemination of the virus to other organs.[1] Our observation that comparable viral RNA levels for the virulent and vaccine strains were produced in the trachea, while lower or delayed viral RNA levels for the vaccine strain were detected in the cloaca and conjunctivae, suggests that the vaccine has a lower ability to reach or to infect these tissues. It is possible, however, that part of the viral RNA came from non-infectious viral particles, as the infectious dose produced was not determined in this study. The extent to which viral shedding from the trachea contributes to the lower viral RNA titres in the conjunctivae and cloaca remains to be confirmed. Other factors, including stability of the virus in various environmental conditions, susceptibility to immune factors, or intrinsic differences between the viruses to replicate in tissues distant from the initial site of infection may play an additional role in reduced replication in secondary organs.

Kidneys from QX vaccine-inoculated animals rarely displayed signs of infection, with only a few animals showing very few virus-positive cells. Thus, attenuation of QX vaccine resulted in a virus with reduced ability to disseminate to this

tissue. This is in accordance with a previous study in which passages of a QX virulent strain in embryonated eggs showed a progressive reduction in ability to replicate in the kidneys of experimentally infected chickens.[14] Kidney lesions induced by D388 did not, however, result in clinical symptoms usually observed in cases of nephritis.[9,21,22] Clinical respiratory symptoms in both groups were mild, but comparable (not shown). As the severity of IBV clinical symptoms also relies on environmental factors, including but not limited to cold and heat stress, food additives and the presence of secondary bacterial or viral infections,[22] the severity of clinical symptoms in an experimental setting is often less than in the field.[23,24]

Finally, our data seem to suggest that an ascending route from the cloaca towards the kidney might contribute to some extent to kidney infection, as the cloaca became RNA positive at an earlier time point than the kidneys. This seems to be supported by the observation that epithelial cells of the distal tubules, collecting ducts and ureter commonly tend to show the only or more prominent viral protein expression, compared to the proximal nephron segments. Comparable observations supporting this theory were made in other studies.[24-26] The cloaca at least seems to be reached by the virus by a descending route via the gastrointestinal tract, likely after swallowing viral particles. Alternatively, the virus might reach the cloaca via an ascending process called cloacal suckling, with uptake of particles from the environment into the cloaca[27] after their excretion from, for example, airways or eyes. From this study, however, it is not clear whether such cloacal uptake of virus takes place.

Vaccines safety studies have previously shown that IBV vaccines have a reduce ability to infect target tissues;[11-13] however, this is the first study to analyse the differences in viral replication and tropism between a virulent IBV-QX field strain (IBV-D388) and the associated attenuated vaccine strain (QX vaccine). We conclude that the attenuation of the QX vaccine results in slower dissemination and lower replication ability in target tissues distant from the initial site of infection, including the kidneys, in broilers during the first week of life.

Declaration of competing interest

The authors declare that they have no known competing financial interests or personal relationships that could have appeared to influence the work reported in this paper.

Acknowledgements

We would like to thank the animal caretakers of the GD for performing the animal experimentation, the personnel of the histology laboratorium of the Department of Pathobiology for processing of the tissues, and Kim Bouwman for help collecting the samples.

Contributions and authorship

AL, EAWSW, JJdW, and MHV designed and conceived the study; JJdW provided the resources and organised the animal experimentation; AL, EAWSW, JB, JPDM, AB, GC, and MHV acquired and analysed the data; AL, EAWSW, and MHV wrote the manuscript. All authors approved the final version of the manuscript.

Funding source and competing interest

Utrecht University (Utrecht, The Netherlands) and GD Animal Health (Deventer, The Netherlands) financially supported this research. The authors have no competing interests to declare.

References

1. Cook JKA, Jackwood M, Jones RC. The long view: 40 years of infectious bronchitis research. Avian Pathol 2012;41:239–50.

2. Cavanagh D. Coronaviridae : a review of coronaviruses and toroviruses 2005:1–54.

3. Valastro V, Holmes EC, Britton P, Fusaro A, Jackwood MW, Cattoli G, et al. S1 gene-based phylogeny of infectious bronchitis virus: an attempt to harmonize virus classification. Infect Genet Evol 2016;39:349–64.

4. YuDong W, YongLin W, ZiChun Z, GenChe F, YiHai J, XiangE L. Isolation and identification of glandular stomach type IBV (QX IBV) in chickens. Chinese J Anim Quar 1998;15:1998.

5. Worthington KJ, Currie RJW, Jones RC. A reverse transcriptase-polymerase chain reaction survey of infectious bronchitis virus genotypes in Western Europe from 2002 to 2006. Avian Pathol 2008;37:247–57.

6. Valastro V, Monne I, Fasolato M, Cecchettin K, Parker D, Terregino C, et al. QXtype infectious bronchitis virus in commercial flocks in the UK. Vet Rec 2010;167:865–6.

7. Krapezˇ U, Slavec B, Rojs OZ. Circulation of Infectious Bronchitis Virus Strains from Italy 02 and QX Genotypes in Slovenia Between 2007 and 2009. Avian Dis Dig 2011;6:e60–1.

8. Abro SH, Renström LHM, Ullman K, Belák S, Baule C. Characterization and analysis of the full-length genome of a strain of the European QX-like genotype of infectious bronchitis virus. Arch Virol 2012;157:1211–5.

9. de Wit JJ, Nieuwenhuisen-van Wilgen J, Hoogkamer A, vande Sande H, Zuidam GJ, Fabri THF. Induction of cystic oviducts and protection against early challenge with infectious bronchitis virus serotype D388 (genotype QX) by maternally derived antibodies and by early vaccination. Avian Pathol 2011;40:463–71.

10. de Wit JJ, Cazaban C, Dijkman R, Ramon G, Gardin Y. Detection of different genotypes of infectious bronchitis virus and of infectious bursal disease virus in European broilers during an epidemiological study in 2013 and the consequences for the diagnostic approach. Avian Pathol 2018;47:140–51.

11. Jackwood MW, Hilt DA, Brown TP. Attenuation, Safety, and Efficacy of an Infectious Bronchitis Virus GA98 Serotype Vaccine Author (s): Mark W. Jackwood, Deborah A. Hilt and Thomas P. Brown Published by: American Association of Avian Pathologists Stable 2003;47:627–32.

12. Gelb JJ, Cloud S. Effect of serial embryo passage of an Arkansas-type avian infectious bronchitis virus isolate on clinical response, virus recovery, and immunity. Avian Dis 1983;27:240.

13. Bijlenga G, Cook JKA, Gelb J, De Wit JJ. Development and use of the H strain of avian infectious bronchitis virus from the Netherlands as a vaccine: a review. Avian Pathol 2004;33:550–7.

14. Geerligs HJ, Tarres-Call J, Stuurman BGE, Bru T, Wijmenga W, Symons J, et al. Efficacy and safety of an attenuated live QX-like infectious bronchitis virus strain as a vaccine for chickens. Avian Pathol 2011;40:93–102.

15. Laconi A, Berends AJ. de Laat ECH, Urselmann TAPMP, Verheije HM. Infectious bronchitis virus Mass-type (GI-1) and QX-like (GI-19) genotyping and vaccine differentiation using SYBR green RT-qPCR paired with melting curve analysis. J Virol Methods 2019;275.

16. Van Beurden SJ, Berends AJ, Krämer-Kühl A, Spekreijse D, Chénard G, Philipp HC, et al. A reverse genetics system for avian coronavirus infectious bronchitis virus based on targeted RNA recombination. Virol J 2017;14:1–13.

17. Brand JMA Van Den, Kreijtz JHCM, Bodewes R, Stittelaar KJ, Amerongen G Van, Kuiken T, et al. Efficacy of vaccination with different combinations of MF59- adjuvanted and nonadjuvanted seasonal and pandemic influenza vaccines against pandemic H1N1 (2009) influenza virus infection in Ferrets 2011;85:2851–8.

18. Hofstad MS, Yoder HW. Avian infectious bronchitis virus distribution in tissues of chicks. Avian Dis 1966:230–9.

19. Amarasinghe A, Abdul-Cader MS, Nazir S, De Silva Senapathi U, Van Der Meer F, Cork SC, et al. Infectious bronchitis corona virus establishes productive infection in avian macrophages interfering with selected antimicrobial functions. PLoS ONE 2017;12:1–21.

20. Reddy VRAP, Trus I, Desmarets LMB, Li Y, Theuns S, Nauwynck HJ. Productive replication of nephropathogenic infectious bronchitis virus in peripheral blood monocytic cells, a strategy for viral dissemination and kidney infection in chickens. Vet Res 2016;47:1–19.

21. Terregino C, Toffan, AnnaBeato M, Serena Beato MS, De Nardi R, Meini A, et al. Pathogenicity of a QX strain of infectious bronchitis virus in specific pathogen free and commercial broiler chickens, and evaluation of protection induced by a vaccination programme based on the Ma5 and 4/91 serotypes. Avian Pathol 2008;37:487–93.

22. Ganapathy K, Wilkins M, Forrester A, Lemiere S, Cserep T, McMullin P, et al. QX-like infectious bronchitis virus isolated from cases of proventriculitis in commercial broilers in England. Vet Rec 2012;171:597.

23. de Wit JJ, Sjaak, Cook JKA. Factors influencing the outcome of infectious bronchitis vaccination and challenge experiments. Avian Pathol 2014;43:485–97.

24. Dolz R, Vergara-Alert J, Pérez M, Pujols J, Majò N. New insights on infectious bronchitis virus pathogenesis : characterization of Italy 02 serotype in chicks and adult hens 2012;156:256–64.

25. Benyeda Z, Szeredi L, Mató T, Süveges T, Balka G, Abonyi-Tóth Z, et al. Comparative Histopathology and Immunohistochemistry of QX-like, Massachusetts and 793/B Serotypes of Infectious Bronchitis Virus Infection in Chickens. J Comp Pathol 2010;143:276–83.

26. Chen BY, Hosi S, Nunoya T, Itakura C. Histopathology and immunohistochemistry of renal lesions due to infectious bronchitis virus in chicks Histopathology and immunohistochemistry of renal lesions due to infectious bronchitis virus in chicks 2007;9457.

27. van der Sluis HJ, Dwars RM, Vernooij JCM, Landman WJM. Cloacal reflexes and uptake of fluorescein-labeled polystyrene beads in broiler chickens. Poult Sci 2009;88:1242–9.

3 Interference between avian corona and influenza viruses: the role of the epithelial architecture of the chicken trachea

E.A.W.S. Weerts [a], K.M. Bouwman [a, #], L. Paerels [a], A. Gröne [a], G.J. Boelm [b], M.H. Verheije [a]

[a] Division of Pathology, Department Biomolecular Health Sciences, Faculty of Veterinary Medicine, Utrecht University, Utrecht, the Netherlands

[b] Royal GD Animal Health, Deventer, the Netherlands

[#] *current address: Department of Population Health, Poultry Diagnostic and Research Center, College of Veterinary Medicine, University of Georgia, Athens GA, 30602*

published: Veterinary Microbiology, 2022; 272: 1-10.

Abstract

Respiratory viral infections are among the major causes of disease in poultry. While viral dual infections are known to occur, viral interference in chicken airways is mechanistically hardly understood. The effects of infectious bronchitis virus (IBV) infection on tissue morphology, sialic acid (sia) expression and susceptibility of the chicken trachea for superinfection with IBV or avian influenza virus (AIV) were studied. *In vivo*, tracheal epithelium of chickens infected with IBV QX showed marked inflammatory cell infiltration and loss of cilia and goblet cells five days post inoculation. Plant lectin staining indicated that sialic acids redistributed from the apical membrane of the ciliated epithelium and the goblet cell cytoplasm to the basement membrane region of the epithelium. After administration of recombinant viral attachment proteins to slides of infected tissue, retained binding of AIV hemagglutinin, absence of binding of the receptor binding domain (RBD) of IBV M41 and partial reduction of IBV QX RBD were observed. Adult chicken trachea rings were used as *ex vivo* model to study the effects of IBV QX-induced pathological changes and receptor redistribution on secondary viral infection. AIV H9N2 infection after primary IBV infection was delayed; however, final viral loads reached similar levels as in previously uninfected trachea rings. In contrast, IBV M41 superinfection resulted in 1000-fold lower viral titers over the course of 48 hours. In conclusion, epithelial changes in the chicken trachea after viral infection coincide with redistribution and likely specific downregulation of viral receptors, with the extend of subsequent viral interference dependent on viral species.

Highlights

Infectious bronchitis virus (IBV) induces sialic acid redistribution in the trachea.

Previous IBV infection changes influenza virus and IBV attachment protein binding.

Adult chicken tracheal organ cultures (TOCs) provide a suitable *ex vivo* model.

Primary IBV infection hampers influenza virus less than secondary IBV infection.

Keywords

chicken – trachea - dual infection - viral interference - avian corona virus - avian influenza virus

Introduction

In the poultry industry, respiratory viral infections have extensive impact on animal welfare and major economic consequences. Two important viruses infecting chicken airways are avian infectious bronchitis virus (IBV) and avian influenza virus (AIV). IBV belongs to the family *Coronaviridae* and many distinct IBV variants circulate worldwide.[30] The virus causes highly contagious, though usually mild respiratory disease and egg production drops and can, depending on the viral variant, induce renal damage.[9] AIV belongs to the *Orthomyxoviridae* family and comparable to IBV, the group of low pathogenic avian influenza viruses (LPAIV) clinically cause mild respiratory symptoms, loss of egg production and growth reduction.[12,28]

IBV and LPAIV both target chicken tracheal epithelial cells via binding to α2,3-linked sialic acid (sia) receptors on the cell surface.[1,20,35] The viral attachment protein of IBV, spike (S), binds a limited set of glycans containing a terminal α2,3-sia, while the viral attachment protein of AIV, haemagglutinin (HA) can bind to a wider range of glycans containing terminal α2,3-sia. More specifically for IBV variants, the receptor-binding domain (RBD) of IBV prototype variant M41 was revealed to bind to Neu5Acα2-3Galβ1-3GlcNAc (Neu5Ac),[1] while the RBD of IBV QX, a nephropathogenic IBV variant, was demonstrated to bind to another, yet unresolved, host sia.[6] IBV and LPAIV infections both cause epithelial cell death with subsequent tracheitis and both viruses are normally shed from the infected mucosa over several days.[5]

Dual infections with a virus and bacteria are frequently reported in chicken, but also dual infections with two viruses[28] and even multiple infectious agents[13,15] are known to occur. Several studies have reported higher susceptibility for secondary respiratory bacterial infections after infection with IBV, AIV, Newcastle disease virus or avian metapneumoviruses.[16,34] In addition,

immunosuppressive viruses like the chicken anemia virus also can predispose for secondary infections.[11] Disease resulting from such dual infections is usually more severe than disease resulting from infection by the individual pathogens separately.[5,14] Mechanisms underlying virus-induced susceptibility for bacterial disease have been investigated quite extensively in several species,[26] but despite the many proposed underlying mechanisms of virus-virus interactions,[18] disease mechanisms behind infection with two viruses have only been studied occasionally and seldom within the topic of chicken respiratory disease.

To understand the role of underlying tissue changes during sequential dual infection with two viruses, the present study evaluated the effect of a primary IBV infection on susceptibility of the chicken tracheal epithelium for superinfection with another IBV variant and AIV by making use of an *ex vivo* chicken tracheal tissue explant model.

Materials and methods

Inoculum

IBV variants QX (D388) and M41 were kindly provided by Royal GD (Deventer, the Netherlands). Avian influenza virus (AIV) strain H9N2 (A/Chicken/Saudi Arabia/SP02525/3AAV/2000), G1-W lineage was kindly provided by C. Jansen, Faculty of Veterinary Medicine, Utrecht University. All three viruses were titrated for infectivity via *in ovo* method in specific pathogen-free (SPF) chicken eggs by determination of the 50% egg (embryonic) infectious dose (EID_{50}) / ml at 7 days post inoculation (dpi).[24]

In vivo experiment design

Six-week-old SPF layer chicken were inoculated by eyedrop with 10^4 EID_{50} IBV QX (D388, Royal GD, Deventer, the Netherlands). At 5 dpi, chickens were euthanized, tracheal samples were collected and immediately fixed in 4% formalin. The experiment was conducted according to the Dutch national regulations on animal experimentation and approved by the Animal Experimentation Committee (DEC, approval number 2015-278).

Ex vivo chicken tracheas cultures

Trachea organ cultures (TOCs) were obtained from tracheas from either 19-day-old embryos (no DEC permission required) or from approximately one-year-old commercial layer hens, kept for experimental and veterinary teaching purposes (DEC approval number AVD108002016642-1, Faculty of Veterinary Medicine, Utrecht University). Embryonic and adult tracheas were flushed three times with warm (30-35° C) PBS, cut into 2-3 mm thick rings and microscopically evaluated for ciliary movement. TOCs were transferred individually to sterile 15 ml tubes (Greiner Bio-One, Germany) with punctured lids allowing gas exchange, and containing Dulbecco's Modified Eagle Medium (DMEM, Thermofisher, US) with 250U/ml penicillin and 250 µg/ml streptomycin (Gibco, US). Incubation was performed in a slowly rotating incubator (with approximately 36 rotations/hr) at 37.5° C and 30-40% humidity for 24 hrs before inoculation.

Design trachea organ culture infection experiments

For single infections, TOCs were incubated in 2 ml DMEM in the presence or absence of 10^5 EID_{50} IBV QX/ml for 2 hrs (t=0). After rinsing three times with PBS, TOCs were transferred to DMEM containing antibiotics, incubated for 24h intervals, and ciliary movement was evaluated before fixation in 4% formalin. In the superinfection experiments, 48 hrs after the initial infection with IBV QX the TOCs were incubated for 2 hrs in 2 ml DMEM containing either 10^5 EID_{50} IBV M41 or LPAIV H9N2 /ml. The 48 hr interval was based on results from validation experiments with the TOC model as described in the results section of the current study. After rinsing three times, TOCs were transferred to DMEM containing antibiotics and incubated as previously described. Superinfection of infected TOCs with IBV QX was not included, due to the inability to technically distinguish between viral genomes generated after the primary (QX) and secondary (QX) infection. Culture supernatant was collected for RT-qPCR and TOCs were fixed in formalin for morphologic evaluation in three-fold (n = 3) per infection group at 24 hr intervals. In addition, culture medium was collected directly after initial (t=2 hpi) and sequential (t=50 hpi) infection. Design for the superinfection experiment is summarized in Figure 1, panel A.

Histopathology

Trachea samples were fixed for 24-48 hrs in 4% formalin and subsequently embedded in paraffin. From each trachea collected from the *in vivo* infection experiment, serial slides were cut and stained with hematoxylin & eosin (HE) or periodic-acid Schiff (PAS) according to standard laboratory procedures. Stained tissue slides were examined using a light-microscope to study epithelial morphology (HE) and presence of mucus-producing mucosal goblet cells (PAS). For TOCs from the *ex vivo* experiments, HE stained tissue slides were used to evaluate mucosal morphology over time.

Immuno- and lectin histochemistry

Serial tissue slides from *in vivo* and *ex vivo* infected tracheas were analyzed for the presence of IBV antigen using a mouse monoclonal antibody (mAb) against IBV S2 as described before.[32] To evaluate presence of AIV antigen, tissue slides were incubated with a mouse mAb against influenza virus nucleoprotein (HB65) (ATCC, US) diluted 1:100 in PBS at room temperature (RT) for 60 min after previous deparaffinization, antigen retrieval with 0.1% Protease 14 (Sigma PSM7, Germany) at 37° C for 10 min, endogenous peroxidase activity blocking with 1% hydrogen peroxide in methanol at RT for 30 min and treatment with normal goat serum diluted 1:10 in PBS at RT for 15 min. Specific mAb binding was visualized with Envision goat anti mouse (DAKO Cytomation, Denmark) and the chromogen amino-ethyl carbazole (AEC) (DAKO Cytomation, Denmark) and the tissue counter-stained with hematoxylin.

To visualize presence of α2,3-linked sialic acids, lectin histochemical staining was performed using the *Maackia amurensis* Lectin I (MAL I) (Vector Laboratories Inc, US) as published[23] (adapted Ambepitiya Wickramasinghe et al., 2011). Binding of MAL I to the tracheal was semi-quantified for three regions within the epithelial lining: 1) apical (ciliated) membrane; 2) goblet cells; 3) basal membrane. For this purpose, tracheal rings were visually split in ten equal circumferential parts and per tenth part the percentage of stained cells per region was estimated in ten percent steps (10, 20, 30% etc). The sum of the ten

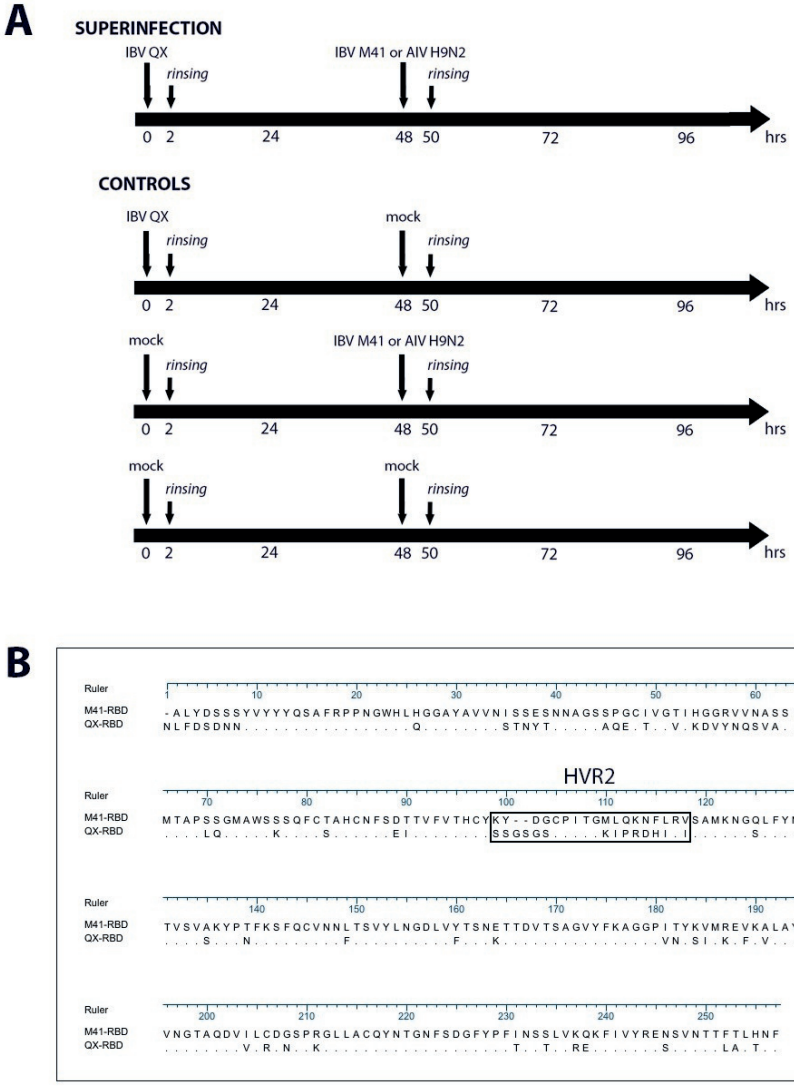

Fig. 1. Schematic presentation of the dual infection experimental design and Alignment of the amino acid sequences of the recombinantly produced IBV receptor binding domains (RBDs) used for viral protein histochemistry. Trachea organ cultures (TOCs) were incubated for 2 hrs with IBV QX, followed 48 hrs later by incubation for 2 hrs with either AIV H9N2 or IBV M41. As controls, TOCs were either initially or secondarily or both times mock-infected by administration of DMEM only without virus. Culture medium samples were taken at a 24hr interval and 2hrs after incubation with virus to define numbers of viral RNA copies over time. TOCs were fixed in formalin and studied microscopically for morphology and receptor distribution (Panel A). Alignment of the IBV QX and M41 amino acid sequences, the box highlights hypervariable region 2 (HVR2) that contains the differences responsible for alternative binding to receptor determinants, as published by Bouwman et al, 2020.

areas was divided by ten to obtain a mean percentage of stained cells per region per trachea.

Protein histochemistry

The receptor binding domains (RBD) of the spikes of IBV M41 and IBV QX, and the hemagglutinin (HA) of AIV H5N1 were produced as described before and recombinant proteins were applied to tissues in protein histochemistry assays as published.[1,6] Alignment of amino acid sequences of the IBV M41 and QX RBDs is presented in Figure 1, panel B (previously published by Bouwman et al., 2020). Neuraminidase pretreatment of tissues was performed using neuraminidase from *Arthrobacter ureafaciens* (AUNA) (Sigma, Germany) as previously published.[6] In anticipation of the use of H9N2 as LPAIV strain in subsequent laboratory infection experiments, several attempts were made to recombinantly produce H9 and comparably allow binding to trachea slides, but this was repeatedly without success (data not shown).

RT-qPCR

RNA was isolated from supernatant using the QIAamp Viral RNA Mini Kit (Qiagen, Germany). Next, one-step RT-qPCRs were used to semi-quantitatively assess viral loads using the iTaq universal SYBR Green one-step kit (Bio-Rad Laboratories, USA). Primers were constructed and obtained (Biolegio, The Netherlands) and the primer sets to detect each virus are listed in Table 1. While the primer set directed against IBV M41 does not detect IBV QX,[32] primers directed against QX also can amplify M41 genomes.[7] The RT-qPCR reactions were carried out in a Bio-Rad CFX Connect real-time PCR system, starting with

Table 1. Primers used for RT-qPCR

		forward primer	
virus	name	sequence (5'-3')	reference
IBV QX	GU391	GCT TTT GAG CCT AGC GTT	Callisson et al. 2006
IBV M41	IBV-RdRp.F41	CAT GCA GTT TGT TGG AGA TCCT	van Beurden et al. 2017
AIV H9N2	IAV M25	AGA TGA GTC TTC TAA CCG AGG TCG	Spackman et al. 2002
		reverse primer	
virus	name	sequence (5'-3')	reference
IBV QX	GL533	GCC ATG TTG TCA CTG TCT ATT G	Callisson et al. 2006
IBV M41	IBV-RdRp.R41	GTG ACC TGG TTT TAC CGT TTG A	van Beurden et al. 2017
AIV H9N2	IAV M124	TGC AAA AAC ATC TTC AAG TCT CTG	Spackman et al. 2002

10 min at 50°C and 1 min at 95°C, followed by 40 cycles of 10s at 95°C and 30s at 60°C, and ending with a dissociation step for the determination of the melting point of the obtained PCR fragment. Serial dilutions of viral stocks of known titer were taken along to determine the viral quantity.

Statistical analysis

Semi-quantified MAL I distribution on tracheal tissue slides was analyzed with the Mann-Whitney U test.

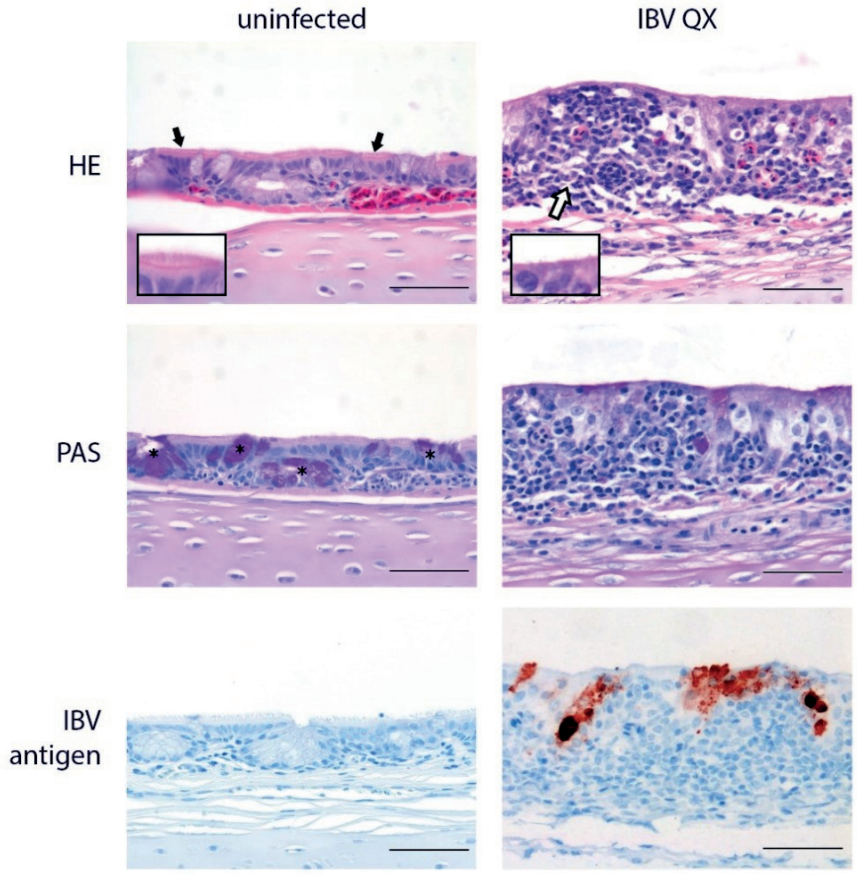

Fig. 2. IBV QX-induced epithelial changes of the chicken trachea *in vivo*, 5 dpi. Chickens were inoculated by eyedrop with IBV QX and euthanized at 5 days post inoculation. Tracheal samples were microscopically analyzed after hematoxylin and eosin (HE) (upper panels) and PAS (middle panels) staining. Viral protein expression was visualized with a monoclonal antibody against IBV S2 (lower panels). Scale bars: 50 µm; black arrows: ciliated epithelial cells, white arrows: inflammatory cells; asterisks: goblet cells; insets in upper panels: presence and loss of cilia at the apical membrane.

Results

IBV infection results in tracheitis with loss of cilia and goblet cells

To characterize detailed histopathological changes induced by IBV in detail, chickens were inoculated with IBV QX and at 5 dpi tracheas were collected. After IBV infection, the tracheal epithelium was markedly thickened due to hyperplasia and inflammatory cell infiltration and cilia were no longer present (Fig. 2, upper panels). PAS-staining highlighted that goblet cells were almost completely absent (Fig. 2, middle panels). Viral protein expression was regularly observed in epithelial cells (Fig. 2, lower panels).

IBV infection induces changes in the tracheal α2,3-linked sia distribution

Next, lectin histochemistry was performed using MAL I to visualize α2,3-linked sia. MAL binding in the IBV-infected chicken trachea was redistributed from mainly the apical membrane of the ciliated cells and the cytoplasm of some of the goblet cells to the cells of the basement membrane region of the mucosa. MAL-binding at the apical membrane and goblet cells was largely lost (Fig. 3). Staining of both the apical membrane and the mucosal glands statistically significantly decreased from on average 40% to 10% or less after infection. The percentage of cells stained in the basal region, albeit with rather large variation between trachea rings, on average statistically significantly increased from 10% to approximately 40%.

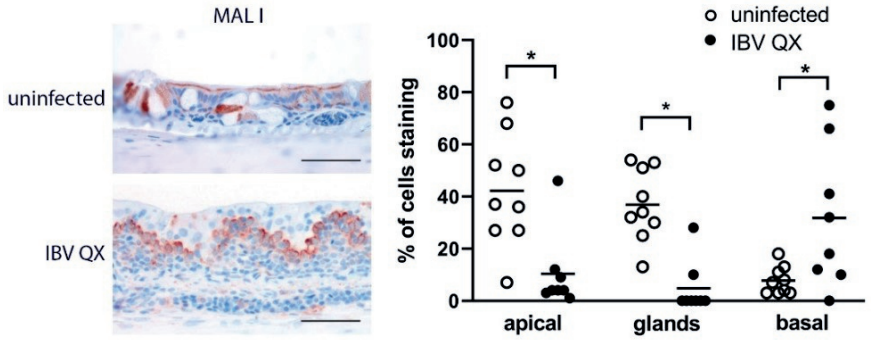

Fig. 3. α2,3-linked sia receptor distribution after IBV QX infection. Slides of infected and uninfected tracheas were stained using the *Maackia amurensis* Lectin (MAL) I. The percentage of cells stained per region were quantified (graph) as described in Materials and Methods and representative examples of MAL I stained tracheas are shown (photo panels). Scale bars: 50 µm. Significant differences ($P < 0.05$) indicated with an asterisk.

Binding of IBV RBDs, but not AIV HA, to IBV QX-infected trachea was partially or completely lost.

To study whether the observed lectin redistribution was predictive for altered viral protein attachment, and therefore viral receptor expression in the IBV-infected trachea, IBV spike RBDs and AIV HA were administered to the previously *in vivo* IBV QX-infected tracheas. AIV H5 bound to the apical membrane of the ciliated epithelial cells and regularly to the cytoplasm of goblet cells in the uninfected trachea. In the previously IBV QX-infected trachea,

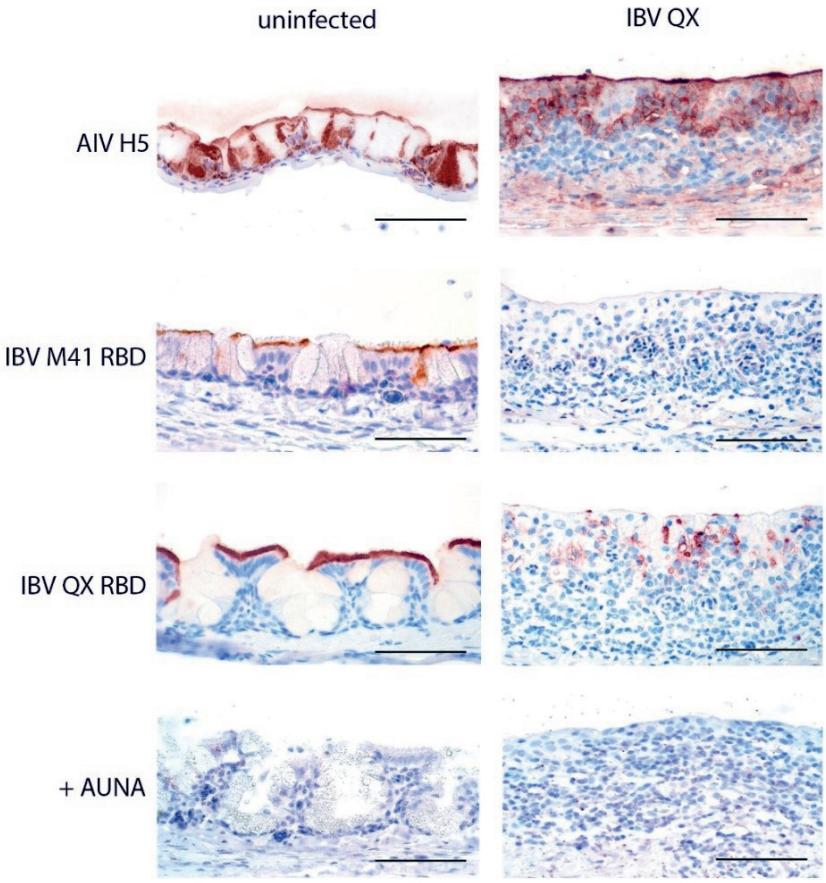

Fig. 4. Viral protein histochemistry on non- and IBV QX-infected chicken trachea. Recombinant viral attachment proteins H5 of AIV (upper row panels) and the RBDs of IBV M41 (second row panels) and QX (third row panels) were incubated onto tissue slides of paraffin-embedded uninfected (left column) and IBV QX-infected (right column) trachea. Binding was visualized using chromogen substrate AEC. All protein binding was dependent on sia presence, since binding of all proteins was lost after neuraminidase (AUNA) pretreatment of the tissue (lowest row panels). Scale bars: 50 µm.

binding to the apical membrane was still clearly present but binding was additionally observed prominently to the basal cell layers (Fig. 4, upper row panels). On uninfected trachea, RBDs of both IBV M41 and QX bound to the same locations in the epithelium as described for AIV HA, albeit with a lower avidity to the goblet cells. In the previously IBV QX-infected trachea, binding of IBV M41 RBD was almost completely lost (Fig. 4, second row panels), while IBV QX RBD binding was markedly diminished and observed only in a faint and scattered pattern in the basal cell layers and seldom at the apical membrane (Fig. 4, third row panels). Pretreatment of tissue slides with *Arthrobacter ureafaciens* neuraminidase resulted in loss of detectable binding for all viral attachment proteins, indicating that binding of the viral attachment proteins was dependent on the presence of sialic acids on both non- and previously IBV-infected trachea (Fig. 4, lowest row panels).

Histomorphological changes in adult chicken tracheal organ cultures (TOCs) are comparable to those in tracheas of in vivo infected chicken.

To further study whether the observed viral protein attachment was predictive for viral interference during dual infection, TOCs were first validated as *ex vivo* model by studying epithelial integrity in the course of time. Histomorphological analysis of TOCs from 19-day-old embryonic chicken, which are often used in IBV research (Winter et al., 2008), revealed that the mucosa was very thin compared to that of the adult chicken trachea and had only few single goblet cells and seldom glandular goblet cell clusters (Fig. 5A, mock-infected). Furthermore, ciliary movement of embryo-derived TOCs often diminished rapidly after incubation (not shown) and extensive loss of intact epithelium already occurred 24 hrs after IBV infection (Fig. 5A, infected). This together rendered embryonal TOCs unsuitable for the purpose to study viral interference over time.

Next, TOCs from adult chickens were collected and initially cultured up to 72 hrs. The mucosa was morphologically stable for the complete studied time period and resembled the tracheal mucosa of birds sampled directly after euthanasia (Fig. 5B, mock-infected). IBV QX infection resulted in loss of most of the

cylindrical epithelial cells, cilia and goblet cell clusters and these changes dominated the TOC morphology from 48 hpi onwards. In addition, MAL staining confirmed that at this similar time point (48 hpi) the α2,3-sia distribution resembled the redistributed pattern observed in tracheas collected from *in vivo* IBV QX-infected birds, with loss of staining of the ciliated apical surface and goblet cells and increased staining in the basal cell region (Fig. 5B, infected). In IBV QX-infected TOCs, viral protein expression was observed over the course of infection, starting from 24 hpi.

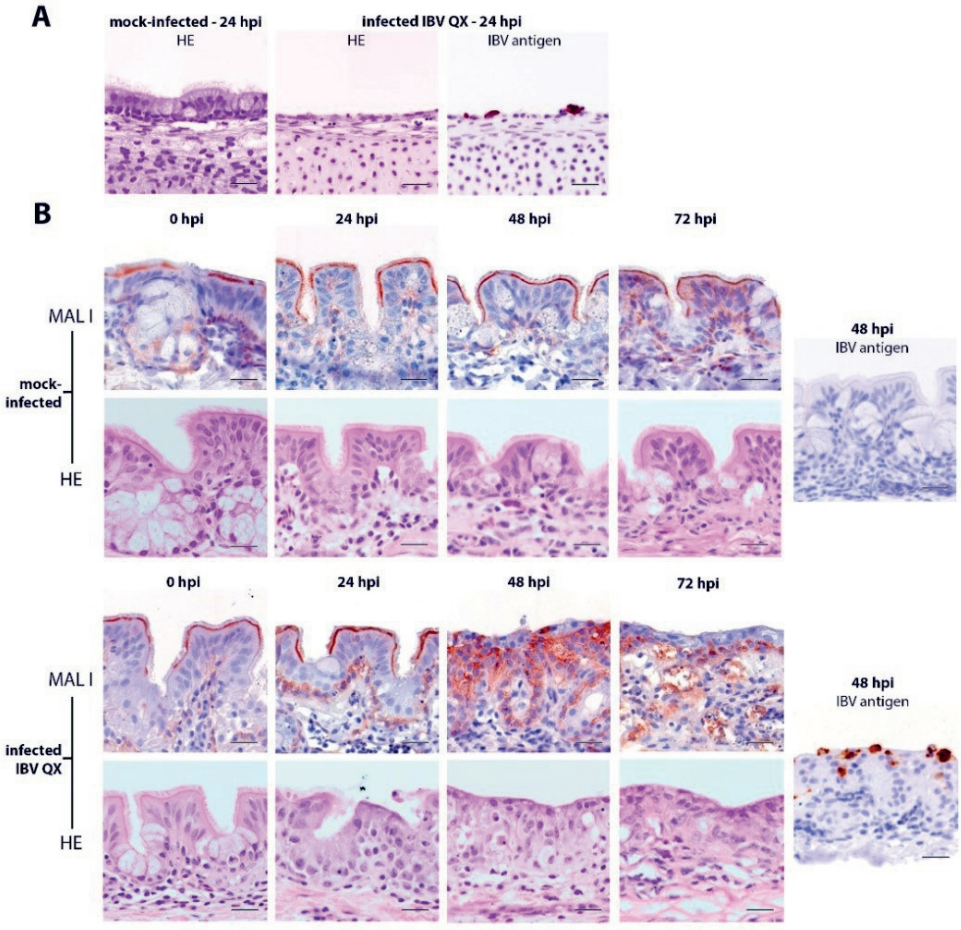

Fig. 5. Analysis of epithelial morphological integrity of *ex vivo* TOCs. Tissue slides of tracheas isolated from chicken embryos (A) or adult chicken (B) were microscopically analyzed for tissue integrity before and during *ex vivo* culture. TOCs were fixed at 24 h intervals and stained with HE, MAL I and anti-IBV S2 monoclonal antibody.

Replication of super-inoculated AIV after primary infection with IBV QX was delayed, while that of IBV M41 was markedly reduced.

Viral growth kinetics of IBV QX-infected tracheas for subsequent secondary viral infection were assessed up to 96 hpi in the validated *ex vivo* TOC model, with dual infection with either IBV M41 or AIV H9N2 induced at 48 hrs after the primary IBV QX infection (Fig. 6, graphs). At 48 hpi after the initial inoculation with IBV QX, the infection had resulted in 10^6 IBV QX genomes/ml. After removal of this initial culture medium before superinfection and subsequent rinsing of the TOCs after the two hour time course of superinfection with the second virus (t=50 hpi), IBV QX viral loads dropped more than 100-fold.

When AIV was inoculated as second virus on these TOCs pre-infected with IBV QX (Fig. 6, left graph), viral RNA production of AIV at 24 hpi (time point 72 hpi for the complete infection sequence) was first delayed when compared to AIV that replicated on control TOCs that were not preinfected (< 10-fold increase in IBV QX infected TOCs compared to a 10^5-fold increase in uninfected control TOCs). At 48 hpi (time point 96 hpi in the complete infection sequence), however, no differences in AIV viral titer were detected after replication in IBV QX pre-infected TOCs and non-pre-infected control TOCs (both 10^9 EID_{50} / ml). In contrast, when IBV M41 was inoculated as the second virus on TOCs pre-infected with IBV QX (Fig. 6, right graph), viral load of IBV M41 only increased a 1000-fold over the whole 48 hrs time course, while a 10^7-fold increase could be observed during this period in control TOCs that were not pre-infected with IBV QX. In the presence of either IBV M41 or AIV H9N2, new viral genomes of IBV QX were both produced in comparable quantities.

Completely uninfected control TOCs retained their mucosal morphological integrity up to the end of the experiment (Fig. 6A), while IBV QX-inoculated TOCs presented with loss of normal epithelium, cilia and goblet cells from 48 hpi onwards (Fig. 6B), which coincided with viral protein expression (Fig. 6C) and was associated with MAL redistribution (Fig. 6D) as expected based on the previously observed *in vivo* and *ex vivo* binding patterns. Upon sequential infection, neither IBV M41 nor AIV H9N2 induced additional morphologic tissue changes compared to TOCs infected with IBV QX only. Viral protein expression

in superinfected TOCs was observed over time after both inoculation with IBV M41 (Fig. 6E,F) and AIV H9N2 (Fig. 6G,H).

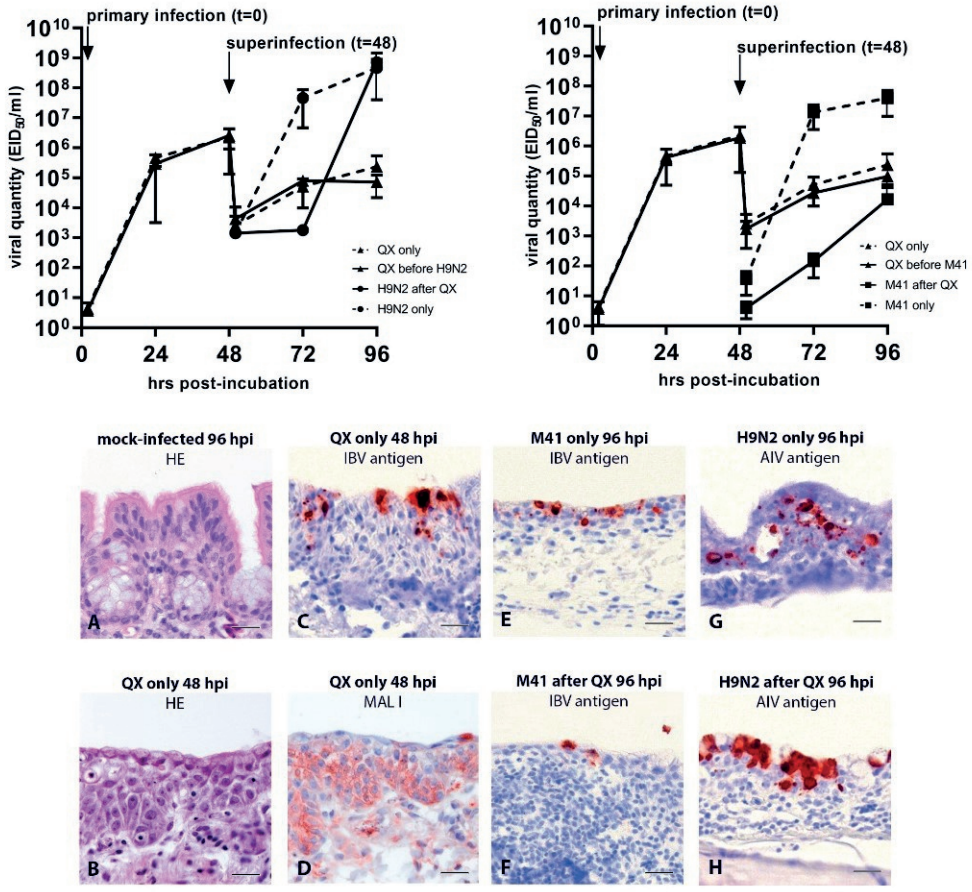

Fig. 6. Viral RNA loads after infection and dual infection of TOCs. TOCs were incubated (t=0) with IBV QX or virus-free medium for 2 hrs after which the inoculum was washed away (t = 2 hpi). At t = 48, TOCS were incubated with H9N2 (left graph) or IBV M41 (right graph); some control TOCS again only received virus-free medium. Culture supernatant was harvested at 24 h intervals after start of incubation throughout the experiment up to 96 hpi and after rinsing upon viral incubation (t = 2 and t = 50 hpi). Viral RNA loads in the culture supernatant were determined after RNA isolation and RT-qPCR using virus-specific primers (table 1) as described in Materials and Methods. Tissue morphology, MAL I binding and viral protein expression were evaluated during the experiment and shown for critical time points (panels A-H).

Discussion

Infectious bronchitis virus-induced tracheitis with loss of cilia and goblet cells is associated with varying epithelial susceptibility for secondary viral infections. Morphologic epithelial changes coincided with sia redistribution and change of binding of viral attachment proteins to the different epithelial regions with clear reduction of IBV protein binding. The extent of reduction of binding varied per virus and viral interference *ex vivo* on the studied parameters was more abundant between the two IBV variants than between IBV and AIV.

Using an *ex vivo* tissue explant model (TOCs), tracheal susceptibility differences for two important avian respiratory viral infections after an initial IBV infection were revealed. After a short delay of AIV replication following IBV pre-infection, viral titers reached similar levels to previously non-infected TOCs, while titers of IBV M41 remained much lower during the total incubation period. Previous studies on viral interference between IBV strains and AIV have only focused on sequential infection with the reciprocal virus and not with the same viral species. Both *in vivo, in ovo*, and *in vitro* (cell cultures), superinfection resulted in reduction of viral titers of the initial inoculated virus; in contrast, no effect on the replication of the second virus was observed, regardless which of the two viruses was initially and which secondarily inoculated.[2,25] The current data demonstrate that replication of a second inoculated virus can get hampered, though, when both the initial and second virus belong to the same virus species. The observed loss of binding of IBV M41 RBD to the previously IBV QX-infected trachea in the protein histochemistry assay suggests that the hampered replication of IBV M41 in the TOC model is likely at least partially the result of loss of ability to bind to the epithelial surface. Considering in addition the observed binding of IBV QX RBD and AIV HA to the IBV QX-infected trachea, this effect seems to be different per virus. These observations might indicate an underlying epithelial antiviral mechanism based surface receptor molecule reduction that varies for different viruses, which could possibly be regulated by an interplay between different cytokine and interferon types[22] or result from specifically induced host sialidase activity,[31] rather than a virus-aspecific

mechanism mostly based on competition for the same susceptible cells, as concluded in one of the previous studies.[25]

As mentioned above, the reduced tissue susceptibility for a virus after exposure to another virus in this study appears to be likely at least partially the result of loss of ability to bind to the epithelial surface. Results from the lectin histochemistry assay demonstrate that this loss of binding coincides with localized downregulation and redistribution of α2,3-linked sia in the epithelial layer**.** Simultaneously with this change of sia expression, the epithelial layer undergoes extensive loss of cilia and goblet cells, which also consistently could be observed in the TOC model. IBV-induced epithelial lesions in the chicken trachea are known to progress over time via three stages,[10] respectively a phase of degeneration (1-2 dpi), a phase of hyperplasia (up to 4-6 dpi) and a phase of recovery (up to 10-20 dpi). Based on the observed lectin binding pattern, α2,3-linked sia receptors seem to be downregulated on the surface of the unciliated stratified epithelium that replaces the normal columnar ciliated epithelium during the so-called hyperplastic phase. This could mainly result from non-specific temporary replacement of infected susceptible epithelial cells by unsusceptible cells. Alternatively, this might imply that the epithelial cells at the surface during the hyperplastic phase specifically downregulate receptors, potentially as defense mechanism to terminate further infection. During this process, infected epithelial cells might influence other, yet uninfected, adjacent epithelial cells via antiviral responses, for example interferon activity, as was likely observed during H5N1 infection in another study.[33] In contrast to the epithelial surface, the basal cells during the hyperplastic phase present with increased sia expression on their cell membrane. These cells, that in the recovery phase accomplish reconstruction of the initial epithelial architecture via proliferation, might very well re-express α2,3-linked sia early during differentiation into new ciliated and mucus-containing cells. However, since these cells are not exposed on the epithelial surface under *in vivo* circumstances, released virus progeny that is present in the tracheal lumen is not able to bind to these cells. In relation to these considerations, it needs to be emphasized that the lectin and protein histochemistry assays are performed on transversal cut sections of the trachea, during which cells, for example the mucus-containing

goblet cells, get cleaved. This mucus is known to contain many sia molecules[8] and during the histochemistry assays, this cleaved surface is artificially exposed to the administered proteins, which explains cytoplasmic binding in addition to the apical membrane binding that would occur *in vivo*.

Observations from the viral protein histochemistry assays point out that redistribution of host factors induced by one virus can have various effects on the binding of viral attachment proteins of other viruses, with complete loss of the IBV M41 receptor, partial loss of the IBV QX receptor and at least partial redistribution of AIV-H5 host attachment factors when IBV QX is the primary infecting virus. The difference in binding ability of QX and M41 RBD is likely influenced by the fact that the QX RBD binds to another, yet undetermined sia due to slight amino acid differences.[6] Based on the protein binding assay, this molecule apparently also gets redistributed, but not completely downregulated similar to that of M41. The marked difference between the binding of AIV HA and IBV RBDs can likely be explained by the fact that AIV HA binds with general higher avidity to a broader set of tissue surface glycans than the IBV spike.[1] This fact in addition likely explains the phenomenon that AIV in the *ex vivo* TOC-experiments seemed to present more rinsing-resistant after 2 hrs incubation than IBV, following administration of similar viral quantities. It would have been interesting to compare the present results with tissues that would have received AIV as primary virus, but unfortunately no *in vivo* AIV infected tracheas could be obtained for comprehensive analysis of morphology, inflammatory changes and protein binding to compare with the *in vivo* IBV QX-infected tracheas. Reduced sia expression after AIV infection is supported by other work,[33] but the extent and exactly involved glycans were not further addressed and might also vary per AIV variant. In the case that AIV, in line with its general broader range of glycan targets, as primary infecting virus would reduce expression of glycans more widely than IBV, binding of IBV variants potentially could very well get influenced and probably reduced; however, this remains highly speculative and needs to be elucidated in future studies.

While several fundamental mechanisms of viral interference have been discovered and suggested,[18] interference during respiratory disease specifically has been studied only to a limited extent. In contrast, mechanisms behind

interference of a primary viral respiratory infection on secondary bacterial infection, which generally leads to aggravation of the resulting lesions and clinical disease, have been repeatedly investigated for several species, including humans.[26] In chickens, such interference is well known in respiratory colibacillosis.[21] There, pivotal roles for the epithelium have been shown by for example the observation that viral infection can increase bacterial adherence to infected cells.[3] In addition, viruses dysregulate antibacterial immune responses, which are partially induced and mediated by the epithelium.[4,26] Such dysregulation enhances the ultimate clinical disease and it is likely that similar mechanisms and disease-aggravating effects also play a role during interference of two viruses. In the case of a dual viral infection, the primary virus might influence the entry efficiency of a secondary virus when viruses target the same cells. Based on the results from the current study, it could be possible that primary IBV QX infection in addition to decrease of IBV M41 binding to the cell surface also has a negative effect on IBV M41 entry. Such effect might potentially also explain the observed delay in AIV H9N2 infection in the TOC-model. The entry process, however, has in the current work not specifically been studied and these considerations therefore also remain speculative.

Finally, the observed epithelial changes and receptor distribution are of major importance for understanding possible viral interference with regard to vaccine efficacy, in particular when using live attenuated viruses. Although such vaccines usually induce fast protection and cause limited damage of host cells,[19] the current results show that adequate vaccine virus infection and thus induction of immunity might under certain circumstances be hampered when birds are suffering already from a potentially subclinical viral infection. Vice versa, vaccination with an attenuated virus might also change susceptibility for infection with simultaneously circulating field strains and predispose for a different, probably even more severe clinical outcome. In one study that involved IBV and AIV variants, neither seemed to occur,[25] but the current results show that both effects may only occur when viruses are of similar species. Such events could under certain circumstances probably explain vaccine failure.[27] Translation of the current results to potential clinical effects of dual viral infection *in vivo* should be done with restriction, though, since clinical effects

will also be influenced by inflammatory and immune responses that could not be simulated within the TOC-model. Based on recent *in vivo* work,[17] a dual infection with first IBV and subsequent AIV indeed seems to induce more severe clinical illness associated with an enhanced inflammatory response, but since no sequential IBV infections or receptor binding were studied, comparison remains difficult. In the end, our results nevertheless seem to stress that extra caution might be needed when considering vaccination against viral disease in a bird flock, that is thought to suffer from previous disease potentially caused by a related viral species, even when clinical symptoms are only very mild.

Conclusion

Epithelial changes in the chicken trachea after IBV infection coincide with redistribution and specific downregulation of viral receptors of IBV variant and AIV, albeit to a different extent. Observed viral interference after sequential infection by either AIV or another IBV variant, which results in delayed and hampered replication respectively, is of importance to both understand and successfully combat viral respiratory infections in the poultry field.

Declaration of competing interest

The authors declare that they have no conflict of interest.

Acknowledgements

We would like to thank the animal caretakers of the Royal GD, Deventer, for performing the animal experimentation and the histology laboratory staff members of the Division of Pathology, Department Biomolecular Health Sciences, Utrecht, for preparing the tissue slides.

References

1. Ambepitiya Wickramasinghe, I. N., de Vries, R.P., Gröne, A., de Haan, C. A. M., Verheije, M.H., 2011. Binding of avian coronavirus spike proteins to host factors reflects virus tropism and pathogenicity. J. Virol. 85, 8903-8912.

2. Aouini, R., Laamiri, N., Ghram, A., 2018. Viral interference between low pathogenic avian influenza H9N2 and avian infectious bronchitis viruses in vitro and in ovo. J. Virol. Methods 259, 92-99.

3. Avadhanula, V., Rodriguez, C.A., Devincenzo, J.P., Wang, Y., Webby, R.J., Ulett, G.C., Adderson, E.E., 2006. Respiratory viruses augment the adhesion of bacterial pathogens to respiratory epithelium in a viral species- and cell type-dependent manner. J. Virol. 80, 1629-1636.

4. Bakaletz, L. O., 2017. Viral-bacterial co-infections in the respiratory tract. Curr. Opin. Microbiol. 35, 30-35.

5. Belkasmi, S. F. Z., Fellahi, S., Touzani, C.D., Faraji, F.Z., Maaroufi, I., Delverdier, M., Guérin, J.L., Fihri, O.F., El Houadfi, M., Ducatez, M.F., 2020. Co-infections of chickens with avian influenza virus H9N2 and Moroccan Italy 02 infectious bronchitis virus: effect on pathogenesis and protection conferred by different vaccination programmes. Avian Pathol. 49, 21-28.

6. Bouwman, K. M., Parsons, L.M., Berends, A.J., de Vries, R.P., Cipollo, J.F., Verheije, M.H., 2020. Three amino acid changes in avian coronavirus spike protein allow binding to kidney tissue. J. Virol. 94, e01363-19, 1-14.

7. Callison, S. A., Hilt, D.A., Boynton, T.O., Sample, B.F., Robison, R., Swayne, D.E., Jackwood, M.W., 2006. Development and evaluation of a real-time Taqman RT-PCR assay for the detection of infectious bronchitis virus from infected chickens. J. Virol. Methods 138, 60-65.
8. Cohen, M., Zhang, X., Senaati, H.P., Chen, H., Varki, N.M., Schooley, R.T., Gagneux, P., 2013. Influenza A penetrates host mucus by cleaving sialic acids with neuraminidase. Virol. J. 10, 1-13.

9. de Wit, J. J., Cook, J.K., van der Heijden, H.M., 2011. Infectious bronchitis virus variants: a review of the history, current situation and control measures. Avian Pathol. 40, 223-235.

10. Dhinakar Raj, G., Jones, R.C., 1997. Infectious bronchitis virus: Immunopathogenesis of infection in the chicken. Avian Pathol. 26, 677-706.

11. Erfan, A.M., Selim, A.A., Helmy, S.A., Eriksson, P., Naguib, M.M., 2019. Chicken anaemia virus enhances and prolongs subsequent avian influenza (H9N2) and infectious bronchitis viral infections. Vet. Microbiol. 230, 123-129.

12. Germeraad, E. A., Elbers, A.R.W., de Bruijn, N.D., Heutink, R., van Voorst, W., Hakze-van der Honing, R., Bergervoet, S.A., Engelsma, M.Y., van der Poel, W.H.M., Beerens, N., 2020. Detection of low pathogenic avian influenza virus subtype H10N7 in poultry and environmental water samples during a clinical outbreak in commercial free-range layers, Netherlands 2017. Front. Vet. Sci. 7, 237, 1-10.

13. Haji-Abdolvahab, H., Ghalyanchilangeroudi, A., Bahonar, A., Ghafouri, S.A., Marandi, M.V., Mehrabadi, M.H.F., Tehrani, F., 2019. Trop. Anim. Health Prod. 51, 689-695.

14. Hassan, K.E., Ali, A., Shany, S.A.S., El-Kady, M.F., 2017. Experimental co-infection of infectious bronchitis and low pathogenic avian influenza H9N2 viruses in commercial broiler chickens. Res. Vet. Sci. 115, 356-362.

15. Hassan, K.E., El-Kady, M.F., El-Sawah, A.A.A., Luttermann, C., Parvin, R., Shany, S., Beer, M., Harder, T., 2019. Respiratory disease due to mixed viral infections in poultry flocks in Egypt between 2017 and 2018: Upsurge of highly pathogenic avian influenza virus subtype H5N8 since 2018. Transbound. Emerg. Dis. 68, 21-36.

16. Jaleel, S., Younus, M., Idrees, A., Arshad, M., Khan, A.U., Ehtisham-Ul-Haque, S., Zaheer, M. I., Tanweer, M., Towakal, F., Munibullah, Tipu, M.Y., Sohail, M.L., Umar, S., 2017. Pathological alterations in respiratory system during co-infection with low pathogenic avian influenza virus (H9N2) and Escherichia coli in broiler chickens. J. Vet. Res. 61, 253-258.

17. Kong, L., You, R., Zhang, D., Yuan, Q., Xiang, B., Liang, J., Lin, Q., Ding, C., Liao, M., Chen, L., Ren, T., 2022. Infectious bronchitis virus infection increases pathogenicity of H9N2 avian influenza virus by inducing severe inflammatory response. Front. Vet. Sci. 8, 1-14.

18. Kumar, N., Sharma, S., Barua, S., Tripathi, B.N., Rouse, B.T., 2018. Virological and immunological outcomes of coinfections. Clin. Microbiol. Rev. 31, e00111017, 1-39.

19. Li, X., Hanson, R.P., 1989. In vivo interference by Newcastle disease virus in chickens, the natural host of the virus. Arch. Virol. 108, 229-245.

20. Matrosovich, M.N., Matrosovich, T.Y., Gray, T., Roberts, N.A., Klenk, H.D., 2004. Human and avian influenza viruses target different cell types in cultures of human airway epithelium. Proc. Natl. Acad. Sci. U.S.A. 101, 4620-4624.

21. Matthijs, M.G.R., van Eck, J.H., Landman, W.J., Stegeman, J.A., 2003. Ability of Massachusetts-type infectious bronchitis virus to increase colibacillosis susceptibility in commercial broilers: a comparison between vaccine and virulent field virus. Avian Pathol. 32, 473-481.

22. Miura, T.A., 2019. Respiratory epithelial cells as master communicators during viral infections. Curr. Clin. Microbiol. Rep. 6, 10-17.

23. Ponder, B.A.J., 1983. 8: Lectin Histochemistry. In: Polak, J.M. and Van Noorden, S. (Eds.), Immunocytochemistry; Practical Applications in Pathology and Biology, Wright & Sons Ltd, Bristol, England, 129-142.

24. Reed, L.J., Muench, H., 1938. A simple method of estimating fifty percent endpoints. Am. J. Hyg. 27, 493-497.

25. Rim, A., Nacira, L., Jihene, N., Said, S., Khaled, M., Ahmed, R., Abdeljelil, G., 2019. Viral interference between H9N2-low pathogenic avian influenza virus and avian infectious bronchitis virus vaccine strain H120 in vivo. Comp. Immunol. Microbiol. Infect. Dis. 65, 219-225.

26. Robinson, K. M., Kolls, J.K., Alcorn, J.F., 2015. The immunology of influenza virus-associated bacterial pneumonia. Curr. Opin. Immunol. 34, 59-67.

27. Roh, H. J., Hilt, D.A., Williams, S.M., Jackwood, M.W., 2013. Evaluation of infectious bronchitis virus Arkansas-type vaccine failure in commercial broilers. Avian Dis. 57, 248-259.

28. Samy, A., Naguib, M.M., 2018. Avian respiratory coinfection and impact on avian influenza pathogenicity in domestic poultry: field and experimental findings. Vet. Sci. 5, 23, 1-12.

29. Spackman, E., Senne, D.A., Myers, T.J., Bulaga, L.L., Garber, L.P., Perdue, M.L., Lohman, K., Daum, L.T., Suarez, D.L., 2002. Development of a real-time reverse transcriptase PCR assay for type A influenza virus and the avian H5 and H7 hemagglutinin subtypes. J. Clin. Microbiol. 40, 3256-3260.

30. Valastro, V., Holmes, E.C., Britton, P., Fusaro, A., Jackwood, M.W., Cattoli, G., Monne, I., 2016. S1 gene-based phylogeny of infectious bronchitis virus: an attempt to harmonize virus classification. Infect. Genet. Evol. 39, 349-364.

31. Varki, A., 2008. Sialic acids in human health and disease. Trends Mol. Med. 14, 351-360.

32. van Beurden, S. J., Berends, A.J., Krämer-Kühl, A., Spekreijse, D., Chénard, G., Philipp, H.C., Mundt, E., Rottier, P.J.M., Verheije, M.H., 2017. A reverse genetics system for avian coronavirus infectious bronchitis virus based on targeted RNA recombination. Virol. J. 14, 109, 1-13.

33. van Riel, D., Leijten, L.M., Kochs, G., Osterhaus, A., Kuiken, T., 2013. Decrease of virus receptors during highly pathogenic H5N1 virus infection in humans and other mammals. Am. J. Pathol. 183, 1382-1389.

34. Weerts, E.A.W.S., Matthijs, M.G.R., Bonhof, J., van Haarlem, D.A., Dwars, R.M., Gröne, A., Verheije, M.H., Jansen, C.A., 2021. The contribution of the immune response to enhanced colibacillosis upon preceding viral respiratory infection in broiler chicken in a dual infection model. Vet. Immunol. Immunopathol. 283, 110276, 1-11.

35. Winter, C., Herrler, G., Neumann, U., 2007. Infection of the tracheal epithelium by infectious bronchitis virus is sialic acid dependent. Microbes Infect. 10, 367-373.

4 The contribution of the immune response to enhanced colibacillosis upon preceding viral respiratory infection in broiler chicken in a dual infection model

E.A.W.S. Weerts [a], M.G.R. Matthijs [b], J. Bonhof [c], D.A. van Haarlem [c], R.M. Dwars [b], A. Gröne [a], M.H. Verheije [a], C.A. Jansen [c,#]

[a] Division of Pathology, Department Biomolecular Health Sciences, Faculty of Veterinary Medicine, Utrecht University, Utrecht, the Netherlands

[b] Division of Farm Animal Health, Department Population Health Sciences, Faculty of Veterinary Medicine, Utrecht University, Utrecht, the Netherlands

[c] Division of Infectious Diseases and Immunology, Department Biomolecular Health Sciences, Faculty of Veterinary Medicine, Utrecht University, Utrecht, the Netherlands

[#] *current address: Cell Biology and Immunology Group, Department of Animal Sciences, Wageningen University and Research, Wageningen, the Netherlands*

published: Veterinary Immunology and Immunopathology, 2021; 238: 1-11.

Abstract

Colibacillosis in chickens caused by avian pathogenic *Escherichia coli* (APEC) is known to be aggravated by preceding infections with infectious bronchitis virus (IBV), Newcastle disease virus (NDV) and avian metapneumovirus (aMPV). The mechanism behind these virus-induced predispositions for secondary bacterial infections is poorly understood. Here we set out to investigate the immunopathogenesis of enhanced respiratory colibacillosis after preceding infections with these three viruses. Broilers were inoculated intratracheally with APEC six days after oculonasal and intratracheal inoculation with IBV, NDV, aMPV or buffered saline. After euthanasia at 1 and 8 days post infection (dpi) with APEC, birds were macroscopically examined and tissue samples were taken from the trachea, lungs and air sacs. In none of the groups differences in body weight were observed during the course of infection. Macroscopic lesion scoring revealed most severe tissue changes after NDV-APEC and IBV-APEC infection. Histologically, persistent tracheitis was detected in all virus-APEC groups, but not after APEC-only infection. In the lungs, mostly APEC-associated transient pneumonia was observed. Severe and persistent airsacculitis was present after NDV-APEC and IBV-APEC infection. Bacterial antigen was detected by immunohistochemistry only at 1 dpi APEC, predominantly in NDV-APEC- and IBV-APEC-infected lungs. Higher numbers of CD4+ and CD8+ lymphocytes persisted over time in NDV-APEC- and IBV-APEC-infected tracheas, as did CD4+ lymphocytes in NBV-APEC- and IBV-APEC-infected air sacs. KUL01+ cells, which include monocytes and macrophages, and TCRγδ+ lymphocytes were observed mostly in lung tissue in all infected groups with transient higher numbers of KUL01+ cells over time and higher numbers of TCRγδ+ lymphocytes mainly at 8 dpi. qPCR analysis revealed mostly trends of transient higher levels of IL-6 and IFNγ mRNA in lung tissue after IBV-APEC and also NDV-APEC infection and persistent higher levels of IL-6 mRNA after aMPV-APEC infection. In spleens, transient higher levels of IL-17 mRNA and more persistent higher levels of IL-6 mRNA were observed after all co-infections. No changes in IL-10 mRNA expression were seen. These results demonstrate a major impact of dual infections with respiratory viruses and APEC, compared to a single infection with

APEC, on the chicken respiratory tract and suggest that immunopathogenesis contributes to lesion persistence.

Highlights

Dual airway infections with viruses and *Escherichia coli* caused severe lesions.

Tracheitis and airsacculitis depended more on viral preinfection than pneumonia.

Lesions persisted eight days after dual infection, bacterial antigen did not.

Immune cell increase in the trachea and air sac was mainly virus-associated.

Infectious bronchitis virus and *E.coli* dual infection increased cytokine mRNA levels.

Key words

broilers - dual infection - avian pathogenic *Escherichia coli* - infectious bronchitis virus - Newcastle disease virus - avian metapneumovirus

Introduction

Colibacillosis in domestic chicken is caused by avian pathogenic *Escherichia coli* (APEC) and induces extensive economic and animal welfare problems worldwide. An important variant of colibacillosis manifests mainly in the respiratory tract of broiler chicken and presents as pneumonia and airsacculitis.[5,7,12,15] Uncomplicated APEC infections, however, can often successfully be cleared by affected chickens in early phase of disease.[11]

Respiratory virus infections are well-known to predispose for subsequent infection with bacterial agents in both humans and animals.[10,13,14,18,29,33] Despite the fact that virus-induced predisposition for secondary bacterial infections often occurs, the diseases resulting from such dual infections are mechanistically poorly understood. These events were first explained by virus-

induced mechanical damage to the mucocilliary respiratory tissue, which was thought to hamper proper bacterial clearance.[3,16] In addition, virus-induced increase of bacterial attachment factors was found to aid bacterial manifestation in the upper respiratory tract.[3,25]

Alternatively, primary viral airway infection is known to facilitate secondary bacterial infection via cell-mediated immune pathways, as was clearly demonstrated in studies on influenza virus-predisposed streptococcal lung infection in mice (reviewed by [32,34]). Macrophages play an important role in the early defence against viruses. Upon phagocytosis or infection, macrophages are able to present foreign antigens to T cells and in this way induce T cell activation.[41] It appears that anti-viral interactions between macrophages and T cells can extensively hamper anti-bacterial activities. Several pro-inflammatory mediators that play a major role in anti-viral defence, such as IL-6 and IFNγ, were in mammals repeatedly associated with increased risks for subsequent bacterial infection.[18,34,38] Type I interferons, released from virus-infected cells, have been reported to impair macrophage activity via decreased release of tumour necrosis factor (TNF)-α and attenuation of macrophage-regulated T helper responses and in this way contribute to the suppression of cell-mediated anti-bacterial clearance.[20,29,34,37,40,46] Other important virus-induced and interferon-driven side effects that contribute to bacterial survival are immunosuppression via increased IL-10 release[17,21,38,43] and hampered antibacterial IL-17 and γδ T cell responses.[17,19,20,30,37]

Although virus-induced predisposition to subsequent bacterial infections will likely vary for different viruses and bacteria, the authors hypothesize that effects on cell-mediated immunity and the macrophage-T cell alliance play a role in bacterial disease preceded by viral infection in the chicken respiratory tract. In broilers, infections by infectious bronchitis virus (IBV), Newcastle disease virus (NDV) and avian metapneumovirus (aMPV) are well known to predispose for severe disease from subsequent APEC infections.[2,11,24,31,42,44] Only few details about the pathogenesis behind these dual infection-based diseases are known and it is especially unclear whether these different viruses predispose for colibacillosis in a similar way or via virus-specific routes. Therefore, the aim of

this study is to focus on the comparative immunopathogenesis of enhanced respiratory colibacillosis after infection with three different viruses in an *in vivo* dual infection model with APEC. The study will give new insights in the similarities and differences between the immune responses that coincide with enhancement of tissue damage following APEC infection after preceding infection with either of these viruses.

Materials and methods

Animal experiments

Eighteen-day-incubated Ross 308 eggs, originating from a *Mycoplasma gallisepticum*-free broiler parent stock, were obtained from a commercial hatchery (Lagerwey, the Netherlands) and hatched at the animal research facility of the Department of Farm Animal Health (Utrecht University). From the day-of-hatch, the birds were housed in negative pressure HEPA (high efficiency particulate air) filtered isolators (Beyer and Eggelaar, Utrecht, the Netherlands). Up to day 15 of age, broilers were fed a commercial feed *ad libitum* with light given for 23 hours a day. To prevent cannibalism, red light was given from day 4 onwards. From 15 days onwards, feed was restricted to 85% and given on a 'skip-a-day' base to reduce leg problems and hydrops ascites with light reduced to 16 hours a day. Drinking water was supplied *ad libitum* throughout the experimental period. From day 1 to 31, temperature was gradually deviated from 37°C to 18°C. From day 31 onwards the temperature was kept at 18°C. The experiments were performed in accordance with the Dutch animal welfare regulations and the experimental protocols approved by the Animal Experimental Committee (Dierexperimentencommissie, DEC) of the Veterinary Faculty of Utrecht University, the Netherlands (DEC approval number 2012.II.08.121).

Viral and bacterial inocula

Virulent IBV M41 strain was kindly provided by MSD Animal Health (Boxmeer, the Netherlands) as freeze-dried vials containing $10^{8.3}$ egg infectious doses

$(EID)_{50}$/1.2ml/vial (batch 00-12-578127). The live Newcastle disease vaccine LASOTA (AviPro ND LASOTA; batch: E029811) was obtained from Lohmann Animal Health (Cuxhaven, Germany) as freeze-dried 5000 doses vials containing $5x10^{9.0}$ EID_{50}/vial. The aMPV live turkey rhinotracheitis (TRT) vaccine (Noblis® TRT; MSD Animal Health; Boxmeer, the Netherlands) was supplied via freeze-dried 1000 doses vials containing $10^{5.5}$ EID_{50}/vial (from here on referred to as aMPV). Just prior to use, inocula were dissolved in phosphate-buffered saline (PBS) at a concentration of $10^{5.0}$ EID_{50}/ml, except for the aMPV inoculum which was dissolved at $10^{4.6}$ EID_{50}/ml.

The APEC strain 506 was used at a concentration of $10^{7.6}$CFU/ml. This APEC strain was originally isolated from a commercial broiler[44] and was prepared as previously published.[24]

Experimental design

Twenty-five female chicken were randomly divided over separate isolators in five experimental groups of five birds. At experimental day -6 (28 days of age), groups 3, 4 and 5 were inoculated with respectively IBV, NDV and aMPV oculo-nasally by administering one droplet of 0.05 ml per bird in both eyes and nostril and 1 ml intra-tracheally per bird, resulting in an infectious viral titre of $1.2x10^{5.0}$ EID_{50} / bird (aMPV $1.2x10^{4.6}$ EID_{50}). Groups 1 and 2 received comparable volumes of PBS. At experimental day 0, all groups except group 1 were intra-tracheally inoculated with 1 ml APEC culture diluted in PBS, group 1 received 1 ml PBS. Broilers were weighed on experimental days -6, 0 and 8.

At day 8, blood samples were collected from the jugular vein to determine the antibody titres against IBV and NDV by haemagglutination inhibition assay (HI) and aMPV titres by enzyme-linked immuno sorbent assay (ELISA) (GD Animal Health, Deventer, the Netherlands). According to standard lab procedures of GD Animal Health, IBV HI titres ≥5, NDV HI titres ≥3 and aMPV ELISA titres ≥9 were considered positive.

At experimental day 1 and 8 (after APEC inoculation) broilers were euthanized. During post-mortem analysis, paired samples were taken of the trachea, lungs

and air sacs. One sample was snap frozen in liquid nitrogen and stored at -20 °C, the other formaline-fixed for 24-48 hours.

Macroscopic and histopathologic lesion scoring

At day 1 and 8, colibacillosis-associated lesions were macroscopically scored in the left and right thoracic air sac, the pericardium and the serosal surface of the liver with a 4-grade system (0-3) to classify birds in mildly, moderately and severely affected as previously published.[44]

For histopathologic lesion evaluation, sections of formalin-fixed and paraffin-embedded (FFPE) trachea, lung and air sac were stained with hematoxylin and eosin (HE) according to standard laboratory procedures. Tissue slides were semi-

Table 1 Histopathologic lesion scoring

Score	Scoring criterium	Multiplication factor
Aspect 1: Epithelial integrity		
0	comparable to PBS group	tissue % affected[1]
1	mild thickening and / or minimal desquamation or cell loss	
2	moderate thickening and / or desquamation, cell death or cell loss (tissue architecture mostly recognizable)	
3	severe thickening and / or desquamation, cell death, cell loss (with loss of normal tissue architecture)	
aspect 2: Granulocyte infiltration		
0	comparable to PBS group	tissue % affected[1]
1	few ('dozens') scattered cells, incidentally in airway lumen	
2	moderate numbers ('hundreds'), scattered cells or small clusters, sometimes in airway lumen	
3	marked numbers ('more than hundreds / uncountable'), scattered and clear clusters, often in airway lumen	
aspect 3: Interstitial cellularity		
0	comparable to PBS group	tissue % affected[1]
1	mild cell increase ('dozens'), few small lymphoid nodules	
2	moderate cell increase ('hundreds'), some interstitial thickening, clear lymphoid nodules	
3	marked increase ('more than hundreds / uncountable'), obvious interstitial thickening, large lymphoid nodules	

Total score per aspect varies between 0 (comparable to PBS group) and 3 (score-3-changes in 100% of the tissue sample. [1] Scale 0.1 – 1.0 with steps of 0.1 (10, 20, 30% etc. of the tissue sample affected)

quantitatively scored using a 4-grade system (0-3) for severity of three separate lesion aspects: 1) epithelial integrity; 2) heterophilic granulocyte infiltration; 3) interstitial / submucosa cellularity (in this category with exclusion of the heterophilic granulocytes). The total lesion scores, which are defined as the sum of the separate scores per category, were corrected for the fraction of tissue containing lesions. The scoring system is depicted in Table 1.

Immunohistochemistry

APEC antigen was detected with APEC 506 specific rabbit serum on sections of FFPE trachea, lung and air sac as previously published.[7] Sections were evaluated by light microscopy for presence of APEC antigen.

Four different immune cell populations were immunohistochemically labelled in 8 µm cryostat sections and transferred to KP Plus slides (Klinipath). CD4+, CD8αβ+ and TCRγδ+ lymphocytes and KUL01+ cells were visualized with mouse-anti chicken CD4 (clone CT-4, IgG1), mouse anti-chicken CD8β (clone EP42, IgG2a), mouse anti-chicken TCRγδ (clone TCR-1, IgG1) and mouse-anti-chicken monocyte/macrophage (KUL01, IgG1) (Southern Biotech, USA) as previously published.[23] The KUL01 antibody binds the mannose receptor MRC1L-B, which is present on monocytes, macrophages and plasmacytoid dendritic cells.[39] The TCR-1 antibody recognizes γδ T cells. Antibodies were diluted 1:1000 (1:2000 for KUL01) in PBS containing 0.5% bovine serum albumin (BSA) and 0.1% sodium azide (PBA) for 1 hour. Antibody binding was visualized with biotinylated horse anti-mouse IgG (Vectastain) diluted 1:200 in PBS for 1 hour, subsequent incubation with the avidin:biotin enzyme complex (Vectastain Elite ABC kit) for 1 hour and the colour substrate 3,3-diaminobenzidine-tetrahydrochloride (DAB, Sigma) in TRIS-HCL buffer (Merck) for 10 minutes. Slides were counterstained with haematoxylin (Sigma) and mounted in fluorescence mounting medium (DAKO). Negative controls were incubated comparably, but without the primary antibody.

For trachea and lung, stained cells were counted light microscopically in three representative sections per slide and averaged per group, resulting in the mean cell count per organ per animal. For the air sacs, positive cells were semi-

quantified per group using four grades: 0 - cell numbers comparable to mock-infected birds, 1 – mildly increased numbers (few up to dozens), 2 – moderately increased numbers (dozens up to approximately one hundred), 3 – markedly increased numbers (hundreds, 'uncountable').

Real time quantitative PCR (RT-qPCR)

Real time qPCR was performed to analyse mRNA levels of the cytokines IL-6, IL-10, IL-17 and IFNγ in lung and spleen of chickens at all post mortem time points. Frozen tissue samples were thawed and homogenized (Retsch Mixer Mill 301, Fisher Scientific) in RLT buffer (Qiagen). Total RNA was isolated using RNeasy Mini Kit (Qiagen) according to the manufacturer's recommendation and eluted in 30 µl RNase-free water. cDNA was generated with reverse transcription of purified RNA, with a maximum of 500ng RNA, using iScript cDNA Synthesis Kit (Bio-Rad). RT-qPCR primers and probes sequences were designed according to previously published sequences[2,48] and are shown in Table 2. IL-6, IL-10, 28S and IFNγ qRT-PCR was performed with 600 nM primers and 100 nM probes using Taqman Universal PCR Master Mix (Life Technologies) on the following cycle profile: one cycle of 50 °C for 2 min, one cycle of 95 °C for 10 min, and 40 cycles

Table 2 RT-qPCR Cytokines, primers and probes

RNA target		Probe / primer sequence (5'-3')	Accession number
28S	probe	(FAM)-AGGACCGCTACGGACCTCCACCA-(TAMRA)	X59733
	F primer	GGCGAAGCCAGAGGAAACT	
	R primer	GACGACCGATTTGCACGTC	
IFNγ	probe	(FAM)-TGGCCAAGCTCCCGATGAACGA-(TAMRA)	YO7922
	F primer	GTGAAGAAGGTGAAAGATATCATGGA	
	R primer	GCTTTGCGCTGGATTCTCA	
IL-6	probe	(FAM)-AGGAGAAATGCCTGACGAAGCTCTCCA-(TAMRA)	AJ309540
	F primer	GCTCGCCGGCTTCGA	
	R primer	GGTAGGTCTGAAAGGCGAACAG	
IL-10	probe	(FAM)-CGACGATGCGGCGCTGTCA-(TAMRA)	AJ621614
	F primer	CATGCTGCTGGGCCTGAA	
	R primer	CGTCTCCTTGATCTGCTTGATG	
IL-17	F primer	ATGGGAAGGTGATACGGC	AM773756
	R primer	GATGGGCACGGAGTTGA	
GAPDH	F primer	GTGGTGCTAAGCGTGTTATC	K01458
	R primer	GCATGGACAGTGGTCATAAG	

of 95 °C for 10 s and 59 °C for 1 min. IL-17 and GAPDH RT-qPCR was performed using 400 nM primers and iQ SYBR Green supermix (Bio-Rad) with the following reaction cycle conditions: one cycle of 95 °C for 5 min, 40 cycles of 92 °C for 10 s, 59 °C for 10 s and 72 °C for 30 s, one cycle of 95 °C for 1 min, one cycle of 65 °C for 1 min and 31 cycles of 65°C for 1 min. mRNA from 24 hour ConA stimulated splenocytes was used as reference line for IL-6, IFNγ, IL-17 and 28S. For GAPDH a GAPDH containing plasmid was used and IL-10 standard curves were generated using mRNA isolated from the chicken macrophage cell line HD11 which was stimulated for 3 hours with LPS. As housekeeping gene for IL-6, IFNγ and IL-10 chicken ribosomal 28S was used. For IL-17 the housekeeping gene GAPDH was used. MyiQ Single-Color Real-Time PCR Detection System (Bio-Rad) was used to amplify and detect specific cytokine products.

qPCR data were analyzed as described by Eldaghayes et al..[8] This method is based on the differences in average Ct values between the gene of interest and the housekeeping gene. For each gene (including a housekeeping gene) 5 serial dilutions of a standard are included, all in triplicate, to generate a linear reference line. In parallel all samples are measured in triplicate, both for the gene of interest as well as the housekeeping gene. A "corrected Ct value" is calculated by the formula =Average Ct gene of interest + ((median Ct value of the housekeeping gene in all standards) – Average Ct housekeeping gene*(slope_standard curve gene of interest/slope standard curve housekeeping gene_)). In this way the data is corrected for variation in RNA input, and tube variations in the housekeeping gene. Next the "corrected Ct value" is subtracted from the number of cycles, and this 40-Ct value is shown.

Statistical analysis

The One-Way ANOVA test was used to analyse the differences in weight of dually-inoculated broilers (IBV-APEC, NDV-APEC and aMPV-APEC) and APEC-inoculated broilers per time point. A generalized linear model was performed on the macroscopic lesion scores, mRNA fold changes and number of positive immune cells in broilers. The explanatory variables were treatment (PBS, APEC, IBV, NDV, aMPV) and time point (day 1 and 8). The dependent variable number

of positive immune cells in trachea and lung underwent log transformation, to meet the assumption of normality, before statistical analysis. A Bonferroni correction was used to investigate differences between dually-inoculated broilers and the APEC-inoculated birds. Histologic lesion scores were analysed with the Mann-Whitney U test. For all statistical analyses a p-value of < 0.05 was considered statistically significant.

Results

Macroscopic lesion scores, antiviral antibody titers and body weights

Colibacillosis-associated lesions were macroscopically observed in all dually- and APEC-only-inoculated birds (Figure 1A and B), most prominently after NDV-APEC inoculation (mean macroscopic lesions scores 3.3 and 3.1 at respectively day 1 and 8), slightly less after IBV-APEC inoculation (scores 2.4 and 2.1) and at mild level after aMPV-APEC inoculation and in the APEC-only-inoculated birds (scores respectively 0.5 and 0.4 versus 0.7 and 0.5). Lesions were most severe in the air sacs; pericardial lesions were only present after NDV-APEC infection. Perihepatitis was not seen in any bird. Birds which were not inoculated with virus or APEC had no macroscopic lesions.

All virus-inoculated birds showed humoral immune responses specifically against the inoculated virus. All IBV-APEC-inoculated chicken had a serum IBV antibody HI titre of ≥7 (threshold ≥5) (Figure 1C). Four of five NDV-APEC-inoculated birds had a serum NDV antibody HI titre of ≥3 (threshold ≥3) (Figure 1D). Four of five aMPV-APEC-inoculated birds had a serum aMPV antibody ELISA titre of 10 (threshold ≥9) (Figure 1E).

No significant body weight differences existed between the groups which had received a dual inoculation, neither at the day of virus inoculation (day -6), nor at the day of APEC inoculation (day 0) or at the end of the experiment (day 8). (data not shown).

Histopathologic lesion scores

Histopathologic lesion scores are shown for the three studied respiratory tissues with representative pictures of the most severe changes in Figure 2.

Trachea (Figure 2, row A)

In the tracheas of birds inoculated with APEC only, mild to moderate granulocytic infiltration was observed with only minimal epithelial hyperplasia

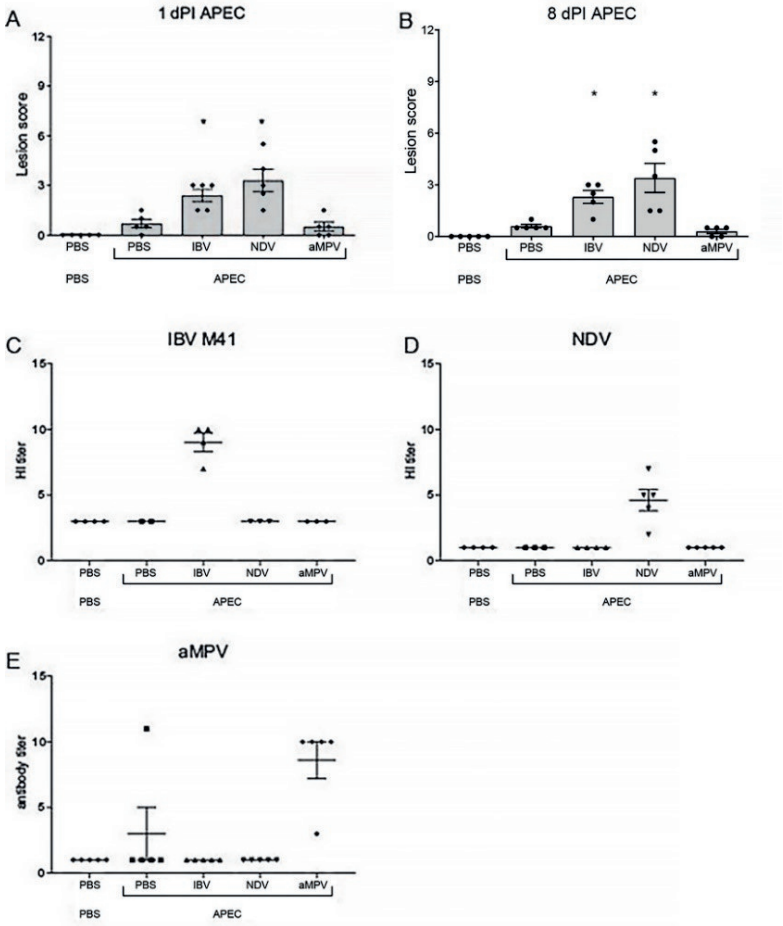

Figure 1: Macroscopic lesion scores and antibody titres. Colibacillosis lesion scores were determined as described by van Eck and Goren, 1991 at 1 (A) and 8 (B) days post APEC infection. Mean + SEM of five birds per group is shown. Antibodies titres against IBV (C) and NDV (D), were determined two weeks post infection by haemagglutination inhibition. Titres ≥5 (IBV) and ≥3 (NDV) were considered positive. Antibody titres against aMPV (E) were determined by ELISA. Titres ≥9 were considered positive. 5 birds per group (few birds not analysed for all titres due to limited amounts of serum).

at day 1. No tracheal lesions were seen in this group at day 8. Moderate lesions were present after IBV-APEC inoculation at day 1, consisting mainly of epithelial hyperplasia, intraepithelial granulocyte infiltration and lymphohistiocytic infiltration in the lamina propria. Compared to the APEC-only and aMPV-APEC groups, these lesions persisted and were significantly ($P < 0.05$) more severe on day 8. At day 1, tracheal lesions were of comparable morphology, but significantly ($P < 0.05$) more severe in NDV-APEC-inoculated birds than in all other groups. Similar to the IBV-APEC-inoculated birds, these lesions showed a

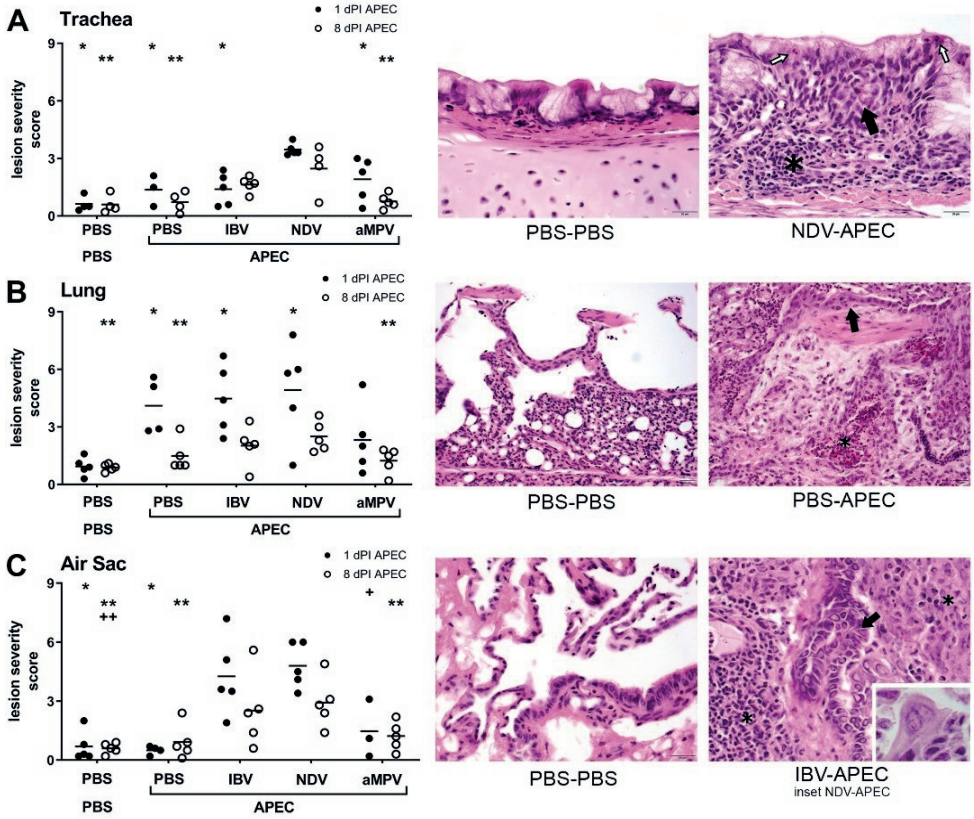

Figure 2: Histopathologic lesion scores with mean for trachea (A), lung (B) and air sac (C), with representative pictures (400x magnification, 20 µm scale bar) of highest score lesions. Black arrow = epithelial lining, white arrow = heterophilic granulocytes in the epithelial lining, asterisk = inflammatory cell accumulations (in the lung mostly heterophilic granulocytes), inset = syncytial cells after NDV-APEC infection. 5 birds per group (few missing values due to tissue artefacts impeding scoring). Significant differences ($P < 0.05$), trachea: * compared to NDV-APEC 1 dpi, ** compared to IBV-APEC 8 dpi; lung: * compared to PBS-PBS 1 dpi, ** compared to NDV-APEC 8 dpi; air sac: * compared to NDV-APEC and IBV-APEC 1 dpi, $^{+}$ compared to NDV-APEC 1 dpi, ** compared to NDV-APEC 8 dpi, $^{++}$ compared to IBV-APEC 8 dpi.

trend to persist at day 8. Tracheal lesions observed in aMPV-APEC-inoculated birds had an average severity that was comparable to those observed in the IBV-APEC-inoculated birds and birds inoculated with APEC only at day 1. In contrast with the tracheas of both IBV-APEC- and NDV-APEC-inoculated birds, tracheal lesions in aMPV-APEC-inoculated birds reduced and did not persist at day 8. Apart from minimal to mild focal infiltration of lymphocytes and histiocytes, no lesions were observed in the tracheas of mock-infected birds.

Lung (Fig. 3, row B)

Lung lesions were of comparable morphology and severity for APEC-only-, IBV-APEC- and NDV-APEC-inoculated birds at day 1 with significant ($P < 0.05$) difference to the PBS group. In contrast, lesions in the lungs of aMPV-APEC-inoculated birds were only mild. Lesions were predominantly characterized by parabronchial epithelial swelling and granulocyte infiltration. In some lungs of APEC-only-, IBV-APEC- and NDV-APEC-inoculated birds, accumulations of cellular debris and degenerate granulocytes were observed within parabronchial lumina. At day 8, lesions in the virus-APEC-inoculated birds consisted more prominently of non-granulocytic interstitial cell increase, whereas those in the lungs of birds inoculated with APEC only contained more granulocytes. Lesions persisted at this time point in NDV-APEC-inoculated birds and were significantly ($P < 0.05$) more severe compared to APEC-only- and aMPV-APEC-inoculated birds. A trend of mild lesion persistence at day 8 was also observed after IBV-APEC inoculation. Lungs of mock-infected birds had minimal to mild focal lymphocytic and histiocytic infiltration, but granulocytic infiltration was not present.

Air sacs (Figure 3, row C)

Differences in lesion severity between the experimental bird groups were most evident in the air sacs. In most of the air sacs of birds inoculated with APEC only, no tissue changes were observed at both day 1 and 8. In contrast, IBV-APEC- and NDV-APEC-inoculated birds had severe air sac lesions at day 1, which was significantly ($P < 0.05$) different to the APEC-only group. These lesions reduced in severity, but persisted moderately on day 8 with significant ($P < 0.05$)

difference between the NDV-APEC and APEC-only group and with a similar trend for persistence in the IBV-APEC group. Air sacs of aMPV-APEC-inoculated birds also showed mild lesions, but these were less severe than in the other virus-APEC groups. Lesions observed after preceding IBV and NDV inoculation consisted of marked granulocytic infiltration and marked epithelial hypertrophy with sometimes epithelial desquamation at day 1. At day 8, cell infiltrates in the air sacs of these birds had changed to less granulocytic and more lymphohistiocytic. Apart from incidental mild focal inflammatory cell infiltration at day 1, no lesions were observed in the air sacs of mock-infected birds.

APEC antigen presence

APEC antigen was not demonstrated in the trachea, but was present at day 1 only in the lungs of IBV-APEC-, NDV-APEC- and APEC-only-inoculated birds and in the air sacs of one NDV-APEC-inoculated bird. It was not demonstrated in aMPV-APEC-inoculated birds and in none of the birds at day 8 (Table 3).

In the lungs, APEC antigen was present in air capillaries and parabronchial lumina (Figure 3, upper panels), in the air sac it was present within the lumen

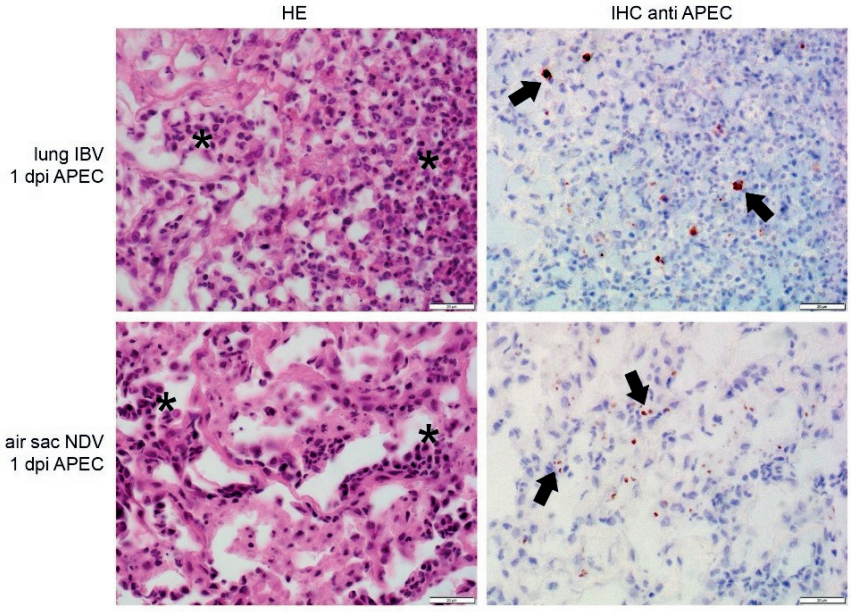

Figure 3: Representative serial sections of chicken lung (upper panels) and air sac (lower panels) showing APEC-antigen presence, HE and IHC anti-APEC (800x magnification, 20 µm scale bar). Asterisk = inflammatory cell infiltrates, arrow = APEC antigen.

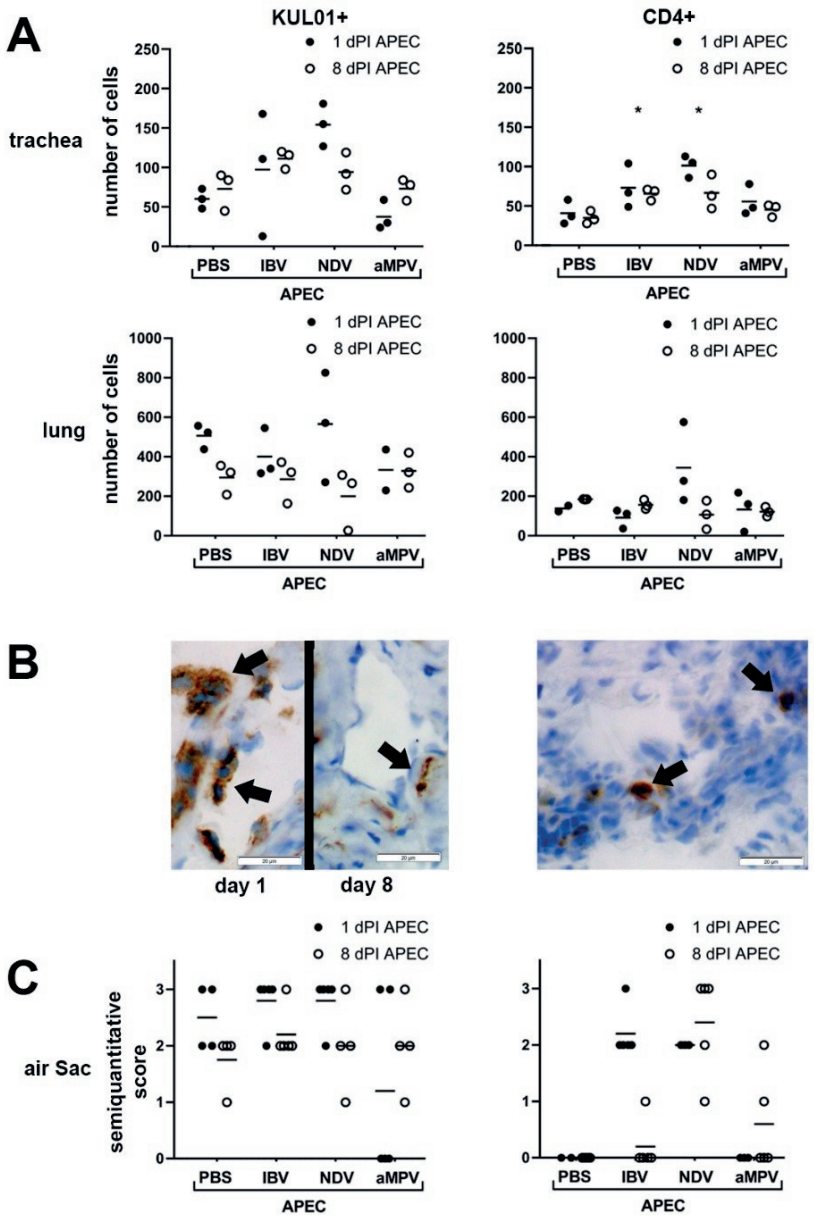

(Figure 3, lower panels). APEC antigen was observed as scattered single dots in association with focal heterophilic granulocyte infiltration, probably representing individual bacteria, and sometimes as small clusters of dots, probably several bacteria taken up by phagocytes or in the lumen of small capillaries.

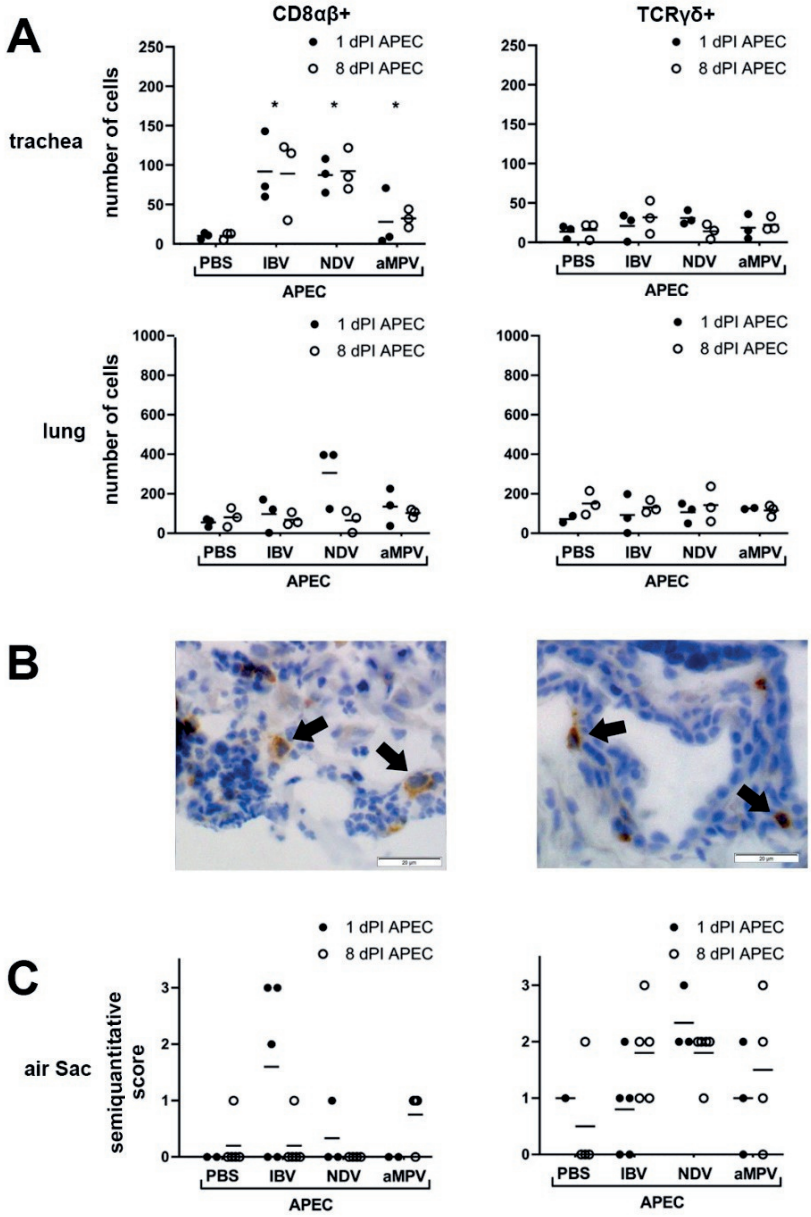

Figure 4: Respiratory tract immune cells counts in trachea and lung (A), with representative pictures of IHC cell labeling (800x magnification, 20 µm scale bar) (B) and semi-quantified immune cell numbers in air sac (C) for KUL01+, CD4+, CD8αβ+ and TCRγδ+ cells. KUL01+ cells were swollen at day 1 and displayed a spindeloid morphology day 8. Arrow = positively labelled, stained cells. Significant differences over time compared to PBS-APEC ($P < 0.05$) are indicated with an asterisk. For trachea and lung, cells were counted in 3 of 5 birds, for the air sac cells were semi-quantitatively scored in all 5 birds.

Immune cell presence

Immune cell counts in tracheas and lungs are shown in Figure 4A, representative examples of the immunohistochemically-labelled cells in Figure 4B and semi-quantified cell numbers in the air sacs in Figure 4C.

KUL01+ cell numbers were highest in tracheas of IBV-APEC- and NDV-APEC-inoculated birds and comparably lower in tracheas of aMPV-APEC and APEC-only-inoculated birds at day 1 and 8. In the lung, KUL01+ cell numbers at day 1 were higher in NDV-APEC- and APEC-inoculated and also slightly higher in IBV-APEC-inoculated birds than in aMPV-APEC-inoculated birds. At day 8, KUL01+ cell numbers remained comparable to day 1 in the aMPV-APEC group. In IBV-APEC-, NDV-APEC and APEC-only-inoculated birds, KUL01+ cell numbers at day 8 were lower compared to day 1 with cell numbers at day 8 comparable to the aMPV-APEC group in all other groups. Compared to all other groups, increase of KUL01+ cells was slightly lower in the air sacs of aMPV-APEC-inoculated birds. Cell numbers were lower at day 8, except for the aMPV-APEC-inoculated birds, and were then comparable for all groups.

Compared to the birds inoculated with APEC only, CD4+ lymphocyte numbers in the trachea were significantly ($P < 0.05$) higher for the IBV-APEC- and NDV-APEC-inoculated birds at both day 1 and 8. NDV-APEC-inoculated birds had more CD4+ lymphocytes in their lungs than the other groups at day 1. In the air sacs, CD4+ lymphocytes were at day 1 mainly observed in the IBV-APEC- and NDV-APEC-inoculated birds. This increase persisted for the NDV-APEC-inoculated birds at day 8.

In contrast to the birds inoculated with APEC only, CD8αβ+ lymphocytes were observed in significantly ($P < 0.05$) higher numbers at day 1 and persisted at day 8 in all virus-infected tracheas. A comparable, but milder trend was seen for CD8αβ+ lymphocytes within the lungs, although these increases did not persist at day 8. Compared to the other virus-APEC groups, the lungs of NDV-APEC-inoculated birds contained more CD8αβ+ lymphocytes at day 1. In the air sacs, higher numbers of CD8αβ+ lymphocytes were only observed in some IBV-APEC-inoculated birds at day 1.

TCRγδ+ lymphocyte numbers did only mildly differ between groups in the trachea. Compared to day 1, this cell type was present in slightly higher numbers at day 8 in IBV-APEC-, NDV-APEC- and APEC-only-inoculated lungs. In the air sacs, these cells were present in higher numbers at both day 1 and 8 after preceding viral inoculation, compared to inoculation with APEC only.

No statistical significances ($P < 0.05$) between groups could be demonstrated for the lungs and air sacs.

Cytokine mRNA levels

To conclude, differences in cytokine mRNA expression were investigated. As shown in Figure 5A, mRNA levels of the pro-inflammatory cytokine IL-6 were significantly ($P < 0.05$) higher in the lungs of IBV-APEC-inoculated birds and tended to be higher in the NDV-APEC-inoculated group compared to the APEC-only group at day 1. In the course of infection, IL-6 levels in the lungs of IBV-APEC- and NDV-APEC-inoculated birds decreased to similar levels on day 8 as observed in birds inoculated with APEC only, while in aMPV-APEC inoculated birds the level of IL-6 did not change, compared to day 1. In the spleen no statistically significant differences between IL-6 mRNA levels were observed at day 1, but IL-6 levels tended to increase in the IBV-APEC- and NDV-APEC-inoculated birds at day 8 (Figure 5B). In the lungs, IFNγ mRNA in IBV-APEC- and NDV-APEC-inoculated birds was only observed at day 1 (Figure 5C). In the spleen, IFNγ was readily detected at day 1 and tended to remain higher at day 8 in the IBV-APEC- and NDV-APEC-inoculated birds, compared to birds inoculated with APEC only (Figure 5D). In the lung, no differences in IL-17 mRNA levels between the groups were observed, except for a slightly but not significantly higher level at day 1 in NDV-APEC-inoculated birds (Figure 5E). In the spleen,

significantly ($P < 0.05$) higher IL-17 mRNA levels were observed in IBV-APEC- and aMPV-APEC-inoculated birds at day 1, compared to APEC-only-inoculated birds (Figure 5F). No IL-10 mRNA was detected in lungs or spleen in any of the groups (data not shown).

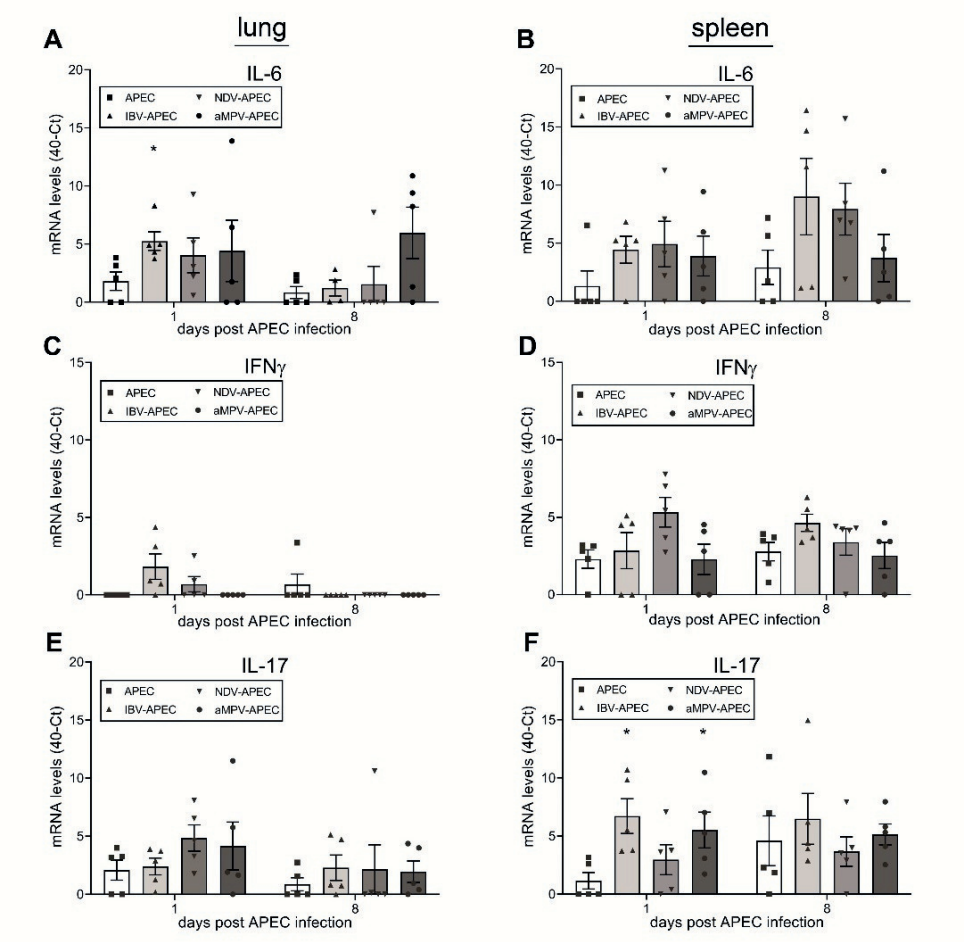

Figure 5: IL-6, IFNγ and IL-17 mRNA levels in lung and spleen. Real-time qRT-PCR IL-6 mRNA levels at 1 and 8 days post APEC infection in lung (A) and spleen (B). Real-time qRT-PCR IFNγ mRNA levels at 1 and 8 days post APEC infection in lung (C) and spleen (D). Real-time qRT-PCR IL-17 mRNA levels at 1 and 8 days post APEC infection in lung (E) and spleen (F).mRNA levels were normalized against 28S and are expressed as 40-Ct. Median + quartiles of five birds per group. Significant differences compared to PBS-APEC ($P < 0.05$) are indicated with an asterisk.

Discussion

This study for the first time compared immunologic and pathologic aspects of dual infections with three very relevant respiratory viruses in poultry (IBV, NDV and aMPV) and APEC. In summary, tracheitis and airsacculitis developed mostly virus-associated, persisted over time after mainly NDV-APEC but also IBV-APEC infection and mainly coincided with respectively higher and persistent CD4+ and CD8αβ+ lymphocyte numbers (trachea) and CD4+ and TCRγδ+ lymphocyte numbers (air sac). Pneumonia, in contrast, developed more APEC-associated, but also persisted mildly after NDV-APEC and IBV-APEC infection. Pneumonia coincided with KUL01+ cell numbers comparable for all groups that were higher early after infection. Furthermore, pneumonia was associated with increased CD4+ and CD8+ cell numbers after NDV-APEC inoculation. Virus-APEC dual infections were furthermore associated with transient higher mRNA levels of pro-inflammatory cytokines locally in the lung and with persisting higher mRNA levels of these cytokines systemically in the spleen. These findings broaden the knowledge on viral influences on colibacillosis in broilers and highlight similarities and differences between viruses in dual infections. Previous studies have focused mostly on either single pathogens or the dual infection IBV-APEC and therefore lack this comparative aspect of the current work.

The presence of CD4+ lymphocytes and CD8αβ+ lymphocytes in the tracheas and air sacs and of KUL01+ cells in the tracheas was virus-associated, coincided mainly with IBV-APEC- and NDV-APEC-induced lesions and persisted over time. In the trachea, numbers of KUL01+ cells (likely mostly macrophages) correlated with increased CD4+ and CD8αβ+ cell numbers, which is likely the result of specific cell interactions – probably in the form of antigen presentation by macrophages to the T cell subsets – that are known to lead to development of adaptive cell-mediated immunity.[41] The fact that these higher immune cell numbers coincided with higher mRNA levels of the pro-inflammatory cytokines IL-6 and IFNγ in both the lungs and spleen, suggests that besides a stronger local immune response also a stronger systemic response plays a role in the pathogenesis of the studied dual infections compared to infection with APEC only. The authors hypothesize that tissue resident macrophages in the

respiratory tract that first encountered the virus as part of the innate immune response will be activated to secrete cytokines and chemokines. This will lead to the recruitment of additional immune cells such as T cells and more macrophages to the infected tissue. Next, also systemic immune responses will be induced by the cytokines and chemokines that easily spread to other organs including the spleen. Such sequence of events seems reflected by the demonstrated higher local IFNγ mRNA levels associated with mainly IBV and NDV infection at day 1 and the trend of higher systemic IFNγ mRNA levels in the spleen persisting at day 8.

Local and systemic immune responses induced by respiratory APEC infection in chicken were recently evaluated in detail, albeit without preceding viral infections.[1] Interestingly, in this study upregulation of IL-6 mRNA levels and the T_h1 pathway was observed, but also an APEC strain specific decrease of both IL-17 mRNA levels and heterophilic granulocyte recruitment. The higher IL-6 and IFNγ mRNA levels and CD4+ and KUL01+ cell numbers after previous viral infection as observed in the current work might therefore imply viral aggravation of an effect also caused by APEC itself. The viruses on the other hand seem to overrule a potentially present IL-17 and granulocyte decrease evoked by APEC, since in this study only higher mRNA levels and cell numbers were found in the virus-APEC groups when compared to the APEC-only group. Alternatively, the demonstrated presence of CD4+ lymphocytes and CD8αβ+ lymphocytes in the trachea after all viral-pre-infections may also be an aspecific consequence of the local inflammatory environment, resulting in attraction of bystander lymphocytes. The presence of such lymphocyte populations may contribute to virus-induced pathology, as has been shown in respiratory infections in mice,[9,36] and such effect might probably continue mechanistically largely independent during subsequent bacterial infection.

In contrast to the air sac and trachea, lesions in the lung seemed more APEC-associated, were more transient over time and mainly coincided with higher KUL01+ cell numbers. In chicken, KUL01+ cells mostly represent monocytes and macrophages. Macrophages and heterophilic granulocytes are important anti-bacterial effector cells.[1,2,27] Via secretion of IL-17, TCR1+ lymphocytes are known to have pro-inflammatory influences on both macrophage and granulocyte

function, promoting effective bacterial clearance.[22,45,47] In the current work, IL-17 expression locally in the lung was not significantly different for the virus-APEC-infected birds and the birds infected with APEC only, but did differ in the spleen. These virus-dependent systemic effects may probably contribute to enhanced clinical disease after dual infection.[26]

The observed limited influence of viral inoculation on lung lesion severity may be explained by the fact that none of the inoculated viruses usually primarily targets lung-specific cell populations (parabronchial and air capillary epithelium), with viral replication in the lung mostly restricted to the more 'upper respiratory tract-like' primary and secondary bronchi.[6,28,35] NDV and IBV nevertheless seemed to have a mild aggravating effect on induction of lung lesions. This may possibly be explained by the observed cellular debris in the parabronchial and air capillary lumina, likely derived via epithelial desquamation in the virus-infected upper respiratory tract and air sacs. Presence of this debris may trigger immune responses and induce pathologic tissue changes. Alternatively, this aggravation might be explained by hematogenous spread of cytokines or probably (mostly bacterial) antigen. Interestingly, compared to the NDV-APEC and IBV-APEC groups, less pathologic tissue changes were observed in the lungs after aMPV-APEC inoculation, which coincided with a trend of higher IL-6 levels at day 8. In chicken, aMPVs usually cause only mild infections of the very upper parts of the respiratory tract (nose, intraorbital sinuses, trachea),[35] which may explain low lesion severity compared to the other viruses. Alternatively, taking the observed IL-6 response and the immune cell increases in the air sacs into account, aMPV infection might coincide with a delayed pro-inflammatory response. This may explain lower immune cell influxes at day 1, as observed for many of the studied cell types, resulting in lower lesion severity. Such effect, however, might in the end enhance the risk of persisting infection with increase of lesion severity and clinical disease at later time points than studied here.[4] Additional temporal analysis for a longer total period and probably over shorter time intervals would be needed to further study this hypothesis.

The infection model investigated in this study has been used previously with the aim to elucidate immunopathologic mechanisms in chicken after dual infection

with IBV and APEC.[7,23,24] Although the observed IBV-APEC-induced lesion distribution and persistence are in line with the previously published data, the overall lesion severity (based on macroscopic scoring) and its effect on the birds' body weight seems lower in the current study. This may be due to epigenetic changes in the commercial broilers used for the experiments, resulting from genetic selection within the commercial parental chicken flocks in the last decades.[49] Nevertheless, the fact that the birds developed antibody titres against the inoculated viruses and the fact that pathogen-dependent lesion differences were observed validate effective use of the current infection model.

In conclusion, this study demonstrates that a dual infection in the broiler respiratory tract, resulting from inoculation with APEC preceded by IBV, NDV or aMPV, may result in development of lesions that can persist for at least eight days. In these persisting lesions, interestingly, based on immunohistochemical analysis the inoculated bacteria could not be demonstrated eight days after infection. Furthermore, lesion severity and distribution over the respiratory tract may be at least partially determined by the tropism of the inoculated virus. These observations together might imply that APEC rather maintains primarily virus-induced tissue damage, instead of that the viruses only facilitate lesion development primarily defined by APEC and antibacterial host responses. In this respect, further studies including virus-PBS-inoculated control birds would be needed to determine in detail the specific contributions of both the virus and bacterium to the enhanced lesions resulting from these dual infection. The data further underscore an important role for the immune system in virus-APEC-induced disease. The results highlight the importance of protection against viral respiratory infections in chicken via vaccination and suggest that extensive antibiotic use in such dual infections might be of limited therapeutic value, since lesions persist in spite of an apparently effective bacterial clearance.

Acknowledgements

Special thanks go out to Robbert van Sambeek, Freek Weites and Marc Kranenburg for performing the animal experiments, the histology laboratory staff members of the Division of Pathology, Department Biomolecular Health

Sciences, for preparing the tissue slides and to Simone Pulles for her help with the immunohistochemical immune cell analyses.

Funding

This project is supported by the European Regional Development Fund and the province of Gelderland, the Netherlands.

Conflict of interest statement

The authors declare that they have no conflict of interest.

Abbreviations

APEC, avian pathogenic Escherichia coli;
IBV, infectious bronchitis virus;
NDV, Newcastle disease virus;
aMPV, avian metapneumovirus;
HEPA, high efficiency particulate air;
DEC, Dierexperimentencommisie;
TRT, turkey rhinotracheitis;
PBS, phosphate-buffered saline;
EID, egg infectious dose;
CFU, colony-forming units;
HI, haemagluttination inhibition;
ELISA, enzyme-linked immuno sorbent assay;
FFPE, formalin-fixed paraffin-embedded;
HE, haematoxylin and eosin;
BSA, bovine serum albumin;
(RT-q)PCR, (reverse transcription quantitative) polymerase chain reaction;
cDNA, complement DNA;
GAPDH, glyceraldehyde-3-phosphate dehydrogenase;
IL, interleukin;
IFN, interferon.

References

1. Alber, A., Morris, K.M., Bryson, K.J., Sutton, K.M., Monson, M.S., Chintoan-Uta, C., Borowska, D., Lamont, S.J., Schouler, C., Kaiser, P., Stevens, M.P., Vervelde, L., 2019. Avian pathogenic *Escherichia coli* (APEC) strain-dependent immunomodulation of respiratory granulocytes and mononuclear phagocytes in CSF1R-reporter transgenic chickens. Front. Immunol. 10, 3055, 1-16.

2. Ariaans, M. P., Matthijs, M.G.R., van Haarlem, D., van de Haar, P., van Eck, J.H., Hensen, E.J., Vervelde, L., 2008. The role of phagocytic cells in enhanced susceptibility of broilers to colibacillosis after infectious bronchitis virus infection. Vet. Immunol. Immunop. 123, 240-250.

3. Bakaletz, L. O., 1995. Viral potentiation of bacterial superinfection of the respiratory tract. Trends Microbiol. 3, 110-114.

4. Bocharov, G., Ludewig, B., Bertoletti, A., Klenerman, P., Junt, T., Krebs, P., Luzyanina, T., Fraser, C., Anderson, R.M., 2004. Underwhelming the immune response: effect of slow virus growth on CD8+-T-lymphocyte responses. J. Virol. 78, 2247-2254.

5. Dho-Moulin, M., Fairbrother, J.M., 1999. Avian pathogenic *Escherichia coli* (APEC). Vet. Res., 30, 299-316.

6. Dolz, R., Vergara-Alert, J., Perez, M., Pujols, J., Majo, N., 2012. New insights on infectious bronchitis virus pathogenesis: characterization of Italy 02 serotype in chicks and adult hens. Vet. Microbiol. 156, 256-264.

7. Dwars, R. M., Matthijs, M.G.R., Daemen, A.J., van Eck, J.H., Vervelde, L., Landman, W.J., 2009. Progression of lesions in the respiratory tract of broilers after single infection with *Escherichia coli* compared to superinfection with *E. coli* after infection with infectious bronchitis virus. Vet. Immunol. Immunop. 127, 65-76.

8. Eldaghayes, I., Rothwell, L., Williams, A., Withers, D., Balu, S., Davison, F. and Kaiser, P., 2006. Infectious bursal disease virus: strains that differ in virulence differentially modulate the innate immune response to infection in the chicken bursa. Viral Immunol. 19, 83-91.

9. Frey, S., Krempl, C. D., Schmitt-Gräff, A., Ehl, S., 2008. Role of T cells in virus control and disease after infection with pneumonia virus of mice. J. Virol. 82, 11619-11627.

10. Golda, A., Malek, N., Dudek, B., Zeglen, S., Wojarski, J., Ochman, M., Kucewicz, E., Zembala, M., Potempa, J., Pyrc, K., 2011. Infection with human coronavirus NL63 enhances streptococcal adherence to epithelial cells. J. Gen. Virol. 92, 1358-1368.

11. Goren, E., 1978. Observations on experimental infection of chicks with *Escherichia coli*. Avian Pathol. 7, 213-224.

12. Guabiraba, R., Schouler, C., 2015. Avian colibacillosis: still many black holes. FEMS Microbiol. Lett. 362, fnv118, 1-8.

13. Hament, J. M., Kimpen, J.L., Fleer, A., Wolfs, T.F., 1999. Respiratory viral infection predisposing for bacterial disease: a concise review. FEMS Immunol. Med. Microbiol. 26, 189-195.

14. Hendaus, M. A., Jomha, F. A., Alhammadi, A. H., 2015. Virus-induced secondary bacterial infection: a concise review. Ther. Clin. Risk Manag. 11, 1265-1271.

15. Horn, F., Correa, A. M., Barbieri, N.L., Glodde, S., Weyrauch, K.D., Kaspers, B., Driemeier, D., Ewers, C., Wieler, L.H., 2012. Infections with avian pathogenic and fecal *Escherichia coli* strains display similar lung histopathology and macrophage apoptosis. PloS One 7, e41031, 1-11.

16. Kotani, T., Odagiri, Y., Nakamura, J., Horiuchi, T., 1987. Pathological changes of tracheal mucosa in chickens infected with lentogenic Newcastle disease virus. Avian Dis. 31, 491-497.

17. Kudva, A., Scheller, E. V., Robinson, K. M., Crowe, C. R., Choi, S. M., Slight, S. R., Khader, S. A., Dubin, P. J., Enelow, R. I., Kolls, J. K., Alcorn, J.F., 2011. Influenza A inhibits Th17-mediated host defense against bacterial pneumonia in mice. J. Immunol. 186, 1666-1674.

18. Kukavica-Ibrulj, I., Hamelin, M. E., Prince, G. A., Gagnon, C., Bergeron, Y., Bergeron, M.G., Boivin, G., 2009. Infection with human metapneumovirus predisposes mice to severe pneumococcal pneumonia. J. Virol. 83, 1341-1349.

19. Lee, B., Robinson, K. M., McHugh, K. J., Scheller, E. V., Mandalapu, S., Chen, C., Di, Y. P., Clay, M. E., Enelow, R. I., Dubin, P. J., Alcorn, J. F., 2015. Influenza-induced type I interferon enhances susceptibility to gram-negative and gram-positive bacterial pneumonia in mice. Am. J. Physiol. – Lung C. 309, L158-167.

20. Li, W., Moltedo, B., Moran, T.M., 2012. Type I interferon induction during influenza virus infection increases susceptibility to secondary *Streptococcus pneumoniae* infection by negative regulation of gammadelta T cells. J. Virol. 86, 12304-12312.

21. Lokken, K. L., Mooney, J. P., Butler, B. P., Xavier, M. N., Chau, J. Y., Schaltenberg, N., Begum, R. H., Muller, W., Luckhart, S., Tsolis, R. M., 2014. Malaria parasite infection compromises control of concurrent systemic non-typhoidal *Salmonella* infection via IL-10-mediated alteration of myeloid cell function. PLoS Pathog. 10, e1004049, 1-13.

22. MacMicking, J., Xie, Q. W., Nathan, C., 1997. Nitric oxide and macrophage function. Annu. Rev. Immunol. 15, 323-350.

23. Matthijs, M. G., Ariaans, M. P., Dwars, R. M., van Eck, J. H., Bouma, A., Stegeman, A., Vervelde, L., 2009. Course of infection and immune responses in the respiratory tract of IBV infected broilers after superinfection with *E. coli*. Vet. Immunol. Immunop. 127, 77-84.

24. Matthijs, M. G., van Eck, J. H., Landman, W. J., Stegeman, J. A., 2003. Ability of Massachusetts-type infectious bronchitis virus to increase colibacillosis susceptibility in commercial broilers: a comparison between vaccine and virulent field virus. Avian Pathol. 32, 473-481.

25. McCullers, J. A., Rehg, J.E., 2002. Lethal synergism between influenza virus and *Streptococcus pneumoniae*: characterization of a mouse model and the role of platelet-activating factor receptor. J. Inf. Dis. 186, 341-350.

26. McGeachy, M. J., Cua, D. J., Gaffen, S.L., 2019. The IL-17 family of cytokines in health and disease. Immunity 50, 892-906.

27. Mellata, M., Dho-Moulin, M., Dozois, C.M., Curtiss, R., Lehoux, B., Fairbrother, J.M., 2003. Role of avian pathogenic *Escherichia coli* virulence factors in bacterial interaction with chicken heterophils and macrophages. Infect. Immun. 71, 494-503.

28. Nakamura, K., Ohtsu, N., Nakamura, T., Yamamoto, Y., Yamada, M., Mase, M., Imai, K., 2008. Pathologic and immunohistochemical studies of Newcastle disease (ND) in broiler chickens vaccinated with ND: severe nonpurulent encephalitis and necrotizing pancreatitis. Vet. Pathol. 45, 928-933.

29. Navarini, A. A., Recher, M., Lang, K.S., Georgiev, P., Meury, S., Bergthaler, A., Flatz, L., Bille, J., Landmann, R., Odermatt, B., Hengartner, H., Zinkernagel, R.M., 2006. Increased susceptibility to bacterial superinfection as a consequence of innate antiviral responses. PNAS 103, 15535-15539.

30. Ouyang, W., Kolls, J. K., Zheng, Y., 2008. The biological functions of T helper 17 cell effector cytokines in inflammation. Immunity 28, 454-467.

31. Peighambari, S. M., Julian, R.J., Gyles, C.L., 2000. Experimental *Escherichia coli* respiratory infection in broilers. Avian Dis. 44, 759-769.

32. Robinson, K. M., Kolls, J.K., Alcorn, J.F., 2015. The immunology of influenza virus-associated bacterial pneumonia. Curr. Opin. Immunol. 34, 59-67.

33. Robinson, K. M., McHugh, K.J., Mandalapu, S., Clay, M.E., Lee, B., Scheller, E.V., Enelow, R.I., Chan, Y.R., Kolls, J.K., Alcorn, J.F., 2014. Influenza A virus exacerbates *Staphylococcus aureus* pneumonia in mice by attenuating antimicrobial peptide production. J. Infect. Dis. 209, 865-875.

34. Rynda-Apple, A., Robinson, K.M., Alcorn, J.F., 2015. Influenza and bacterial superinfection: Illuminating the immunologic mechanisms of disease. Infect. Immun. 83, 3764-3770.

35. Saif, Y. M., Fadly, A. M., Glisson, J.R., McDougald, L.R., Nolan, L.K., Swayne, D.E., 2008. Diseases of Poultry (12th Ed.), Iowa State University Press, Arnes, AI, US.

36. Schmidt, M. E., Knudson, C. J., Hartwig, S. M., Pewe, L. L., Meyerholz, D. K., Langlois, R. A., Harty, J. T., Varga, S.M., 2018. Memory CD8 T cells mediate severe immunopathology following respiratory syncytial virus infection. PLoS Pathog. 14, e1006810, 1-10.

37. Shahangian, A., Chow, E. K., Tian, X., Kang, J. R., Ghaffari, A., Liu, S. Y., Belperio, J. A., Cheng, G., Deng, J.C., 2009. Type I IFNs mediate development of postinfluenza bacterial pneumonia in mice. J. Clin. Invest. 119, 1910-1920.

38. Smith, M. W., Schmidt, J. E., Rehg, J. E., Orihuela, C. J., McCullers, J. A., 2007. Induction of pro- and anti-inflammatory molecules in a mouse model of pneumococcal pneumonia after influenza. Comp. Med. 57, 82-89.

39. Staines, K., Hunt, L.G., Young, J.R., Butter, C., 2014. Evolution of an expanded mannose receptor gene family. PloS One 9, e110330, 1-10.

40. Sun, K., Metzger, D.W., 2008. Inhibition of pulmonary antibacterial defense by interferon-gamma during recovery from influenza infection. Nat. Med. 14, 558-564.

41. Unanue, E.R., 1984. Antigen-presenting function of the macrophage. Annu. Rev. Immunol. 2, 395-428.

42. van de Zande, S., Nauwynck, H., Pensaert, M., 2001. The clinical, pathological and microbiological outcome of an *Escherichia coli* O2:K1 infection in avian pneumovirus infected turkeys. Vet. Microbiol. 81, 353-365.

43. van der Sluijs, K. F., van Elden, L. J., Nijhuis, M., Schuurman, R., Pater, J.M., Florquin, S., Goldman, M., Jansen, H.M., Lutter, R., van der Poll, T., 2004. IL-10 is an important mediator of the enhanced susceptibility to pneumococcal pneumonia after influenza infection. J. Immunol. 172, 7603-7609.

44. van Eck, J. H., Goren, E., 1991. An Ulster 2C strain-derived Newcastle disease vaccine: vaccinal reaction in comparison with other lentogenic Newcastle disease vaccines. Avian Pathol. 20, 497-507.

45. Walliser, I., Göbel, T.W., 2018. Chicken IL-17A is expressed in αβ and γδ T cell subsets and binds to a receptor present on macrophages, and T cells. Dev. Comp. Immunol. 81, 44-53.

46. Wu, Y., Tu, W., Lam, K.T., Chow, K.H., Ho, P.L., Guan, Y., Peiris, J.S., Lau, Y.L., 2015. Lethal coinfection of influenza virus and *Streptococcus pneumoniae* lowers antibody response to influenza virus in lung and reduces numbers of germinal center B cells, T follicular helper cells, and plasma cells in mediastinal lymph Node. J. Virol. 89, 2013-2023.

47. Ye, P., Rodriguez, F.H., Kanaly, S., Stocking, K. L., Schurr, L., Schwarzenberger, P., Oliver, P., Huang, W., Zhang, P., Zhang, J., Shellito, J.E., Bagby, G.J., Nelson, S., Charrier, K., Peschon, J. J., Kolls, J.K., 2001. Requirement of interleukin 17 receptor signaling for lung CXC chemokine and granulocyte colony-stimulating factor expression, neutrophil recruitment, and host defense. J. Exp. Med. 194, 519-527.

48. Yoo, J., Chang, H.H., Bae, Y. H., Seong, C. N., Choe, N. H., Lillehoj, H. S., Park, J. H., Min, W., 2008. Monoclonal antibodies reactive with chicken interleukin-17. Vet. Immunol. Immunop. 121, 359-363.

49. Zou, A., Nadeau, K., Wang, P.W., Lee, J.Y., Guttman, D.S., Sharif, S., Korver, D.R., Brumell, J.H., Parkinson, J., 2020. Accumulation of genetic variants associated with immunity in the selective breeding of broilers. BMC Genet. 21, 5, 1-14.

5 The histopathological phenotype of enhanced airsacculitis after dual infection with infectious bronchitis virus strain H52 and avian pathogenic *Escherichia coli* strain 506

E.A.W.S. Weerts [a], C.A. Jansen [b], M.G.R. Matthijs [c], R.M. Dwars [c], M.H. Verheije [a], A. Gröne [a],

[a] Division of Pathology, Department Biomolecular Health Sciences, Faculty of Veterinary Medicine, Utrecht University, Utrecht, the Netherlands

[b] Cell Biology and Immunology Group, Department of Animal Sciences, Wageningen University and Research, Wageningen, the Netherlands

[c] Division of Farm Animal Health, Department Population Health Sciences, Faculty of Veterinary Medicine, Utrecht University, Utrecht, the Netherlands

in preparation

Abstract

Viral respiratory infection is known to predispose for secondary bacterial disease across species. In chickens, infectious bronchitis virus (IBV) facilitates respiratory colibacillosis, caused by avian pathogenic *Escherichia coli* (APEC). Chicken air sacs often are severely affected by such dual infections and this study aimed to elucidate the contributions of IBV and APEC to these air sac changes. To reduce experimental animal use, surplus uninfected control chickens from another experiment were inoculated with IBV strain H52 and APEC strain 506 as single or dual infection. Air sacs were scored microscopically for presence of viral and bacterial antigen, epithelial changes and immune cell quantities. IBV infection caused marked heterophilic and lymphoplasmacytic airsacculitis with epithelial necrosis and intralesional viral protein at 5 days post infection (dpi.) At 12 dpi, epithelial linings in IBV-infected air sacs were intact with a markedly decreased inflammatory cell infiltrate rich in Bu1+ cells (mostly B cell lineages). After APEC infection only, the epithelium was intact, though swollen with an increased proliferative state indicated by expression of proliferative cell nuclear antigen (PCNA). This coincided with fairly mild infiltration of heterophils and KUL01+ cells (monocytes / macrophages). Birds coinfected with IBV and APEC showed the most severe lesions with marked epithelial loss and presence of many heterophils, KUL01+ cells and Bu1+ B cells. Intralesional APEC antigen was detected only in few dually-infected birds. These findings demonstrate that exacerbated airsacculitis after dual infection with the studied IBV and APEC strains phenotypically shares many morphologic aspects with lesions caused by IBV only.

Highlights

Dual infection of IBV and APEC induced severe airsacculitis in broiler chickens.

Epithelial damage and lymphocyte infiltration seemed mostly IBV-associated.

APEC mostly induced monocyte/macrophage increase and PCNA expression.

Persistent IBV damage might predominantly define IBV+APEC-induced airsacculitis.

Keywords

chicken - airsacculitis - dual infection - infectious bronchitis virus (IBV) - avian pathogenic *Escherichia coli* (APEC) – epithelium – immune cells

Introduction

Dual infection of a virus and bacterium often induces tissue damage that is more severe than the damage that is caused by both pathogens separately. This is a well-known phenomenon across animal species and humans and is often seen in respiratory disease. Ineffective bacterial clearance from the airways and facilitation of bacterial adherence to the airway surface have been classically attributed to virus-induced damage to the mucociliary apparatus.[4,5,14,30] However, dysregulation of the anti-bacterial immune response by viruses has been proposed as alternative or coinciding mechanism and is quite extensively studied mainly in mammals. Although data on immune cell involvement and cytokine release are often difficult to interpret, the current scientific consensus is that bacterial airway disease following a viral infection is mainly influenced by aberrant immune responses.[28,31]

Infectious bronchitis virus (IBV) is an important pathogen of chickens that is primarily known as cause of respiratory disease. IBV is one of the viral pathogens that predisposes the chicken respiratory tract to secondary bacterial infection. Avian pathogenic *Escherichia coli* (APEC) is often involved in such dual infections. Depending on the bacterial strain, APEC can cause respiratory disease of variable severity.[1,12] Chickens that would normally be able to recover from single infection by certain APEC strains after several days, can develop severe respiratory and even systemic colibacillosis after prior IBV field infection or IBV vaccination, as is often seen in broiler chickens.[13,15,22] After sequential infection by IBV and APEC, these birds tend to develop extensive pneumonia, airsacculitis and polyserositis, which often remain present up to slaughter age. These diseases contribute to reduction of animal welfare, result in extensive economic losses due to growth rate reduction, raised mortality and higher condemnation rates at slaughter and also lead to increased antibiotic treatment.[16]

Previous studies that compared the effect of preexposure to IBV field and vaccine strains on APEC infection demonstrated that the extent of IBV-induced mucociliary damage in the respiratory tract was unlikely to be the major determinant for increased APEC pathogenicity.[22,23] Thereafter, research focus mostly switched towards IBV-driven immune modulation. Studies have shown that IBV can decrease bactericidal activity of macrophages *ex vivo*.[3] Other hampering effects on the anti-APEC response by prior IBV infection were considered to depend on T-helper, cytotoxic and γδ lymphocyte populations and alteration of expression of pro- and anti-inflammatory cytokines.[23] However, interpretation of the influences of immune parameters and tissue lesions on the development of IBV-induced colibacillosis has been difficult, in particular because chickens sequentially infected with both IBV and APEC were not consistently compared to chickens infected with IBV only.

Since the air sacs have been pinpointed as important site for enhancement of colibacillosis after IBV infection,[9,12,38] the present study aimed to compare air sac lesions induced by single infections of both APEC and IBV with lesions caused after sequential infection by both pathogens with specific focus on epithelial changes and immune cell presence.

Materials and methods

Experimental birds

With the aim to reduce the use of experimental animals, surplus uninfected control chickens from another experiment were used. Commercial Ross 308 eggs (Lagerwey, the Netherlands, *Mycoplasma gallisepticum* free) were hatched and broiler chicks were housed in negative pressure high-efficiency particulate air (HEPA)-filtered isolators. Up to day 15, animals were kept in light for 23 hours a day with food ad libitum. After day 15, light was reduced to sixteen hours a day and feed was restricted to prevent growth-related health problems. Drinking water was provided ad libitum during the whole experiment. Light was changed from white to red from day four on to prevent cannibalism. During the first 31 days, the isolator temperature was gradually reduced from 35° C to 18°

C and thereafter kept at 18° C. For the experimental infection 27 female birds were used.

Ethical statement

All experiments were approved by the Animal Experimental Committee of Utrecht University, according to the Dutch regulation on experimental animals (DEC number 2014.III.12.19).

IBV and APEC inocula

IBV vaccine strain H52 (AviPro IB H52, Lohmann Animal Health GmbH, Cuxhaven, Germany), titer $1.0 \times 10^{5.68}$ EID_{50}/ml, was prepared in phosphate buffered saline (PBS). Birds were inoculated both oculonasally (0.2 ml per bird, 0.05 ml per eye and nostril) and intratracheally (1 ml per bird) with a total of $1.2 \times 10^{5.68}$ EID_{50} of virus applied per bird. APEC strain 506 (isolated by Van Eck and Goren, 1991)[36] was administered at $1.0 \times 10^{7.6}$ CFU per bird via the intratracheal route. The APEC inoculum was prepared as previously described.[22]

Experimental design

At day 16 of age (day 0 of the infection experiment), chickens were randomly divided into one group of ten birds, one group of seven birds and two groups of five birds and these were housed in separate isolators. The group of ten birds was inoculated with IBV. At 5 days post inoculation (dpi) five birds of this group were euthanized (referred to as group 'IBV 5 dpi'), the other birds were then mock-inoculated with PBS only and euthanized seven days later at 12 dpi (referred to as group 'IBV 12 dpi'). The group of seven birds was mock-inoculated with PBS only. At 5 dpi two of these birds were euthanized and the remaining five birds were again mock-inoculated with PBS and euthanized at 12 dpi (referred to as combined group 'mock'). One group of five birds was first mock-inoculated with PBS only. At 5 dpi this group received APEC inoculum and the birds were euthanized at 12 dpi (referred to as group 'APEC'). The other group of five birds was at 0 dpi first inoculated with IBV, sequentially received APEC inoculum at 5 dpi and the birds were also euthanized at 12 dpi (referred to as group 'IBV+APEC') (Table 1).

Table 1. Experimental groups with inoculations per time point. 16 day-old broilers were inoculated with IBV or mock-infected with PBS and sequentially infected with APEC or mock-infected with PBS at 5 dpi. Birds were euthanized 5 or 12 dpi.

Name of group	0 dpi	5 dpi	12 dpi
IBV 5 dpi [a]	IBV H52	euthanized	-
IBV 12 dpi [a]	IBV H52	PBS	euthanized
APEC	PBS	APEC strain 506	euthanized
IBV+APEC	IBV H52	APEC strain 506	euthanized
mock	PBS	PBS (n = 5), euthanized (n = 2)	euthanized (n = 5)

All groups (n = 5), except PBS (n = 7); [a] groups initially housed together (n = 10), of which 5 birds were taken out and euthanized at 5 dpi before the other 5 were sequentially mock-infected and euthanized at 12 dpi.

Post-mortem examination was performed directly after euthanasia and two adjacent tissue samples of the caudal thoracic air sacs (overlying and adjacent to the kidneys) were taken; one sample was fixed in 10% formalin, the other one was snap-frozen in liquid nitrogen and stored at -80° C. In addition, the middle segment of the trachea and a cranial piece of lung were taken and fixed in formalin. After 24-48 hours, formalin-fixed tissue samples were dehydrated and embedded in paraffin.

Histochemical and immunohistochemical tissue staining

Four µm thick slides were cut from formalin-fixed, paraffin-embedded tissues and stained histochemically for morphologic evaluation with haematoxylin and eosin (HE) according to standard laboratory procedures.

Presence of IBV within the tissue was demonstrated using a monoclonal antibody (Mab) against spike protein 2 (S2) with incubation details as previously published.[35] The presence of APEC was visualized using a polyclonal antiserum as previously published.[9]

The epithelium was labeled with an antibody against pancytokeratin (PCK). Proliferating epithelial cells were visualized with an antibody against proliferating cell nuclear antigen (PCNA). For visualization of PCK and PCNA expression, slides were deparaffinized and rehydrated in ethanol series. Antigen retrieval was performed by boiling slides in citrate buffer, pH 6.0, for fifteen minutes and endogenous peroxidase activity was blocked with 1% hydrogen

peroxidase solution in methanol. Slides were incubated overnight at 4°C with Mab anti-PCK diluted 1:1600 and Mab anti-PCNA diluted 1:1000 in phosphate-buffered Normal Antibody Diluent (NAD, ScyTek Laboratories, Logan, USA). Positive controls included skin for PCK and intestine for PCNA, in negative controls the first Mab was replaced by mouse IgG2a control reagent (Agilent Technologies, Santa Clara, USA). Antibody binding was visualized with Envision+ System- HRP-labelled Polymer anti-mouse (Agilent Technologies, Santa Clara, USA), undiluted with 30 minute incubation at room temperature (RT).

Five immune cell subsets were visualized via immuno-labelling of cryosections: KUL01+ cells (monocytes / macrophages),[21] CD4+ cells (T-helper cells), CD8αβ+ cells (cytotoxic T cells), TCRγδ+ cells (γδ T cells) and Bu-1+ cells (mostly B cells, in addition also a minor subpopulation of macrophages).[17] Eight µm thick sections were cut from frozen air sac samples on KP Plus slides (VWR International, Radnor, PA, USA), which were air-dried for two hours and then fixed in cold acetone for ten minutes. Endogenous peroxidase activity was blocked with 1% hydrogen peroxidase. All Mabs (Table 2) were diluted 1:1000 (KUL01 1:2000) in PBS + 0,5% bovine serum albumin (BSA) and incubated for one hour at RT. Chicken spleen and other airway mucosa samples functioned as positive control tissues, in negative controls the first Mab was replaced by the same control reagent as mentioned above. Mab binding was visualized with the similar Envision Polymer, diluted 1:1 in PBS with one hour incubation at RT.

All Envision Polymer binding was visually demonstrated with 3-amino-9-ethylcarbazole chromogen substrate (AEC) (Agilent) after incubation for fifteen minutes at RT. All slides were counterstained with haematoxylin, mounted with Aquatex (Merck, Darmstadt, Germany) and evaluated via light microscopy. Details on all used antibodies are listed in Table 2.

Histopathological scoring

HE-stained tissue slides were evaluated for epithelial changes, infiltration of heterophils and presence of mononuclear inflammatory cells (macrophages, lymphocytes and plasma cells), based on recommendations for histopathological scoring.[11,26] Epithelial changes were assigned to four

Table 2. Antibodies used for immunohistochemical stainings

Target	Antibody	Antibody type	Manufacturer
IBV S2	Ch/IBV 26.1	mouse Mab	ThermoFischer Scientific, Waltham, USA
APEC 506	APEC 506	rabbit polyclonal antiserum	Matthijs *et al*. 2009
cytokeratin	PCK	rabbit polyclonal antiserum	Agilent Technologies, Santa Clara, USA
PCNA	PCNA	mouse Mab	ThermoFischer Scientific, Waltham, USA
monocytes / macrophages	KUL01	mouse Mab, anti-chicken	Southern Biotech, Birmingham, USA
T-helper cells	CD4	mouse Mab, anti-chicken	Southern Biotech, Birmingham, USA
cytotoxic T cells	CD8αβ	mouse Mab, anti-chicken	Southern Biotech, Birmingham, USA
γδ T cells	TCRγδ	mouse Mab, anti-chicken	Southern Biotech, Birmingham, USA
B cells (+ minor macrophage subpopulation)	Bu-1	mouse Mab, anti-chicken	Southern Biotech, Birmingham, USA

categories (flat, cuboidal, ciliated columnar and unrecognizable / lost due to inflammatory changes) and an estimation was made of the percentages (10% steps) per category per air sac sample and converted to a score: grade 0 = normal morphology; grade 1 = mild changes; grade 2 = moderate changes; grade 3 = marked changes (detailed scoring criteria in Table 3, adapted from [38]). Heterophils and mononuclear cells were identified based on cell morphology and counted in five representative light microscopic captured images (CIs) of 0,0775 mm^2 (in total 0,39 mm^2) per air sac sample. The average cell count for the five images was converted to a severity grade per bird (grades 0 to 3), which was adapted for the percentage of tissue affected by cell infiltration (see Table 3 for details). Lymphoid nodules were excluded from these counts and recorded separately. In addition, the average thickness of the air sacs was defined per bird by use of a measuring tool in the captured images via imaging software (Olympus cellSens®).

Table 3. Histopathologic lesion scoring. Air sac lesions were semi-quantifically scored per group per bird for 3 parameters (epithelium, heterophilic infiltration, mononuclear cell infiltration). The scores for heterophilic and mononuclear cell infiltration (based on cell counts, average of 5 captured images) were corrected for the percentage of tissue affected by this infiltration.

Score	Parameter	Correction factor (CF)
	Epithelium	
0	mainly flat and ciliated cells, <10% cuboidal cells, no necrosis	
1	mild: 10-50% cuboidal cells, no necrosis	
2	moderate: > 50% cuboidal cells and / or 1-49% necrosis / cell loss	
3	severe: > 50% necrosis / cell loss	
	Heterophils	
0	< 1 cell, average of 5 CIs	% affected tissue [a]
1	mild: < 10 cells, average of 5 CIs	
2	moderate: 10-50 cells, average of 5 CIs	
3	severe: > 50 cells, average of 5 Cis	
	Mononuclear cells	
0	< 50 cells, average of 5 CIs	% affected tissue [a]
1	mild: 50-100 cells, average of 5 CIs	
2	moderate: 101-200 cells, average of 5 CIs	
3	severe: > 200 cells, average of 5 Cis	

[a] e.g. 10% of the tissue affected = CF 0.1; 50% of the tissue affected = CF 0.5; etc. CI = captured image of 0.0775 mm^2

Epithelial PCNA index

Within five representative CIs of 0,0775 mm^2 that always included areas within the tissue with the highest expression, a 1000 nuclei of epithelial cells were counted per air sac sample and the number of nuclei that expressed PCNA was registered. This was converted to a PCNA index per air sac sample by calculating the percentage of positive nuclei per 1000 cells.

Immune cell quantification

Per cryoslide, ten representative areas of 0.34 mm^2 (= one high power field (HPF), 400x magnification) were selected per tissue sample and individual cells showing specific antibody binding were counted. The total cell count was

divided by ten for an average count per immune cell type per bird. For the purpose of interpretation, average fold changes per experimental group compared to the mock-infected birds were calculated per cell type by dividing the average cell count of the experimental group (x) minus the average cell count in the mock-infected group (y) by the average cell count in the mock-infected group ((x-y)/y).

Statistical analysis

Variation in histopathologic lesion scores and immune cell counts was analyzed using the Kruskal-Wallis test and the Mann-Whitney U test for between-group variation (GraphPad Prism ®, version 9). Differences were considered significant with a p-value of 0.05 or lower, but in addition p-values ≤0.10 were also defined.

Results

IBV-induced lesions

Air sacs of IBV-infected chickens showed marked epithelial swelling and several areas where epithelium was completely obscured due to inflammatory cell infiltration or lost due to necrosis in 3/5 birds at 5 dpi. These air sacs were infiltrated by large numbers of heterophils and macrophages, lymphocytes and plasma cells (Fig. 1A). In contrast, air sacs of 5/5 IBV-infected chickens at 12 dpi had an intact, though multifocally to diffusely swollen epithelial lining when compared to those of mock-infected birds (Fig. 1B). This coincided with minimal infiltration of heterophils, though with presence of many lymphocytes and plasma cells and fewer macrophages. In these birds, the interstitium showed multifocal fibrosis. Lymphoid follicles were seen in 3/5 birds in both groups (table 4).

Table 4. Presence of lymphoid nodules within the air sac samples

Group	Lymphoid nodules	
	birds with nodules	nodules per air sac sample
IBV 5 dpi	3/5	9 – 12 – 25
IBV 12 dpi	3/5	2 – 15 – 22
APEC	0/5	-
IBV+APEC	4/5	2 – 2 – 5 - 9
mock	2/6	2 - 5

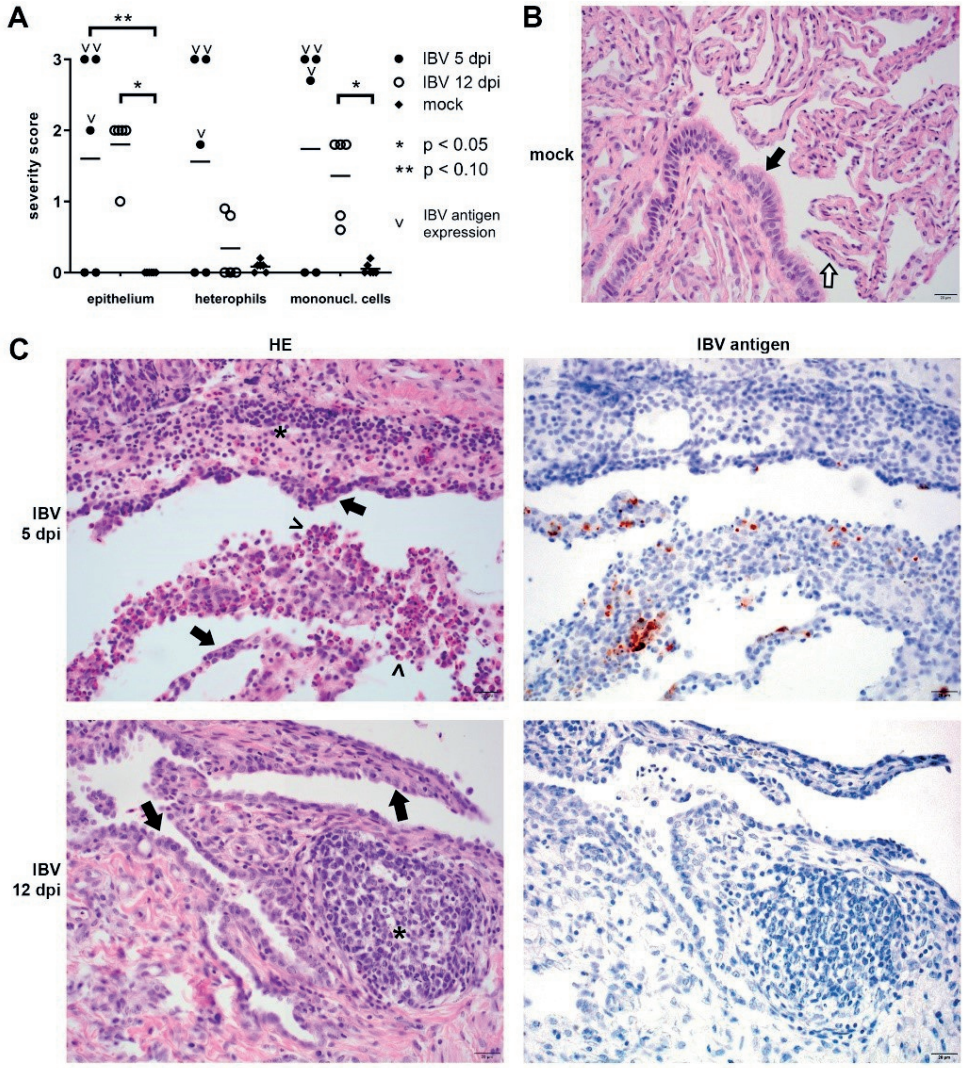

Figure 1 IBV-induced air sac lesions. A) Histopathological lesion scores: comparison of air sac lesion severity for three parameters (1: epithelium; 2: heterophilic infiltration; 3: mononuclear cell infiltration; scores defined as shown in table 3) of individual birds with average per group for three bird groups, group 1: IBV 5 dpi; group 2: IBV 12 dpi; group 3: mock. V = individual bird with intralesional IBV antigen expression. **B)** air sac of mock-infected chicken with normal morphology, HE-staining. The tissue consist of a thin layer of connective tissue, covered by mostly flat cells (white arrow) and sometimes foci of ciliated columnar cells (black arrows); **C)** representative histological examples of air sacs of birds infected with IBV 5 dpi and 12 dpi, HE-staining with serial tissue slides showing viral antigen expression. Epithelium or epithelial remnants (arrows), heterophils (arrow heads), mononuclear cells or lymphoid nodules (asterisks). All scale bars: 20 µm.

Tissue changes coincided with viral protein expression in the air sac epithelium at 5, but not at 12 dpi (Fig. 1C). Additionally, viral protein expression was observed in the trachea (4/5 birds) and lungs (2/5) birds at 5 dpi (Table 5). One mock-inoculated bird at 12 dpi was excluded from further evaluation, because its air sac samples contained large pieces of plant material that, considering associated lesions, likely were inhaled during the experiment. The other mock-inoculated birds had air sacs with similar morphology at 5 and 12 dpi and were further considered as one group.

APEC-induced lesions with and without preceding IBV infection

Air sacs of 5/5 chickens that were first mock-infected and then received APEC showed an intact, but multifocally markedly swollen epithelial lining. This often coincided with loosely arranged interstitial collagen, likely due to oedema. Mild to moderate numbers of heterophils were present multifocally in 4/5 birds. Numbers of lymphocytes, plasma cells and macrophages were similar to those in mock-infected birds.

Air sacs of chickens that sequentially received IBV and APEC, however, showed either large coalescing areas with complete obscuring of the epithelium due to extensive heterophilic and mononuclear cell infiltration (3/5 birds) or an intact, though markedly swollen epithelial lining with diffuse presence of mild to moderate numbers of heterophils and mononuclear cells (2/5 birds). Compared to IBV-infected birds at 12 dpi that did not receive APEC, both epithelial changes and inflammatory cell infiltrates were more severe with significant differences in numbers of heterophils (Fig. 2A-B). Several lymphoid nodules were seen in 4/5 IBV+APEC-infected birds, but none were observed in birds that only received APEC (Table 4).

Mild amounts of APEC antigen was detected in the air sacs of 1/5 and in addition more abundantly in the lungs of 2/5 IBV+APEC-infected birds (Fig. 2C), but no antigen was found in birds that only were only inoculated with APEC. No IBV protein expression was observed in any of the IBV+APEC-infected birds (Table 5).

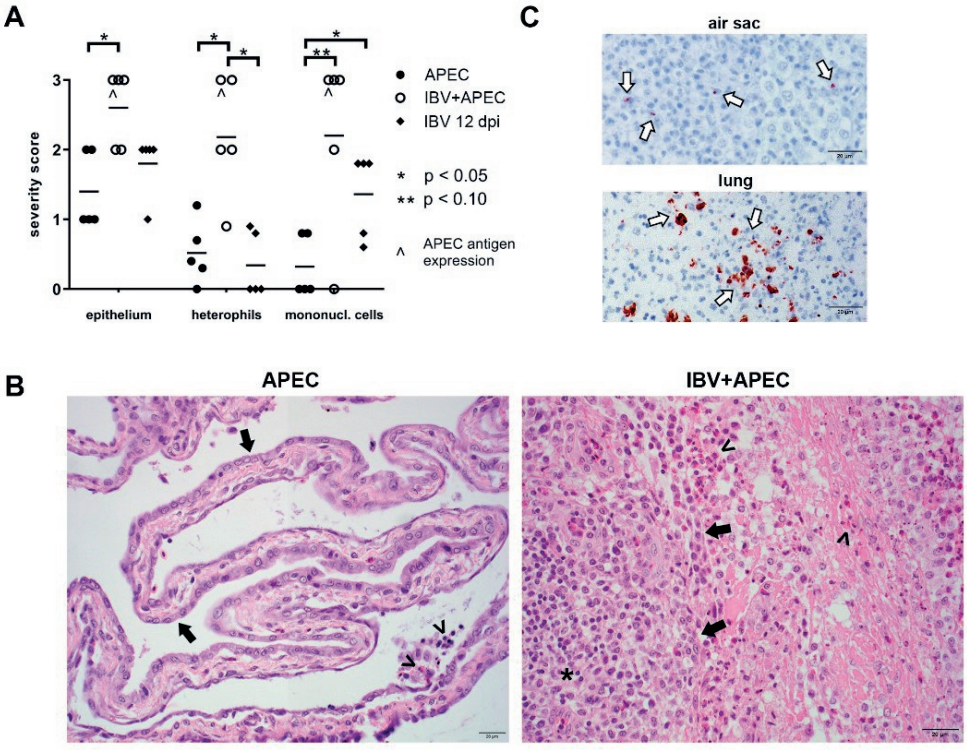

Figure 2 APEC-induced air sac lesions with and without previous IBV infection. A) Histopathological lesion scores: comparison of air sac lesion severity for three parameters (1: epithelium; 2: heterophilic infiltration; 3: mononuclear cell infiltration; scores defined as shown in table 3) of individual birds with average per group for three bird groups, group 1: APEC; group 2: IBV+APEC; group 3: IBV 12 dpi. Λ = individual bird with intralesional APEC antigen expression. **B)** representative histological examples of air sacs of APEC and IBV+APEC infected birds, HE-staining. Epithelium or epithelial remnants (arrows), heterophils (arrow heads), mononuclear cells (asterisk); **C)** APEC antigen expression (white arrows) in the air sac and lung of IBV-APEC-infected birds. All scale bars: 20 µm.

Table 5. IBV and APEC antigen expression. Presence of IBV and APEC was demonstrated via immuno-histochemical staining within the air sacs and additionally in the trachea and lung.

Group	air sac		trachea		lung	
	IBV	APEC	IBV	APEC	IBV	APEC
IBV 5 dpi	**3/5**	0/5	**4/5**	0/5	**2/5**	0/5
IBV 12 dpi	0/5	0/5	0/5	0/5	0/5	0/5
APEC	0/5	0/5	0/5	0/5	0/5	0/5
IBV+APEC	0/5	**1/5**	0/5	0/5	0/5	**2/5**
mock	0/6	0/6	0/6	0/6	0/6	0/6

Air sac thickness and epithelial PCNA index

Air sac thickness was increased in most of the infected chickens in all experimental groups compared to the mock-infected birds (on average 25.6 µm). This increase was significantly different for respectively the IBV+APEC (325.4 µm), the IBV 12 dpi (97.56 µm) and the APEC group (56.88 µm) and also clearly, though not statistically different in the IBV 5 dpi group (91.58 µm) (Fig. 3A). Increased air sac thickness in the IBV 5 dpi group resulted mainly from heterophilic and mononuclear cell infiltration. Increase of thickness in the IBV 12 dpi group was caused by epithelial swelling and increase of connective tissue with densely packed collagen fibres, in addition to mononuclear cell presence. In contrast, increase of air sac thickness in the APEC group in addition to epithelial swelling mostly coincided with loosely arranged collagen and optical clear spaces, which were likely the result of oedema. In the IBV+APEC group, in which on average the most severe air sac thickness increase was observed, all of the mentioned tissue changes were variably present with an emphasis on heterophilic and mononuclear cell infiltration.

Staining intensity of PCNA in nuclei was mostly faint to mild, but a group of nuclei with higher expression intensity could often be distinguished, which usually coincided with increased nuclear size (Fig. 3B). The PCNA index of the intact air sac epithelium on average increased for all infected birds with exception of the IBV 12 dpi group (26.6 on average, compared to 26.9 of the mock-infected group). The increase was significant for the IBV 5 dpi group (49.6), but the highest significant change was observed in the APEC group (65.1). In addition, increase of the PCNA index in the APEC group seemed to coincide with a marked increase of nuclei with high expression intensity. An average increase with rather broad variation was observed in the IBV+APEC group (40.0) (Fig. 3C).

No epithelial PCNA expression could be distinguished in the areas with epithelial necrosis and desquamation in the IBV 5 dpi and the IBV+APEC groups, in which nuclei of inflammatory cells also often showed PCNA expression. The ciliated columnar epithelium often presented with many PCNA positive nuclei, while only limited numbers of nuclei were PCNA positive in the flat epithelium. PCNA expression in cuboidal cells was most variable, but regularly abundant and with high intensity (Fig. 3D-E).

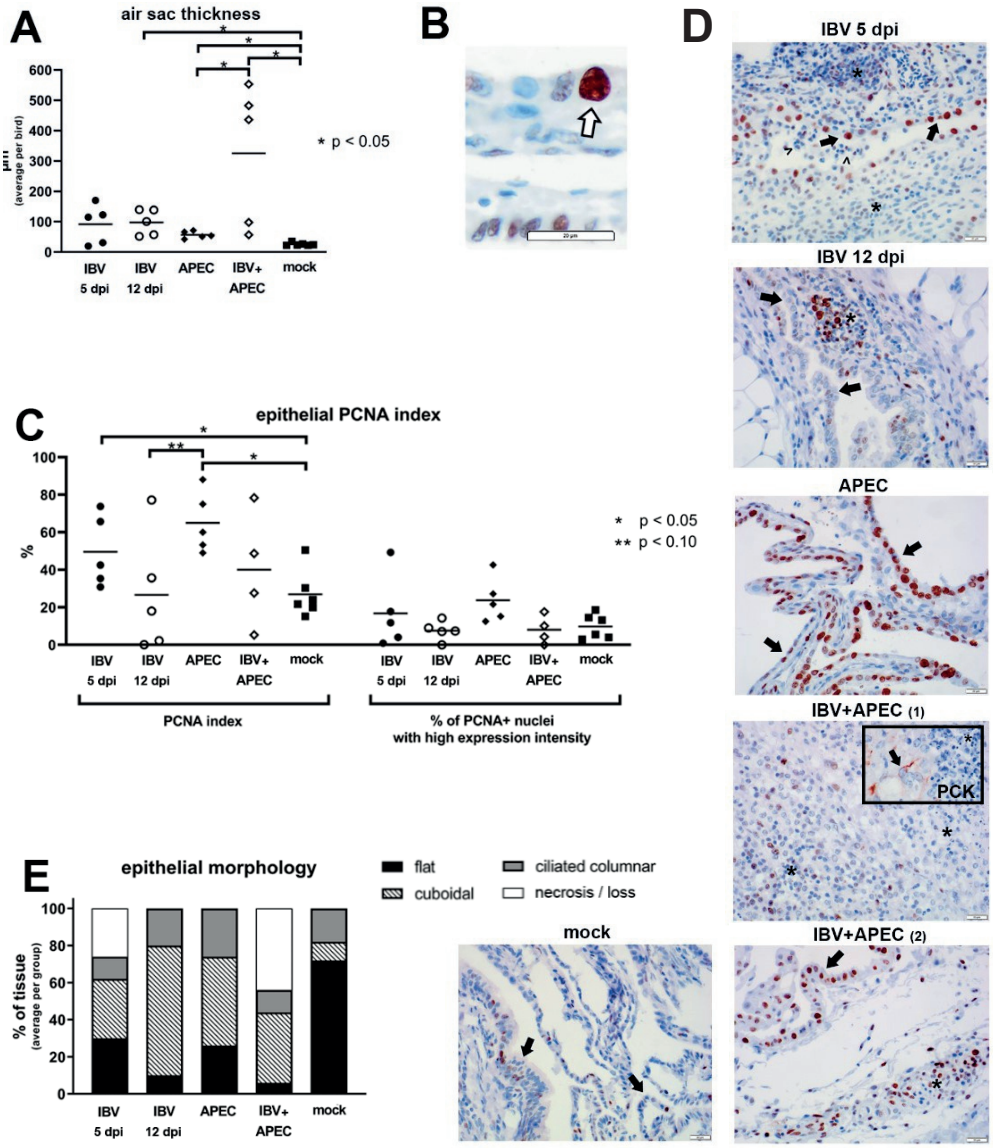

Figure 3 Interstitial thickness and epithelial proliferative cell nuclear antigen (PCNA) index. A) average air sac thickness per bird per group; **B)** PCNA expression, example of staining intensities. Nuclear staining with mild to moderate intensity and one example of a swollen nucleus with high expression intensity (arrow); **C)** epithelial PCNA index per bird per group (% of nuclei with any staining intensity per 1000 nuclei) (left), with % of stained nuclei with high expression intensity separately visualized (right, not statistically analyzed); **D)** representative air sac examples, immunohistochemistry anti-PCNA. Epithelium or epithelial remnants (arrows), heterophils (arrow heads), mononuclear cells (asterisks). Inset picture: cytokeratin (PCK) expression, highlighting epithelial remnants within the severe air sac lesions of IBV-APEC-infected birds; **E)** epithelial morphology, average distribution per group over 4 morphologic categories. All scale bars: 20 μm.

Immune cell presence

Statistically significant increased numbers of heterophils were observed in the selected areas of the air sacs of the IBV+APEC group compared to the IBV 12 dpi group, the APEC group and the mock group (Fig. 4A). Compared to the mock group, the IBV 5 dpi and IBV+APEC group showed similar fold changes of heterophil numbers of respectively 16.6 and 17.2, with a more modest fold change within the selected areas of the APEC group of 0.6 (Table 6).

KUL01+ cells on average increased in all infected groups with fold changes of 2.1, 3.8, 4.7 and 9.5 for the IBV 5 dpi group, the IBV 12 dpi group, the APEC group and the IBV+APEC group respectively. These increases where statistically significant compared to the mock group for the APEC and IBV+APEC groups (Fig. 4B). Bu-1+ cells were on average increased in all groups (Fig. 4C) with highest fold changes in the IBV 12 dpi group (36.5) and the IBV+APEC group (24.7), a lower fold change in the IBV 5 dpi group (7.8) and the lowest fold change in the mock-APEC group (0.84) (Table 6).

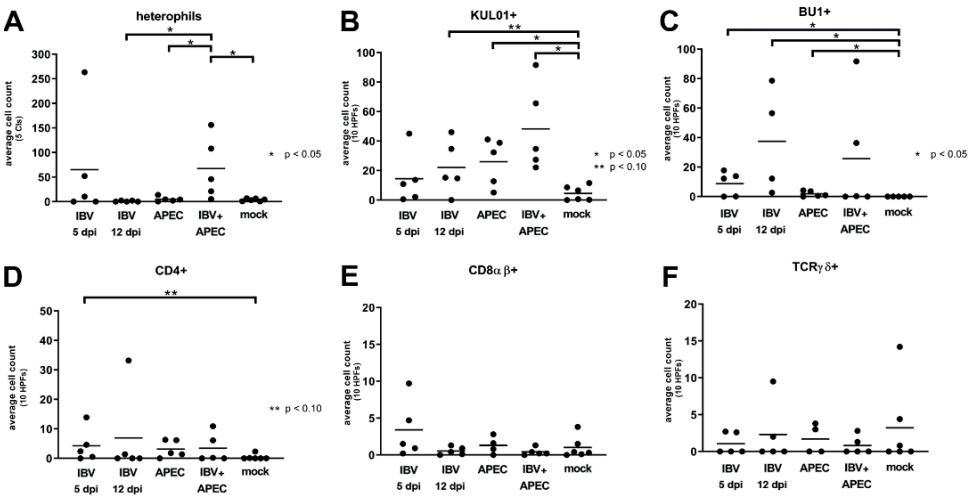

Figure 4 Quantification of immune cell populations within the air sacs. Average cell counts per bird per group for 6 cell populations; **A)** heterophils; **B)** KUL01+ cells (monocytes / macrophages); **C)** Bu1+ cells (majority B cells, minority certain subpopulation of macrophages); **D)** CD4+ cells (T helper cells); **E)** CD8αβ+ cells (cytotoxic T cells); **F)** TCRγδ+ cells (γδ T cells). CI = captured image (0,0775 mm^2), HPF = high power field, 400x magnification (0.34 mm^2).

Table 6. Immune cell population fold changes compared to mock-infected birds

Group	Immune cell populations					
	heterophils	KUL01+	Bu1+	CD4+	CD8αβ+	TCRγδ+
IBV 5 dpi	16.6	2.1	7.8	3.3	2.4	- 0.7
IBV 12 dpi	- 0.7	3.8	36.5	5.9	- 0.5	- 0.3
APEC	0.6	4.7	0.84	2.1	0.3	- 0.5
IBV+APEC	17.2	9.5	24.7	2.4	- 0.6	- 0.7

Increase of CD4+ cells was compared to mock-infected birds only statistically significant in the IBV 5 dpi group (Fig. 4D). However, increased cell numbers, albeit with lower fold changes compared to the mock-infected birds (Table 6), were also observed in the IBV 12 dpi group, the APEC group and the IBV+APEC group.

CD8αß+ cells were observed in higher numbers in the IBV 5 dpi group and slightly higher numbers in the APEC group (Fig. 4E) with fold changes compared to the mock-infected birds of respectively 2.4 and 0.3 (Table 6), but compared to the mock group lower numbers were counted in the IBV 12 dpi group and the IBV+APEC group.

TCRγδ+ cells were present in lower numbers in all infected groups (Fig. 4F). No statistically significant differences were observed between groups for the CD8αß+ and TCRγδ+ cells.

Discussion

In the present study, air sac lesions in broiler chickens were studied after a sequential dual infection with IBV and APEC and compared with birds that only received either IBV or APEC. Based on morphologic comparison, the air sac lesions that resulted from a dual infection with the studied variants of IBV (strain H52) and APEC (strain 506) phenotypically presented as a mixture of characteristics observed after 5 and 12 days after infection with IBV only. Therefore, these lesions might be explained as persisting damage primarily caused by IBV and further enhanced by APEC, rather than injury mostly caused by APEC and merely facilitated by tissue changes made by IBV. After dual infection, lesions in general had higher average severity, but this seldom coincided with intralesional presence of APEC antigen and never with remaining

IBV antigen. Infection with only IBV at 5 dpi caused marked heterophilic and mononuclear airsacculitis with multifocal epithelial necrosis, which were also prominent hallmark changes after dual infection. 12 days after IBV infection only, the air sac epithelium was intact but swollen and air sacs were often thickened by fibrosis, which was also observed after dual infection in areas with less severe inflammatory cell infiltration and intact epithelium. Air sacs of birds that only received APEC also had a swollen epithelial lining, but in contrast with air sacs after dual infection the epithelium nowhere showed necrosis or desquamation and was diffusely intact. Furthermore, in contrast with dually infected birds the inflammatory cell infiltration, especially of mononuclear cells, was very limited. The present work here adds considerably to the findings from earlier studies on dual respiratory infections with virus (mostly IBV) and APEC in chickens, because these studies either lacked the virus/IBV-only infected control groups,[9,38] the histopathological analysis[33] or both.[23]

The observed IBV-induced epithelial damage will likely affect the subsequent tissue response to APEC. Several studies have shown that the respiratory epithelium influences local immune responses and that virus-induced epithelial damage not only destroys the physical anti-bacterial epithelial barrier, but also hampers moderation of local immunologic reactions.[2,13,25,27,31] In the current study, predominantly the APEC strain 506 but also the IBV vaccine strain H52 both induced upregulation of PCNA expression by the air sac epithelium. PCNA is a protein that has a key function in cell replication, DNA repair and genome stability.[18,24] A recent study has demonstrated that specific APEC strains produce colibactin.[37] This is a genotoxin produced by several *E. coli* strains that can cause extensive DNA damage.[6,29,37] Upregulation of PCNA expression in the air sacs of birds inoculated with APEC might therefore potentially be explained as repair mechanism for such genotoxic effects established by APEC. It would need to be determined though whether the studied APEC strain 506 is truly able to produce this toxin and to which extent for better interpretation. IBV infection at 5 dpi also coincided with upregulated PCNA expression by morphologically intact and hence likely uninfected epithelial cells. Since it has been demonstrated that IBV causes cell cycle arrests and apoptosis within infected cells, it seems unlikely though that such upregulation would also be executed by IBV-infected epithelial

cells.[8,19] A lower average PCNA upregulation was observed in the intact air sac epithelium of birds infected with both pathogens compared to birds that received APEC only. Type I and III interferons, which are also important in avian antiviral defence, have been shown to hamper epithelial repair via proliferation in lungs of mice infected with influenza virus.[20] Further study would be needed to determine whether IBV can induce comparable negative influence on PCNA-mediated epithelial proliferation and DNA repair after sequential APEC infection and whether this effects contributes to enhanced lesion severity.

Single infections of IBV and APEC were associated with different composition of immune cell populations and some of these pathogen-associated differences seemed to be distinguishable within the air sacs of birds that were given both pathogens. Abundant heterophil infiltration was induced by IBV infection and this persisted with similar cell fold changes after introduction of APEC. In contrast, this infiltration reduced when no sequential APEC was given and persisted only mildly when APEC was inoculated alone. Heterophils can contribute to tissue damage via nonspecific enzymatic destruction and this might explain lesion enhancement after dual infection.[13] KUL01+ cells (monocytes / macrophages) were present in highest numbers in birds that received APEC, especially when IBV was inoculated first. Although KUL01+ cells were on average also increased after IBV inoculation alone, based on statistical significance the infiltration of this cell type seemed more APEC than IBV driven. This finding is supported by the fact that macrophages, together with heterophils, are known to be important effector cells in the first antibacterial defense in chicken colibacillosis.[1-3,13] However, since their number also increased after only IBV was given, KUL01+ positive cells might also be present for antigen presentation as part of cell-mediated adaptive immune responses. This could be supported by the observed presence of CD4+ cells, which did increase several folds in all infected birds and are key-mediators of such responses.[34]

In contrast with the KUL01+ cell influx, presence of Bu-1+ cells and lymphoid nodule formation were predominantly observed after IBV inoculation. These findings, which are mainly indicative of a B cell response, are in agreement with the fact that humoral immune responses play an important role in anti-IBV

defence.[7] Although scarce studies have indicated that humoral responses likely also play a role in defence against APEC,[2] in this study only limited observations supportive of B cell presence were made when APEC was inoculated alone. Apart from some mild increase of CD8αβ+ in the IBV 5 dpi group, which might suggest a cytotoxic anti-viral response,[7] no conclusions can be made about this cell type and TCRγδ+ cells, because numbers of both cells were rather low. CD8αβ+ cells in addition can also invade areas of inflammation as 'by-stander cells' and such cells can at their turn non-specifically contribute to tissue damage.[10,32]

In addition to epithelial changes and immune cell infiltration also changes in air sac thickness were observed. Both infections with IBV and APEC respectively, but especially dual infection with both pathogens were associated with marked increase of air sac thickness. After IBV infection this mostly resulted from inflammatory cell presence and at 12 dpi additionally from fibrosis, whereas after APEC infection this mostly seemed to result from oedema and epithelial swelling. After dual infection, a combination of all these changes contributed to air sac thickening. Thickening of the air sacs will likely decrease their elasticity, which might reduce proper air circulation and hamper oxygen exchange.

This study was performed as follow-up of another experiment with the aim to make better use of surplus uninfected control chickens and thereby in the end to reduce the use of experimental animals. Due to restricted numbers of available surplus birds and the number of available isolators at the research facility, choices needed to be made on the number of experimental groups and their size. This resulted in quite small group sizes and lack of a group inoculated with APEC only that could be studied earlier than 7 dpi after inoculation, for example 1 dpi as performed in earlier studies.[9,23] In these studies, in which the same APEC strain was used as in the current work, tissue changes caused by APEC only at 1 dpi however seemed to resolve quickly over time. Therefore, and due to the restricted number of available birds, this 1 dpi group was omitted in favor of the 7 dpi group, which was expected to be more indispensable to compare lesion persistence between groups over time.

In conclusion, this study demonstrates that severe airsacculitis caused by a dual infection of IBV strain H52 and APEC strain 506 displays several morphological characteristics that seem more attributable to the virus than to the bacterium. Important to note is that it remains to be seen whether the findings of this study are valid when other IBV variants and APEC strains are used and when the reciprocal inoculation sequence with the bacterium preceding the virus would be applied. Nevertheless, this view could change opinions on how to treat or prevent this type of airsacculitis and potentially other associated airway lesions in chickens, especially when future studies would further confirm that persistence of intralesional bacteria is indeed truly minimal and antibiotic treatment therefore might have limited effect.

Competing Interests

The authors declare that they have no competing interests.

Funding

The authors received no specific funding for this work.

Acknowledgements

The authors thank the animal care takers from the Division of Farm Animal Health, Department Population Health Sciences, Faculty of Veterinary Medicine of Utrecht University for their help during the in vivo experiment; colleague researchers and technical staff from the Division of Pathology, Department Biomolecular Health Sciences, Faculty of Veterinary Medicine of Utrecht University for their help during the necropsies and for tissue and slide processing; Jesper Bergmans, Tijmen van den Burght and Simone Pulles for participating in the immune cell analyses and Guy Grinwis for his critical reading and commenting on the manuscript.

References

1. Alber, A., Morris, K.M., Bryson, K.J., Sutton, K.M., Monson, M.S., Chintoan-Uta, C., Borowska, D., Lamont, S.J., Schouler, C., Kaiser, P., Stevens, M.P., Vervelde, L. (2019). Avian pathogenic *Escherichia coli* (APEC) strain-dependent immunomodulation of respiratory granulocytes and mononuclear phagocytes in CSF1R-reporter transgenic chickens. *Frontiers in Immunology*, 10, 1-16.

2. Alber, A., Stevens, M.P., Vervelde, L. (2021). The bird's immune response to avian pathogenic *Escherichia coli*. *Avian Pathology*, 50, 382-391.

3. Ariaans, M.P., Matthijs, M.G.R., van Haarlem, D.A., van de Haar, P., van Eck, J.H.H, Hensen, E.J., Vervelde, L. (2008). The role of phagocytic cells in enhanced susceptibility of broilers to colibacillosis after infectious bronchitis virus infection. *Veterinary Immunology and Immunopathology*, 123, 240-250.

4. Bakaletz, L.O. (1995). Viral potentiation of bacterial superinfection of the respiratory tract. *Trends in Microbiology*, 3, 110-114.

5. Brogden, K.A., Guthmiller, J.M. (2002). *Polymicrobial Diseases*. ASM Press, Washington.

6. Cuevas-Ramos, G., Petit, C.R., Marcq, I., Boury, M., Oswald, E., Nougayrède, J. (2010). *Escherichia coli* induces DNA damage in vivo and triggers genomic instability in mammalian cells. *Proceedings of the National Academy of Sciences of the United States of America*, 107, 11537-11542.

7. Dhinakar Raj, G., Jones, R.C. (1997). Infectious bronchitis virus: immunopathogenesis of infection in the chicken. *Avian Pathology*, 26, 677-706.

8. Dove, B., Brooks, G., Bicknell, K., Wurm, T., Hiscox, J.A. (2006). Cell cycle perturbations induced by infection with the coronavirus infectious bronchitis virus and their effect on virus replication. *Journal of Virology*, 80, 4147-4156.

9. Dwars, R. M., Matthijs, M.G.R., Daemen, A.J., van Eck, J.H., Vervelde, L., Landman, W.J., 2009. Progression of lesions in the respiratory tract of broilers after single infection with *Escherichia coli* compared to superinfection with *E. coli* after infection with infectious bronchitis virus. Vet. Immunol. Immunop. 127, 65-76.

10. Frey, S., Krempl, C.D., Schmitt-Gräff, A., Ehl, S. (2008). Role of T cells in virus control and disease after infection with pneumonia virus of mice. *Journal of Virology*, 82, 11619-11627.

11. Gibson-Corley, K.N., Olivier, A.K., Meyerholz, D.K. (2013). Principles for valid histopathologic scoring in research. *Veterinary Pathology*, 50, 1007-1015.

12. Goren, E. (1978). Observations on experimental infection of chicks with *Escherichia coli*. *Avian Pathology*, 7, 213-224.

13. Guabiraba, R., Schouler, C. (2015). Avian colibacillosis: still many black holes. *FEMS Microbiology Letters*, 362, 1-8.

14. Hendaus, M.A., Jomha, F.A., Alhammadi, A.H. (2015). Virus-induced secondary bacterial infection: a concise review. *Therapeutics and Clinical Risk Management*, 11, 1265-1271.

15. Jackwood, M.W. (2012). Review of infectious bronchitis virus around the world. *Avian Diseases*, 56, 634-641.

16. Ignjatovic, J., Sapats, S. (2000). Avian infectious bronchitis virus. *Revue Scientifique et Technique (Office International des Epizooties)*, 19, 493-508.

17. Igyártó, B.Z., Nagy, N., Magyar, A., Oláh, I. (2008). Identification of the avian B-cell-specific Bu-1 alloantigen by a novel monoclonal antibody. *Poultry Science*, 87, 351-355.

18. Kelman, Z. (1997). PCNA: structure, functions and interactions. *Oncogene*, 14, 629-640.

19. Li, F.Q., Tam, J.P., Liu, D.X. (2007). Cell cycle arrest and apoptosis incuded by the coronavirus infectious bronchitis virus in absence of p53. *Virology*, 365, 435-445.

20. Major, J., Crotta, S., Llorian, M., McCabe, T.M., Gad, H.H., Priestnall, S.L., Hartmann, R., Wack, A. (2020). Type I and III interferons disrupt lung epithelial repair during recovery from viral infection. *Science*, 369, 712-717.

21. Mast, J., Goddeeris, B.M., Peeters, K., Vandesande, F., Berghman, L.R. (1998). Characterisation of chicken monocytes, macrophages and interdigitating cells by the monoclonal antibody KUL01. *Veterinary Immunology and Immunopathology*, 61, 343-357.

22. Matthijs, M.G.R., van Eck, J.H.H., Landman, W.J.M., Stegeman, J.A. (2003). Ability of Massachusetts-type infectious bronchitis virus to increase colibacillosis susceptibility in commercial broilers: a comparison between vaccine and virulent field virus. *Avian Pathology*, 32, 473-481.

23. Matthijs, M.G.R., Ariaans, M.P., Dwars, R.M., van Eck J.H.H., Bouma, A., Stegeman J.A, Vervelde, L. (2009). Course of infection and immune responses in the respiratory tract of IBV infected broilers after superinfection with *E. coli*. *Veterinary Immunology and Immunopathology*, 127, 77-84.

24. Mayland, N., Gibbs-Seymour, I., Bekker-Jensen, S. (2013). Regulation of PCNA-protein interactions for genome stability. *Nature Reviews. Molecular Cell Biology*, 14, 269-282.

25. Melvin, J.A., Bomberger, J.M. (2016). Compromised Defenses: Exploitation of epithelial responses during viral-bacterial co-infection of the respiratory tract. *PLoS Pathogens*, 12,1-7.

26. Meyerholz, D.K., Beck, A.P. (2018). Principles and approaches for reproducible scoring of tissue stains in research. *Laboratory Investigation; A Journal of Technical Methods and Pathology*, 98, 844-855.

27. Mol, N., Peng, L., Esnault, E., Quere, P., Haagsman, H.P., Veldhuizen, E.J.A. (2019). Avian pathogenic *Escherichia coli* infection of a chicken lung epithelial cell line. *Veterinary Immunology and Immunopathology*, 210, 55-59.

28. Navarini, A.A., Recher, M., Lang, K.S., Georgiev, P., Meury, S., Bergthaler, A., Flatz, L., Bille, J., Landmann, R., Odermatt, B., Hengartner, H., Zinkernagel, R.M. (2006). Increased susceptibility to bacterial superinfection as a consequence of innate antiviral responses. *Proceedings of the National Academy of Sciences of the United States of America*, 103, 15535-15539.

29. Nougayrède, J., Homburg, S., Taieb, F., Boury, M., Brzuszkiewicz, E., Gottschalk, G., Buchrieser, C., Hacker, J., Dobrindt, U., Oswald, E. (2006). *Escherichia coli* induces DNA double-strand breaks in eurkaryotic cells. *Science*, 313, 848-851.

30. Peters, B.M., Jabra-Rizk, M.A., O'May, G.A., Costerton, J.W., Shirtliff, M.E. (2012). Polymicrobial interactions: impact on pathogenesis and human disease. *Clinical Microbiology Reviews*, 25, 193-213.

31. Robinson, K.M., Kolls, J.K., Alcorn, J.F. (2015). The immunology of influenza virus-associated bacterial pneumonia. *Current Opinion in Immunology*, 34, 59-67.

32. Schmidt, M.E., Knudson, C.J., Hartwig, S.M., Pewe, L.L., Meyerholz, D.K., Langlois, R.A., Harty, J.T., Varga, S.M. (2018). Memory CD8 T cells mediate severy immunopathology following respiratory syncytial virus infection. *PLoS Pathogens*, 14, 1-10.

33. Smith, H.W., Cook, J.K.A., Parsell, E. (1985). The experimental infection of chickens with mixtures of infectious bronchitis virus and *Escherichia coli*. *The Journal of General Virology*, 66, 777-786.

34. Unanue, E.R. (1984). Antigen-presenting function of the macrophage. *Annual Review of Immunology*, 2, 395-428.

35. van Beurden, S.J., Berends, A.J., Kramer-Kuhl, A., Spekreijse, D., Chenard, G., Philipp, H.C., Mundt, E., Rottier, P.J.M., Verheije, M.H. (2017). A reverse genetics system for avian coronavirus infectious bronchitis virus based on targeted RNA recombination. *Virology Journal*, 14, 1-13.

36. van Eck, J.J.H., Goren, E. (1991). An Ulster 2C strain-derived Newcastle disease vaccine: vaccinal reaction in comparison with other lentogenic Newcastle disease vaccines. *Avian Pathology*, 20, 497-507.

37. Wang, P., Zhang, J., Chen, Y., Zhong, H., Wang, H., Li, J., Zhu, G., Xia, P., Cui, L., Li, J., Dong, J., Gao, Q., Meng, X. (2021). Colibactin in avian pathogenic *Escherichia coli* contributes to the development of meningitis in a mouse model. *Virulence*, 12, 2382-2399.

38. Weerts, E.A.W.S., Matthijs, M.G.R., Bonhof, J., van Haarlem, D.A., Dwars, R.M., Gröne, A., Verheije, M.H., Jansen, C.A. (2021). The contribution of the immune response to enhanced colibacillosis upon preceding viral respiratory infection in broiler chicken in a dual infection model. *Veterinary Immunology and Immunopathology*, 238, 1-11.

6 Transmission kinetics and histopathology induced by European turkey coronavirus during experimental infection of specific pathogen free turkeys

P.A. Brown [a, b, #], C. Courtillon, E.A.W.S. Weerts [a, #], M. Andraud [a], C. Allée [a], A. Vendembeuche [a], M. Amelot [c], N. Rose, M.H. Verheije [d], N. Eterradossi [a]

[a] VIPAC Unit, Agence Nationale de Sécurité Sanitaire (ANSES), Laboratoire de Ploufragan-Plouzané, Université Bretagne Loire, Ploufragan, France

[b] EPICOREM Consortium, Unité de Recherche Risques Microbiens (U2RM), Université de Caen, Caen, France

[c] Division of Pathology, Department Biomolecular Health Sciences, Faculty of Veterinary Medicine, Utrecht University, Utrecht, the Netherlands

[d] EBEP Unit, Agence Nationale de Sécurité Sanitaire (ANSES), Laboratoire de Ploufragan-Plouzané, Université Bretagne Loire, Ploufragan, France

[e] SELEAC Unit, Agence Nationale de Sécurité Sanitaire (ANSES), Laboratoire de Ploufragan-Plouzané, Université Bretagne Loire, Ploufragan, France

published: Transboundary and Emerging Diseases, 2019; 66: 234-242.

Abstract

Numerous viruses, mostly in mixed infections, have been associated worldwide with poult enteritis complex (PEC). In 2008 a coronavirus (Fr-TCoV 080385d) was isolated in France from turkey poults exhibiting clinical signs compatible with this syndrome. In the present study, the median infectious dose (ID_{50}), transmission kinetics and pathogenicity of Fr-TCoV were investigated in 10-day-old SPF turkeys. Results revealed a titre of $10^{4.88}$ ID_{50}/ml with 1 ID_{50}/ml being beyond the limit of genome detection using a well-characterized qRT-PCR for avian coronaviruses. Horizontal transmission of the virus via the airborne route was not observed however, via the oro-faecal route this proved to be extremely rapid (one infectious individual infecting another every 2.5 hr) and infectious virus was excreted for at least 6 weeks in several birds. Histological examination of different zones of the intestinal tract of the Fr-TCoV-infected turkeys showed that the virus had a preference for the lower part of the intestinal tract with an abundance of viral antigen being present in epithelial cells of the ileum, caecum and bursa of Fabricius. Viral antigen was also detected in dendritic cells, monocytes and macrophages in these areas, which may indicate a potential for Fr-TCoV to replicate in antigen-presenting cells. Together these results highlight the importance of good sanitary practices in turkey farms to avoid introducing minute amounts of virus that could suffice to initiate an outbreak, and the need to consider that infected individuals may still be infectious long after a clinical episode, to avoid virus dissemination through the movements of apparently recovered birds.

Keywords

Coronavirus – histopathology – transmission - turkeys

Introduction

Coronaviruses, order *Nidovirales* family *Coronaviridae* are enveloped viruses with a genome of single stranded positive sense RNA. To date four genera of coronaviruses exist, alpha, beta, delta and gamma, defined on the basis of

phylogenetic groups. The genus gamma-coronavirus is mainly composed of viruses isolated from birds (avian coronaviruses, AvCoVs), including infectious bronchitis virus (IBV), Turkey coronavirus (TCoV) and guinea fowl coronavirus (GfCoV).[11,13,21]

Infectious bronchitis virus is a highly contagious virus transmitted very quickly among naive birds in the field. It is responsible worldwide for respiratory diseases, egg drop with poor eggshell quality, reduced hatchability, nephritis and sometimes, in early infection of future breeders, genital atrophy responsible for the syndrome of "false laying" in chicken breeders or layers.[18]

Turkey coronavirus, originally identified in the USA in the 1970s as one of the agents responsible for an acute enteritis named bluecomb[24,27] and since with a multifactorial disease known as poult enteritis complex of turkeys (PEC),[2] has now been detected in most areas where turkeys are farmed,[4,8-10,20,23,29] although TCoVs isolated in Europe have been shown to have a different genetic lineage to those isolated in the USA.[6,22] PEC includes several intestinal disorders that occur in turkeys mostly within the first three weeks of life[16] and its clinical signs often include diarrhea, stunting, anorexia, dehydration, weight loss, and immune dysfunction (atrophy of the thymus and the bursa of Fabricius) that promotes secondary infections. The wide distribution of both IBV and TCoV and their highly contagious nature have considerable economic repercussions.

The contagious nature of a disease can be measured by the "reproduction number" (R0) defined as "the expected number of secondary cases produced by a single (typical) infection in a totally susceptible population".[21] The parameters necessary to calculate R0 are (a) the speed of transmission and (b) the shedding duration of the infectious viruses. Generally, a virus with an R0 less than 1 will disappear quickly because an infected individual will have a low ability to infect another. A virus with an R0 greater than one will spread in the susceptible population. For IBV, an R0 of 19.95 has been estimated,[32] which is a figure comparable to the R0 of highly contagious human viruses such as measles virus (R0 12-18).[21] For TCoV, R0 has not yet been fully calculated; however, a study with an American TCoV isolate demonstrated that infectious virus particles can be shed up to six weeks post-infection in experimentally infected turkeys.[4]

The current study focused on strain Fr-TCoV 080385d that was detected in France in 2008 in turkeys with clinical signs compatible with PEC. Fr-TCoV is the only European TCoV strain isolated to date, although coronaviruses have been detected in turkeys in Poland, Great Britain and Italy.[8,10,20] The aim of this study was to determine the transmission properties of the virus by evaluating its ID_{50} and reproduction number (R0) under experimental conditions in 10-day-old SPF turkeys, in order to better understand the diffusion of the disease. Histopathological examination and in-situ detection of TCoV antigen at the sites of replication in the intestinal tract were also performed.

Materials and Methods

Ethics statement

Three animal experiments (Exp 1, 2 and 3) were performed in agreement with the national regulations of the French Ministry for higher education and research on animal welfare and after approval from the French Agency for Food, Environmental and Occupational Health & Safety's (ANSES) ethical committee.

Virus preparation and titration

Virus Fr-TCoV 080385d isolated from duodenal contents of 42-day-old turkeys affected by PEC in November 2008 was propagated by inoculating embryonated SPF turkey eggs (Anses, Ploufragan, France) via the intra-amniotic route, as previously described.[15] Because Fr-TCoV 080385d does not induce clinical lesions in the embryo, the intestines of inoculated embryos were screened 4 days post-inoculation by qRT-PCR,[22] and the intestines of positive embryos were collected and pooled to prepare a virus stock. Five-fold serial dilutions of this stock were inoculated into seven eggs per dilution, and a titre of $10^{4.01}EID_{50}$/ml was calculated according to Reed & Muench.[26]

RNA extraction and qRT-PCR RT-PCR

One hundred microliters of intestinal or cloacal swab material was lysed with 300 µl of Buffer RLT (Qiagen, France) by mixing and incubating at room temperature for 15 min. RNA was extracted using MagAttract RNA Tissue Mini

M48 kit or MagAttract Virus Mini M48 kit for BioRobot M48 (Qiagen, France) and eluted in 100 µl of buffer AVE following the manufacturer's instructions. The presence of TCoV genome was detected using a qRT-PCR specific for Avian Coronaviruses.[22] The limit of detection (LoD) and the linear phase of this qRT-PCR were described as 2 log10 and from 3 to 9 log10 copies per microliter of extracted RNA, respectively. In this study, samples were considered positive with a result higher than 2 log10 copies per microliter of extracted RNA. All results are given as copy number (cp)/µl of extracted RNA expressed in log10 together with the SD

Exp 1. Titration of Fr-TCoV in 10-day-old SPF Turkeys

Thirty 10-day-old SPF turkeys were separated in 5 groups of 6 birds, and housed for 3 days in negative pressure isolators allowing ad lib feeding and drinking. Each isolator had a cardboard floor with a metal grid platform underneath and a surface area of 1.4 m^2. Groups 1, 2, 3 and 4 were inoculated via the oral route with 0.25 ml of strain Fr-TCoV 080385d diluted to $10^{-1.5}$, $10^{-3.0}$, $10^{-4.5}$ and $10^{-6.0}$ respectively in MEM Hepes (Gibco, France) supplemented with penicillin (200 µ/ml final concentration) and streptomycin (0.2 mg/ml final concentration). Control group 5 was inoculated with MEMH plus antibiotics alone via the same route. At 1-day post-inoculation (dpi), two SPF turkey contacts were introduced into groups 1–4 as sentinels to demonstrate horizontal transmission of infectious virus. From 1 to 3 dpi, cloacal swabs were collected from all subjects, sampling the contacts first, followed by those that had been inoculated. RNA was extracted from these samples for molecular analysis as described above. The 50% endpoint was calculated using the method of Reed and Muench.[26]

Exp 2.: Transmission by contact from a seeder bird

Thirty-two 10-day-old SPF turkeys were separated into groups, one containing 29 subjects and a second containing 3. Each group was housed in a separate negative pressure room at a density of seven birds per m^2 and floors were covered with wood chippings (reproducing common commercial rearing conditions in France). The group of three subjects was inoculated with 0.25 ml

of strain Fr-TCoV 080385d diluted at $10^{-4.5}$ in the same media as used in Exp. 1, via the oral route. At 1 dpi, cloacal swabs were collected to confirm their Fr-TCoV 080385d positive status by qRT-PCR. At 2 dpi, one positive subject was placed as a seeder infected bird among the group of 29 SPF subjects (contacts). Cloacal swabs were collected from all subjects every 2 hr until 16 hr post-contact (hpc), at 24 hpc and 2 days post-contact (dpc) then weekly until 41 dpc.

During the 2-hr-sampling regime, the order in which the subjects were taken was respected throughout. This ensured that each subject was sampled precisely every two hours. Sampling staff wore a new pair of sterile gloves for each sampled bird, so as not to transfer the virus through bird-handling. RNA was extracted from these samples to perform qRT-PCR, to determine infection and the excretion period for each subject.

The transmission characteristics were assessed considering the evolution of individuals through the susceptible, infectious and recovered stages (SIR model). Susceptible (S) animals correspond to naïve individuals who are exposed to the virus shed by infectious (I) animals. The individuals then turn to the recovered (R) stage at the end of the shedding period. The transmission rate, denoted as β, reflects the number of new infections generated by one typical infectious individual per time unit. In this study, owing to the high transmissibility of the virus, a two-hourly time scale was selected. With these notations, the probability for a susceptible individual to become infected on a time interval $[t, t + \Delta t]$ is given by $p_t = 1 - \exp(-\beta I_t \Delta t/N)$, where N is the total number of individuals involved in the experiment (here, $N = 30$). Therefore, the number of new cases on each time interval $[t_i, t_{i+1}]$ follows a binomial distribution with parameters S_{ti}, the number of susceptible individuals at time t_i, and p_{ti}, the probability of infection. The number of susceptible and infectious animals was updated for each sampling interval, as well as the number of new cases, allowing the estimation of the transmission rate parameter β. The generalized linear model approach was used for the estimation, using the complementary log-log link function and taking log(I/NΔt) as offset variable.[3,12,31]

The duration of excretion of Fr-TCoV 080385d was measured in terms of presence of viral RNA during the course of this experiment, independently from

the infective capacity of the detected viral particles. A further experiment (Exp 3.) was therefore conducted in SPF turkeys, to assess the infectivity of the samples confirmed positive by qRT-PCR.

Exp 3. – Assessing infectivity of TCoV at different sampling times

Exp 3 objectives were (a) to assess the shedding duration of infectious virus in samples collected at different time points during Exp 2, (b) to evaluate tissue distribution of Fr-TCoV in infected birds, (c) to perform a preliminary assessment of the airborne route of transmission.

One representative positive sample selected at 6 dpc of Exp 2. (codified T6) was diluted (same media as Exp. 1) so as to inoculate via the oral route $10^{5.7}$ RNA copies in three 10-day-old SPF turkeys. They were housed in a negative pressure room, under the same rearing conditions as in Exp 2, with three 11-day-old SPF turkeys introduced as contact-birds at 1 dpi to demonstrate horizontal transmission. Cloacal swabs were collected daily for qRT-PCR analyses from all birds until 3 dpi, when the birds were humanely euthanized and duodenum, jejunum, ileocaecal junction and bursa of Fabricius were collected. These samples were fixed for 24 hr in 4% formaldehyde then transferred to 70% ethanol and finally embedded in paraffin wax for histopathology and anti-TCoV immunohistochemistry (see section Histopathology). This process was repeated using one representative positive sample from 13, 21, 27, 34 and 41 dpc of Exp 2. (codified T13, T21, T27, T34 and T41, respectively) to make a total of six experiments. Airborne transmission was evaluated in each of these experiments by using six 10-day-old SPF turkeys housed in a park in the same containment cell but separated from the other animals, at a distance of 3 meters. The sampling programme was as described above. Housing, circulation of personal, change of boots, clothes and gloves was organized to minimize physical contamination.

Histopathology and anti-TCoV immunohistochemistry

Duplicate tissue slides were cut from formalin-fixed, dehydrated, and paraffin-embedded intestinal samples (duodenum, jejunum, ileocaecal junction, bursa of Fabricius), collected from Exp. 3. For routine histopathologic evaluation, one

slide was stained with haematoxylin and eosin (HE) according to standard laboratory procedures. The other duplicate slide was deparaffinized with xylene and rehydrated in alcohol series and subsequently subjected to endogenous peroxidase inactivation in 1% hydrogen peroxide in methanol for 20 min, antigen retrieval via boiling in Tris-ethylenediaminetetraacetic acid (EDTA), pH 9.0 for 10 min and double washing in phosphate buffered Normal Antibody Diluent (NAD, ScyTek Laboratories, Logan, USA) containing 0.1% Tween-20. Tissue sections were then incubated with mouse monoclonal Ab anti IBV M-protein 25.1 (D274, Centraal Veterinair Instituut, Lelystad, the Netherlands) diluted 1:400 in NAD for 60 min at room temperature. Based on pilot experiments (data not shown), this Ab successfully cross-reacted with Fr-TCoV which is likely due to the highly conserved nature of the targeted protein in avian gamma coronaviruses (>90% amino acid identity).[5]

Primary antibody binding was detected via subsequent incubation with Dako Envision HRPO labeled polymer goat anti-mouse (Dako, by Agilent Technologies, Santa Clara, USA) diluted 1:1 in NAD (30 min, room temperature), and visualized by administration of 3-Amino-9-ethylcarbazole (AEC, Dako). Fr-TCoV-induced histopathology and Fr-TCoV protein expression were assessed by light microscopy (BX40, Olympus, Tokyo, Japan).

Results

Exp 1. Titration of Fr-TCoV in 10-day-old SPF Turkeys

Fr-TCoV was detected with qRT-PCR at 1 dpi in all six inoculated subjects of group 1 (dilution $10^{-1.5}$, mean ± SD 5.19 ± 0.94 $\log_{10}$ cp/µl), in 5 out of 6 subjects of group 2 (10^{-3}, 4.46 ± 1.81 $\log_{10}$ cp/µl) and in 3 out of 6 subjects in group 3 ($10^{-4.5}$, 3.59 ± 1.37 $\log_{10}$ cp/µl). At 2 and 3 dpi, all subjects of these groups, including contact-birds, were positive, demonstrating horizontal transmission. No viral RNA was detected throughout the experiment in groups 4 (10^{-6}) and 5 (MEMH). The result obtained at 1 dpi (before horizontal transmission) gave a virus titre of $10^{4,88}$ ID_{50}/ml.

Exp 2. Transmission by contact from a seeder bird

The following data are shown graphically in Figure 1. An inoculated subject with a viral RNA load of 5.28 log_{10} cp/µl at 1 dpi that had been placed among 29 contacts, transmitted the virus to one contact between 8 and 10 hpc, though the level of viral RNA detected at 10 hpc in this newly infected bird (2.05 log_{10} cp/µl) was almost at the LoD. However, between 10 and 12 hpc the level of viral RNA detected in the same bird increased to 3.39 log_{10} cp/µl and a second contact was positive at 2.19 log_{10} cp/µl. Between 12 and 14 hpc, seven contacts were positive with values ranging from 2.24 to 4.77 log_{10} cp/µl. Between 14 and 26 hpc, 23 contacts were positive with a mean ± *SD* of 4.86 ± 0.99 log_{10} cp/µl. In the subsequent days (2–13 dpc), all contacts were positive with mean ± *SD* values of 6.05 ± 0.54, 5.07 ± 0.76, 5.57 ± 0.38, 4.80 ± 0.76 log_{10} cp/µl at 2, 3, 6, 13 dpc respectively. The transmission rate β was estimated to be 0.42 $Turkey^{-1}$ h^{-1} (confidence interval [0.27, 0.62]). Otherwise stated, one infected animal had, on average, infected 1 animal every 2.5 hr. For the following 2 weeks (21 and 27 dpc), viral RNA was detected in almost all contacts (N = 25, mean ± SD 3.46 ± 0.79 and N = 27, mean ± *SD* 3.58 ± 0.80 log_{10} cp/µl respectively). At 34 and 41 dpc, the number of positive contacts was reduced to

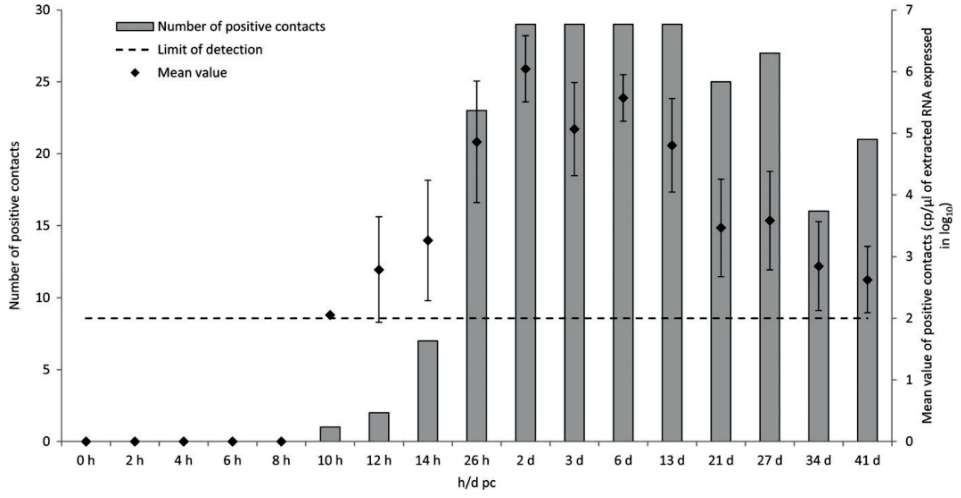

Figure 1. Detection of Fr-TCoV080385d viral RNA in 29 SPF turkeys placed in contact with one seeder turkey at 10 days of age. The x-axis represents sampling dates (hours (h) or days (d) post-contact). The 2 hr sampling period is underlined. The y-axis to the left represents the number of positive contacts. The y-axis to the right represents the viral RNA load in positive subjects, expressed as mean log10 copy number per microliter.

16 and 21 respectively with RNA loads near to the LoD (mean ± SD 2.85 ± 0.72 and 2.63 ± 0.54 $\log_{10}$ cp/µl). This result would suggest the shedding period to be longer than 41 dpc. However, this estimation was based on the detection of viral RNA, ignoring the infective potential of the viral particles, which was investigated as Exp. 3.

Exp 3: Assessing infectivity of TCoV at different sampling times

The data are shown graphically in Figure 2. In three out of six Exp 2. samples (T6, T27 and T41), the number of positive inoculated birds and the level of viral RNA detection increased over time during the sampling period, culminating at 3 dpi with RNA detected in all birds including contacts (mean ± *SD* = 4.89 ± 0.69, 5.75 ± 0.32 and 4.55 ± 0.70 cp/µl, respectively). No viral RNA was detected throughout the period, neither in inoculated or contact subjects exposed to T13, T21 and T34, nor in subjects assigned to the assessment of airborne transmission.

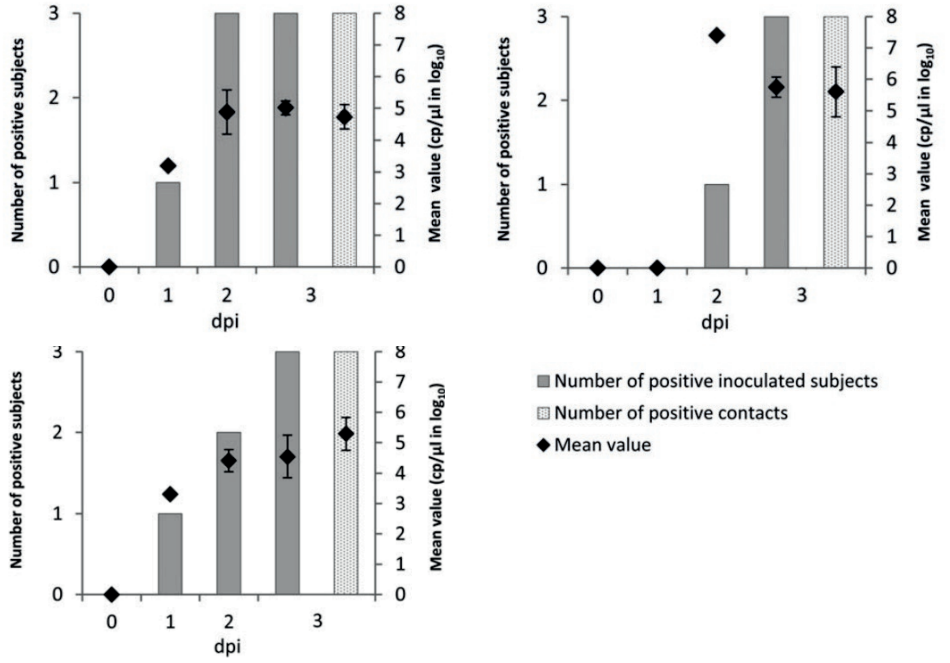

Figure 2. Exp 3 = Detection of infectious Fr-TCoVin SPF turkeys inoculated with intestinal samples collected in Exp2 at 6, 27 or 41 days post-exposure (a, b or c, respectively). The x-axis represents sampling dates (days post-inoculation in Exp 3). The y-axis to the left represents the number of positive subjects. The y-axis to the right represents the mean viral RNA copy number in positive subjects.

Histopathology and anti-TCoV immunohistochemistry: Widespread antigen distribution in lower gut in the absence of microscopic lesions

Intestinal samples taken from infected subjects at 3 dpi from Exp. 3 showed well-preserved characteristic architectural features. Except for some very mild hyperemia and rare epithelial desquamation, no clear histopathological changes were seen in any of the samples (Figure 3a). Immunohistochemical staining showed an abundance of viral protein expressed in the ileum, caeca and bursa of all inoculated or contact subjects exposed to T6, T27 and T41 (expression in

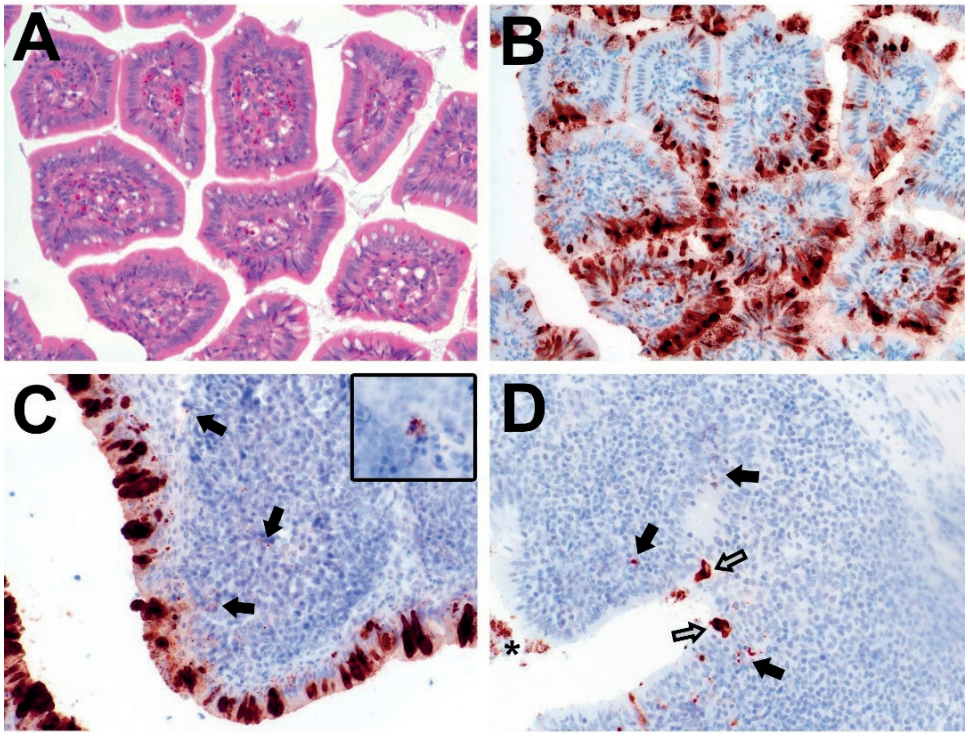

Figure 3. TCoV histopathology and protein expression, 3 dpi. Panels a and b: Serial transversal sections of the caecal mucosal folds (villi). Although no clear virus-induced histopathologic epithelial changes are present, besides very mild hyperemia of the lamina propria (a), abundant viral protein expression in the caecal enterocytes is seen (brown staining in b). Panels c and d: Viral protein expression in the epithelium (white arrows) and more fragmented and dotted, finely dispersed immunohistochemical signal subepithelially (black arrows) in the lymphoid follicles of the Bursa of Fabricius (c) and the caecal tonsil (d). Panel c inset: occasional single cells in the bursal lymphoid follicles, demonstrating the intracytoplasmic presence of viral protein. All depicted tissues are taken from the same T41 contact subject. All tissues are visualized by light microscopy at 200× (a, b, d), 400× (c) or 800× (inset c) magnification. A = hematoxylin and eosin staining; B, C + inset, D: immunohistochemistry anti TCoV. Asterisk: desquamated cells in the intestinal lumen.

the caecum and bursa is shown for T41 in Figure 3). As shown in Figure 4 histograms, antigen detection in the other regions of the intestine (duodenum or jejunum) was inconsistent in both the inoculated and contact-birds exposed to the same samples, as illustrated by the fact that no viral protein was detected in the duodenum of any contact subject exposed to T6, T27 and T41. No viral protein expression was seen in any of the intestines taken from the inoculated and contact subjects exposed to T13, T21 and T34.

In all positive cases, viral protein prominently presented in both enterocytes and goblet cells and in limited situations in desquamated cells and intraluminal debris. Viral protein expressing enterocytes and goblet cells were mainly situated in the villar region and hardly in the crypt region. The number of cells per tissue section containing viral protein varied from only few to very many. In general, the highest number of cells containing viral protein was found in the caudal intestinal tract (ileum, caecum and bursa). A positive sample (a subject inoculated with T41) showing virus protein in caecal enterocytes is shown in Figure 3b. In the bursa of Fabricius and near the caecal tonsil, viral protein

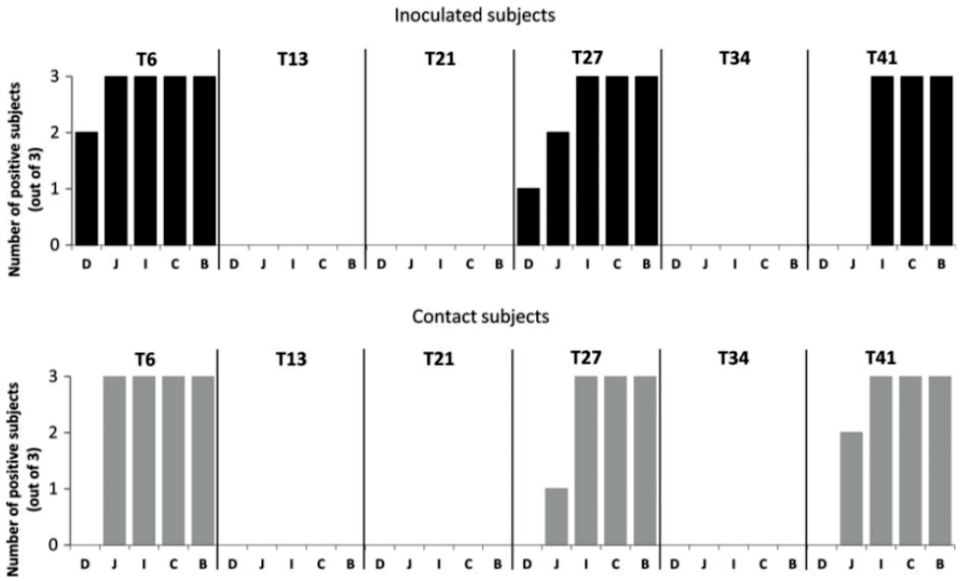

Figure 4. Detection of viral antigen in intestinal tissues. Immunohistochemistry of: intestinal tissues D = duodenum, J = jejunum, I = ileum, C = caeca B = bursa of Fabricius, taken 3 dpi from subjects inoculated with samples T6, T13, T21, T27, T34 orT41 of Exp 2 (a) and from their corresponding contacts (b).

expression was mostly restricted to the epithelium covering the lymphoid tissue (Figure 3c,d), but less distinct and fragmented staining was also regularly seen subepithelially in the lymphoid follicles. Incidentally, individual cells in the lymphoid follicles seemingly showed viral protein comparable (in terms of quantity) to the epithelial viral protein expression. One subject (negative control from airborne transmission experiment), which was negative by qRT-PCR, was used as a control for histopathology. This subject neither showed histopathological changes nor viral protein expression in any of the examined intestinal samples.

Discussion

When considering viral infection in animals the infectious dose, the transmission rates, the age of animal infected and environmental conditions are all influencing factors of efficacy. In the current study the infectious dose, transmission rate, duration of excretion and induced histopathology in ten-day-old SPF turkeys for the European strain of turkey coronavirus Fr-TCoV 080385d were evaluated.

The controlled experimental infections performed in this study demonstrated the Fr-TCoV080385d virus stock to have a titre in 10-day-old SPF turkeys of $10^{4,88}$ ID_{50}/ml. Considering the same virus stock had been titrated previously in embryonated turkey eggs and found to have a virus titre of $10^{4,01}$ EID_{50}/ml, this would suggest that 10-day-old SPF turkeys are more sensitive than embryonated eggs (1 EID_{50} = 7 ID_{50}) in recovering infectious TCoV, although the repeatability of Reed & Muench titration needs to be taken into consideration. Similarly, at one ID_{50}/ml, viral RNA levels were also beyond the limit of detection of a well characterized qRT-PCR,[22] so that 10-day-old turkeys might be also more sensitive than qRT-PCR to detect infectious TCoV. Such a high susceptibility of young hosts was also reported in a recent paper where an enteric coronavirus of pigs (porcine epidemic diarrhea virus, PEDV) was shown to infect more efficiently 5-day-old piglets than tissue culture (minimal infectious dose = 0.056 $TCID_{50}$).[30] RNA levels at the PEDV MID have also been reported to be beyond the limit of detection by qRT-PCR.[14] The effects of turkey age on the ID_{50} of Fr-

TCoVwere not investigated in the current study however, the fact that TCoV associated enteric disorders such as PEC or poult enteritis mortality syndrome (PEMS) are predominantly diseases of younger subjects[2] lends support to more resistance in older birds.

An extremely rapid transmission via the oro-faecal route was observed under the current experimental conditions for 10-day-old SPF turkeys resulting in almost all of the naïve contact subjects being infected from one infectious individual within 24 hr. No airborne transmission over a distance of 2–3 m was observed. Mathematically the results of the oro-faecal transmission gave a calculated rate of one newly infected individual every 2.5 hr and provided a figure for the first parameter in estimating an Fr-TCoV R0. This transmission rate was measured in terms of detection of viral RNA and the passage of each individual from a negative to positive status above the threshold of the qRT-PCR used. Considering what was discussed previously regarding the relative sensitivity of qRT-PCR and 10-day-old turkeys to detect infectious TCoV, the actual rate of transmission could be quicker. The qRT-PCR used in this study is in the authors' experience the most sensitive tool for detecting Fr-TCoV and thus until a more sensitive method becomes available the calculated figure of 2.5 hr cannot be refined. Nevertheless, these results showed that Fr-TCoV can be transmitted extremely rapidly and also draw attention to the fact that when calculating transmission rates, no matter the pathogen, results will relate to the sensitivity of the diagnostic tools applied. In other words, more sensitive tools for detection equals increased transmission rates.

The shedding duration of infectious virus, as the second R0 parameter, was more complicated to determine, as detection of viral RNA could not be taken to represent infectious particles. Thus, this parameter could only be solidly determined if individual re-infection of SPF turkeys with each of the samples at every date was performed. This requisite could not be fulfilled in the current study and was also difficult to justify on an ethical level in respect to the principals of the 3 Rs.[28]

Although the "duration of excretion" for every individual could not be obtained, the experiments performed in the current study (in which one sample from each

date was re-inoculated) revealed that some subjects continued to shed infectious virus for at least six weeks when others ceased at two. At this time the authors have no data on why some subjects stopped excreting infectious virus four weeks in advance of others or if, in fact, excretion detected at six weeks was representative of subjects with intermittent excretion profiles as has been observed in cats experimentally infected with FECV.[19] In cats, this intermittent excretion has been suggested to be linked with persistent infection in the colon (lower intestine) from which viruses then have the potential to re-infect the small intestine at any time. The presence of virus in both regions of the gut can then result in renewed excretion.[19] Concerning Fr-TCoV these questions should be assigned to specifically designed trials and histopathological examination, however, the present study seems to indicate a clear tropism of Fr-TCoV for lower intestine, as described for FECV.[19] Indeed, in the current study, Fr-TCoV's ability to infect the turkey intestinal tract was successfully demonstrated with immunohistochemical staining. The virus showed preferred tropism for the lower intestines similar to what has been also observed for US lineage TCoV (NC95),[17] which likely reflects distribution of the TCoV receptor.[1] This distribution pattern could be time-dependent though and since all tissue samples were collected at a single time point (3 dpi in Exp 3), evaluation of intestinal segments taken at different time points after infection would be needed to fully confirm these observations.

Regarding specific cell tropism within the target tissue, gut-associated lymphoid tissue (among which the so-called caecal tonsil) and the lymphoid tissue in the bursa of Fabricius might be of special interest. Although viral protein expression was most distinctively seen in epithelial cells (enterocytes) overlying these subepithelially-located lymphoid tissues, in several birds a delicate, finely dispersed and dotted immunohistochemical staining signal was present subepithelially within these lymphoid tissues. Taking into account both the signal's fragmented subtle aspect compared to the signal at the epithelial level and otherwise the biological function of these lymphoid aggregates, the authors speculate that this might be the result of immunohistochemical demonstration of degraded viral protein within phagocytozing antigen-presenting cells. Occasionally, as shown in the inset picture in Figure 3c, individual cells in the

subepithelial lymphoid tissues displayed a 'full-cytoplasmic' immuno-histochemical staining signal comparable to the signal seen in the majority of infected enterocytes. Since, upon viral inoculation of an animal, such abundant intracellular signal is usually seen in cells known to be within the virus' tropism (in other words 'presumably correlated with true viral replication'), it is therefore possible that Fr-TCoV can incidentally replicate in antigen-presenting cells (APCs), represented by dendritic cells and monocytes/macrophages. APC tropism was recently demonstrated for subtypes of TCoVs relative IBV, with this ability to infect APCs being a determinant for cell-mediated viremic systemic spread and subsequent infection of the chicken's urinary tract.[25] However, although the stellate morphology and the localization of the depicted cell (see inset Figure 3c) suggest that it likely belongs to one of the mentioned APC families, additional assays characterizing these cell types (for example double immunohistochemical staining for both viral protein expression and cell-characterizing protein epitopes) are needed to confirm a APC tropism for TCoV.

Fr-TCoV viral protein expression was not correlated with histopathologic changes in the sampled tissues collected here, contrary to previous observations following inoculation with a TCoV of US lineage that did induce lesions, albeit without associated clinical signs.[17] This discrepancy could be explained by the difference in age of the birds inoculated as in the US TCoV study, birds had been inoculated at 6 days of age; alternatively, like the distribution pattern discussed above, this discrepancy might be a time-dependent feature, with 3 dpi in our study being too early for morphologic changes – resulting from epithelial damage, local tissue reactions and influx of immune cells to manifest. Furthermore the specific date post- inoculation when microscopic lesions were observed in the US TCoV study was not given.[17] It is equally possible that under experimental conditions the European lineage of TCoV simply has a different pathogenic profile to those of the US lineage. Infection studies for EU and US TCoVs in turkeys of the same age and under the same controlled conditions are required for comparative analysis into the pathological profiles of these different lineages.

In conclusion an extremely low dose of European isolate Fr-TCoV strain 080385d is required for infection of 10-day-old turkey poults under experimental

conditions. The virus spreads very quickly via the oro-faecal route among susceptible subjects (a new subject at least every 2.5 hr) and infectious virus may continue to be excreted for at least six weeks after the initial infection which may be linked to a preferential tropism for the lower intestines. These results stress the importance of good sanitary practices at the entrance to livestock buildings and the need to consider that infected individuals may still be infectious long after the clinical episode.

Conflict of Interest

The authors declare that they have no conflict of interest.

Acknowledgements

The authors wish to thank the Département des Côtes d'Armor/Conseil Régional de Bretagne/Conseil Régional des Pays de Loire/France Agrimer/Office de l'élevage/Comité Interprofessionnel de la Dinde Française for their financial support. This research was part of the EPICOREM ANR programme: Eco-epidemiology of Coronaviruses: From wildlife to human & emergence threat assessment.

References

1. Ambepitiya Wickramasinghe, I. N. , de Vries, R. P. , Weerts, E. A. , van Beurden, S. J. , Peng, W. , McBride, R. , Verheije, M. H. (2015). Novel receptor specificity of avian gammacoronaviruses that cause enteritis. *Journal of Virology*, 89, 8783–8792.

2. Barnes, H. J. , Guy, J. S. , & Vaillancourt, J. P. (2000). Poult enteritis complex. *Revue Scientifique et Technique*, 19, 565–588.

3. Becker, N. G. (1989). *Analysis of Infectious Disease Data*. London: Chapman and Hall Ltd.

4. Breslin, J. J. , Smith, L. G. , Barnes, H. J. , & Guy, J. S. (2000). Comparison of virus isolation, immunohistochemistry, and reverse transcriptase-polymerase chain reaction procedures for detection of turkey coronavirus. *Avian Diseases*, 44, 624–631.

5. Brown, P. , Touzain, F. , Briand, F. , De Boisseson, C. , Courtillon, C. , Allée, C. , … Eterradossi, N. 2014: First full length sequence of European Turkey coronavirus XIIIth Nidovirus 2014 Symposium, p. 104. Salamanca Spain.

6. Brown, P. A. , Touzain, F. , Briand, F. X. , Gouilh, A. M. , Courtillon, C. , Allee, C. , … Eterradossi, N. (2016). First complete genome sequence of European turkey coronavirus suggests complex recombination history related with US turkey and guinea fowl coronaviruses. *Journal of General Virology*, 97, 110–120. 10.1099/jgv.0.000338

7. Cavanagh, D. (2001). A nomenclature for avian coronavirus isolates and the question of species status. *Avian Pathology*, 30, 109–115.

8. Cavanagh, D. , Mawditt, K. , Sharma, M. , Drury, S. E. , Ainsworth, H. L. , Britton, P. , & Gough, R. E. (2001). Detection of a coronavirus from turkey poults in Europe genetically related to infectious bronchitis virus of chickens. *Avian Pathology*, 30, 355–368.

9. Dea, S. , & Tijssen, P. (1988). Viral agents associated with outbreaks of diarrhea in turkey flocks in Quebec. *Canadian Journal of Veterinary Research*, 52, 53–57.

10. Domańska-Blicharz, K. , Seroka, A. , Lisowska, A. , Tomczyk, G. , & Minta, Z. (2010). Turkey coronavirus in Poland - Preliminary results. *Bulletin of the Veterinary Institute in Pulawy*, 54, 473–477.

11. Ducatez, M. F. , Liais, E. , Croville, G. , & Guerin, J. L. (2015). Full genome sequence of guinea fowl coronavirus associated with fulminating disease. *Virus Genes*, 50, 514–517.

12. Eblé, P. , De Koeijer, A. , Bouma, A. , Stegeman, A. , & Dekker, A. (2006). Quantification of within- and between-pen transmission of foot-and-mouth disease virus in pigs. *Veterinary Research*, 37, 647–654.

13. Fehr, A. R. , & Perlman, S. (2015). Coronaviruses: An overview of their replication and pathogenesis. *Methods in Molecular Biology*, 1282, 1–23.

14. Goyal, S. 2014: PEDV research updates: Environmental stability of PED (porcine epidemic diarrhea virus) University of Minnesota, US National Pork Board.

15. Guionie, O. , Courtillon, C. , Allee, C. , Maurel, S. , Queguiner, M. , & Eterradossi, N. (2013). An experimental study of the survival of turkey coronavirus at room temperature and +4 degrees C. *Avian Pathology*, 42, 248–252.

16. Guy, J. S. (2013). Turkey coronavirus enteritis, In Swayne D. E. (Ed.), *Diseases of poultry*, 13 edn., (pp. 376–381). Ames Iowa: John Wiley & Sons, Inc.

17. Guy, J. S. , Smith, L. G. , Breslin, J. J. , Vaillancourt, J. P. , & Barnes, H. J. (2000). High mortality and growth depression experimentally produced in young turkeys by dual infection with enteropathogenic Escherichia coli and turkey coronavirus. *Avian Diseases*, 44, 105–113.

18. Jackwood, M. W. , & Wit, S. D. (2013). Infectious Bronchitis In Swayne D. E. (Ed.), *Diseases of Poultry*, 13 edn., (pp. 139–159). Ames, Iowa: John Wiley & Sons, Inc.

19. Kipar, A. , Meli, M. L. , Baptiste, K. E. , Bowker, L. J. , & Lutz, H. (2010). Sites of feline coronavirus persistence in healthy cats. *Journal of General Virology*, 91, 1698–1707.

20. Martin, A. M. , Vinco, L. J. , Cordioli, P. , & Lavazza, A. 2002: Diagnosis of turkey viral enteric diseases by electron microscopy and identification of coronavirus in a case of turkey enteritis. 4th International Symposium on Turkey Diseases, pp. 114–119. Berlin, Germany.

21. Masters, P. S. , & Perlman, S. (2013) Coronaviridae In Knipe D. M. & Howley P. M. (Eds.), *Fields Virology*, 6 edn., (pp. 825–858). Philadelphia, PA: Lippincott Williams & Wilkins.

22. Maurel, S. , Toquin, D. , Briand, F. X. , Queguiner, M. , Allee, C. , Bertin, J. , … Eterradossi, N. (2011). First full-length sequences of the S gene of European isolates reveal further diversity among turkey coronaviruses. *Avian Pathology*, 40, 179–189.

23. Maurel, S. , Toquin, D. , Que'guiner, M. , Le Men, M. , Alle'e, C. , Lamande', J. , … Eterradossi, N. 2009: Molecular identification and characterization of a turkey coronavirus in France. The 6th International Symposium on Avian Corona- and Pneumovirus and Complicating Pathogens, pp. 209–218. Rauischholzhausen, Germany.

24. Panigrahy, B. , Naqi, S. A. , & Hall, C. F. (1973). Isolation and characterization of viruses associated with transmissible enteritis (bluecomb) of turkeys. *Avian Diseases*, 17, 430–438.

25. Reddy, V. R. , Trus, I. , Desmarets, L. M. , Li, Y. , Theuns, S. , & Nauwynck, H. J. (2016). Productive replication of nephropathogenic infectious bronchitis virus in peripheral blood monocytic cells, a strategy for viral dissemination and kidney infection in chickens. *Veterinary Research*, 47, 70

26. Reed, L. J. , & Muench, H. (1938). A simple method of estimating fifty percent end points. *American Journal of Hygiene*, 27, 493–497.

27. Ritchie, A. E. , Deshmukh, D. R. , Larsen, C. T. , & Pomeroy, B. S. (1973). Electron microscopy of coronavirus-like particles characteristic of turkey bluecomb disease. *Avian Diseases*, 17, 546–558.

28. Russell, W. M. S. , & Burch, R. L. (1959). *The Principles of Humane Experimental Technique*. Wheathapstead, England: U. F. f. A. W.

29. Teixeira, M. C. , Luvizotto, M. C. , Ferrari, H. F. , Mendes, A. R. , da Silva, S. E. , & Cardoso, T. C. (2007). Detection of turkey coronavirus in commercial turkey poults in Brazil. *Avian Pathology*, 36, 29–33.

30. Thomas, J. T. , Chen, Q. , Gauger, P. C. , Gimenez-Lirola, L. G. , Sinha, A. , Harmon, K. M. , … Zhang, J. (2015). Effect of porcine epidemic diarrhea virus infectious doses on infection outcomes in naive conventional neonatal and weaned pigs. *PLoS ONE*, 10, e0139266

31. Velthuis, A. G. , De Jong, M. C. , Kamp, E. M. , Stockhofe, N. , & Verheijden, J. H. (2003). Design and analysis of an *Actinobacillus pleuropneumoniae* transmission experiment. *Preventive Veterinary Medicine*, 60, 53–68.

32. de Wit, J. J. , de Jong, M. C. , Pijpers, A. , & Verheijden, J. H. (1998). Transmission of infectious bronchitis virus within vaccinated and unvaccinated groups of chickens. *Avian Pathology*, 27, 464–471.

7 Coronaviral intestinal disease in poultry: comparative histopathology in three domestic galliform species

E.A.W.S. Weerts [a], J.P. Deniz Marrero [a], P.A. Brown [b], M. Ducatez [c], J.L. Guérin [c], M. Delverdier [c], J.J. de Wit [d,e], M.H. Verheije [a], A. Gröne [a]

[a] Division of Pathology, Department Biomolecular Health Sciences, Faculty of Veterinary Medicine, Utrecht University, Utrecht, the Netherlands

[b] VIPAC Unit, ANSES (French Agency for Food, Environmental and Occupational Health Safety), Ploufragan-Plouzané-Niort Laboratory, Ploufragan, France

[c] IHAP, Université de Toulouse, INRAE, ENVT, Toulouse, France

[d] Division of Farm Animal Health, Department Population Health Sciences, Faculty of Veterinary Medicine, Utrecht University, Utrecht, the Netherlands

[e] Royal GD Animal Health, Deventer, the Netherlands

in submission
(Veterinary Pathology)

Abstract

Poultry regularly suffers from diseases induced by avian gammacoronaviruses. Infectious bronchitis virus (IBV) causes respiratory disease, egg production decrease and strain-dependent nephritis in chickens. Although IBV is not primarily associated with clinical intestinal disease, several strains are also known to infect the gastrointestinal tract. Turkey and Guinea fowl coronavirus (TCoV and GfCoV) in contrast to IBV mainly target the gastrointestinal tract in turkeys and Guinea fowl respectively and both pathogens are associated with marked clinical enteric disease. The current study aimed to analyze and compare lesions and viral tissue tropism underlying IBV-, TCoV- and GfCoV-induced intestinal disease, based on histopathologic analysis of tissues from experimentally- and naturally-infected birds. Additionally other tissues were also evaluated. Viral protein expression was associated with heterophilic infiltration within the intestines of all three studied poultry species, but the abundance of inflammatory cells did not always correlate with the abundance of viral protein. In chickens and turkeys, cell infiltrates and viral protein were most prominently observed in the lower intestines, while in Guinea fowl the duodenum was mostly targeted. In addition, rhinotracheitis and tubulointerstitial nephritis were observed in IBV-infected chickens, but neither lesions, nor viral protein expression were seen in respiratory and urinary tract samples of turkeys and Guinea fowl. This study demonstrates that GfCoV targets a different intestinal region than IBV and TCoV and reconfirms that IBV, although genetically closely related, has a broader tissue tropism than TCoV and GfCoV.

Keywords

Infection – coronavirus – poultry - comparative histopathology - viral protein distribution - intestinal disease

Introduction

Poultry regularly suffers from diseases caused by avian coronaviruses, which to date belong to the genus gammacoronaviruses. Infectious bronchitis virus (IBV)

of chickens and turkey coronavirus (TCoV) of turkeys are well-documented representatives of this group of viruses, responsible for clinical diseases with major animal welfare and economic impact in the poultry industry.[16,25]

In 1931, IBV was the first avian coronavirus[40] and also the first of all coronaviruses to be discovered.[33] Its prototype, IBV Massachusetts 41 (M41), was described in the United States (US) as causative agent of respiratory disease and reduction in egg production in chickens.[4] Since then, many new variants were discovered that were all associated with respiratory disease and some additionally proved to be able to variably induce nephritis, genital tract dysfunction and intestinal infection.[36] These variant-related differences in disease are not well understood. Receptor affinity within the sialic acid family likely plays a role,[7] but no specific protein receptors or post-binding differences in the viral life cycle have been pinpointed that fully explain the clinical and pathologic differences.[47] Although some IBV variants are known to cause gastrointestinal (GI) infections, the virus is generally not considered to cause clinically relevant enteritis or typhlocolitis.[12]

In the 1970s, TCoV was discovered.[38] Originally also found in the US (US TCoV), this virus was associated with enteric disease and mortality in young turkeys. In recent years a genetically different European variant of this virus was identified in France (Fr TCoV), which is also associated with significant enteric disease.[31] TCoVs do not cause respiratory, renal or reproductive tract disease. However, it is not completely clear whether this implicates that TCoVs are unable to replicate in tissues other than the GI tract.[39]

Another more recently discovered avian coronavirus associated with GI tract disease is the Guinea fowl coronavirus (GfCoV), found in farmed Guinea fowl. In 1991, isolation of an IBV-like coronavirus in this bird species was reported,[24] but at that time it was unknown whether this was a truly new avian coronavirus or an already identified IBV strain that infected another bird species. GfCoV existence was confirmed in 2011 based on RNA detected in domestic Guinea fowl that showed high mortality in correlation with diarrhea, a clinical presentation referred to as 'fulminating disease'.[20] Up to date, only few publications on GfCoV exist and none of those address virus-induced lesions in

much detail or report potential tissue tropism besides the GI tract.[15,20,28] Knowledge on the potential extent of the GfCoV tissue tropism mainly relies on analysis of *ex vivo* receptor binding to guinea fowl tissue slides.[6]

Studies on avian coronaviruses in recent years mostly focused on genotyping of newly discovered viral strains[42]. In addition, a minority of studies on avian coronaviruses aimed to elucidate intracellular effects of viral replication[29] and *ex vivo* and *in vitro* tissue receptor binding.[47] New studies on avian coronavirus-induced lesions and viral tissue tropism would help to better understand virus-associated differences in disease. Since the clinical impact of IBV, TCoV and GfCoV infection on the GI tract is very different, the present study focused on histopathological comparison of IBV-, TCoV- and GfCoV-induced lesions in especially the GI tract, but also other tissues. The study aims to improve understanding of the differences in coronavirus-induced pathology in chickens, turkeys and Guinea fowl and the potential effects on clinical disease.

Materials and Methods

Tissue samples

Archived formalin-fixed and paraffin-embedded tissue samples were collected from several scientific institutes that collaborated in the European Cooperation in Science and Technology (COST) Action FA2017 'Towards Control of Avian Coronaviruses: Strategies, Surveillance and Vaccination and / or initials'. These samples originated from different previously performed experiments with chickens and turkeys (IBVs M41, 793B and QX and TCoVs). For Guinea fowl (GfCoV), tissues came from naturally-infected birds in field-outbreaks, since no isolated virus and hence no experimentally-infected bird tissues were available. Experimental samples all came from infection trial studies with comparable construction, but since slightly varying experimental protocols were used by the different institutes, samples differ regarding viral infectious dose, route of inoculation or infection, interval between infection and euthanasia and the type and age of the birds. Three parts of the intestinal tract (duodenum, at least one piece of a lower intestinal segment and the mucosa of cloaca / bursa) were available for all three bird species from approximately comparable time points

Table 1. Sources of Studied Intestinal Samples

Infection	Birds	Age at moment of infection	Viruses	Sampling time points
Exp.	SPF broiler and layer chickens	day of hatch	IBV QX	4 dpi
Exp.	SPF turkeys	10-day-old	Fr TCoV	3 dpi
Nat.	Guinea fowl, farmed	7-wk-old	GfCoV	unknown[a]

Abbreviations: exp, experimental; nat, natural; SPF, specific pathogen free;

[a] Four days after the onset of mortality in the bird flock.

during infection (Table 1). These samples were systematically analyzed in detail for histopathological changes with grading of viral protein expression and then compared for the three bird species. Further samples, roughly categorized as further segments of the gastrointestinal tract, the respiratory tract, the urinary tract and other tissues, were also evaluated for lesions and presence of viral protein. Specific information on all samples, birds and viruses used for this study is summarized in Supplemental Table 1, with further details given in Supplemental Materials and Methods.

All experiments were performed in agreement with the national regulations on animal experiments of the country where the experiment was performed and approved by the either the Dutch Animal Ethical Committee (DEC) (ethical animal experimentation approvals 2015-278, 2013.II.10.107 and 2017-071) or the French Ministry for Higher Education and Research on Animal Welfare (N° APAFIS#6680-201 609091 3457475 v3) after approval from the French Agency for Food, Environmental and Occupational Health & Safety's (ANSES) ethical committee (N°016).

Histopathology and Anti-Virus Immunohistochemistry

All tissue samples were originally fixed in 10% neutral buffered formalin for 24-48 hours (experimental) or unknown time (naturally-infected) and subsequently routinely embedded in paraffin. For the present comparative study, duplicate serial sections of four µm were cut. One slide was stained with hematoxylin and eosin (HE); the duplicate slide was used for immunohistochemistry as previously

Table 2. **Antibodies and Immunohistochemical Procedures**

Antigen	Ab	Dilution	Source of Ab
S2 (IBV)	mouse mAb Ch/IBV 26.1	1:100	Thermo Fischer
N (TCoV)	mouse mAb anti N TCoV	1:100	Kindly provided by J. Guy
M (TCoV + GfCoV)	mouse mAb anti IBV M 25.1[a]	1:400	Prionics

All pretreatments with Tris-EDTA (pH 9.0), all Ab dilutions in Normal Antibody Diluent (Immunologic), all Ab detections with EnVision anti-mouse (Dako). Abbreviations: S2, spike protein 2; IBV, infectious bronchitis virus; mAb, monoclonal antibody; N, nucleocapsid protein; TCoV, turkey coronavirus; M, membrane protein; GfCoV, guinea fowl coronavirus. [a] Antibody cross-reacting with TCoV and GfCoV

described.[3,6,9,43] Details on antibodies and immunohistochemical procedures are given in Table 2. Trachea and nasal mucosa were additionally stained with the periodic acid-Schiff (PAS) stain to highlight mucus-containing cells. All tissue samples were evaluated for morphological characteristics, distribution and severity of lesions and expression of viral protein.

Samples of the duodenum, at least one piece of lower intestine (ileum region for chickens and turkeys, unknown precise location for Guinea fowl) and the mucosa of the cloaca or bursa (referred to as 'bursal mucosa') were analyzed in detail for numbers of heterophils, lymphocytes, plasma cells and macrophages in six IBV QX-infected chickens at 4 days post inoculation (dpi), nine Fr TCoV-infected turkeys at 3 dpi and nine naturally-infected Guinea fowl in which GfCoV was detected by qPCR four days after the onset of mortality. Due to variable and sometimes suboptimal tissue morphology and regular presence of highly cellular areas with cells lying very close together, lymphocytes, plasma cells and macrophages were not always well individually distinguishable. Abundance of these cells was therefore scored cumulatively and referred to as 'mononuclear cells'. Cells were counted using the counting tool of graphic software (Adobe Photoshop CC 2018®) in digital images covering a total defined area (DA) of 0.16 mm^2, split over two multifocally selected 0.08 mm^2 areas that were morphologically representative for the tissue sample and that cumulatively contained parts of 4 to 6 representative villi and their lamina propria. Grades (0-3) were given based on the average cell numbers counted within the DA (Supplemental Table 2). In addition, for the Guinea fowl duodenum relative

villus-crypt lengths were estimated using the ruler tool of graphic software (Adobe Photoshop CC 2018®) and compared to the villus to crypt ratio of uninfected commercially-farmed Guinea fowl (n = 5) that were used as negative control group in an *in vivo* experiment and identified as GfCoV-negative by qPCR.

Viral protein expression in the intestinal samples was semi-quantified with a two-parameter scoring system (Supplemental Table 3), comparable to a previously published study.[22] The first parameter comprised the percentage of tissue where viral protein was observed: 0%, <10% (usually focal), 10-50% (usually multifocal), >50% (usually coalescing to diffuse). For the second parameter the number of cells with viral protein were counted in a DA of 0.34 mm^2 (one 40x objective, field number (FN) 26.5) where the number of cells that showed immunohistochemical signal was highest. A combined total grade was assigned to each sample for further comparison and interpretation by adding the grades of both parameters: a total sum of 1 or 2 would be grade 1, a total sum of 3 or 4 would be grade 2, a total sum of 5 an 6 would be grade 3.

Results

Gastrointestinal Tract

In IBV QX-infected chicken intestines at 4 dpi, heterophils were only present individually scattered in very low numbers (<10/DA) in 2/6 ileum samples and 5/6 bursal mucosa samples, but never in the duodenum. Moderate numbers (11-50/DA) of mononuclear cells were observed in almost all of these intestinal tissue samples (Fig. 1). No epithelial changes, villus thickening or villus fusion were noticed and no differences were observed between broilers and layers.

In contrast, in the selected Fr TCoV-infected turkeys at 3 dpi higher numbers (mostly 1-50, but sometimes >50/DA) of heterophils were observed in 6/9 duodenum samples, 8/9 ileum samples and 9/9 bursal mucosa samples. The number of mononuclear cells was similar in almost all intestinal tissue samples (Fig. 2). No epithelial changes, villus thickening or villus fusion were noticed

The most abundant inflammatory cell infiltration was observed in the intestinal samples of the naturally-infected Guinea fowl (9/9) with moderate to high

numbers of heterophilic granulocytes (1-50 and sometimes >50/DA) in 9/9 duodenum samples and low to moderate numbers (1-50/DA) in 7/9 lower intestine and bursal mucosa samples. Almost all segments contained high numbers (>50/DA) of mononuclear cells (Fig. 3). Within the duodenum, villi were regularly thickened and plump and sometimes showed fusion (3-5 crypts covered by one plump villus) with an average villus : crypt ratio of 2.2 (1.2-3.9).

In none of the three bird species, lesions were present in the gut-associated lymphoid tissues (GALT), including the cecal tonsil, and the lymphoid component of the bursa of Fabricius.

Quantity and distribution of viral protein over the intestinal regions differed between bird species (Fig. 4-6). Viral protein expression was most prominently observed in the Guinea fowl duodenum, whereas protein expression in chickens

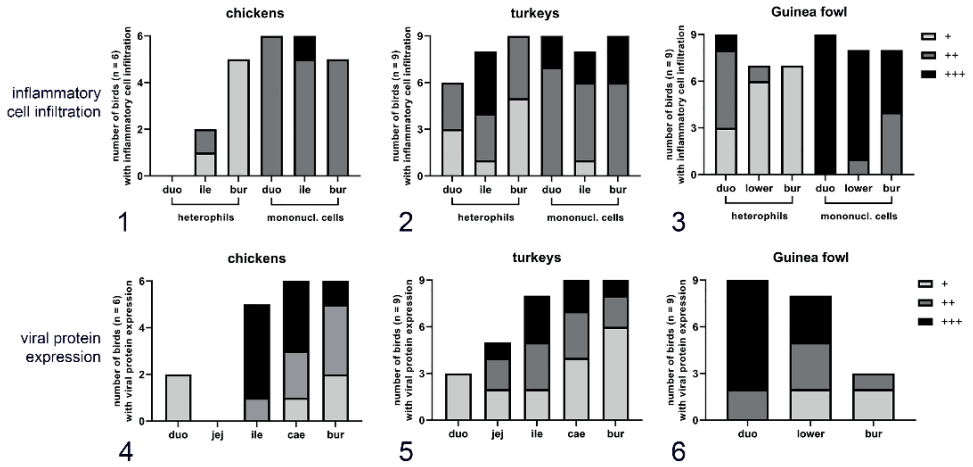

Figures 1-6. IBV QX, US TCoV and GfCoV infection, intestines of chicken, turkey and Guinea fowl. Semi-quantification of inflammatory cell infiltration and viral protein expression. **Figure 1**. IBV QX-infected chicken (4 dpi), mild heterophilic infiltration of the lower intestine, moderate mononuclear infiltration throughout the intestines. **Figure 2**. Fr TCoV-infected turkey (3 dpi), moderate to marked heterophilic infiltration of mainly the lower intestine, moderate to marked mononuclear infiltration throughout the intestines. **Figure 3**. GfCoV-infected Guinea fowl (4 days after onset of mortality), moderate heterophilic infiltration of mainly the upper intestine, marked mononuclear infiltration throughout the intestines. **Figure 4**. IBV QX-infected chicken (4 dpi), moderate to marked viral protein expression of the lower intestine. **Figure 5**. Fr TCoV-infected turkey (3 dpi), moderate viral protein expression of mainly the lower intestine. **Figure 6**. GfCoV-infected Guinea fowl (4 days after onset of mortality within the bird flock), marked viral protein expression of mainly the upper intestine. Duo = duodenum; jej = jejunum; ile = ileum; cae = caecum; bur = bursal / cloacal mucosa; lower = lower intestine (other than duodenum).

and turkeys was more abundant in lower intestinal segments. Presence of viral protein seemed to coincide with presence of heterophils, but less with presence of lymphocytes, plasma cells and macrophages. Viral protein was observed in the cytoplasm of enterocytes and goblet cells (Fig. 7-9). In addition, in IBV QX-

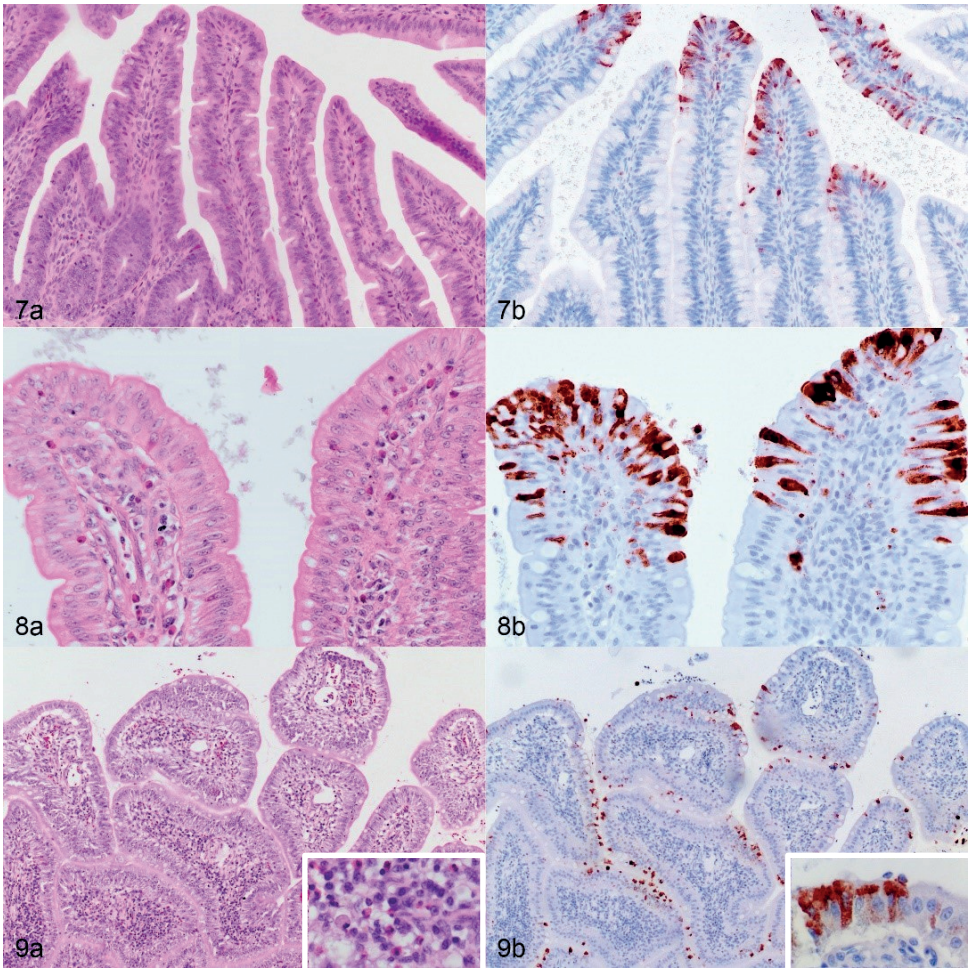

Figures 7-9. IBV QX, US TCoV and GfCoV infection, intestines of chicken, turkey and Guinea fowl. Representative pictures of morphologic changes and viral protein expression. **(a)** Hematoxylin and eosin. **(b)** Immunolabeling IBV, TCoV or GfCoV antibody. **Figure 7**. IBV QX infection (7 dpi), ileocolonic junction, chicken. **(a)** Mild mononuclear enterocolitis. **(b)** Viral antigen expression within the enterocyte cytoplasm. **Figure 8**. Fr TCoV infection (3 dpi), ileocolonic junction, turkey. **(a)** Moderate heterophilic and mild mononuclear enterocolitis. **(b)** Viral antigen expression within the enterocyte cytoplasm. **Figure 9**. GfCoV infection (4 days after onset of mortality within the bird flock), duodenum, Guinea fowl. **(a)** Thickened villi with moderate heterophilic and marked mononuclear enteritis. **(b)** Viral antigen expression within the enterocyte cytoplasm.

infected chickens and Fr TCoV-infected turkeys, viral protein was sometimes visible in mononuclear cells in the lower intestine GALT and the lymphoid component of the bursa (Supplemental Fig. S1, S2).

Intestinal tissue samples of uninfected birds incidentally contained few (<10/DA) and seldom higher numbers (11-50/DA) of heterophils. Mononuclear cells were observed in moderate numbers (11-50/DA) in all uninfected chicken and turkey intestines and abundantly (>50/DA) in those of Guinea fowl (Supplemental Fig. S3-S5). No villus fusion was observed in any of these uninfected tissues. The duodenum of uninfected Guinea fowl had an average villus : crypt ratio of 4.7 (3.1-5.2).

Heterophilic and lymphoplasmacytic enterocolitis (Supplemental Fig. S6) that mildly progressed over time at 6, 14 and 21 dpi was observed in the small additional sample collection of one-day-old Fr or US TCoV-infected turkeys and incidentally mild proventriculitis (Supplemental Fig. S7) and ventriculitis (Supplemental Fig. S8) were seen in IBV-infected chickens. No lesions or viral protein were observed in any esophagus and crop assessed.

Respiratory Tract

In 30/30 (100%) six- and nine-week-old chickens inoculated intraocularly with IBV M41, IBV 793B and IBV QX, moderate to severe, diffuse, lymphohistiocytic and heterophilic rhinitis, tracheitis and milder aerosacculitis were observed at 5 dpi (Supplemental Fig. S9, S10). Lungs of all birds showed very mild diffuse interstitial heterophilic infiltration with often moderate multifocal nodular lymphoid hyperplasia and regularly (10/30 (33%) birds) heterophils and debris in the parabronchial lumina. Viral protein expression (Supplemental Table 4) was observed in the nasal and tracheal epithelium, incidentally the epithelium of primary and secondary bronchi and the air sacs and sometimes in cellular debris in parabronchial lumina, but never in the parabronchial and air capillary epithelium.

Respiratory tract inflammatory cell infiltration was observed in one-week-old IBV M41-infected chicks from 24 hours post infection (hpi) with mild progression over time and lesions comparable to those in the six- and nine-week-old birds

described above at 7 dpi. Viral protein was found in the nasal mucosa of most of these birds from 24 hpi up to 7 dpi, but was observed in only few tracheas and air sacs (Supplemental Table 5). No viral protein was found in any lung.

None of the turkey and Guinea fowl airway samples showed any lesions or viral protein expression.

Urinary Tract

Minor focal lymphohistiocytic interstitial nephritis and periureteritis were observed in 7/18 (39%) chickens infected with IBV QX at day of hatch at 1-3 dpi. Similar focal infiltration was also present in 3/10 uninfected control birds. From 4 dpi on, lesions in IBV QX-infected birds progressed to moderate, multifocal lymphoplasmacytic and milder heterophilic tubulointerstitial nephritis with epithelial necrosis in 23/30 (77%) birds, of which 13/23 (57%) were broilers and 10/23 (43%) layers (Supplemental Fig. S11a). In samples 4-8 dpi that contained a piece of ureter (n=11), moderate to severe lymphoplasmacytic and heterophilic ureteritis was seen in 10/11 (91%) kidneys. No glomerular lesions were observed in any bird. Viral protein expression (Supplemental Fig. S11b) was observed in tubular, collecting duct and ureteral epithelium from 4-8 dpi in 16/30 (53%) birds, of which 11/16 (69%) were broilers and 5/16 (31%) layers. No viral protein was observed in any kidney at 1-3 dpi.

None of the kidneys of the one-week-old IBV M41-infected chickens or any turkey or Guinea fowl showed any lesions or viral protein expression.

Other Tissues

Of all other tissues that were studied, only several Harderian glands (15/45, 33%) sampled from the various IBV-infected chickens showed very mild lymphoplasmacytic and minimal heterophilic adenitis, which coincided with viral protein expression in 10/15 (66%) glands (Supplemental Fig. S12). In addition, very mild focal viral protein expression was present without lesions in few lacrimal glands and the conjunctiva of some IBV-infected chicken (not further quantified). In 3/30 (10%) of the six- and nine-week-old IBV M41-, 793B- or QX-infected chickens, single viral protein-containing cells (likely

macrophages) were observed in the spleen (Supplemental Fig. S13). Lesions and viral protein were absent in any oviduct, gonad, liver, pancreas, skeletal and cardiac muscle or brain tissues that were assessed.

Discussion

In this study, tissues of chickens, turkeys and Guinea fowl infected with IBV, TCoV and GfCoV respectively were analyzed for presence of pathologic changes and expression of viral protein. Since enterotropism is the trait most characteristically shared by the three viruses, intestinal tracts of the three bird species were compared in detail to explain reported differences in clinical presentation. In the present study, IBV has been shown to induce milder inflammatory cell infiltration than TCoV and GfCoV and while IBV and TCoV mostly infected the lower intestines, GfCoV clearly more prominently targeted the duodenum. These findings suggest differences in lesion severity and tropism of these viruses in the intestines, which may contribute to differences in clinical signs and mortality. The relative physiologic importance of the avian small intestine and especially the duodenum and jejunum outweighs that of the ceca, rectum and cloaca significantly on levels of total absorptive surface, retention time of digesta, enzymatic digestion, nutrient absorption and digestive hormone release.[18] Other intestinal diseases, for example the so-called 'malabsorption syndrome' (MAS) in broiler chickens, also illustrate the negative impact of extensive small intestine pathology on poultry's health.[37] The fact that Guinea fowl are reported to suffer clinically more severely from intestinal CoV infection than turkeys and chickens, might therefore be explained by the observed preference of GfCoV for the upper small intestine. The present work does further confirm that TCoV to lesser extent also targets the duodenum, an intestinal segment that is often not specifically reported in earlier studies on TCoV infections.[1,8,17,23] In contrast to the Guinea fowl however, this was observed only in a minority of birds and associated with only small amounts of viral protein when compared to the amounts of viral protein in the turkeys' lower intestines.

Heterophilic and mononuclear enterocolitis was observed in all three bird

species with variable distribution and severity over the different regions of the intestines. The distribution of the heterophilic infiltrate over the different intestinal segments in all three bird species coincided with distribution of viral protein. The number of heterophils, on the other hand, seemed to be positively associated with the abundance of viral protein within the turkey and Guinea fowl intestines, but less within the chickens. In the latter species, only limited heterophilic infiltration was observed in the several intestinal regions, although viral protein was often prominently expressed in especially the lower intestinal segments. This might imply that TCoV and GfCoV evoke a more severe intestinal inflammatory response than IBV variants, which might explain the greater clinical GI tract impact that is usually observed. It has been under debate whether IBV truly causes relevant GI disease[12]. Earlier studies that demonstrate presence of IBV genome and protein within the GI tract seldom report associated clinical signs, but are often also less specific about distribution of virus and often lack details on associated lesions.[2,19,21,46] Although the current results confirm that the acute heterophilic infiltration of the GI tract after CoV infection in chickens seems quite mild compared to the responses in turkeys and Guinea fowl, the relevance of the mononuclear cell infiltrate is more doubtful since such infiltration was also observed in uninfected control birds. More data are also needed for solid interpretation of especially lesion progression over time and the response in the Guinea fowl in general. For this species, comparison with earlier data is particularly difficult, since the birds within the current work were the only ones available for the study presented here and originate from the only confirmed cases reported so far.[20,28] In these reports no specifications were given on histopathology and (semi)quantification of virus, though, and the present study for the first time provides detailed information on both aspects under *in vivo* circumstances.

Within the current comparative study, no additional tissue tropism besides the intestinal tract was demonstrated for TCoV and GfCoV. It needs to be considered though, that these observations are based on immunohistochemical detection of viral protein and not on more sensitive techniques like ISH and PCR. The observed respiratory tract and renal lesions in IBV-infected chickens largely resembled the hallmark IBV-associated lesions reported over the last

decades.[5,13,14,35] Consistent with some previous studies, the epithelium of the parabronchi, atria, infundibula and air capillaries never revealed viral protein in any of the lungs.[19,32] Presence of IBV specifically in the parabronchial epithelium has been reported, but in that rare case birds additionally suffered from immune-incompetence due to infectious bursal disease.[21] Additional other studies report parabronchial and air capillary inflammation during IBV infection, but without specific demonstration of viral presence within these locations.[26,30,39] The present work now more comprehensively than the earlier work tried to find associations between specific lesions and precise location of the virus within the lungs of chickens of different type and age and inoculated with different IBV variants. Based on these results, the tropism of IBV seems to differ from respiratory alpha- and betacoronaviruses which often replicate within pneumocytes.[34,44,45,48] Pneumocyte infection can induce a severe acute respiratory distress syndrome (ARDS), which is often lethal.[41] In contrast, mortality from uncomplicated airway disease is seldom observed in IBV infections.[11] The mild interstitial pneumonia observed in some chickens might have resulted either from viremia or potentially have been triggered by intraluminal cellular debris that contained virus, which was observed in several otherwise lesion-free parabronchi and atria and therefore might have originated from the more prominently infected primary and secondary bronchi.

A restriction regarding interpretation of the findings in this study is the fact that tissues were collected via convenience sampling from various experiments at multiple institutes. This is especially true for the Guinea fowl samples. Since no tissues from experimentally infected Guinea fowl were available, archived paraffin-embedded tissues were obtained that were initially used for diagnostic examination of naturally-infected flocks and these sometimes came from birds that had been dead for some time before sampling. These Guinea fowl were not SPF birds and therefore lesion morphology might have been influenced by triggers other than GfCoV only. Tissue samples were therefore matched as much as possible regarding time frame and completeness of tissue collections and compared with available uninfected birds if possible.

In conclusion, this study demonstrates that GfCoV infection is associated with heterophilic enteritis most prominently in the upper small intestine, which is in

contrast with TCoV and IBV that more prominently target the lower intestine. These differences in tropism and severity of associated heterophilic infiltration might explain differences in clinical outcome of intestinal CoV infection in chickens, turkeys and Guinea fowl. The study helps to understand the presentation of coronaviral disease in poultry, but also demonstrates that infection, for example by IBV in the intestine, can coincide with very little pathological changes.

Acknowledgements

The authors gratefully thank G.J. Boelm, I. Jorna and the necropsy floor staff of Royal GD Animal Health, Deventer, the Netherlands; M. Delpont, R. Berger and the necropsy floor staff of IHA, Université de Toulouse, Toulouse, France; M. Matthijs, K. Bouwman and the histology laboratory staff of the Faculty of Veterinary Medicine, Utrecht, the Netherlands; and A. Laconi, J. Bloodgood, B. Saucedo, I. Ambepitiya-Wickramasinghe, F. van Asten, G. de Vrieze, S. Nguyen, S. Schouwenburg, J. Bergmans, T. van den Burgh and S. Pulles for their participation during the necropsies, making slides and performing immunohistochemical stainings; M. Dwars for constructive debate on avian histopathology; G. Grinwis for critical reading and commenting during revision of the manuscript.

Declaration of Conflicting Interests

The authors declared no potential conflicts of interest with respect to the research, authorship, and/or publication of this article.

Funding

This article is based upon work from COST Action FA1207 (Towards Control of Avian Coronaviruses: Strategies for Diagnosis, Surveillance and Vaccination and/or initials), supported by COST (European Cooperation in Science and Technology).

References

1. Adams NR, Ball RA, Hofstad MS. Intestinal lesions in transmissible enteritis of turkeys. *Avian Dis*. 1970;**14:**392-399.

2. Ambali AG, Jones RC. Early pathogenesis in chicks of infection with an enterotropic strain of infectious bronchitis virus. *Avian Dis*. 1990;**34:**809-817.

3. Ambepitiya Wickramasinghe IN, de Vries RP, Weerts EAWS, et al. Novel receptor specificity of avian gammacoronaviruses that cause enteritis. *J Virol*. 2015;**89:**8783-8792.

4. Beaudette FR, Hudson CB. Cultivation of the virus of infectious bronchitis. *J Am Vet Med Ass*. 1937;**90:**51-60.

5. Benyeda Z, Szeredi L, Mato T, et al. Comparative histopathology and immunohistochemistry of QX-like, Massachusetts and 793/B serotypes of infectious bronchitis virus infection in chickens. *J Comp Pathol*. 2010;**143:**276-283.

6. Bouwman KM, Delpont M, Broszeit F, et al. Guinea fowl coronavirus diversity has phenotypic consequences for glycan and tissue binding. *J Virol*. 2019;**93**:1-11.

7. Bouwman KM, Parsons LM, Berends AJ, de Vries RP, Cipollo JF, Verheije MH. Three amino acid changes in avian coronavirus spike protein allow binding to kidney tissue. *J Virol*. 2020;**94**:1-14.

8. Breslin JJ, Smith LG, Barnes HJ, Guy JS. Comparison of virus isolation, immunohistochemistry, and reverse transcriptase-polymerase chain reaction procedures for detection of turkey coronavirus. *Avian Dis*. 2000;**44:**624-631.

9. Brown PA, Courtillon C, Weerts EAWS, et al. Transmission kinetics and histopathology induced by European turkey coronavirus during experimental infection of specific pathogen free turkeys. *Transbound Emerg Dis*. 2019;**66**:234-242.

10. Brown PA, Touzain F, Briand FX, et al. First complete genome sequence of European turkey coronavirus suggests complex recombination history related with US turkey and Guinea fowl coronaviruses. *J Gen Virol*. 2016;**97:**110-120.

11. Cavanagh D. Coronavirus avian infectious bronchitis virus. *Vet Res*. 2007;**38:**281-297.

12. Cavanagh D. Coronaviruses in poultry and other birds. *Avian Pathol*. 2005;**34:** 439-448.

13. Chen BY, Hosi S, Nunoya T, Itakura C. Histopathology and immunohistochemistry of renal lesions due to infectious bronchitis virus in chicks. *Avian Pathol*. 1996;**25:**269-283.

14. Chong KT, Apostolov K. The pathogenesis of nephritis in chickens induced by infectious bronchitis virus. *J Comp Pathol*. 1982;**92:**199-211.

15. Courtillon C, Briand F-X, Allée C, et al. Description of the first isolates of Guinea fowl corona and picornaviruses obtained from a case of Guinea fowl fulminating enteritis. *Avian Pathol*. 2021;**50:**507-521.

16. De Wit JJ, Cook JK, van der Heijden HM. Infectious bronchitis virus variants: a review of the history, current situation and control measures. *Avian Pathol*. 2011;**40:**223-235.

17. Dea S, Verbeek A, Tijssen P. Transmissible enteritis of turkeys: experimental inoculation studies with tissue-culture-adapted turkey and bovine coronaviruses. *Avian Dis*. 1991;**35:**767-777.

18. Denbow DM. Gastrointestinal Anatomy and Physiology. In: Scanes CG, ed. *Sturkie's Avian Physiology*. 6th ed. San Diego, CA: Academic Press; 2015:337-366.

19. Dolz R, Vergara-Alert J, Perez M, Pujols J, Majo N. New insights on infectious bronchitis virus pathogenesis: characterization of Italy 02 serotype in chicks and adult hens. *Vet Microbiol*. 2012;**156:**256-264.

20. Ducatez MF, Liais E, Croville G, Guerin JL. Full genome sequence of Guinea fowl coronavirus associated with fulminating disease. *Virus Genes*. 2015;**50:**514-517.

21. França M, Woolcock PR, Yu M, Jackwood MW, Shivaprasad HL. Nephritis associated with infectious bronchitis virus Cal99 variant in game chickens. *Avian Dis*. 2011;**55:**422-428.

22. Giglia G, Agliani G, Munnink BBO, et al. Pathology and pathogenesis of Eurasian blackbirds (*Turdus merula*) naturally infected with Usutu virus. *Viruses*. 2021;**13**:1-16.

23. Gomes DE, Hirata KY, Saheki K, Rosa AC, Luvizotto MC, Cardoso TC. Pathology and tissue distribution of turkey coronavirus in experimentally infected chicks and turkey poults. *J Comp Pathol*. 2010;**143:**8-13.

24. Ito NM, Miyaji CI, Capellaro CE. Studies on broiler's IBV and IB-like virus from Guinea fowl. In: II International Symposium on Infectious Bronchitis. Giessen, Germany: Justus Liebig University; 1991:302-307.

25. Jindal N, Mor SK, Goyal SM. Enteric viruses in turkey enteritis. *VirusDisease*. 2014;**25:**173-185.

26. Jones RC, Jordan FT. Persistence of virus in the tissues and development of the oviduct in the fowl following infection at day old with infectious bronchitis virus. *Res Vet Sci*. 1972;**13:**52-60.

27. Laconi A, Weerts EAWS, Bloodgood JC, et al. Attenuated live infectious bronchitis virus QX vaccine disseminates slowly to target organs distant from the site of inoculation. *Vaccine*. 2020;**38:**1486-1493.

28. Liais E, Croville G, Mariette J, et al. Novel avian coronavirus and fulminating disease in Guinea fowl, France. *Emerg Infect Dis*. 2014;**20:**105-108.

29. Maier HJ, Hawes PC, Cottam EM, et al. Infectious bronchitis virus generates spherules from zippered endoplasmic reticulum membranes. *mBio*. 2013;**4:**1-12.

30. Martin MP, Wakenell PS, Woolcock P, O'Connor B. Evaluation of the effectiveness of two infectious bronchitis virus vaccine programs for preventing disease caused by a California IBV field isolate. *Avian Dis*. 2007;**51:**584-589.

31. Maurel S, Toquin D, Briand FX, et al. First full-length sequences of the S gene of European isolates reveal further diversity among turkey coronaviruses. *Avian Pathol*. 2011;**40:**179-189.

32. Nakamura K, Cook JK, Otsuki K, Huggins MB, Frazier JA. Comparative study of respiratory lesions in two chicken lines of different susceptibility infected with infectious bronchitis virus: histology, ultrastructure and immunohistochemistry. *Avian Pathol*. 1991;**20:**241-257.

33. Peiris JSM. Coronaviruses. In: Greenwood D, ed. *Medical Microbiology*. 18th ed. London, UK: Churchill Livingstone; 2012:587-593.

34. Priestnall SL. Canine respiratory coronavirus: A naturally occurring model of COVID-19? *Vet Pathol*. 2020;**57:**467-471.

35. Purcell DA, McFerran JB. The histopathology of infectious bronchitis in the domestic fowl. *Res Vet Sci*. 1972;**13:**116-122.

36. Raj GD, Jones RC. Infectious bronchitis virus: immunopathogenesis of infection in the chicken. *Avian Pathol.* 1997;**26:**677-706.

37. Rebel JMJ, Balk FRM, Post J, Van Hemert S, Zekarias B, Stockhofe N. Malabsorption syndrome in broilers. *Worlds Poult Sci J*. 2006;**62:**17-30.

38. Ritchie AE, Deshmukh DR, Larsen CT, Pomeroy BS. Electron microscopy of coronavirus-like particles characteristic of turkey bluecomb disease. *Avian Dis*. 1973;**17:**546-558.

39. Saif YM, Fadly AM, Glisson JR, McDougald LR, Nolan LK, Swayne DE. *Diseases of Poultry*. 12th ed. Arnes, AI, US: Iowa State University Press; 2008.

40. Schalk AF, Hawn MC. An apparently new respiratory disease of baby chicks. *J Am Vet Med Ass*. 1931;**78:**413-422.

41. Torres Acosta MA, Singer BD. Pathogenesis of COVID-19-induced ARDS: implications for an ageing population. *Eur Respir J*. 2020;**56:**1-12.

42. Valastro V, Holmes EC, Britton P, et al. S1 gene-based phylogeny of infectious bronchitis virus: an attempt to harmonize virus classification. *Infect Genet Evol*. 2016;**39:**349-364.

43. Van Beurden SJ, Berends AJ, Kramer-Kuhl A, et al. A reverse genetics system for avian coronavirus infectious bronchitis virus based on targeted RNA recombination. *Virol J*. 2017;**14:109:**1-13.

44. Van den Brand JM, Haagmans BL, Leijten L, et al. Pathology of experimental SARS coronavirus infection in cats and ferrets. *Vet Pathol*. 2008;**45:**551-562.

45. Van den Brand JM, Smits SL, Haagmans BL. Pathogenesis of Middle East respiratory syndrome coronavirus. *J Pathol*. 2015;**235:**175-184.

46. Villarreal LY, Brandão PE, Chacón JL, et al. Molecular characterization of infectious bronchitis virus strains isolated from the enteric contents of Brazilian laying hens and broilers. *Avian Dis*. 2007;**51:**974-978.

47. Wickramasinghe IN, van Beurden SJ, Weerts EAWS, Verheije MH. The avian coronavirus spike protein. *Virus Res*. 2014;**194:**37-48.

48. Yao XH, Li TY, He ZC, et al. A pathological report of three COVID-19 cases by minimally invasive autopsies. *Zhonghua Bing Li Xue Za Zhi*. 2020;**49:**411-417.

Supplementary Data

Materials and Methods

Experimental Setup 1 (IBV M41, 793B, QX)

Tissues were obtained from challenged control group birds from three vaccination trials performed by GD Animal Health, Deventer, the Netherlands. Per trial, a group (n = 10) of specific pathogen free (SPF) chickens (GD Animal Health, Deventer, the Netherlands) was infected intraocularly with 0.1 ml inoculum (0.05 ml per eye) containing respectively $4\log^{10}$ EID_{50} IBV M41, $5\log^{10}$ EID_{50} IBV 793 (both groups nine week old broilers) or $4\log^{10}$ EID_{50} IBV QX (type D388) (six week old layers). During the experiment, animals were housed in HEPA-filtered isolators with ad lib food and water. At five days post inoculation (dpi), all animals were euthanized and submitted for necropsy. Tissue samples were taken from all animals from the trachea, nasal mucosa, air sac (caudal, adjacent to cranial pole of kidney), lung and spleen. From two animals per group Harderian and lacrimal glands were taken and fixed. Experiments were performed in agreement with the Dutch national regulations on animal experiments and approved by the Dutch Animal Ethical Committee (DEC) (ethical animal experimentation approval 2015-278).

Experimental Setup 2 (IBV M41)

42 one-week-old female SPF chickens (GD Animal Health, Deventer, the Netherlands) were infected intraocularly with 0.1 ml inoculum (0.05 ml per eye) containing $5\log^{10}$ EID_{50} IBV. Animals were housed in HEPA-filtered isolators with ad lib food and water during the whole experimental period. At six, 12, 24, 36, 48 hpi and three and seven dpi, animals (five or six per time point) were euthanized and submitted for necropsy. Tissue samples were taken from all animals from the respiratory tract (trachea, nasal mucosa, lung, caudal air sac), the digestive tract (crop, proventriculus, gizzard, duodenum, pancreas, jejunum, ileum, caeca, colon, cloaca, liver), the urogenital tract (kidney, ovarium, oviduct), lymphoid tissues (spleen, bursa of Fabricius, thymus, cecal tonsil), peri-ocular tissues (lacrimal gland, Harderian gland, ductus nasolacrimalis), heart,

skeletal muscle, brain and smears from jugular blood. Additionally, on every time point, comparable samples were also taken from two euthanized PBS inoculated birds. Experiments were performed in agreement with the Dutch national regulations on animal experiments and approved by the DEC (ethical animal experimentation approval 2013.II.10.107).

Experimental Setup 3 (IBV QX)[27]

24 SPF broiler and 24 SPF layer chickens (GD Animal Health, Deventer, the Netherlands) were inoculated intratracheally at day of hatch with 0.1 ml inoculum containing $3\log^{10}$ EID_{50} IBV QX (type D388). At day one to day eight post inoculation, three animals were euthanized per time point per bird type and submitted for necropsy. Kidney samples were taken from all animals at all time points. At 1, 4, 7 and 8 dpi samples were also taken from the digestive tract (esophagus, proventriculus, gizzard, duodenum, jejunum, ileum, caeca, colon, cloaca). At every time point, additionally a PBS inoculated broiler and layer were euthanized and comparable tissue samples were taken. Experiments were performed in agreement with the Dutch national regulations on animal experiments and approved by the DEC (ethical animal experimentation approval 2017-071).

Experimental Setup 4 (Fr TCoV)[9]

Eighteen 10-day-old SPF turkeys were divided in six groups of n = 3 per group and inoculated orally with $10^{5.7}$ RNA copies of Fr TCoV. For each group, a fecal inoculum taken from donor birds from a previous experiment was used, sampled at six, 13, 21, 27, 34 and 41 dpi from these donor birds; all these birds were inoculated with the same TCoV stock. Three additional contact animals were added at to each group at one dpi (additionally n = 18, in toto 36 birds). All animals were euthanized at 3 dpi and samples were taken from the gastrointestinal tract (duodenum, jejunum, ileocolonic junction, caecum, cloaca with bursa of Fabricius), respiratory tract (trachea, lung, air sac), liver, kidney, spleen and thymus. Experiments were performed in agreement with the national regulations of the French Ministry for higher education and research on animal welfare (N° APAFIS#6680-201 609091 3457475 v3) and after approval

from the French Agency for Food, Environmental and Occupational Health & Safety's (ANSES) ethical committee (N°016).

Experimental Setup 5 (US TCoV, Fr TCoV)[3]

12 1-day-old SPF turkeys were inoculated orally with $10^{4.7}$ EID_{50} of either TCoV-US or TCoV-Fr (n = 6 per virus). Animals were euthanized at six, 14 and 21 dPI (n = 2 per virus per time point) and intestinal samples were taken (for the purpose of the original experiment not precisely labelled per location). Experiments were performed in agreement with the national regulations of the French Ministry for higher education and research on animal welfare and after approval from the French Agency for Food, Environmental and Occupational Health & Safety's (ANSES) ethical committee (performed 2009).

Samples of naturally-infected birds (GfCoV)[28]

Tissues were obtained from several field cases spread over France in the period 2014 to 2016. Dead or moribund 7 to 13-week-old birds (n = 34) were collected from commercially-housed flocks showing more than ten percent mortality in association with diarrhea. For diagnostic histopathological purposes, a variable set of tissues per case was sampled, always including the duodenum and pancreas (n = 34), often containing an additional intestinal segment caudal to the duodenum (usually caudal part of small intestine or colon), lung and trachea (n = 22) and sometimes the cloaca and bursa of Fabricius (n = 14) or the kidney (n = 11). For detailed comparison of the digestive tracts, nine animals (7-week-old) were selected from which always a piece of duodenum, an intestinal segment caudal to the duodenum and the bursa of Fabricius with attached cloacal epithelium was present. In these birds, presence of avian coronaviral RNA in the intestinal contents was confirmed with real-time RT-PCR targeting a part of the N protein gene. Based on later full genome sequencing, it was concluded that the discovered viral genomic material differed from that of TCoVs and IBVs.[10,20,28]

Supplemental Table 1. Sources of Studied Tissue Samples

Infection	Birds + Age at day of infection	Viruses	Tissues	Sampling time points
Exp.	SPF broiler and layer chickens, day of hatch	IBV QX	gi[a], kid	1-8 dpi[b]
Exp.	SPF turkeys, 10-day-old	Fr TCoV	gi[a], resp, kid, spl, thy, liv	3 dpi
Nat.	Guinea fowl, farmed, 7-wk-old	GfCoV	gi[a], resp, kid, bu	unknown[c]
Exp.	SPF broiler chickens, 9-wk-old	IBV M41 / 793B	resp, spl, pg	5 dpi
Exp.	SPF layer chickens, 6-wk-old	IBV QX	resp, spl, pg	5 dpi
Exp.	SPF layer chickens, 1-wk-old	IBV M41	resp, gi, kid, lymph, pg, liv, other	6, 12, 24, 36, 48 hpi, 3, 7 dpi
Exp.	SPF turkeys, 1-day-old	Fr / US TCoV	gi	6, 14, 21 dpi

Abbreviations: exp, experimental; nat, natural; SPF, specific pathogen free; resp, respiratory tissues (nasal mucosa (IBVs only) – trachea – lung – caudal air sac); spl, spleen; pg, periocular glands (lacrimal gland, Harderian gland); gi, GI tract (duodenum – pancreas – jejunum - ileocolonic junction – caecum – cloaca, additionally for IBV infected birds esophagus or crop – proventriculus – gizzard. Archived turkey gi samples 6, 14 and 21 dpi were only partially specified); kid, kidney; lymph, lymphoid tissues (spleen - bursa of Fabricius – thymus - cecal tonsil); liv, liver; thy, thymus; bu, bursa; d/hpi: days/hours post inoculation. other: conjunctiva – ovary – oviduct - cardiac and skeletal muscle – brain - blood smear.

[a] Intestines used for comparative analysis (Figs. 1-6, main text). For this analysis, IBV QX-infected chickens 4 dpi were used.

[b] GI tract sampled on 1, 4, 7 and 8 dpi. [c] Four days after the onset of mortality in the bird flock.

Supplemental Table 2. Grading of Heterophilic and Mononuclear Infiltration

Grade	cells / DA[a]
0	0
1	1 - 10
2	11- 50
3	>50

[a] Heterophilic granulocytes and mononuclear cells were countred in a total area of 0.16 mm^2, split over two multifocally selected 0.08 mm^2 areas that cumulatively contained parts of 4 to 6 morphologically representative villi and their lamina propria. Grades (0-3) were given for both cell types based on the average cell numbers counted within these two areas (referred to as 'defined area', DA)

Supplemental Table 3. Two-Parameter Grading of Viral Protein Expression

grade	1st Parameter: % of tissue involved	2nd Parameter: cells / DA[a]	combined total grade[b]
0	0%	0	0
1	<10% (focal)	1-20	1 = sum 1 or 2
2	10-50% (multifocal)	21-50	2 = sum 3 or 4
3	>50% (coalescing / diffuse)	>50	3 = sum 5 or 6

[a] one defined area (DA) measures 0.34 mm^2 (one 40x objective, FN 26.5)

[b] combined grade of a sample is defined as the sum of the grades of both parameters.

Results

Supplemental Table 4. Airway Viral Protein Expression in IBV-infected Chickens, 5 dpi

IBV strain	nasal mucosa	trachea	air sac	lung[a]
M41	9/9	7/10	3/10	4/10
793B	7/10	7/10	0/10	2/10
QX	7/10	8/10	6/10	2/10

[a] Viral protein only observed in primary and secondary bronchi and cellular debris in the parabronchial lumen, but never in the parabronchial, atrial, infundibular or air capillary epithelium.

Supplemental Table 5. Number of Chickens showing IBV M41 Protein Expression per Tissue per Time Point

hpi / dpi	nasal mucosa	trachea	air sac
6 hpi	1/5	1/5	0/5
12 hpi	2/6	0/6	0/6
24 hpi	5/6	0/6	0/6
36 hpi	6/6	1/6	0/6
48 hpi	4/6	1/6	0/6
3 dpi	4/6	1/6	0/6
7 dpi	3/5	1/6	1/6

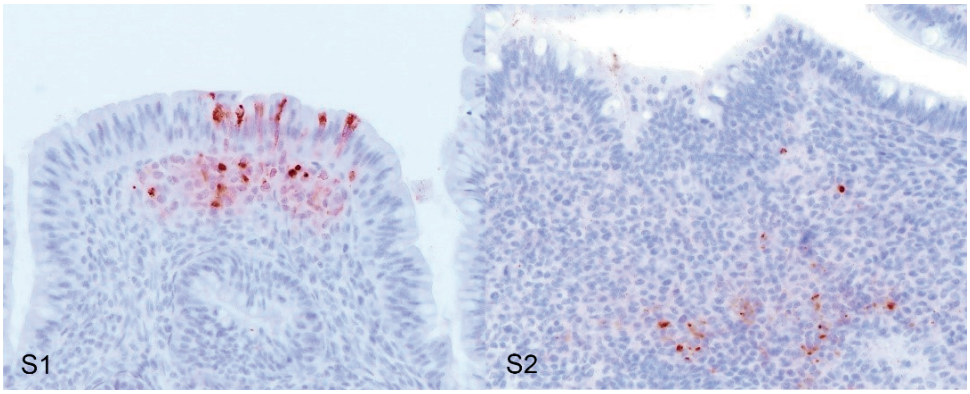

Supplemental Figures 1-2. IBV QX protein expression, GALT, chicken. Immunolabeling IBV antibody. **Figure 1**. Cloaca, enterocytes and mononuclear cells containing viral protein. **Figure 2**. Cecal tonsil, mononuclear cells containing viral protein.

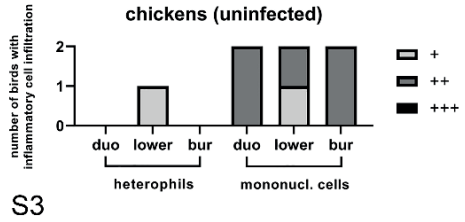

S3

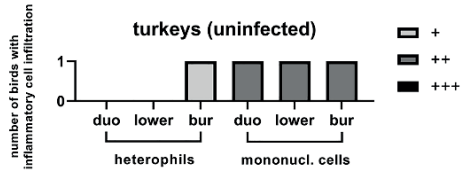

S4

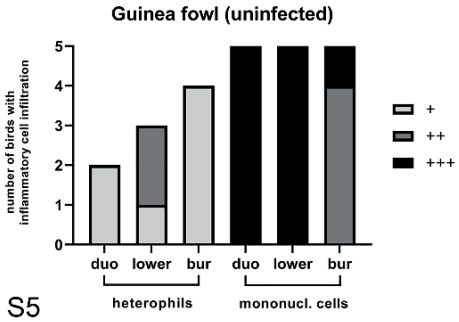

S5

Supplemental Figures 3-5. Intestines of uninfected chickens, turkeys and Guinea fowl, semi-quantification of inflammatory cell infiltration. **Figure 3**. Uninfected chickens, minimal heterophilic infiltration of the lower intestine, moderate mononuclear infiltration throughout the intestines. **Figure 4**. Uninfected turkey, minimal heterophilic infiltration of the bursal mucosa, moderate mononuclear infiltration throughout the intestines. **Figure 5**. Uninfected Guinea fowl, mild heterophilic and marked mononuclear infiltration throughout the intestines. duo, duodenum; lower, lower intestine other than duodenum (ileum in chickens and turkey); bur, bursal / cloacal mucosa.

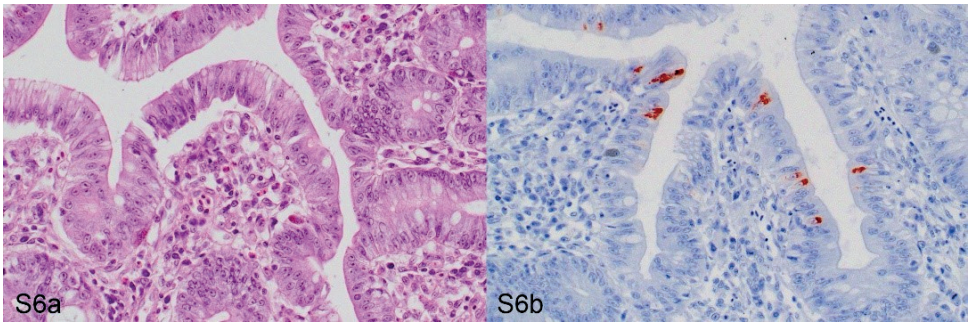

Supplemental Figure 6. US TCoV infection (14 dpi), transition rectum to cloaca, turkey. **(a)** mild heterophilic and moderate mononuclear colitis, hematoxylin and eosin. **(b)** Viral antigen expression within the enterocyte cytoplasm, immunolabeling TCoV antibody.

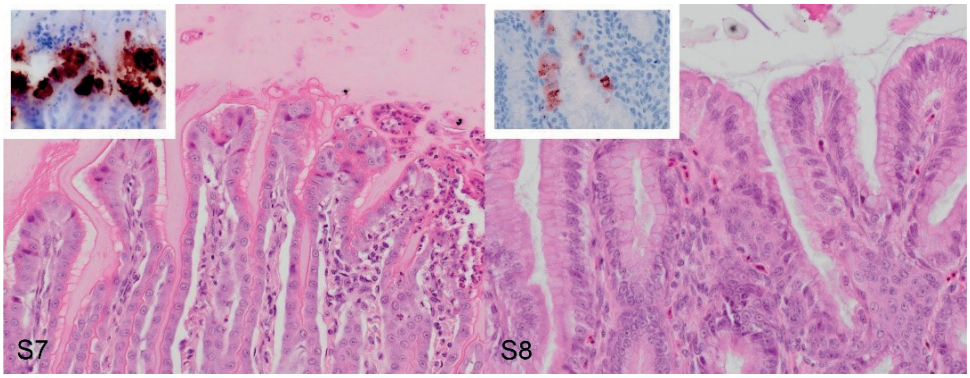

Supplemental Figures 7-8. IBV infections, gizzard and proventriculus, chicken. Hematoxylin and eosin. Insets: Immunolabeling IBV antibody. **Figure 7**. IBV QX-infection, gizzard, focal heterophilic ventriculitis. **Figure 8**. IBV M41-infection, mild mononuclear proventriculitis.

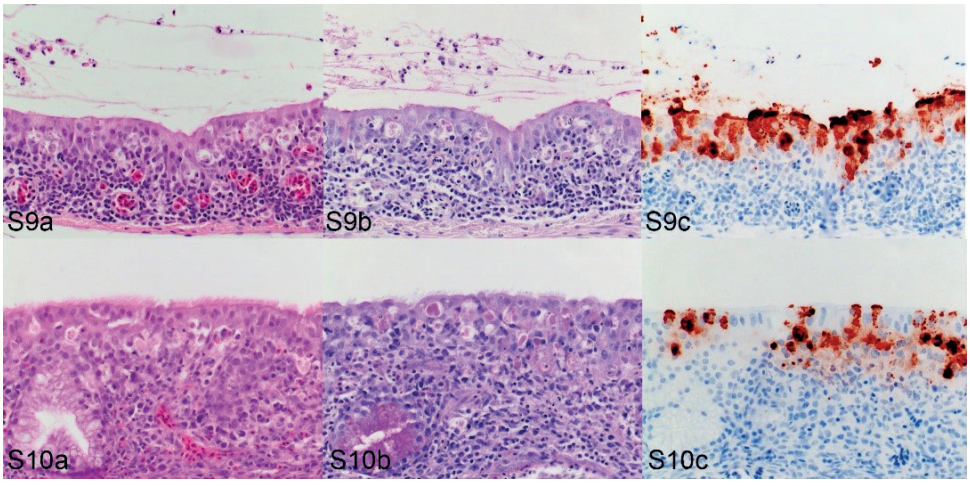

Supplemental Figures 9-10. IBV 793B respiratory tract infection (5 dpi), trachea and nasal mucosa, chicken. **(a)** Hematoxylin and eosin. **(b)** Periodic-acid Schiff. **(c)** Immunolabeling IBV antibody. Lesions were identical for IBVs 793B, M41 and QX. **Figure 9**. Trachea. **(a)** Diffuse lymphohistiocytic tracheitis with single-cell necrosis, loss of cilia and intraluminal heterophils. **(b)** Diffuse loss of mucus-containing goblet cells. **(c)** Viral protein expression within the epithelial cytoplasm. **Figure 10**. Nasal mucosa. **(a)** Diffuse lymphohistiocytic rhinitis with single-cell necrosis. **(b)** Multifocal loss of glandular mucus-containing goblet cells. **(c)** Viral protein expression within the epithelial cytoplasm.

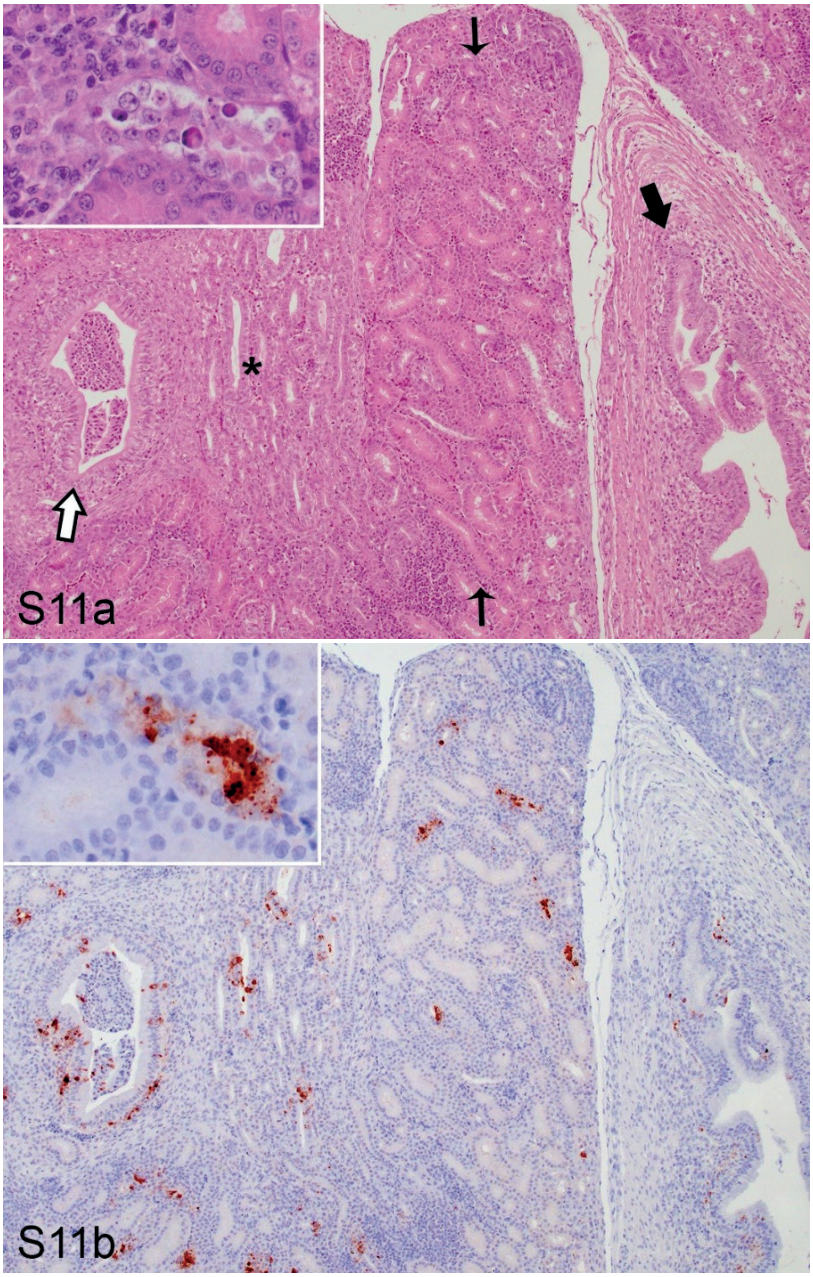

Supplemental Figure 11. IBV QX infection (6 dpi), moderate multifocal lymphoplasmacellular and histiocytic tubulointerstitial nephritis and ureteritis, kidney, chicken. **(a)** Hematoxylin and eosin. **(b)** Immunolabeling IBV antibody. Ureter (thick black arrow), cortical zone (thin black arrows), medullary cone (asterisk) with large collecting duct (white arrow).

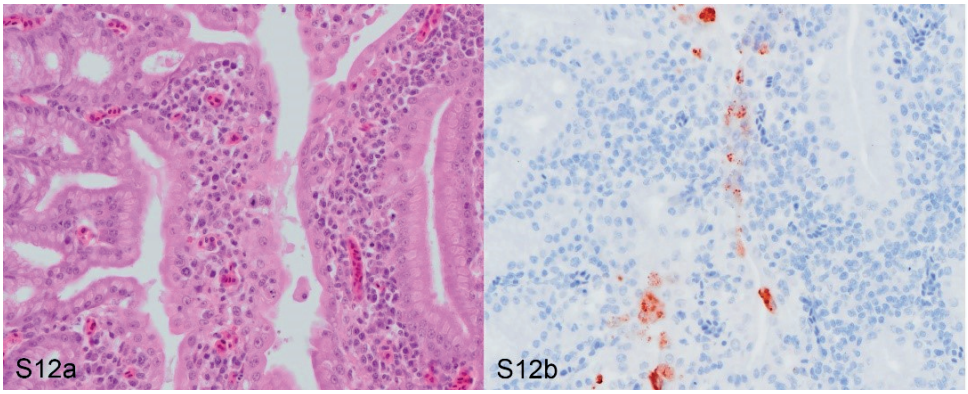

Supplemental Figure 12. IBV 793B infection (5 dpi), mild mononuclear adenitis with epithelial cell necrosis and desquamation, Harderian gland, chicken. Moderate plasmacellular infiltration is considered normal in this gland. **(a)** Hematoxylin and eosin. **(b)** Immunolabeling IBV antibody.

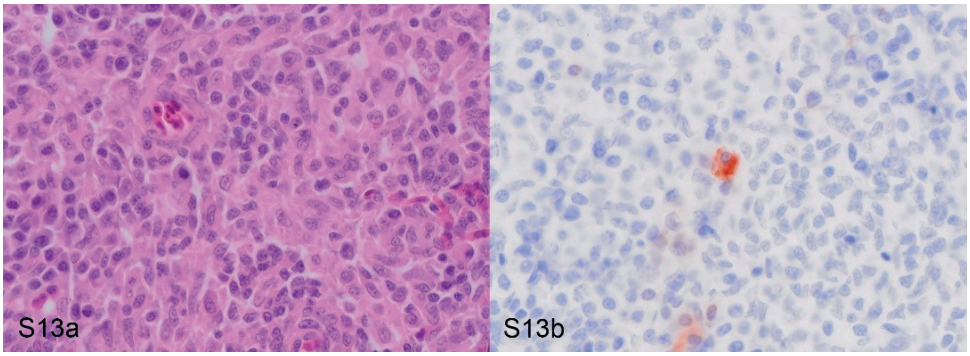

Supplemental Figure 13. IBV 793B infection, viral protein expression in single mononuclear cells without coinciding lesions, spleen, chicken. **(a)** Hematoxylin and eosin. **(b)** Immunolabeling IBV antibody.

8 General discussion

Avian coronaviruses (AvCoVs) continue to threaten poultry species and livestock farmers to date and at the same time carry on to challenge and intrigue veterinarians and researchers. In this thesis, AvCoV infections were studied with emphasis on pathogenesis and virus-induced histomorphological changes to improve knowledge on AvCoV-induced diseases in chickens, turkeys and Guinea fowl.

Over the last years, studies on AvCoVs and especially infectious bronchitis virus (IBV) often focused on virus phylogeny, genotyping of new virus variants and improvement of vaccination strategies to prevent infection and disease.[7,20,31,32] To lesser extent, researchers aimed to elucidate coronavirus-associated immune responses and functions of the viral replication machinery.[13,26] Although understanding of virus-induced histomorphological changes is very important to properly explain disease, studies on AvCoVs that involved histomorphological analysis seem to have been somewhat underrepresented. This thesis helps to fill this gap, since histomorphological analysis of pathological tissue changes – in short 'histopathology' - was used in **all chapters** as a leading approach to gain new insights into AvCoV-induced diseases. Histopathological examination on the one hand helps to create an overview of morphologic tissue changes that together underlie a disease process. On the other hand, it can be used to dissect this overview to pinpoint and quantify the separate general tissue reactions patterns, such as epithelial cell death and immune cell presence, that contribute to the microscopic phenotype of the disease. It further enables to discover associations between these separate tissue reaction patterns and also creates the opportunity to visualize presence of the causative agent within the lesions, for example via techniques such as immunohistochemistry and in-situ hybridization. These properties together make histopathological analysis of indispensable value to fully characterize and understand disease.

All chapters of this thesis incorporate approaches that could be categorized as 'comparative pathology' in narrower or broader sense. In narrow sense, the term 'comparative pathology' is primarily used for comparison between species, but in broader sense it could also be used to refer to studies that compare breeds and age groups. In even broader sense, it could include different routes of infection of a single pathogen. Furthermore, comparison of pathogens that

are genetically closely related or seem to have very similar clinical effects within a specific host might also be incorporated. **Chapter 2** compares pathogenicity of an attenuated IBV vaccine strain with its direct virulent field ancestor, **chapters 3 to 5** compare the impact of different respiratory viral pathogens and a bacterium in different airway regions, **chapter 6** compares the intestines of turkeys inoculated with the turkey coronavirus (TCoV) via two routes of administration and **chapter 7** compares lesions and tropism in different intestinal segments of three AvCoVs in three poultry species. Studying similarities and differences of infectious diseases in all variants above helps to quicker and better understand and potentially predict the clinical impact of future emerging pathogens that could evoke new pandemics in animal species, as well as in the human population.[25]

Furthermore, a significant part of the thesis, represented by **chapters 3 to 5**, is attributed to dual infections in the respiratory tract. Here, lesion development is not only driven by an AvCoV, but after sequential inoculation with a certain time interval also by a bacterium or other virus. Understanding the role of coronaviruses (CoVs) in dual infections is very important, since such infections often significantly increase disease severity and therefore aggravate animal welfare problems and economical losses. Gain of knowledge on the pathogenesis of dual infections may contribute to more critical use of therapeutic drugs, for example antibiotics when a bacterium is involved in order to avoid antibiotic resistance.[14] It may also help to improve vaccination strategies in order to avoid complications like vaccine failure or unintentional vaccine-associated enhanced disease when virulent field viruses are present in a flock at the time of administration of an attenuated vaccine virus.

Chapter 2 provides new insights into differences in pathogenicity that result from the attenuation of a vaccine virus (IB Primo QX) when compared to its direct virulent field ancestor (IBV D388). Where many studies on virus attenuation for vaccine production mostly aim to show successful reduction of pathogenicity combined with good protection against challenge with virulent virus,[19] no studies truly seem to directly compare an IBV vaccine virus with its virulent field ancestor *in vivo* in order to elucidate the mechanisms behind the reduced pathogenicity. The study in **chapter 2** demonstrates that attenuation of

this specific IBV QX-like variant D388 is either based on a decreased ability to disseminate through the chicken from the inoculation site (trachea, nasal mucosa) or a decreased ability to replicate in target tissues more distant from the inoculation site (for example the urogenital tract and intestines), rather than on loss of tissue tropism or loss of pathogenicity at the inoculation site. Based on mRNA levels and viral protein expression, the vaccine virus was able to replicate and induce lesions similar to the wild type progenitor in the trachea. Although the vaccine virus was also found in the kidneys, replication here was very limited compared to the virulent field ancestor and no lesions were induced. A possible explanation for this difference might be that the vaccine virus lost the ability to enter the bloodstream and cause viremia.[28] Since occurrence of viremia was not specifically evaluated, the findings however do not exclude the possibility that decreased ability to bind to or replicate in the renal epithelium play an additional role. In distant target tissues that likely do not necessarily require viremia to get infected by the virus, for example the conjunctiva and intestinal tract, viral mRNA and protein were nevertheless found fairly abundant and this seems to contradict that attenuation is mostly based on a general decrease of replication potency.

In addition to the findings that help to understand the mechanism underlying the attenuation, the work in **chapter 2** provides new support for the possibility that nephropathogenic IBV variants might reach the kidneys via ascending infection through the ureters.[10] This support comes from the finding that mRNA of the virulent field ancestor virus was already abundantly found in the cloaca before mRNA and viral protein were demonstrated in the kidney. Although viral presence in the cloaca at that time point therefore could not be the result of renal infection yet, it could be the cause for subsequent renal infection with the ureter as port of entry. This theory could be substantiated by the fact that the ureters and renal collecting ducts consistently showed more abundant viral protein expression compared to the numbers of cells that contained viral protein in the proximal and distal tubules. Viremic spread of IBV has been difficult to prove and quantify *in vivo* and some details on the underlying pathogenesis only recently were elucidated.[28] The ability of the virus to reach

the kidneys via ascending route through the ureters would make successful renal infection less dependent on or even independent from viremia.

While the work in **chapter 2** reconfirms that lesion severity can change based on properties of the virus, **chapter 3** demonstrates that also changes within the target cells of the host can contribute to the decreased ability of a virus to infect or replicate. Results in this chapter show that IBV infection of tracheal epithelium decreases the ability of this epithelium to get reinfected by another IBV variant. The results further demonstrate that the initial IBV infection can delay reinfection by at least one variant of low pathogenic avian influenza virus (AIV). Binding studies with the attachment proteins of both virus families indicate that this is likely associated with changes of sialic acid expression by the epithelial cells, which is the group of receptors used by both viruses. This could be explained as an antiviral response of the epithelium aimed to prevent further infection of adjacent cells to allow the epithelium to recover. Such responses could be based on virus-specific intracellular pathways, but also represent a general anti-viral effect via for example the activation of certain Toll-like receptors or other generic anti-viral responses.[17] Changes in cell susceptibility to a certain virus that result from infection by another virus might be very important with regard to vaccination strategies and vaccine failure.[3] Based on this study, the effectivity of a live-attenuated vaccine can potentially be reduced by epithelial changes that have been caused by a subclinical or unnoticed field infection at the time of, or shortly before, vaccine administration. Conversely, and although not truly demonstrated in this study, it needs to be further determined whether circulating field viruses could probably also undesirably benefit from changes in surface molecule expression induced by a vaccine virus and thereby cause more severe tissue damage and disease.

Besides, as studied in **chapter 3**, that epithelial cells modify mucosal membranes to the disadvantage of viruses, they also have been recognized as important modulators of immune responses during both viral and bacterial infections. Within the scope of dual infections, antibacterial immune responses in mammals have been shown to be dysregulated extensively by prior viral infections, and there are several indications that virus-induced epithelial malfunction is mechanistically of major influence.[29] Virus-induced immune

responses in chickens that might result in enhanced inflammation evoked by subsequent infection by avian pathogenic *Escherichia coli* (APEC) were studied in **chapters 4 and 5**.

The data presented in **chapter 4** demonstrate that respiratory lesions that result from dual infections with one of three respiratory viruses - either IBV, Newcastle disease virus (NDV) or avian metapneumovirus (aMPV) – and APEC are all associated with altered immune responses when compared to infection with APEC only. Mostly in the lung, and to lesser extent in the trachea and air sac, inoculation of APEC without preceding virus exposure was associated with an increase of KUL01+ phagocytic antigen presenting cells, that was mostly transient. Dual infection with prior exposure to one of the three viruses led to various and sometimes persistent influxes of T cells, which were not observed after inoculation with APEC only. Furthermore, the dual infections were associated with upregulated mRNA levels of pro-inflammatory cytokines interleukin (IL) 6, interferon (IFN) γ and IL-17, which were transient in the lung but persistent over the studied time interval in the spleen.

These observed differences in immune responses were associated with lesions that were generally more severe after dual infection than after inoculation with APEC only. The severity of mainly airsacculitis but also tracheitis varied depending on which virus was initially inoculated and seemed influenced to only a limited extent by APEC. Although it is known that pathogenicity of APEC isolates can vary,[2] previous studies have indeed demonstrated that APEC-induced lesions in the trachea and air sacs are often resolve rather quickly.[12,27] NDV and IBV were correlated with more severe lesions than aMPV and these persisted over time whereas lesions after aMPV infection were mostly transient over the time period studied. In contrast, severity of pneumonia after the various dual infections resembled the severity that was observed after inoculation of APEC only and was less influenced by the three viruses. In chickens, aMPV mostly causes mild upper respiratory tract infection, whereas IBV and NDV are known to more extensively target the epithelium of bronchi and the air sacs.[23,30] Within the lungs, these viruses generally prefer bronchial over air capillary epithelium,[30] which could explain the relatively limited viral influence on severity and persistence of lesions in the deeper lung tissue. Since

the severity and distribution of airway lesions in this chapter seemed to be determined mainly by the tropism and pathogenicity of the initially inoculated virus, these virus-related characteristics probably define the phenotype of the resulting disease more than APEC, at least in broiler chickens under the conditions as in this experiment.

Chapter 5 provides observations that substantiate this theory on the phenotype of lesions and disease after dual infection further, at least when inoculation of the virus precedes inoculation of the bacterium. Dual infection with IBV and APEC was studied with specific focus on the air sacs, because these showed the most severe and persistent lesions in the respiratory tract in the work of both **chapter 4** and previous studies.[12,27] Seven days after inoculation with APEC, the air sacs of birds that were infected with IBV twelve days earlier had severe lesions with marked epithelial damage in three of five birds and infiltration of many heterophils and mononuclear cells with several lymphoid nodules in four of five birds. Epithelial damage and marked heterophilic infiltrates were also the main characteristics seen five days after inoculation in the air sacs of three of five control birds that only received IBV, while mononuclear cell infiltration with formation of lymphoid nodules was the main observation in three of five birds twelve days after inoculation with only the virus. In contrast, air sacs of birds that only received APEC seven days after inoculation showed an intact epithelial lining with mild multifocal inflammatory cell infiltrates. Within this experiment and with the IBV and APEC variants used, the observed lesion morphology after dual infection therefore also to large extent seems to be defined by the virus. This conclusion needs to be drawn with caution though, since IBV and APEC isolates can vary in pathogenicity.[2,18,30] Furthermore, the outcome might be different when APEC inoculation would precede IBV infection.

In the studies of both **chapter 4 and 5**, enhanced and persistent airway lesions after dual infection seemed mostly free of bacteria, based on intralesional APEC antigen detection. This could mean that antibiotic therapy at this stage of disease might be of lesser value, but more sensitive techniques like PCR or classical culture are likely needed for a better and more quantitative foundation of this finding. Nevertheless, the fact that severe lesions persist in absence or rather limited intralesional presence of bacteria again stresses the importance

of prevention of the initial IBV infection via vaccination strategies. In addition, it theoretically could reopen the discussion on potential advantages of the use of anti-inflammatory drugs in progressed stages of disease, although this might be undesirable under practical circumstances because of residues in carcasses for human consumption, for example.[4,22]

While **chapters 2 to 5** deal with IBV as representative of the AvCoV family, **chapters 6 and 7** introduce two additional AvCoVs in two other poultry species, respectively TCoV in turkeys and the Guinea fowl coronavirus (GfCoV) in Guinea fowl. In contrast to **chapters 3 to 5** that report on respiratory infections, **chapter 6 and 7** focus on the intestinal tract.

Based on the results of the study in **chapter 6**, presence of TCoV RNA in fecal samples of orally infected turkeys did not always correlate with presence of infectious viral particles. Fecal samples taken from TCoV-infected turkey poults with one-week-intervals up to 6 weeks after infection that all contained abundant viral RNA were used to inoculate other poults. Inoculation of fecal material from only three of six sampling time points successfully lead to infection of the intestinal tract of these poults as demonstrated by both qPCR and immunohistochemistry. Viral protein was mostly discovered in the cytoplasm of enterocytes, but in several poults it was also found in cells within the lymphoid component of the cecal tonsil, probably due to phagocytosis but potentially also due to replication in these cells. An explanation for the intermittent excretion of infective viral particles could be that the virus resides within this lymphoid tissue for a longer period without concurrent production of infective particles or release of such particles within the feces. Viral genetic material could probably end up in the intestinal contents via exocytosis of lymphocytes or histiocytes that contain viral RNA. It might be possible that revival of viral replication in the intestinal epithelium occurs from this latent stage, and this would normally result in production of infective viral particles. This explanation seems supported by an earlier proposed theory in which the cecal tonsils were considered as potential place of latent infection for IBV in chickens.[9] Further support follows from the fact that cyclic revival of viral replication with intermittent fecal shedding was also observed for the feline enteric coronavirus.[21] In the study of **chapter 6** it could not be determined

definitively whether the presence of TCoV protein within the cecal tonsils resulted from phagocytosis or replication. Previous studies nevertheless demonstrated that IBV is indeed able to replicate in peripheral blood monocytes.[28] As alternative explanation for failure of infection from some of the inocula, it could have been possible that infectious viral particles were actually present but that successful infection or replication were hampered within the inoculated poults. It seems unlikely though that this would happen systematically in all birds within a certain experimental group.

The work in **Chapter 7** demonstrates that severity of disease might be reflected by differences in intestinal viral tropism, but that on the other hand abundant viral replication (here based on viral protein expression) does not necessarily correlate with inflammatory lesions and therefore potentially not with clinical effects. In contrast to TCoV and IBV, that in this study were mainly found in the lower intestines, GfCoV protein was extensively present within the upper intestines. Although no clinical signs were recorded during the experiments that underlie this retrospective study, this difference in tropism might very well be explanative for the severe clinical presentation of disease in GfCoV-infected Guinea fowl as reported in literature, compared to the relatively milder enteric signs evoked by TCoV and especially IBV.[1,5,9,11,15,24] The more severe clinical impact of an upper intestine tropism could be explained by the fact that in birds the small intestines and mostly the duodenum and jejunum are physiologically significantly more important regarding absorption, enzymatic digestion and excretion of digestive hormones than the lower intestinal segments.[8] It remains unclear why viral protein expression in the intestines of the chicken does seem to induce so little tissue damage and, based on literature, in general seems to cause neglectable intestinal disease.[5,9]

Several perspectives for potential future research perspectives are raised by this thesis. Based on the findings in **chapter 2**, new studies on demonstration of viremia over time and the likelihood of occurrence of ascending renal infection could be initiated to better understand viral migration through the host. Especially the latter aspect would be challenging though, since it will likely require systematic analysis of specifically the ureter, which can be difficult to prepare well for histological analysis. Theoretically a possible approach might be

to create a luciferase producing virus, that can be monitored longitudinally under *in vivo* circumstances.[16] With regard to **chapter 3**, consequences of changes in receptor expression induced by AIV could be studied in the trachea organ culture (TOC) model under condition of first an infection with AIV followed by an infection with IBV. Furthermore, infection experiments in chickens could be performed to evaluate whether the proposed receptor expression changes are *in vivo* also associated with similar repression of viral RNA production as observed in the TOC model. The studies in **chapter 4 and especially chapter 5** would benefit from larger experimental group size. The virus-APEC comparison in **chapter 4** would benefit from addition of extra control groups infected with virus only to better understand the impact of the viral agents on distribution and persistence of lesions. The study of **chapter 5** was designed to make profitable use of surplus chickens from another experiment to reduce unnecessary wasting of useful experimental animals. Due to the limited number of available birds on the one hand and available isolators in the research facility on the other hand though, choices had to be made regarding group size and not all experimental groups ideally needed for best interpretation could be created. Furthermore, the studies in both chapters could also be improved with more sensitive evaluation of pathogen dynamics by additional culturing and PCR analysis, since this might give useful knowledge to improve therapeutic intervention and prevention. Finally, from **chapters 6 and 7** it becomes clear that controlled *in vivo* studies on GfCoV infection in Guinea fowl are needed for improved understanding of disease severity, viral tropism and viral transmission.[6] In addition, studies on potential latency of AvCoV infection in lymphoid tissues might change thoughts on disease prevention. This could probably be studied *ex vivo* on lymphocytes and monocytes isolated from lymphoid tissues or peripheral blood in culture media.

In conclusion, the major findings from this thesis are:

Chapter 2: Attenuation of the IBV vaccine virus IB Primo QX ® results from diminished ability to disseminate to or replicate in target organs distant from the site of inoculation, although it causes lesions with comparable morphology and severity as its wild-type progenitor at the inoculation site.

Chapter 3: IBV induces changes in receptor expression in the chicken trachea that negatively influence the possibility for a sequential infection by another IBV variant and potentially also other viruses that use the same receptors.

Chapter 4: Respiratory lesions that result from dual infections with a virus - either IBV, NDV or aMPV - and APEC are correlated with enhanced pro-inflammatory immune responses in comparison with infection by APEC only. The tropism and pathogenicity of the involved virus seem to define severity and localization of tissue damage, which likely have a direct influence on severity of disease in addition to the virus-induced immune reactions that might indirectly hamper a proper antibacterial response.

Chapter 5: Airsacculitis after dual infection with the selected variants of IBV (vaccine strain H52) and APEC (strain 506) in this study displayed morphological characteristics that seem to better resemble tissue changes observed after infection with IBV, rather than with APEC only, but with increased severity and wider distribution. Although this needs further study, especially involving other variants of both IBV and APEC and the reciprocal inoculation sequence with the bacterium preceding the virus, this could imply that 'virus-induced colibacillosis' under certain circumstances might be better explained as 'APEC-enhanced viral damage'.

Chapter 6: Fecal shedding of infective TCoV particles seems to take place intermittently, although viral RNA is continuously found in fecal contents. This might be explained by revival of replication in the intestinal epithelium after latency of the virus in the gut-associated lymphoid tissue.

Chapter 7: Intestinal disease in GfCoV-infected Guinea fowl might be more severe than intestinal disease in IBV-infected chickens and TCoV-infected turkeys due to preference of GfCoV for the duodenum, whereas IBV and TCoV more prominently seem to replicate in the lower intestines.

Following from the findings above, this thesis demonstrates the value of histopathology as a tool to provide new insights in the contribution of morphologic tissue changes to disease, here caused by AvCoVs in three poultry species.

References

1. Adams NR, Ball RA, Hofstad MS. Intestinal lesions in transmissible enteritis of turkeys. *Avian Dis*. 1970;14:392-399.

2. Alber A, Morris KM, Bryson KJ, et al. Avian pathogenic *Escherichia coli* (APEC) strain-dependent immunomodulation of respiratory granulocytes and mononuclear phagocytes in CSF1R-reporter transgenic chickens. *Front Immunol*. 2019;10:3055,1-16.

3. Bhuiyan MSA, Amin Z, Bakar AMSA, et al. Factor influences for diagnosis and vaccination of avian infectious bronchitis virus (gammacoronavirus) in chickens. *Vet Sci*. 2021;8:47,1-25.

4. Caplen G, Colborne GR, Hothersall B, et al. Lame broiler chickens respond to non-steroidal anti-inflammatory drugs with objective changes in gait function: a controlled clinical trial. *Vet J*. 2013;196:477-482.

5. Cavanagh D. Coronavirus avian infectious bronchitis virus. *Vet Res*. 2007;38:281-297.

6. Courtillon C, Briand F-X, Allée C, et al. Description of the first isolates of Guinea fowl corona and picornaviruses obtained from a case of Guinea fowl fulminating enteritis. *Avian Pathol*. 2021;50:507-521.

7. De Wit JJ, Cook JK, van der Heijden HM. Infectious bronchitis virus variants: a review of the history, current situation and control measures. *Avian Pathol.* 2011;40:223-235.

8. Denbow D. Gastrointestinal anatomy and physiology. In: Scanes C, ed. *Sturkie's Avian Physiology*. 6th ed. Academic Press; 2015:337-366.

9. Dhinakar Raj G, Jones RC. Infectious bronchitis virus: immunopathogenesis of infection in the chicken. *Avian Pathol.* 1997;26:677-706.

10. Dolz R, Vergara-Alert J, Pérez M, et al. New insights on infectious bronchitis virus pathogenesis: characterization of Italy 02 serotype in chicks and adult hens. *Vet Microbiol*. 2012;156:256-264.

11. Ducatez MF, Liais E, Croville G, Guerin JL. Full genome sequence of Guinea fowl coronavirus associated with fulminating disease. *Virus Genes*. 2015;50:514-517.

12. Dwars RM, Matthijs MGR, Daemen AJ, et al. Progression of lesions in the respiratory tract of broilers after single infection with *Escherichia coli* compared to superinfection with *E. coli* after infection with infectious bronchitis virus. *Vet Immunol Immunopathol*. 2009;127:65-76.

13. Ellis S, Keep S, Britton P, de Wit S, et al. Recombinant infectious bronchitis viruses expressing chimeric spike glycoproteins induce partial protective immunity against homologous challenge despite limited replication *in vivo. J Virol*. 2018;92:e01473-18,1-18.

14. Fancher CA, Thames HT, Colvin MG, et al. Prevalence and molecular characteristics of avian pathogenic *Escherichia coli* in "No Antibiotics Ever" broiler farms. *Microbiol Spectr*. 2021;9:e00834-21,1-11.

15. Gomes DE, Hirata KY, Saheki K, et al. Pathology and tissue distribution of turkey coronavirus in experimentally infected chicks and turkey poults. *J Comp Pathol*. 2010;143:8-13.

16. Heaton NS, Leyva-Grado VH, Tan GS, et al. In vivo bioluminescent imaging of influenza A virus infection and characterization of novel cross-protective monoclonal antibodies. *J Virol*. 2013;87:8272-8281.

17. Ichinohe T. Respective roles of TLR, RIG-I and NLRP3 in influenza virus infection and immunity: impact on vaccine design. *Expert Rev Vaccines*. 2010;9:1315-1324.

18. Jackwood MW. Review of infectious bronchitis virus around the world. *Avian Dis*. 2012;56:634-641.

19. Jackwood MW, Jordan BJ, Roh HJ, et al. Evaluating protection against infectious bronchitis virus by clinical signs, ciliostasis, challenge virus detection, and histopathology. *Avian Dis*. 2015;59:368-374.

20. Keep S, Sives S, Stevenson-Leggett P, et al. Limited cross-protection against infectious bronchitis provided by recombinant infectious bronchitis viruses expressing heterologous spike glycoproteins. *Vaccines (Basel)*. 2020;8:330,1-19.

21. Kipar A, Meli ML, Baptiste KE, et al. Sites of feline coronavirus persistence in healthy cats. *J Gen Virol*. 2010;91:1698-1707.

22. Landman WJM, Matthijs MGR, van Eck JHH. Effect of anti-inflammatory drugs on colibacillosis lesions in broilers after infectious bronchitis virus and subsequent *Escherichia coli* infection. *Vet Q*. 2012;32:25-29.

23. Li X, Hanson RP. In vivo interference by Newcastle disease virus in chickens, the natural host of the virus. *Arch Virol*. 1989;108:229-245.

24. Liais E, Croville G, Mariette J, et al. Novel avian coronavirus and fulminating disease in Guinea fowl, France. *Emerg Infect Dis*. 2014;20:105-108.

25. Lin CN, Chan KR, Ooi EE, et al. Animal coronavirus diseases: parallels with COVID-19 in humans. *Viruses*. 2021;13:1507,1-15.

26. Maier HJ, Hawes PC, Cottam EM, et al. Infectious bronchitis virus generates spherules from zippered endoplasmic reticulum membranes. *mBio*. 2013;4:e00801-13,1-12.

27. Matthijs MGR, Ariaans MP, Dwars RM, et al. Course of infection and immune responses in the respiratory tract of IBV infected broilers after superinfection with *E. coli*. *Vet Immunol Immunopathol*. 2009;127:77-84.

28. Reddy VRAP, Trus I, Desmarets LMB, et al. Productive replication of nephropathogenic infectious bronchitis virus in peripheral blood monocytic cells, a strategy for viral dissemination and kidney infection in chickens. *Vet Res*. 2016;47:70,1-19.

29. Robinson KM, Kolls JK, Alcorn JF. The immunology of influenza virus-associated bacterial pneumonia. *Curr Opin Immunol*. 2015;34:59-67.

30. Saif YM, Fadly AM, Glisson JR, et al. *Diseases of Poultry*. 12th ed. Iowa State University Press; 2008.

31. Valastro V, Holmes EC, Britton P, et al. S1 gene-based phylogeny of infectious bronchitis virus: an attempt to harmonize virus classification. *Infect Genet Evol.* 2016;39:349-364.

32. Van Beurden SJ, Berends AJ, Krämer-Kühl A, et al. Recombinant live attenuated avian coronavirus vaccines with deletions in the accessory genes 3ab and/or 5ab protect against infectious bronchitis in chickens. *Vaccine*. 2018;36:1085-1092.

Addenda

Nederlandse samenvatting

De recente Covid-pandemie heeft de wereldbevolking als nooit tevoren kennis doen maken met coronavirussen. Dierenartsen en wetenschappelijk onderzoekers in het diergeneeskundig werkveld waren echter al decennia in touw om diverse coronavirussen enerzijds te beteugelen en anderzijds beter te leren begrijpen. Begin jaren 30 van de vorige eeuw werd in Massachusetts in de Verenigde Staten bij kippen een luchtwegziekte vastgesteld, die met het beter worden van de onderzoeksmethoden retrospectief aan een coronavirus kon worden toegeschreven. Hiermee was deze ziekte, infectieuze bronchitis (IB) genoemd, de eerste ziekte ooit die bewezen veroorzaakt werd door een coronavirus. Tegenwoordig is het infectieuze bronchitis virus (IBV) wereldwijd in gedomesticeerde kippenpopulaties aanwezig en de oorzaak van bedrijfsproblematiek in zowel de leg- als vleeskuikensector.

IBV veroorzaakt zoals gezegd in beginsel een luchtweginfectie. Het infecteert epitheel, een laag van gespecialiseerde bekledende en beschermende cellen, in voornamelijk de voorste luchtwegen (neus, luchtpijp) van de kip. Hierdoor verliest deze cellaag tijdelijk gedeeltelijk functie, wordt er een ontstekingsreactie op gang gebracht en begint het dier ziekteverschijnselen als snotteren en waterige neusuitvloeiing te vertonen. Als er geen verdere complicaties optreden, dan kan het dier – afhankelijk van de leeftijd - binnen een aantal dagen min of meer restloos herstellen. Gedurende deze infectie dalen echter groei en eiproductie, waardoor het virus behoorlijke economische impact kan hebben.

IBV kent verschillende varianten en sommige hiervan zijn in staat om dieper in de kip door te dringen dan in enkel de voorste luchtwegen. Naarmate de specifieke IBV variant beter in staat is om dit te doen, worden geïnfecteerde kippen over het algemeen zieker en zeker voor jonge dieren kan dat met permanente weefselschade gepaard gaan of dodelijk aflopen. IBV kan dieper doordringen in de luchtwegen en schade maken in de luchtzakken; dit zijn uitbreidingen van de luchtwegen specifiek gevonden in vogels. Vogels zijn voor correcte functionering van hun ademhaling sterk van deze anatomische structuren afhankelijk. Sommige IBVs kunnen nog dieper doordringen, de bloedbaan bereiken en uiteindelijk de nieren en het legapparaat infecteren. Infectie van het legapparaat van jonge leghennen kan op

latere leeftijd leiden tot verminderde eiproductie, misvormende eieren en zelfs tot totaal verlies van het vermogen om eieren te leggen.

Een andere, doorgaans vrij ernstig verlopende complicatie, betreft de situatie waarin een door IBV geïnfecteerde kip vervolgens aanvullend met een bacterie geïnfecteerd raakt. Aviaire pathogene *Escherichia coli* (APEC) is op dit vlak één van de meest beruchte bacteriën en de oorzaak van forse dierwelzijnsproblematiek en economische verliezen in de pluimveesector. APEC veroorzaakt in verschillende pluimveetypen diverse ziekteproblemen. In geval van interferentie met een eerdere IBV infectie, gaat het vaak om infectie van de luchtwegen. De ontstekingen in deze luchtwegen verlopen dan meestal vele malen ernstiger met vaak uitgebreide permanente weefselschade tot diep in de longen en luchtzaken. Geïnfecteerde dieren ervaren hiervan ernstige hinder.

Uit het bovenstaande wordt duidelijk dat de gevolgen van een IBV infectie variabel, doch zeer ernstig kunnen zijn, zowel in het kader van dierwelzijn als in economisch opzicht. De sector wil vogels daarom middels vaccinatie beschermen tegen infectie. Omdat er echter zoveel verschillende IBV varianten zijn, is dat een uitdagende klus, omdat niet alle vaccins goede bescherming bieden tegen deze verschillende virusvarianten. Het is daarom dat er een continue behoefte is aan vergroting van de kennis over IBV, zodat de ziekte beter begrepen kan worden, de impact van nieuwe virusvarianten beter kan worden voorspeld en er betere vaccins kunnen worden ontwikkeld die uitgebreidere bescherming bieden. Dit proefschrift draagt hieraan bij en beschrijft een aantal studies waarin bepaalde delen van het ziekteproces – de zogenaamde 'pathogenese' – nader onder de loep werden genomen.

Om verschillende redenen is het gebruikelijk om kippen middels besproeiing (spray) of aerosolvorming (fijne verneveling van virusdeeltjes in de lucht) te vaccineren, waarbij dan wordt getracht de dieren op een zo gecontroleerd mogelijke wijze en in zeer beperkte mate de eerder beschreven luchtweginfectie door te laten maken, waarna in ieder geval tijdelijk een zekere immuniteit wordt gegenereerd. Om deze infecties dusdanig gecontroleerd te laten verlopen, is het als vaccin te gebruiken virus stapsgewijs afgezwakt. In **hoofdstuk 2** is het effect bekeken van het afzwakken (attenueren) van een nierziekte-veroorzakende (nephropathogene) IBV variant tot zogenaamde 'vaccinstam' op de verspreiding van het virus door de kip wanneer het dier eraan wordt blootgesteld. Studie naar dergelijke effecten, waarbij het ziekmakende, directe 'vooroudervirus' uit het pluimveeveld één op één vergeleken

wordt met de daaruit afgezwakte vaccinstam, is op deze gedetailleerde schaal voor IBVs vrij zeldzaam. Waargenomen is dat de vaccinstam op microscopisch niveau weliswaar vrijwel identieke weefselveranderingen in de luchtwegen bewerkstelligt, maar dat dit wel vertraagd plaatsvindt. Het aantal geproduceerde virusdeeltjes blijft daarbij op luchtwegniveau redelijk gelijk. Een groot verschil werd echter waargenomen op nierniveau. De vaccinstam blijkt sterk verminderd in staat om de nieren te bereiken en het aantal geproduceerde virusdeeltjes is duidelijk minder. Tevens werd gezien dat het virus het darmkanaal van de kippen infecteerde, een verschijnsel wat maar in beperkte mate bestudeerd is. Het aantal virusdeeltjes in de cloaca (opening bij de vogel waar zowel darminhoud, urinezuur vanuit de nieren én bij vrouwelijke dieren eieren worden uitgescheiden) was daarbij eerder dan in de nieren opvallend hoog. Omdat de urineleiders van de dieren vaak viruseiwit bleken te bevatten, lijkt het niet onmogelijk dat IBV potentieel via een opklimmende (ascenderende) infectie de nieren zou kunnen bereiken, hetgeen doorgaans voornamelijk aan verspreiding via het bloed (viraemie) wordt toegedicht.

Een ander virus dat in de pluimveesector (en ook daarbuiten) wereldwijd tot grote problemen leidt, is het vogelgriepvirus (aviaire influenza virus, AIV). In het bovenstaande werd aangehaald dat IBV infecties tot extra problemen kunnen leiden wanneer er vervolgens een tweede (secundaire) infectie met een bacterie zoals APEC optreedt. Dergelijke dubbele infecties zijn in enige mate in kippen bestudeerd. In veel mindere mate is echter studie verricht naar de effecten van een infectie met twee virussen en wat de gevolgen van een dergelijke infectie op de pathogenese zijn. In **hoofdstuk 3** werd middels een model van op kweek gezette (geïncubeerde) stukjes luchtpijp van kippen (zogenaamde 'trachea organ cultures', TOCs) onderzocht wat het effect van een eerste IBV infectie op enerzijds een daarop volgende AIV infectie en anderzijds een tweede IBV infectie is. Waar AIV met enige vertraging redelijk ongestoord leek te kunnen infecteren en vermenigvuldigen in de reeds door IBV geïnfecteerde luchtpijp, bleek het voor een tweede IBV virus veel moeilijker om de epitheellaag opnieuw binnen te komen. Door de aanhechting van de bindingseiwitten van AIV en IBV aan de met IBV geïnfecteerde luchtpijp microscopisch te bestuderen en vergelijken, lijken deze verschillen in ieder geval deels voort te komen uit een verminderd vermogen van de tweede IBV variant om aan de luchtpijp te binden. Dit lijkt vervolgens samen te hangen met veranderingen aan het oppervlak van de te infecteren epitheellaag, waarbij bepaalde moleculen (siaalzuren, sialic acids) die IBV specifiek voor aanhechting nodig heeft grotendeels

van dit oppervlak lijken te verdwijnen onder invloed van de initiële IBV infectie. Interacties als deze zouden in het pluimveeveld kunnen optreden wanneer er bij aanwezigheid van AIV voor IBV wordt gevaccineerd en deze zouden ziekteverloop en mogelijk opbouw van immuniteit kunnen beïnvloeden.

Indien na een IBV infectie een secundaire bacteriële infectie optreedt, dan kunnen de gevolgen voor het dier en uiteindelijk ook de pluimveehouder desastreus zijn. Omdat antibioticumgebruik wegens het optreden van bacteriële ongevoeligheid (resistentie) voor deze middelen idealiter met hernieuwde kritische blik zou moeten aangewend, is het wenselijk om meer kennis over deze dubbele infecties met virus en bacterie te verwerven. In **hoofdstukken 4 en 5** zijn een aantal aspecten van zulke infecties bestudeerd. Hoewel in het verleden de interacties tussen kip, IBV en APEC eerder werden bestudeerd, is een vergelijking van IBV met andere luchtwegvirussen in deze context vernieuwend. Zodoende zijn in **hoofdstuk 4** tevens dieren naast IBV met respectievelijk een Newcastle Disease Virus (NDV) en een aviair metapneumovirus (aMPV) (beide eveneens belangrijke luchtwegziekte-veroorzakers bij kippen) geïnfecteerd alvorens ze aan APEC werden blootgesteld. Het virus lijkt hierbij in grote mate bepalend voor wáár in de luchtwegen na APEC infectie schade optreedt en tevens voor de uitgebreidheid en ernst daarvan. Na aMPV infectie, een virus waarvan bekend is dat het bij kippen vaak niet dieper dan neus en luchtpijp infecteert, werden nauwelijks APEC gecorreleerde weefselveranderingen gezien, terwijl na IBV en nog het meest na NDV infectie (virussen waarvan bekend is dat deze in variabele mate ook diepere luchtwegen infecteren) veel uitgebreidere schade in de longen en luchtzakken werd ontdekt. In vergelijking met dieren die alleen APEC toegediend hadden gekregen, waren de ontstekingsveranderingen vooral bij IBV en NDV veel uitgebreider. Opvallend genoeg werd de bacterie zelf maar zelden in de persisterende weefselschade terug gevonden. Deze veranderingen waren in verschillende infectiegroepen gecorreleerd met variaties in aanwezigheid van typen immuuncellen. Aanwezigheid van APEC bleek met name in het longweefsel voornamelijk gepaard te gaan met aanwezigheid van fagocyterende celtypen (zogenaamde granulocyten en macrofagen, die de bacterie kunnen opnemen en onschadelijk maken), terwijl aanwezigheid van de verschillende virussen invloed had op verschillende populaties zogenaamde T cellen (waarvan sommige specifiek met virus geïnfecteerde cellen onschadelijk kunnen maken). Met name wanneer IBV en NDV aan APEC infectie vooraf gingen, bleven deze cellen langer over tijd in het weefsel aanwezig en werden langere tijd hogere

waarden van zogenaamde cytokinen gemeten (moleculen gebruikt voor signaaloverdracht tussen immuuncellen). In **hoofdstuk 5** werd daarbij nog meer specifiek naar de effecten van IBV en APEC in de luchtzakken gekeken. Uit deze studie lijken signalen zichtbaar dat de persisterende weefselschade na blootstelling aan APEC mogelijk nog in grote mate de door het virus veroorzaakte en door de bacterie verergerde schade is. Dit is een subtiel andere kijk op deze veranderingen dan gebruikelijk, waarbij meestal wordt geredeneerd dat het virus de antibacteriële immuunrespons hindert, waardoor de bacterie langere tijd ongehinderd schade aan kan richten.

In het bovenstaande werd aangehaald dat IBV behalve de luchtwegen afhankelijk van de virusvariant ook het darmkanaal kan infecteren. Over de jaren is het hierbij enigszins discutabel gebleven in hoeverre de dieren hiervan ook hinder en ziekte ondervinden. Een nauw gerelateerd virus bij kalkoenen echter, het turkey coronavirus (TCoV), is juist bekend om zijn effecten op het maagdarmkanaal, waarbij dieren in reactie op TCoV-infectie in variabele mate daadwerkelijk darmontsteking (enteritis) en daarmee gepaard gaande diarree krijgen. TCoV werd aanvankelijk eveneens in de Verenigde Staten ontdekt (TCoV-US variant), maar veel recentelijker werd in Europa (Frankrijk) een nauw verwant, doch genetisch weldegelijk verschillend TCoV ontdekt (TCoV-Fr variant). In **hoofdstuk 6** werd deze TCoV-Fr variant onder de loep genomen voor wat betreft virale transmissie tussen dieren, de uitscheiding van virale deeltjes tijdens de infectie en de microscopische effecten op darmniveau. Uit deze studie blijkt dat geïnfecteerde dieren over een infectieperiode van meerdere weken al vrij snel na infectie en daarna gedurende lange tijd virusdeeltjes met hun darminhoud uitscheiden. Opmerkelijk is dat deze virusdeeltjes tijdens sommige van deze uitscheidingsmomenten wel en tijdens sommige momenten niet (of minder) infectieus lijken voor een gezond dier dat ze opneemt. Dieren die succesvol door deze virusdeeltjes werden geïnfecteerd, hadden enkele dagen na infectie erg veel viruseiwit in voornamelijk hun achterste (dikke) darmsegmenten, maar darmschade was erg beperkt. Deze bestond uit geringe, vrij moeilijk te ontdekken ontstekingscelinfiltratie, maar echte epitheelschade (zoals gezien bij IBV infecties in luchtwegen) was nergens aanwezig.

In de studie van **hoofdstuk 7** zijn tot slot de gevolgen van infectie van een darmziekte-veroorzakende (enteropathogene) IBV variant microscopisch op darmniveau vergeleken met die van TCoV en een derde pluimvee-geassocieerd coronavirus dat ernstige diarree en sterfte kan veroorzaken in parelhoenders, het

Guinea fowl coronavirus (GfCoV). Uit deze studie lijkt zichtbaar te worden dat GfCoV in tegenstelling tot de bestudeerde IBV variant en TCoV veel meer de direct na de maag komende, voorste dunne darmsegmenten (duodenum en jejunum) infecteert en daar veel uitgebreider tot ontsteking leidt dan infecties met TCoV en met name IBV in de meer achterste (dikke) darmsegmenten (ileum, caecum, colon, cloaca-regio). Deze voorste darmsegmenten spelen bij vogels veel meer dan de achterste segmenten een grote rol op de vertering, metabolisme en homeostase en bij uitgebreide ontsteking van die voorste segmenten zou een correlatie met ernstiger ziekteverloop niet onlogisch zijn. Er is zeker behoefte om GfCoV, dat pas een ruim decennium geleden als oorzaak aan het al decennia geziene ernstige ziektebeeld in de Franse parelhoenderhouderij kon worden gekoppeld, verder te onderzoeken voor wat betreft ziekteverloop, verspreiding door het dier, transmissie en immuunresponsen.

In conclusie brengt dit proefschrift nieuwe inzichten in het ziekteverloop van en immuunresponsen op infecties door IBV, TCoV en GfCoV in respectievelijk kippen, kalkoenen en parelhoenders. In alle studies werd daarbij de waarde van microscopisch onderzoek en het nauwkeurig middels dergelijk onderzoek in kaart brengen van details in weefselafwijkingen voor het voetlicht gebracht. Op deze wijze kan de precieze locatie van aanwezigheid van een virus of ander pathogeen worden gerelateerd aan opgetreden weefselafwijkingen en met het in kaart brengen van de ernst van deze afwijkingen kan impact op het individu mogelijk worden verklaard, dan wel voor toekomstige ziektegevallen worden ingeschat. De verworven kennis zou daarnaast potentieel van waarde kunnen zijn bij het begrijpen van toekomstige uitbraken van nieuwe virussen, waarvan recent door het severe acute respiratory syndrome coronavirus 2 (SARS-CoV2) wereldwijd aangetoond is dat deze juíst door hun ‘onbekendheid’ en onvoorspelbaarheid van enorme impact op de maatschappij en het leven kunnen zijn.

JA, DAT VOELEN WIJ

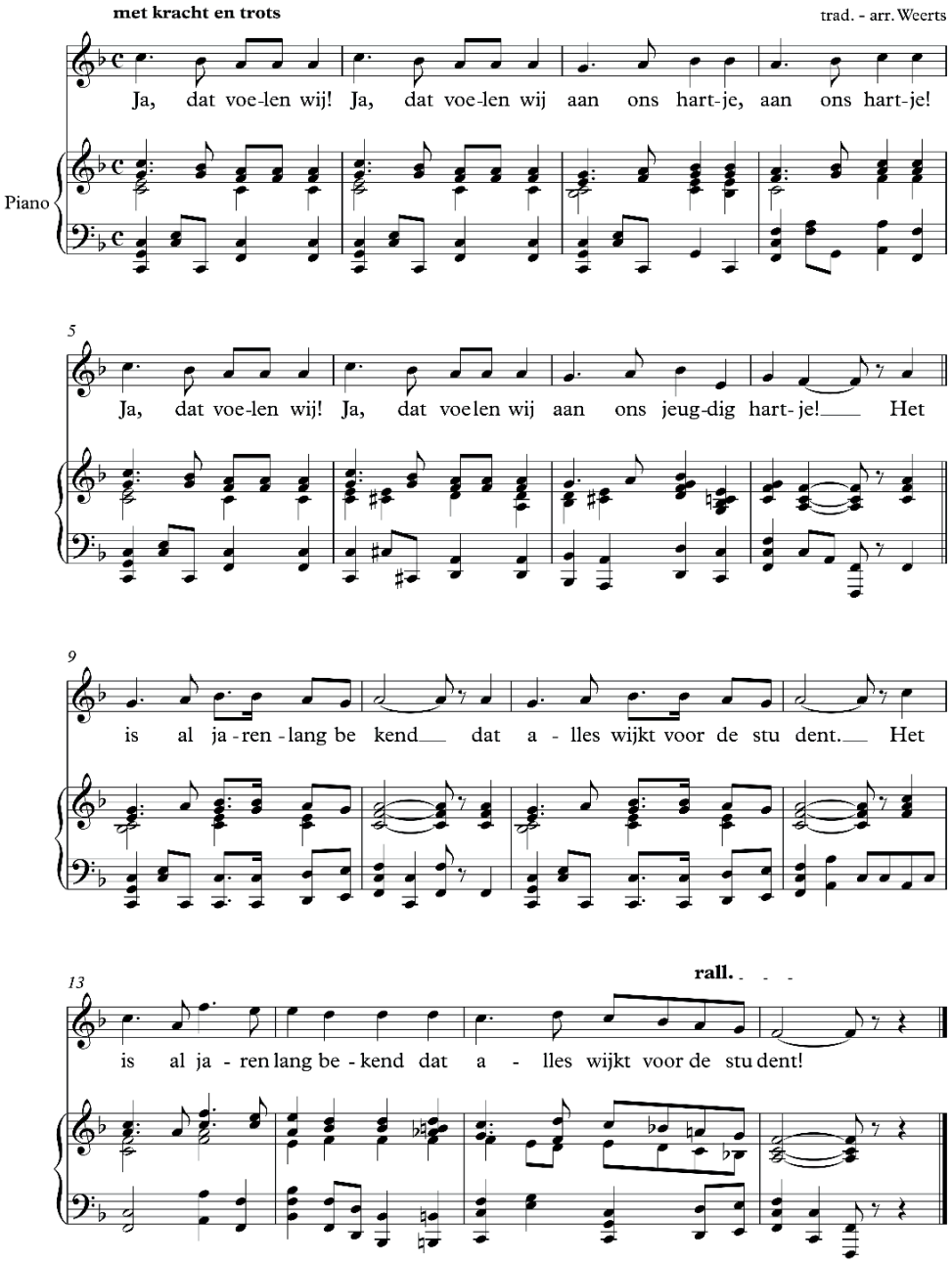

Voetnoot: *Ik zie sommigen bij het bovenstaande al denken: dat is niet compleet! Daarover het volgende: het op de pagina hiernaast aangestipte ritueel schrijft volgens Vlaamse Codices voor dat de lofzang traditioneel niet verder reikt dan hetgeen hierboven is weergegeven en dat de zogenaamde 'Blauwe Bladzijden' van de Codex daarbij vermelden: 'Het klinkt als hoon na deze lofzang vulgaire straatliedjes te zingen van het slag "En hedde gaai meubele..." etc.'*

Dankwoord

Volgens de Nederlandse veterinaire traditie is er maar één geëigende manier om de hoogst mogelijke dankzegging over te brengen en deze traditie biedt mij - bijna aan het einde van mijn boekje - op toepasselijke wijze de kans een andere van mijn vaardigheden in mijn proefschrift te vervlechten. Het hiernaast afgebeelde zal de meeste collegae en aanstaand collegae die in Utrecht hun opleiding tot dierenarts hebben genoten of nog genieten bekend voorkomen. Van oorsprong dient dit lied te worden aangeheven ter besluit van de Vlaams-Nederlandse variant van de zogenaamde '*Salamander*', een ritueel dat vermoedelijk is ontstaan in Duitsland in de 19e eeuw en dient ter bezegeling van vriendschap of om iets of iemand op de krachtigst mogelijke wijze te eren. Aangaande dit proefschrift komt deze hoogst mogelijke dankzegging toe aan allen die op welke manier dan ook betrokken zijn geweest bij de totstandkoming - zij het inhoudelijk, ondersteunend, aanmoedigend, relativerend en / of ter afleiding en ontspanning om de spreekwoordelijke batterij weer te helpen opladen:

Andrea… voor de discussies, de kansen, het geduld en vertrouwen, 'vissen op het droge'… en ja: Shakespeare! ;-)

Hélène… voor een totaal andere kijk op zaken, sterke wetenschappelijk gedachten, de warme band. 't.z.t. is gekomen' ;-) *'Suuuuucces!'*

Mie(ke)… voor uw onvoorwaardelijke support, uw medeleven, het Flandrienekke, dé meet, de ruimhartige bourgondische gezelligheid *'Schaamt ge u nie, da ge da nie weet?!'* ;-)

Guy… voor de ultieme collegialiteit, je onvolprezen verdiensten, de lach en de traan, de culinaria… je verdient met recht een gouden standbeeld! *'Never a boring moment, toch?!'*

Tim en Steven… voor het mee-zweten, de inzichten, de technische ondersteuning, de luisterende oren en het trouwe verbond dat muzikaal ontstond

Ruud… in gróte mate ten grondslag aan het feit dat ik een veterinaire carrière ging ambiëren en verwierf … en nog altijd even dicht in de buurt *'Aan mijn lijf geen polonaise!'*

de heeren **Simons, Gerrits** en **Beulens**… vakinhoudelijk en vriendschappelijk van ruime invloed op mijn veterinaire worden en zijn

Willie… samen in het schuitje ;-) – **Judith**… op het juiste moment de steun in mijn rug, *'táá tà tà, táá tà tà tà, tà-dáá á!'* ;-) – **Marja**… kleurrijk, relativerend, aanmoedigend - **Jooske**… het delen van ervaringen met dat tussenschot tussen ons in ;-) – **Nynke**… de koffiepraat en collegialiteit

ál mijn fantastische collega's – stuk voor stuk – van het VPDC, het 'Patho-lab', de zeezoogdierhelden, het DWHC… al dik 13 jaar iedere dag weer met veel plezier in jullie aanwezigheid aan de slag! :-)

mijn ex-(lab)collegae: **Henny, Johan, Ronald, Mieke, Bernardo, Iresha , Kim, Nika, Alinda, Geert, Fons, Laca, Vera, Famke**… tijdperk na tijdperk omringd door toppers!

Margreet, Sandra, Liesbeth en Lineke…'tijdgenoten', 'study buddies'… wát een belevenissen! ;-)

de 'Gevederde Vrienden' & Co: **Thijs, Andreas, Jasper, Sjaak, Jan, Ewout, Miel, Thomas & Thomas** en natuurlijk **Marius**!!!, wandelende encyclopedie en 'microscoop-vrind'… tijd voor Sauternes?! :-)

alle coauteurs van de studies in dit proefschrift

de **mannen op ski's en board**, relaxed met peertje

al mijn **muzikale amices-collegae van Syrinx**… voor alle in- en ontspanning tijdens al het muzikale moois dat we doen, brengen en laten weerklinken!

mijn altijd betrokken schoonouders **Mieke en Max** en **al mijn lieve schoonfamilieleden**

Wendy, Yuri en **Bram** *'Zullen we naar Disneyland gaan?'*:p

pa & ma… altijd vol vertrouwen, doorzetters!, nooit klagen of pretentieus, onvoorwaardelijk liefdevol

Ivo… je weet het!

… en ja, cliché, edoch: iedereen die ik onverhoopt vergeten ben :-)

Over de auteur

Erik Anthonius Wilhelmus Siebertus Weerts werd geboren te Oeffelt in het Land van Cuijk, Noord-Brabant, op 30 juni 1983. Na het afronden van zijn Gymnasium-opleiding op het Merletcollege te Cuijk begon hij in 2001 aan de studie Diergeneeskunde aan de Universiteit Utrecht en deze voltooide hij met de differentiatierichting Landbouwhuisdieren in de nazomer van 2009. In grofweg de tweede helft van deze studieperiode ontstond bij hem een voorliefde voor de discipline Pathologie en in februari 2010 mocht hij aan het werk als specialist-in-opleiding Veterinaire Pathologie op wederom de Faculteit Diergeneeskunde te Utrecht. In 2014 slaagde hij voor zijn certificeringsexamens en werd hij officieel diplomate of the European College of Veterinary Pathologists (ECVP). In het daaraan voorgaande jaar kon hij instromen in een promotietraject bij de onderzoeksgroep van de afdeling Pathologie onder leiding van Andrea Gröne en Hélène Verheije: dit proefschrift is thans het stoffelijke resultaat daarvan. Hij participeerde als deel van deze groep onder andere in de Europese COST Action 'Towards control of avian coronaviruses: strategies for diagnosis, surveillance and vaccination', was in 2016 en 2022 mede-organisator van 2 edities van het 'International Symposium on Avian Corona- and Pneumoviruses' (vanaf 2022 'International Symposium on Avian Viral Respiratory Diseases') en in 2019 mede-organisator van het Joint European Congress of Veterinary Clinical Pathologists and Veterinary Pathologists te Koninklijke Burgers' Zoo, Arnhem NL. Thans is hij nog altijd werkzaam als veterinair patholoog op de Faculteit Diergeneeskunde van de Universiteit Utrecht en participeert daar onder andere in onderzoekssamenwerkingen met de pluimveegroep van de afdeling Landbouwhuisdieren onder leiding van Sjaak de Wit en Mieke Matthijs. Daarnaast is hij bedreven ambassadeur van 'veterinair-muzikale zaken' en in die hoedanigheid mede-oprichter, h.t. bestuurslid, muzikant en huisarrangeur van het Collegium Musicum Veterinarium 'Syrinx', dat onder andere op bovengenoemde congressen in grote, kleurrijke bezetting op concertante wijze van zich heeft laten horen.